ISSN 1718-3200 VOLUME 21, SPECIAL ISSUE 2026

THE JOURNAL OF OCEAN TECHNOLOGY

www.thejot.net

marine renewables canada 2025

conference proceedings

IN THIS ISSUE

marinerenewables.ca/vision

marine renewables canada

THE JOURNAL OF
OCEAN TECHNOLOGY

Contents

Papers

The Journal of Ocean Technology

www.thejot.net

A publication of

Marine Institute

Memorial University

bsi. ISO 9001:2015 Quality Management

Printed in Canada

Academic and Scientific Credentials

The Journal of Ocean Technology is a scholarly periodical with an extensive international editorial board comprising experts representing a broad range of scientific and technical disciplines. Editorial decisions for all reviews and papers are managed by Dr. David Molyneux, Memorial University of Newfoundland, and Dr. Katleen Robert, Fisheries and Marine Institute.

The Journal of Ocean Technology is indexed with Scopus, EBSCO, Elsevier, and Google Scholar. Such indexing allows us to further disseminate scholarly content to a larger market; helps authenticate the myriad of research activities taking place around the globe; and provides increased exposure to our authors and guest editors. All content in the JOT is available online in open access format. **www.thejot.net**

A Note on Copyright

On the Cover

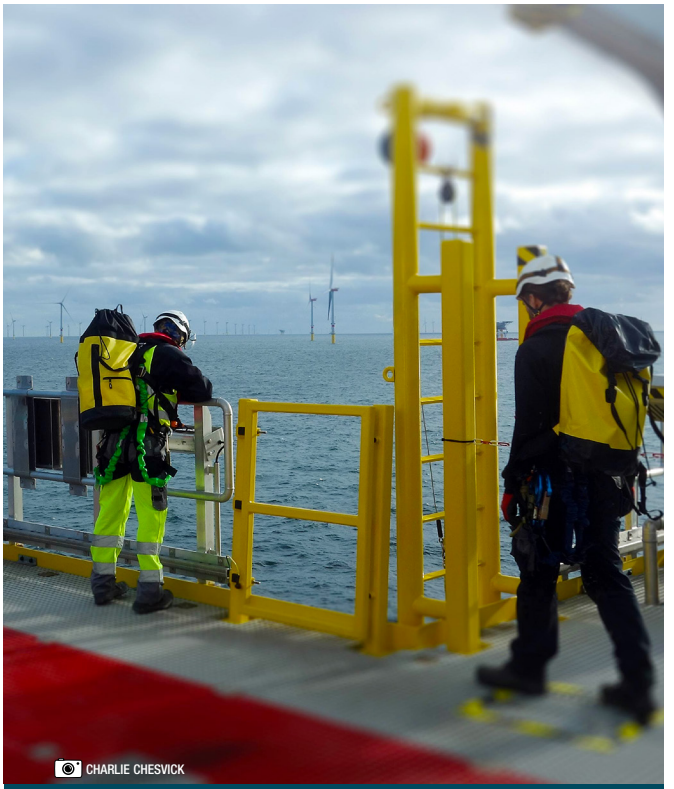

Offshore wind farm in Germany.

Publishing Schedule at a Glance

The JOT production team invites the submission of technical papers, essays, and short articles based on upcoming themes. **Technical papers** describe cutting edge research and present the results of new research in ocean technology or engineering, and are no more than 7,500 words in length. Student papers are welcome. All papers are subjected to a rigorous peer-review process. **Essays** present well-informed observations and conclusions, and identify key issues for the ocean community in a concise manner. They are written at a level that would be understandable by a non-specialist. As essays are less formal than technical papers, they do not include abstracts, listing of references, etc. Typical essay lengths are up to 3,000 words. **Short articles** are between 400 and 800 words and focus on how a technology works, evolution or advancement of a technology as well as viewpoint/commentary pieces. All content in the JOT is published in open access format, making each issue accessible to anyone, anywhere in the world. There are no costs to publish in the JOT. Submissions and inquiries should be forwarded to info@thejot.net.

Upcoming Themes

All themes are approached from a Blue Economy perspective.

Spring 2026	Women and the Ocean
Summer 2026	Ocean startups
Fall 2026	Youth and the ocean
Winter 2026	Citizen science
Spring 2027	Floating laboratories: research at sea
Summer 2027	Dual-use technologies: defence in the North Atlantic
Fall 2027	Harsh environment technology: working in the cryosphere
Winter 2027	Maritime transport: moving people and goods

Stay informed

Each issue of the JOT provides a window into important issues and corresponding innovation taking place in a range of ocean sectors – all in an easy-to-read format with full colour, high-resolution graphics and photography.

CONTACT US

The Journal of Ocean Technology
c/o Marine Institute
P.O. Box 4920
155 Ridge Road
St. John's, NL
A1C 5R3 Canada
+001 (709) 778-0763
info@thejot.net
www.thejot.net

Don't forget to follow us!

Welcome Note

MRC

When planning the Marine Renewables Canada 2025 Conference and Exhibition, our team reflected on the progress and opportunities ahead in Canada's marine renewable energy sector. Over the past year, offshore wind and tidal energy have been advancing to a point where they present real potential to play a role in meeting Canada's net zero and economic growth goals. Our conference needed to reflect this momentum by focusing on technical, regulatory, and infrastructure aspects of sector development. We re-introduced a Research and Technical Track for 2025 and this second special edition with the Journal of Ocean Technology (JOT) focuses on work that will shape the next chapter of marine renewable energy development.

Our industry has seen significant progress since our last JOT special issue in 2018. At that time, research was centred on foundational topics: understanding wake behaviour, refining acoustic monitoring tools, improving measurements in high-flow tidal sites, and identifying variables that influence wave energy performance. These efforts laid critical groundwork, but today, the conversation has changed. The sector is focused on building an industry and preparing to build the projects that will deliver it.

The past year underscores that transition. The Wind West project proposed by Nova Scotia's Premier, Tim Houston, and recognized by Prime Minister Mark Carney as a prospective nation-building project, outlines how more than 60 GW of offshore wind potential could supply up to 27% of Canada's future electricity needs. The launch of the Major Projects Office now sets a two-year timeline for reviewing strategic infrastructure projects, signalling strong federal alignment. The Canada-Nova Scotia Offshore Energy Regulator has initiated its first Call for Information and Prequalification for offshore wind, with an upcoming Call for Bids slated for 2026.

Tidal energy continues to advance with lessons learned from past deployments in the Bay of Fundy and in British Columbia. These insights have helped industry, regulators, researchers, and communities address regulatory barriers and challenges to improve readiness for future projects. Recent developments include a new *Fisheries Act* authorization, the first under the new adaptive regulatory framework, for a project at Fundy Ocean Research Centre for Energy, on the heels of the Province of Nova Scotia awarding two additional berths to Eauclaire Tidal Limited Partnership and Orbital Marine Power. The federal government has also committed CAD$10.7 million in new funding for monitoring platforms and fish-turbine interaction studies.

On the West Coast, there was the launch of the BC Marine Energy and Decarbonization Hub, an initiative between COAST, Accelerating

Community Energy Transformation, the Pacific Regional Institute for Marine Energy Discovery (PRIMED), and the Institute for Integrated Energy Systems, with the goal of creating new pathways for the development and commercialization of marine renewable energy and decarbonization technologies in British Columbia. Projects such as the University of Victoria (UVic) PRIMED Discovery's Blind Channel Tidal Energy Demonstration Centre and the Yourbrook Energy Systems Kamdis Tidal Power Demonstration Project further prove the region's commitment to advancing tidal as a scaled energy system. Significant progress is also being made through an Indigenous-led wave energy project by the Mowachaht/Muchalaht First Nation (MMFN) in collaboration with UVic's PRIMED. Together, MMFN and UVic are working to build local knowledge, assess community priorities, and gather the data needed to determine how, and when, wave energy can support the Nation's clean energy future. This ensures energy solutions are guided by Indigenous leadership, and align with their goals, values, and future energy needs.

Across the region, projects are helping Indigenous and remote communities deploy microgrid systems, reduce diesel reliance, and accelerate commercialization pathways for tidal, wave, and river-current technologies.

In addition to regulatory progress and partnerships, the research featured in this issue reflects a sector advancing from pilot projects to building a national industry from coast to coast to coast.

Several papers examine the engineering and environmental considerations of offshore wind. New methodologies for scaled physical modelling outline how geological and geotechnical conditions in Nova Scotia and Newfoundland and Labrador guide siting decisions and technology selection. Regional modelling work highlights how hurricanes, ice, and seabed conditions unique to Atlantic Canada may require adaptation of global design standards.

Digital and Artificial Intelligence (AI) tools are also featured. MESO, an AI-supported modelling platform, evaluates hybrid energy systems that combine offshore wind with energy storage to support grid stability. Real-time species recognition technology demonstrates how machine learning is transforming ecological monitoring and building public trust. One paper presents Waterfront, a digital tool to improve transparency and coexistence between offshore wind developers and commercial fisheries, a key issue for those communities.

Tidal energy research in this issue continues to advance environmental understanding and deployment readiness. Numerical model comparison work helps predict performance and simplify the design of turbine arrays. New modelling of fish trajectories through Minas Passage improves our ability to assess interaction risks with tidal turbines. International efforts

to advance tidal energy with Smart Data Application show how shared frameworks and environmental data can accelerate responsible tidal deployment globally.

Together, these papers demonstrate a sector that is maturing. They offer new tools and methodologies that will strengthen understanding and decision-making as Canada moves deeper into offshore wind development and tidal energy commercialization.

Thank you to the paper authors and a special thanks to the 2025 Research and Technical Committee, including co-chairs Dr. Anna Redden (Acadia University) and Dr. Matthew Asplin (ASL Environmental), for shaping this year's program.

Chelsi Bennett is the communications and events coordinator with Marine Renewables Canada.
marinerenewables.ca

Editor's Note: All extended abstracts were peer-reviewed prior to presentation at the 2025 Marine Renewable Energy conference and the full papers were peer-reviewed by Marine Renewables Canada prior to publication.

Informative

Cutting Edge

Provocative

Challenging

Informative

International

thejot.net

Peer-Reviewed Papers

Energy Extraction Efficiency

Yanran Xia

Philippe Rochefort

Prof. Guy Dumas

Two simplified models for numerical turbine array simulations

Who should read this paper?

The contributions presented in this paper are valuable for researchers and practitioners researching reliable methods for analyzing turbine layout performance during the design phase of hydrokinetic turbine farms; for researchers interested in wake-turbine interactions; and for Computational Fluid Dynamics (CFD) specialists interested in hydrokinetic and wind turbine modelling.

Why is it important?

This work presents the first direct comparison of two simplified turbine models based on volumetric force-prediction techniques, namely the Effective Performance Turbine Model and the Actuator Line Method, for multi-turbine configurations. These models not only make such farm analysis computationally feasible compared to high-fidelity blade-resolved simulations, they also provide accurate performance and wake predictions for array-scale analysis.

This paper also provides new physical insights for tandem and clustered turbine arrangements – configurations that remain sparsely documented in the literature. The strengths and limitations of each approach are evaluated, leading to recommendations on their appropriate use depending on the turbine array configuration.

As the ocean will increasingly host larger turbine farms, modelling tools that are both accurate and computationally efficient will be needed to support the planning, the optimization, and the environmental assessment for turbine array deployment.

About the authors

Yanran Xia is a PhD candidate at the CFD laboratory LMFN at Université Laval. Her research focuses on numerical modelling of hydrokinetic turbines and optimization of turbine farm deployment in marine environments. Her expertise includes fluid mechanics and CFD. She has experience working with CFD solvers such as Star-CCM+.

Philippe Rochefort is an M.Sc. candidate at the CFD laboratory LMFN at Université Laval with expertise in fluid mechanics and CFD, particularly using Star-CCM+. His research focuses on the modelling of vertical-axis turbines using the Actuator Line Method, aiming to improve performance prediction under realistic conditions while reducing computational cost.

Prof. Guy Dumas is a professor as well as the founder and director of the CFD laboratory LMFN at Université Laval, where he specializes in aero-hydrodynamics and numerical simulations. He investigates vortical and turbulent flows to shed light on the complex physics of fluid-structure interactions and to optimize systems of renewable energy production. His group has contributed to advancing hydrokinetic turbine technologies and developing various concepts of oscillating-foils turbine.

COMPARISON OF TWO SIMPLIFIED MODELS FOR NUMERICAL TURBINE ARRAY SIMULATIONS

Yanran Xia, Philippe Rochefort, Guy Dumas*
CFD Laboratory LMFN, Department of Mechanical and Industrial Engineering, Université Laval, Québec, QC, Canada
**Corresponding author: guy.dumas@gmc.ulaval.ca*
DOI: https://doi.org/10.48336/TMT0-7G93

ABSTRACT

To improve the energy extraction efficiency of hydrokinetic turbine farms, it is necessary to study the performance of different turbine array configurations. However, predicting and analyzing the performance of turbine arrays using high-fidelity blade-resolved simulations is unrealistic due to excessive computational cost. A solution to reduce computational demand while maintaining realistic performance predictions and accurate representation of flow physics is to use simplified turbine models. This work presents a comparison between two simplified modelling approaches developed at Université Laval for cross-flow turbines of the H-Darrieus type: the Actuator Line Method (ALM) and the Effective Performance Turbine Model (EPTM). Both approaches consist of representing the real rotor by equivalent volumetric forces, thus bypassing the resolution of the blades and their boundary layers. The ALM is an unsteady method that requires the computation, at each time step, of the force distribution to be applied along the span of the turbine's blades. Thus, this method accurately reproduces the local impact of the blade on the flow field and to generate realistic near-wake structures. On the other hand, the steady-state EPTM imposes time-averaged blade forces within an annular cylindrical actuating region to reproduce the mean effects of the rotor on the flow, which predicts the mean turbine performance and generates a reasonably accurate mean wake. Compared to the EPTM, the ALM is of higher fidelity, capturing more physical details, but computationally more expensive.

Three turbine configurations (single turbine, tandem array, and triangular cluster) are simulated using both approaches. The two methods are evaluated and compared in terms of the prediction of key performance metrics (i.e., power and drag coefficients) and in terms of their wake reproduction capability. Recommendations for turbine farm analysis are formulated.

Keywords: Hydrokinetic energy, cross-flow turbine, turbine arrays, simplified modelling, actuator line, actuator disk

1. INTRODUCTION

Hydrokinetic turbines are technologies that allow the extraction of kinetic energy from freestream water flows, such as river and tidal currents, in a manner analogous to wind turbines. This work focuses on the H-Darrieus Cross-Flow Turbine (CFT) technology, which is composed of straight blades rotating at a constant radius along the entire span. The CFTs, deployed vertically, are well adapted to the bi-directional or multi-directional tidal flows. They can also be deployed horizontally in shallow water applications where their rectangular extraction plane allows to maximize the power. Thus, their adaptability to different environments and their ease of installation [1], [2] make them advantageous compared to axial-flow turbines. In this work, we consider CFTs deployed vertically.

Deploying these turbines in arrays or farms becomes an interesting option to minimize installation and maintenance costs while maximizing energy extraction on regional scales. Dabiri [3] also demonstrated in 2011 that the energy density of turbine farms is increased when using CFTs compared to axial-flow turbine farms, which makes this technology even more attractive for farm-scale deployment.

The main challenges when considering turbine farms are related to total power prediction and configuration optimization. Hydrokinetic turbine arrays are not simple superposition of isolated turbines; instead, complex interactions exist among turbines, such as the local blockage effects caused by closely placed side-by-side turbines [4], [5], as well as the impact of upstream wakes on downstream turbines [5], [6], [7]. Moreover, resource-related factors – such as the global blockage induced by the channel bed and the free surface [8], [9], free surface deformation [6], and inflow characteristics [10], [11], [12] – also have a significant influence on the array performance. Therefore, it is essential to account for these aspects in turbine array studies.

During the design phase of turbine farms, Computational Fluid Dynamics (CFD) is an important tool to assess the array performance and optimize the turbine layout. High-fidelity Blade-Resolved (BR) simulations are often applied for the performance and wake characterization of single turbines [13], [14], [15]. However, BR simulations are highly demanding in computational cost due to the boundary layers resolution near the solid bodies. As a result, using BR simulations for configuration with multiple turbines becomes unrealistic due to the excessive computational cost. A solution to reduce computational demands while still providing reliable predictions is to use simplified turbine models, such as force prediction-based modelling techniques like the Effective Performance Turbine Model (EPTM) [16] and the Actuator Line Method (ALM) [17]. These two simplified approaches, which have been adapted for CFTs at Université Laval, are used in this study.

This work thus aims to compare these two simplified models adapted to the turbine geometry described in Section 2.1 based on their performance predictions, wake reproduction, and computational costs for three deployment scenarios: single turbine and

two different multi-turbine configurations. The modelling details of both approaches are presented in Sections 2.2 and 2.3, while the results for the three configurations (single turbine, tandem array, and triangular cluster) are discussed in Section 4. Finally, recommendations for the analysis of turbine farms using these two simplified models are provided in order to highlight the advantages and limitations of each approach and to address the following question: Which model is best suited to optimize turbine farm configurations?

2. TURBINE MODELLING

As mentioned earlier, resolving boundary layers in BR simulations requires a very fine computational mesh near solid bodies to capture the strong normal gradient of velocity, which significantly increases the computational cost. The simplified models EPTM and ALM presented in this work are both actuator-type turbines models, which replace solid bodies with actuating regions in which estimated volumetric forces are imposed. As a result, boundary layer resolution is bypassed in these models, which reduces computational cost while still maintaining accurate performance predictions.

This section first presents the reference turbine, along with the normalized parameters that typically characterize CFTs. Then, the general working principles of the two simplified models EPTM and ALM are described.

2.1 Description of the Reference Turbine

The reference turbine, shown in Figure 1, consists of a three-bladed CFT with a simplified cylindrical hub, originally designed and tested by Mavi Innovations. Supporting struts and foundation structures are not considered for simplification purpose. Detailed parameters of geometric characteristics and operating conditions are presented in Table 1. In this study, the turbine operates always at its rotational speed corresponding to its optimal power extraction point whatever its deployment conditions. The tip-speed ratio is a normalized value of the rotational speed Ω, defined as:

$$\lambda \equiv \Omega R / U_{\infty}, \tag{1}$$

where $R \equiv D/2$ is the rotor radius and U_{∞} is the freestream velocity. The optimal tip-speed ratio (λ_{opt}) of a specific turbine design varies depending on the blockage ratio:

$$B = A / A_{\mathrm{channel}}, \tag{2}$$

where $A = bD$ is the turbine's frontal area and A_{channel} is the cross-sectional area of the channel. For the investigated CFT, the optimal tip-speed ratio is of 3 in a confined environment with a blockage ratio of 20% [18]. The diameter-based rotor Reynolds number is fixed at $Re_D \equiv U_{\infty} D/\nu = 1.07 \cdot 10^7$ (with ν being the fluid kinematic viscosity), which is high enough to assume Reynolds independence [19] and fully turbulent boundary layers.

Conventional turbine performance metrics include several non-dimensional parameters, such as the mean power coefficient, defined as the ratio of time-averaged (mean) power extraction ($\overline{P}$) to the available power across the turbine's extraction window:

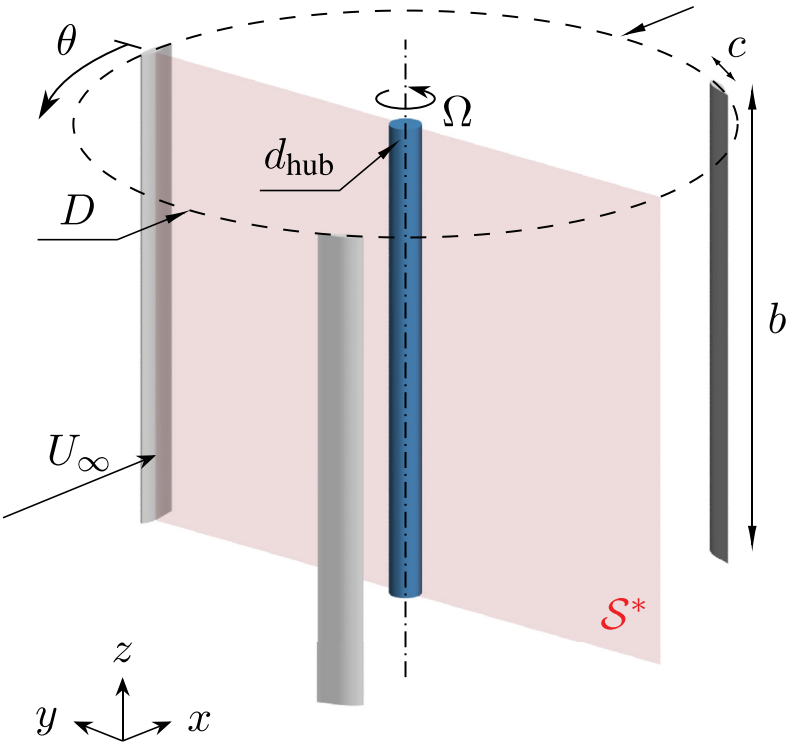

Figure 1: Three-bladed turbine geometry and main parameters.

Table 1: Main normalized geometric and operational characteristics of the reference turbine.

Parameter	Symbol	Value
Turbine geometry		
Blade number		3
Blade profile		NACA 63-021
Blade span	b/D	0.75
Blade chord	c/D	1/14
Blade attachment point	x_p/c	0.25
Blade pitch angle	β	0°
Hub diameter	d_{hub}/D	0.05
Operating conditions		
Blockage ratio	B	20%
Tip-speed ratio design	λ	3
Rotor Reynolds number	Re_D	1.07×10^7
Blade Reynolds number	$Re_c = (\Omega R)c/\nu$	2.29×10^6

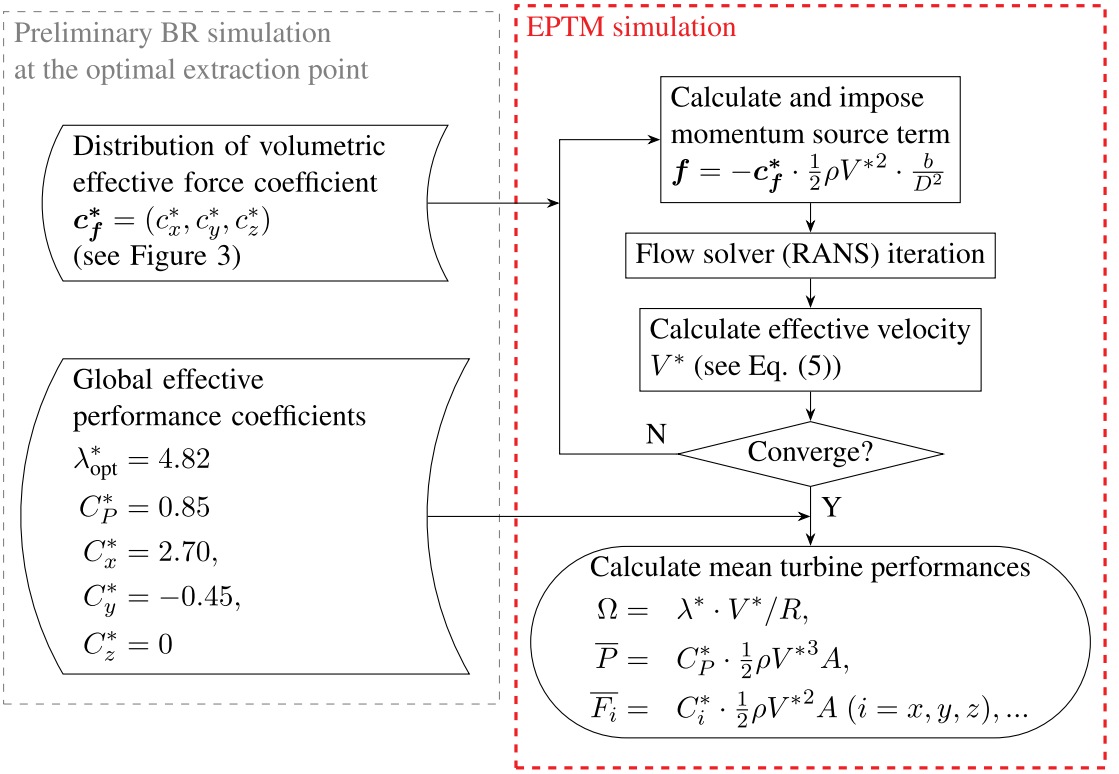

Figure 2: Overall computational workflow of an Effective Performance Turbine Model (EPTM) simulation.

$$\overline{C_P} \equiv \frac{\overline{P}}{\frac{1}{2}\rho U_\infty^3 A}, \tag{3}$$

and the mean drag coefficient (also referred to as the mean thrust coefficient), defined as a normalized value of the drag force, i.e., the mean streamwise force acting on the turbine ($\overline{F_x}$):

$$\overline{C_x} \equiv \frac{\overline{F_x}}{\frac{1}{2}\rho U_\infty^2 A}, \tag{4}$$

where ρ is the fluid density.

2.2 Low-fidelity Simplified Turbine Model: EPTM

The EPTM is a steady-state simplified turbine model for use in a three-dimensional Reynolds-Averaged Navier-Stokes (RANS) CFD simulation of the deployment site, originally developed at Université Laval by Bourget in 2018 [16], which has been specially formulated for the reference CFT considered here and further validated and applied under various operating environments [20]. As an actuator-disk type model, the EPTM imposes volumetric forces (i.e., momentum source terms in the RANS equation) directly into the fluid domain to mimic the time-averaged impact of the real turbine. The cylindrical actuating region replicates the geometry of the CFT's blades swept area. This approach avoids not only the resolution of boundary layers but also the long temporal resolution.

Figure 2 presents the overall calculation process of an EPTM simulation. The key feature of EPTM is that the applied volumetric forces *f* and the mean performance metrics

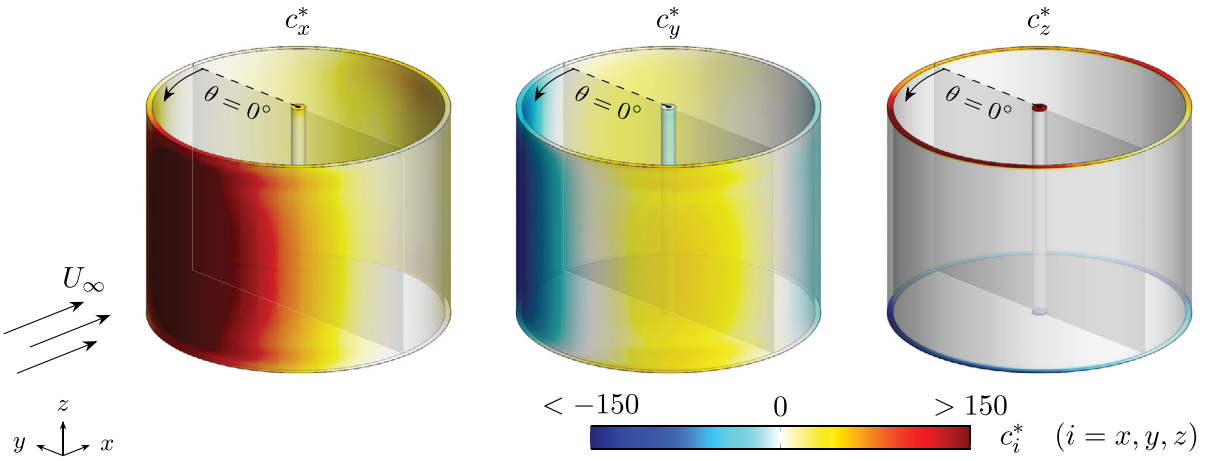

Figure 3: Distribution of the streamwise (c_x^*), transverse (c_y^*), and axial (c_z^*) components of the volumetric effective force coefficient c_f^*. The transparent grey plane denotes the turbine extraction plane.

(e.g., the optimal rotational speed Ω, the mean output power $\overline{P}$, and the mean drag force $\overline{F}_x$) are all scaled with the effective velocity V^*, which is defined as the time- and space-averaged velocity passing through the rotor (see the pink plane denoted S^* in Figure 1):

$$V^* \equiv Q/A \tag{5}$$

with Q being the mean flowrate through the rotor. This effective velocity is not known a priori, but results from the simulation. Indeed, V^* is the main performance metric provided by the EPTM. Other performance metrics are computed from it as expressed in the chart of Figure 2. At each RANS iteration step, the effective velocity V^* is recalculated and is used to update the volumetric force f. Once the solution converges, final prediction of the mean turbine performance can be derived. It is important to note that the input data, i.e., the distribution of the volumetric effective force coefficient (c_f^*) illustrated in Figure 3, as well as the global effective coefficients, including the effective tip-speed ratio (λ^*), the effective power coefficient (C_P^*), and the effective force coefficients ($C_{x,y,z}^*$) are all extracted from a preliminary BR simulation of an isolated turbine at its optimal extraction point. Note that the global mean force $\overline{F_{x,y,z}}$ are the volume integrals over the actuating region of the components of f in their corresponding directions [16].

Since the effective velocity V^* represents the local flow "effectively experienced" by the turbine, the EPTM is intrinsically able to account for the rotor-scale local flow effects such as the blockage effect and velocity variations in the upstream vicinity. The former may be due to the channel confinement or the presence of neighbouring turbines while the latter may be associated to the velocity deficit produced by upstream turbines. Moreover, in all circumstances, the EPTM tracks the optimal power extraction point automatically.

2.3 Medium-fidelity Simplified Turbine Model: ALM

The ALM is a medium-fidelity and unsteady model that can be used to predict the time evolution of the performances [21], [22] and to accurately replicate the unsteady turbine wake structures due to the blade rotation

[23]. In this approach, the solid bodies, i.e., the blades and hub of the CFT, are replaced by straight actuating lines in rotation (for the blades) along which varying volumetric forces are applied into the Navier-Stokes equations, as shown in Figure 4. The actuating lines are formed with actuating points uniformly spaced in the spanwise (z) direction, and the force distribution is constructed based on the force contributions from individual point. The lift ($\Delta_p f_l$) and drag ($\Delta_p f_d$) forces for each actuating point are calculated with the estimated local flow properties [24]: the blade-scale effective local freestream velocity (V) and the effective angle of attack (α), as well as the precomputed 2D aerodynamic polars (i.e., lift and drag curves) of the blade's profile:

$$\Delta_p f_l = \frac{1}{2}\rho|\boldsymbol{V}|^2 \Delta_p A C_l(\alpha), \tag{6}$$

$$\Delta_p f_d = \frac{1}{2}\rho|\boldsymbol{V}|^2 \Delta_p A C_d(\alpha), \tag{7}$$

where $C_l(\alpha)$ and $C_d(\alpha)$ are the lift and drag coefficients corresponding to α, and $\Delta_p A = \Delta_p z \cdot c$ is the area attributed to each point. Resulting forces are implemented in the fluid domain to replicate the actual blades' effects on the flow. Since CFT blades operate in curved flow, it is necessary to apply analytical curvature corrections to the lift and drag coefficients [25] to adapt the ALM to CFT. Additionally, near-tip correction functions developed specifically for the ALM [26] are used to adapt the force loading near the blade tips, as the standard ALM struggles to accurately reproduce tip loading due to a poor representation of tip vortices. The instantaneous power coefficient (C_P) is computed using the tangential force component along the blade chord, which results from the projection of $\Delta_p f_l$ and $\Delta_p f_d$ onto the chord direction, as well as the resulting moment at the attachment point. Compared to other ALM adaptations for CFTs previously proposed in the literature [27], [28], [29], the ALM used in this work is improved through the incorporation of new analytical curvature corrections and near-tip correction functions. These enhancements maintain the simplicity of the ALM while significantly improving its predictive capabilities [17].

3. NUMERICAL SETTINGS

The EPTM, ALM, and BR simulations in this work are all performed using the finite-volume commercial CFD software Simcenter™ STAR-CCM+™ [30]. The BR simulations have been realized by Bourget [16] and Gauvin-Tremblay and Dumas [6].

Table 2 provides a summary of the general numerical setups for the two types of simplified turbine simulations and the reference BR simulations.

The EPTM simulations are conducted with the steady-state solver while the ALM and BR simulations are non-stationary with time advancing using a second-order implicit scheme. The time discretization corresponds to 1,000 time steps per turbine revolution period for unsteady simulations. (U)RANS approaches are applied to account for the turbulence with either the k-ω SST or the Spalart-Allmaras model.

Three turbine configuration scenarios are considered in this work: #1 single turbine, #2 tandem array, and #3 triangular cluster,

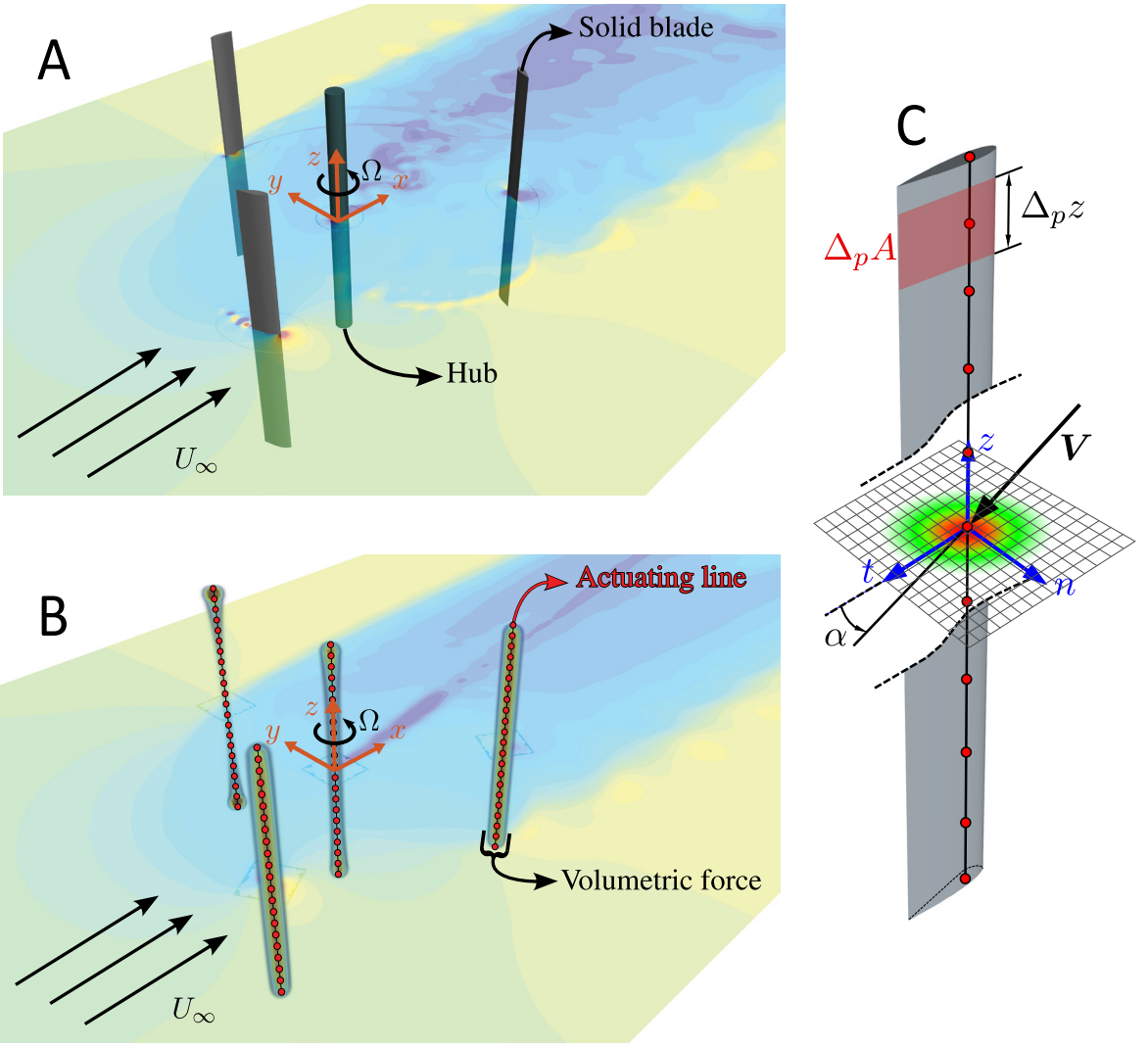

Figure 4: Comparison of (a) the actual blades of the Cross-Flow Turbine (CFT) and (b) the Actuator Line Method (ALM) representation via volume rendering of the actuating forces. The actuator line concept of a single blade is shown in (c), with the control points (in red), their associated coordinate frame (in blue), as well as the actuating force contour on a plane section passing a control point.

Table 2: Summary of numerical setups for the three types of simulations. SST = Shear Stress Transport. SIMPLE = Semi-Implicit Method for Pressure-Linked Equations.

	EPTM	ALM	BR
Solver			
Time advancement	Steady-state	Second-order implicit unsteady (1,000 steps/cycle)	
Pressure-velocity coupling	Segregated SIMPLE	Coupled	Segregated SIMPLE
Turbulence model	RANS k-ω SST	URANS Spalart-Allmaras	URANS k-ω SST
Boundary conditions			
Inlet	Uniform velocity: U_∞ Uniform low turbulence: • $\nu_t/\nu = 10$, $I = 1\%$ for k-ω SST (EPTM and BR) • $\nu_t/\nu = 0.2$ for Spalart-Allmaras (ALM)		
Outlet	Uniform static pressure: $p = 0$		
Lateral	Symmetry plane		

as illustrated in Figure 5. The computational domains are in the shape of a rectangular channel, extending at least $10D$ upstream and $15D$ downstream of the turbine (or turbine array). For the single turbine and tandem array scenarios, the cross section of the channel has the same aspect ratio as that of the turbine. The channel width is doubled for the triangular cluster scenario. The blockage ratio (see Equation (2)) based on the frontal area of one turbine for scenarios #1 and #2 and on the frontal area of two turbines for scenario #3, is always maintained at 20% in all cases. Constant and uniform inflow with low turbulence level is specified at the inlet boundary and a zero static pressure is imposed at the outlet boundary. The lateral boundaries are simplified as symmetry planes.

The overset mesh approach supported by Star-CCM+ is used here. The background channel and the inner domains, which contain the actuating regions or the rotor geometry, are meshed separately using hexahedral or polyhedral cells (as shown in Figure 6). Overset mesh technique is applied to connect the background mesh and the meshes of the inner domains. The inner mesh cells are refined to about $0.01D$ in the vicinity of the actuating region of the EPTM and ALM, which are much finer around the BR rotor geometry ($\leq 0.0025D$ and $\leq 0.005D$ for the scenario #1 and #2, respectively) with boundary layers discretized to ensure $y^+ \sim 1$. The background mesh is progressively coarsened away from the turbine surrounding regions, but a resolution not coarser than $0.05D$ is maintained up to at least

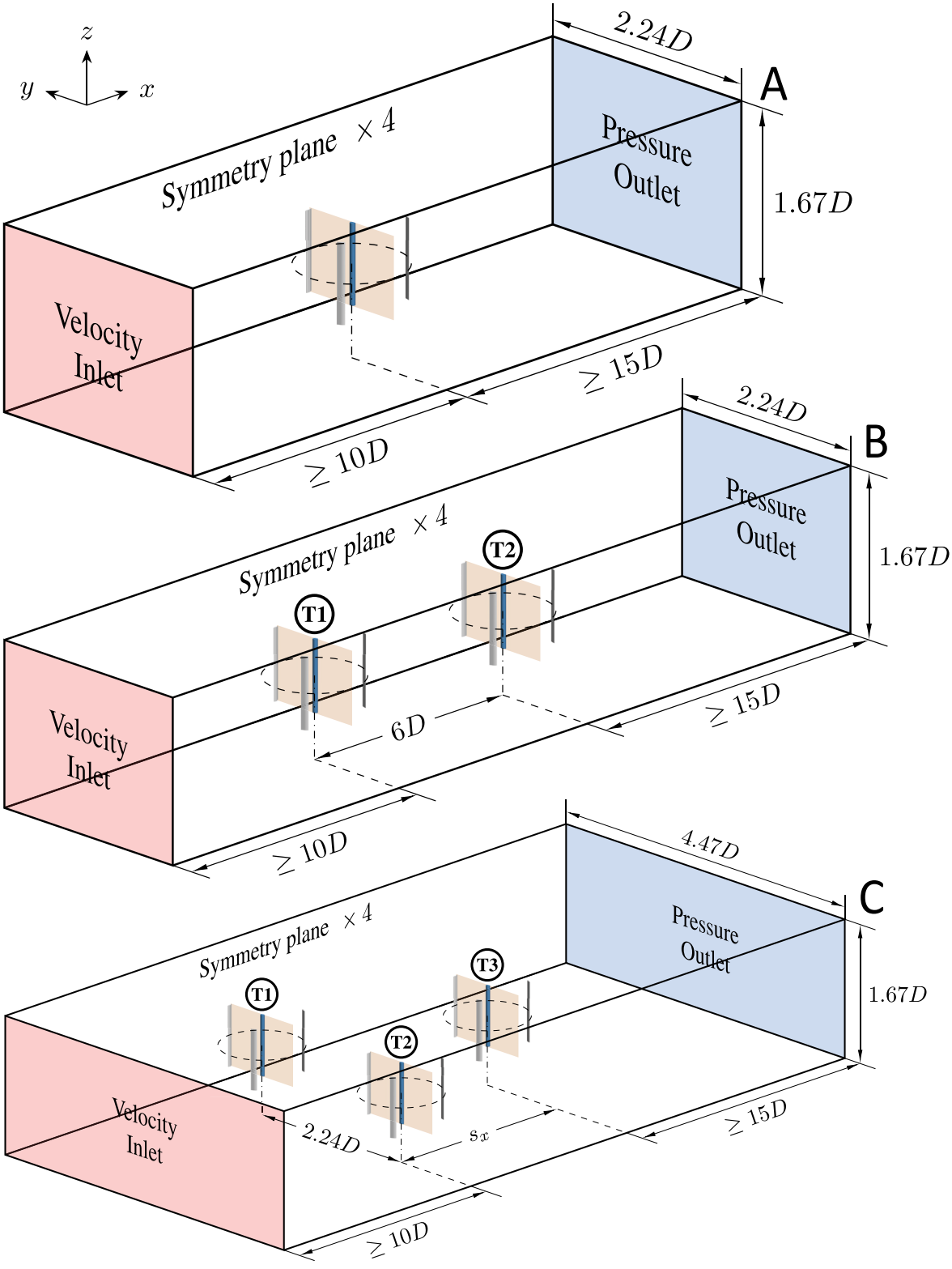

Figure 5: Geometry of the computational domain and boundary conditions for the three scenarios. The dimensions in the streamwise (x) direction are not drawn to scale for illustrative purposes. (a) Scenario #1 Single turbine. (b) Scenario #2 Tandem array. (c) Scenario #3 Triangular cluster.

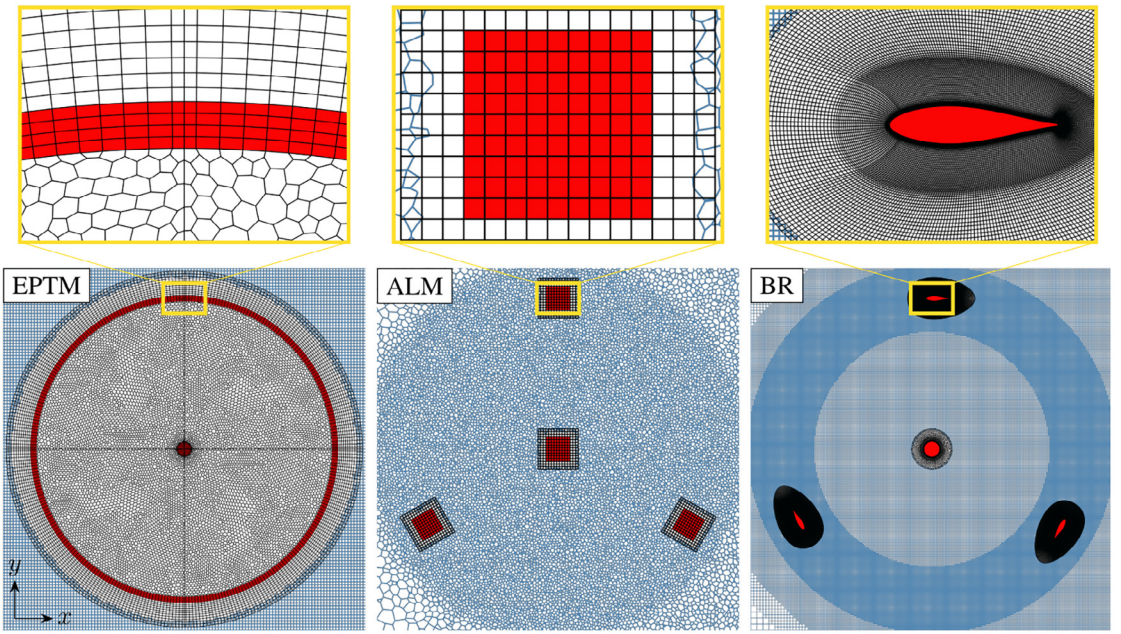

Figure 6: Illustration of the meshes around the turbine models on the mid-span horizontal plane section (at $z = 0$) for the three types of simulation. The background mesh is drawn in blue and the overset mesh is drawn in black. The actuating zones of the Effective Performance Turbine Model (EPTM) and Actuator Line Method (ALM) as well as the solid blades in the Blade-Resolved (BR) simulation are filled in red.

$7D$ downstream of the turbines to well capture the wake structures for all the simulations.

4. RESULTS AND DISCUSSION

In this section, the two simplified turbine models EPTM and ALM are compared in terms of the performance prediction, wake reproduction, and computational costs for the three investigated scenarios shown in Figure 5. High-fidelity BR simulation results are provided for the first two scenarios as reference for comparison. For the unsteady ALM and BR simulations, mean results are derived from time-averaging over at least three additional turbine revolution periods after statistical convergence, while the steady-state EPTM simulations give directly time-averaged predictions.

4.1 Scenario #1: Single Turbine

In this basic scenario, a single CFT operates in a confined environment with a blockage ratio of $B = 20\%$ (see Figure 5a).

The ALM and BR simulations are conducted at various tip-speed ratios (λ) to characterize the mean performances of the isolated turbine. The EPTM, by design, can only provide the predictions at the optimal operation point with maximum power extraction. The results are presented in Figure 7. The $\overline{C_P}$ curves (Figure 7a) show that a same optimal tip-speed ratio $\lambda_{opt} = 3$ is predicted by all the three approaches. The mean power coefficients estimated by the EPTM, which was constructed based on an unconfined BR simulation of that CFT, match well the value from the reference BR simulation carried out at the 20% confinement level. The ALM overpredicts the turbine power but within an acceptable margin (~15% in relative). As for the mean drag coefficient $\overline{C_x}$ (see Figure 7b), it is found that the three modelling approaches yield comparable

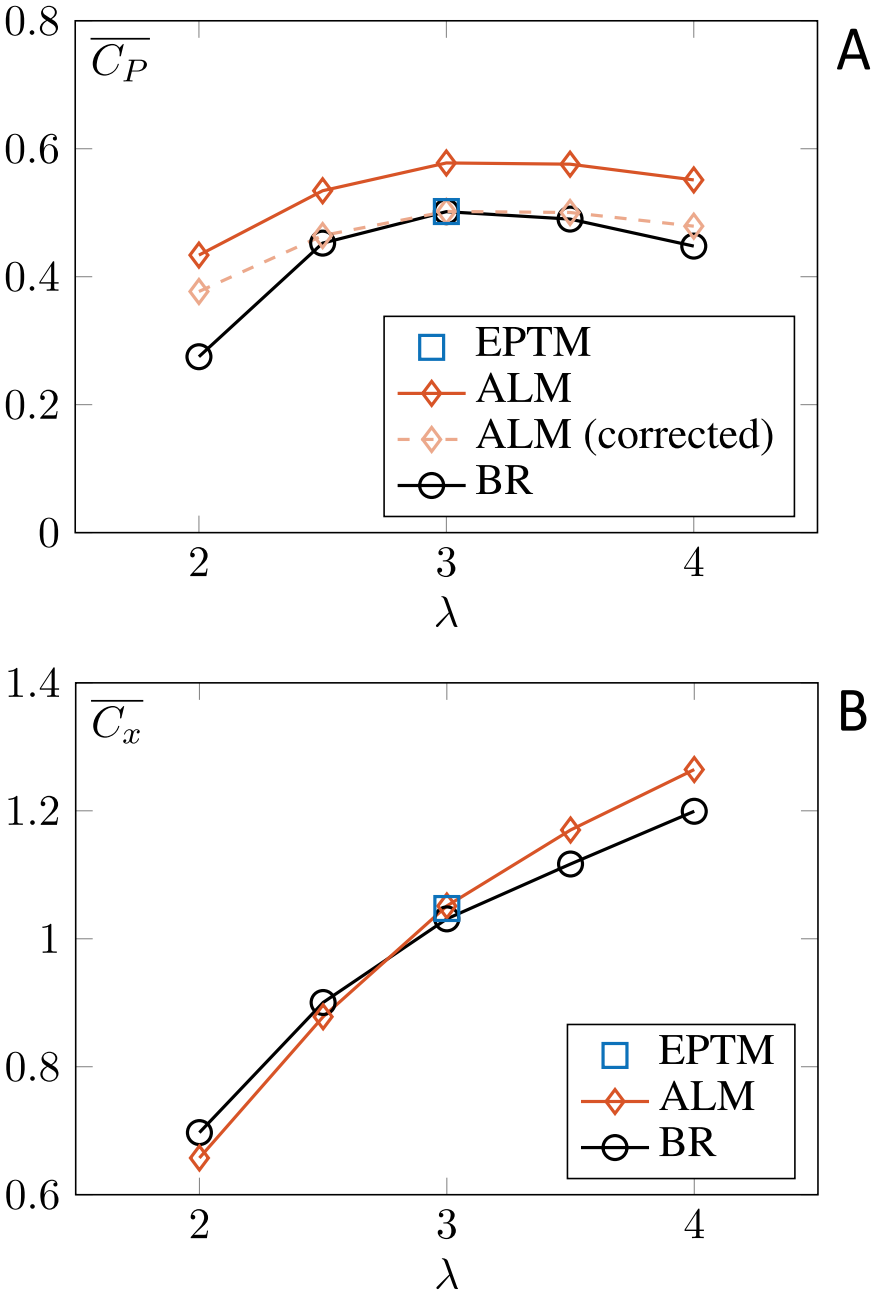

Figure 7: Mean performance curves of a single turbine at various tip-speed ratios (λ) under a fixed blockage ratio of B = 20%, predicted by different turbine modelling approaches. (a) Power coefficient. (b) Drag coefficient.

predictions with only a 2% relative difference at the optimal point, signifying that the EPTM and the ALM both exert a similar mean effect on the fluid in the streamwise direction as the BR turbine does.

The overprediction of $\overline{C_P}$ with the ALM can be explained by its poor representation of tip vortices. Figure 8a shows that the overprediction of the instantaneous power coefficient C_P of one single blade occurs

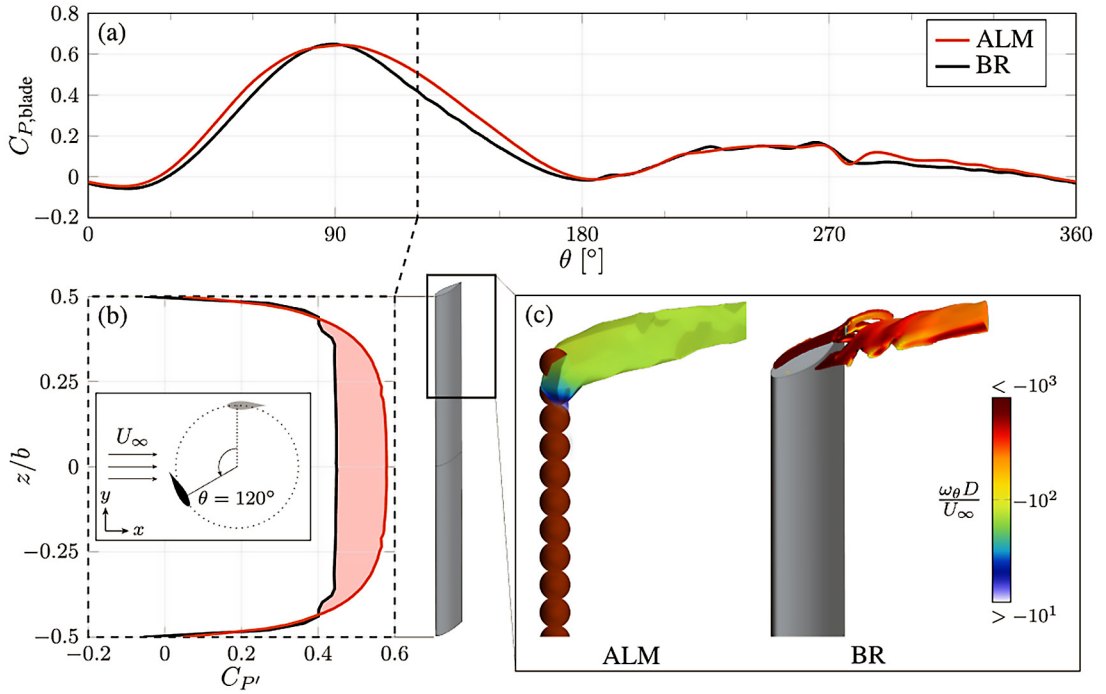

Figure 8: Graphical illustration for the overprediction of the power with the ALM. (a) Evolution of C_P of one blade over a turbine revolution. (b) Spanwise distribution of the section power coefficient ($C_{P'}$) along a blade at $\theta = 120°$. (c) Isosurface of the Q-criterion coloured with tangential vorticity (ω_θ), representing the tip vortex generated by the Blade-Resolved (BR) and Actuator Line Method (ALM) turbines.

mainly in the upstream phase of rotation (θ ϵ [0°, 180°]), especially around the angular position $\theta = 120°$. At such positions, the ALM overpredicts the spanwise distribution of the blade's section power coefficient $C_{P'}$ mostly at the mid-span region of the blade, which is highlighted with red shaded area in Figure 8b. These discrepancies are related to 3D aerodynamic effects, which are revealed through the comparison of the tip vortices shown in Figure 8c. The tip vortex generated by the ALM exhibits a larger core with significantly lower vorticity than that in the BR simulation. This leads to a reduced downwash along the blade span, a phenomenon also reported by Breault et al. [31]. With a weaker downwash induced by the ALM's tip vortices, abnormally larger effective angles of attack (α) are perceived around the mid-span. As a result, the tangential force on the blade generated by the lift-drag combination (and therefore C_P) is overestimated. This occurs because the volumetric forces implemented in the fluid domain extend beyond the actual blade thickness (i.e., a larger force spreading). As mentioned in Breault et al. [31], using a smaller spreading of the volumetric forces in the thickness direction of the blade could generate stronger tip vortices. This would involve unsymmetric Gaussian smoothing of the applied volumetric forces. This is out of the scope of the present work and has been rejected.

This issue does not arise with the EPTM since it is constructed using global turbine performance metrics extracted from a representative BR simulation. Considering that the ALM's overprediction of power is considered to be systematic, a simple ad hoc

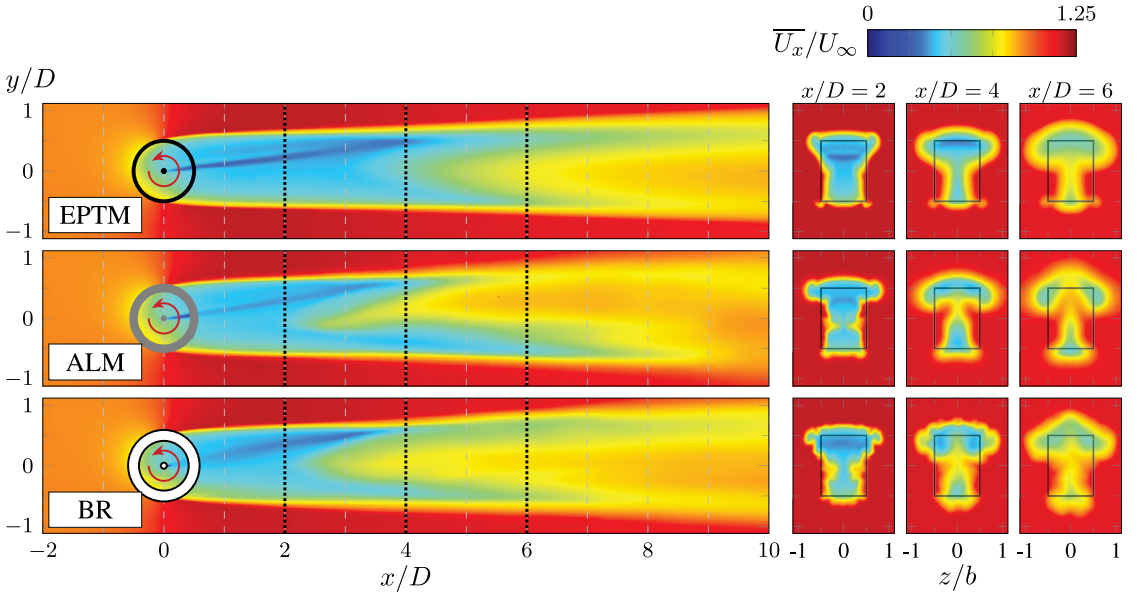

Figure 9: Comparison of the mean wake for the single turbine scenario (#1) generated by the three turbine modelling approaches through contours of mean streamwise velocity from a top view on the mid-span plane section (left) and a cross-section view at x/D = 2, 4, and 6 (right). Rectangles on the cross-section view represent the projection of the turbine extraction plane on the cross section.

correction is proposed based on the relative difference in the maximum mean power of the isolated turbine (at $\lambda_{opt} = 3$) between the ALM and the BR simulations:

$$\left(\overline{C_P}\right)_{\text{ALM}}^{\text{corr}} = \frac{\left(\overline{C_P}\right)_{\text{opt, BR}}}{\left(\overline{C_P}\right)_{\text{opt, ALM}}} \cdot \left(\overline{C_P}\right)_{\text{ALM}}$$

$$\approx 0.87\left(\overline{C_P}\right)_{\text{ALM}}. \quad (8)$$

The corrected $\overline{C_P}$ curve of the ALM shows improved agreement with the curve derived from the BR simulations, as shown in Figure 7a. This ad hoc correction will be systematically used for all the ALM power predictions in this work.

In addition to the performance prediction, the wake reproduction is also a key capability of a turbine model, which may affect significantly the performance prediction accuracy for downstream turbines in array deployments. Figure 9 compares the mean wake generated by the EPTM and the ALM with that of the reference BR simulation through mean streamwise velocity contours, confirming that the characteristic wake topology is reasonably well reproduced by both simplified models. The wakes are all found to be deflected transversely toward the positive y direction (i.e., toward the upper part of rotation ($\theta \in$ [-90˚, 90˚])) and contracted in the spanwise (z) direction, forming a similar T-shaped deficit viewed on downstream cross-section planes. The rapidly recovered centre zone, observed from 2D downstream of the ALM and BR rotors, but only from 4D downstream of the EPTM, is effectively attributed to this wake deformation. In fact, it has been previously proved by Boudreau and Dumas [32] that the convection of the mean flow contributes predominantly to the wake recovery along the centreline.

Wake recovery could be globally estimated with the space-averaged mean streamwise velocity on successive wake plane sections,

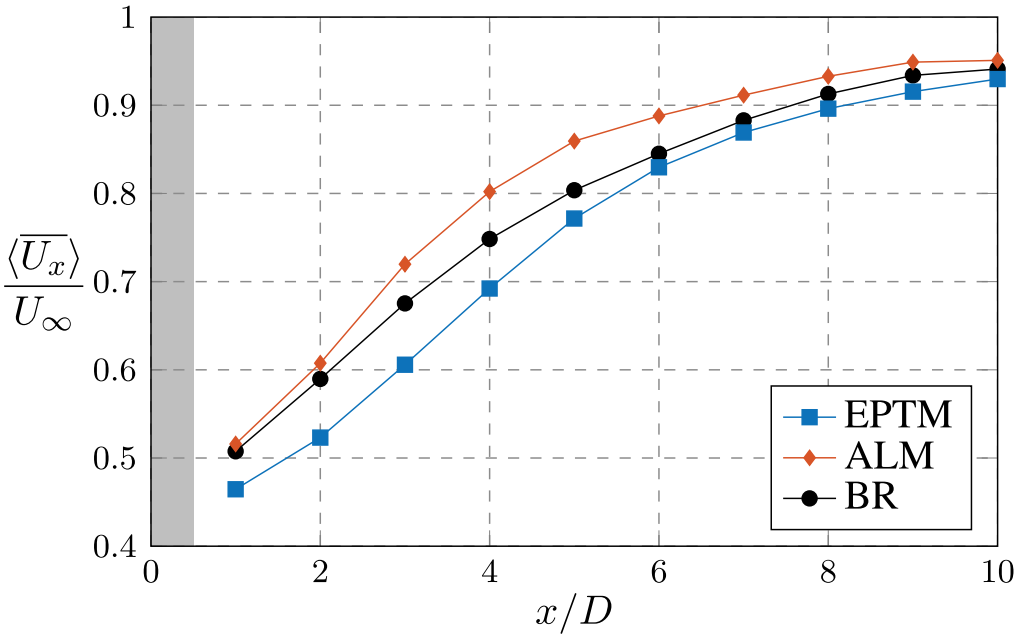

Figure 10: Streamwise evolution of the section-averaged mean streamwise velocity in the wake of the Effective Performance Turbine Model (EPTM), Actuator Line Method (ALM), and Blade-Resolved (BR) rotors. The streamwise extent of the turbine sweeping region is shaded in grey.

which are aligned with the turbine extraction plane and geometrically identical. This section-averaging operation is denoted by angle brackets (‹·›). As shown in Figure 10, the ALM's mean wake shares comparable recovery rate with that of the BR rotor in the near-wake region ($0 < x/D < 3$), owing to the correctly predicted spanwise contraction, which itself is induced by the blade's tip vortices. Its overly rapid recovery around $4D$ – $5D$ downstream is supposed to be attributed to the overpredicted transverse convection toward $+y$.

The EPTM wake shows slower recovery in the near-wake region due to a spanwise contraction less pronounced. Nonetheless, in the far-wake zone ($x/D > 6$), which exhibits higher potential for downstream aligned turbine deployment, the mean wake profiles regenerated by the two simplified approaches match well that of the BR turbine, with a relative difference in $\langle\overline{U_x}\rangle$ lower than 5% for the ALM and 2% for the EPTM.

4.2 Scenario #2: Tandem Array

In the tandem scenario, a second turbine (T2) is placed $6D$ downstream of the first turbine (T1), as illustrated in Figure 5b. The domain retains the same cross section as in scenario #1; thus, the blockage ratio of the two turbines remains $B = 20\%$.

As the longitudinal spacing between the turbines is sufficiently large, it is reasonable to assume that the ambient flow conditions of the upstream turbine T1 are unaffected by the turbine T2. With the same blockage ratio and inflow conditions as in the single turbine scenario, it is expected that the optimal tip-speed ratio of the T1 is unchanged (i.e., $\lambda_{\mathrm{opt,T1}} = 3$). However, as the turbine T2 operates in the T1's wake flow, which is not fully recovered, its inflow should be slower than the reference velocity U_∞, and thus $\lambda_{\mathrm{opt,T2}}$ is anticipated to be lower than 3. Through manual tuning in the BR simulation, it was

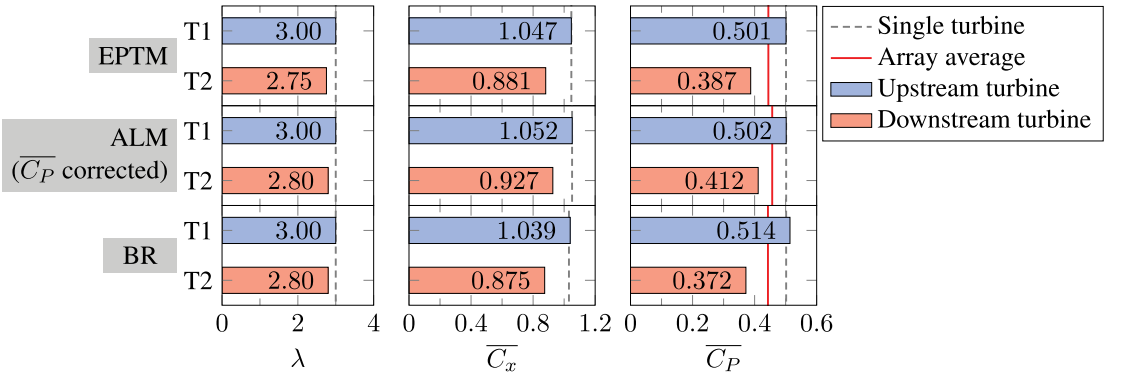

Figure 11: Mean performance prediction for each turbine in the tandem array scenario (#2) from different turbine modelling approaches. For the Actuator Line Method (ALM) simulation, the power correction (Equation (8)) is applied. The grey dashed lines represent the performances of the single turbine (scenario #1) as reference. The red solid lines indicate the mean power coefficient averaged across the array.

indeed confirmed in a previous study that $\lambda_{opt,T2} = 2.8$ [6]. These values of $\lambda_{opt,T1}$ and $\lambda_{opt,T2}$ were prescribed for the BR and ALM simulations, which align well with the optimal tip-speed ratios auto-detected by the EPTM ($\lambda_{opt,T1} = 3$ and $\lambda_{opt,T2} = 2.75$, see Figure 11).

Predictions of the mean drag and power coefficients within the array are presented in Figure 11 as well. For the upstream turbine T1, the mean drag and power coefficients remain unchanged compared to the values of the single turbine at its optimal operating point (see Figure 7), confirming the fact that the influence of T2 on T1 is negligible. One may observe minor discrepancies between the T1 and the single turbine in the BR simulations, which are probably attributed to the slight differences in mesh resolution adopted in the two scenarios #1 and #2.

The mean drag and power of the downstream turbine T2 are respectively reduced by 16% and 28% compared to T1, as predicted by the reference BR simulation, which is not surprising since T2 encounters the slower incoming flow from T1 with lowered momentum and power flux than the free stream. This trend is correctly reproduced by both simplified models (see Figure 11). The T2's actuating lines (i.e., the ALM blades), dynamically acting as real solid blades, perceive non-uniformly decelerated effective local freestream velocity V along the blade trajectory, and generate overall lower forces over the revolution (through Equations (6) and (7)), leading to a reduced power prediction. More precisely, as shown in Figure 12, the ALM predicts an instantaneous blade power reduction comparable to the BR prediction, occurring primarily in the upstream phase of rotation and with similar peak values, not exactly at the same moment in the cycle (at the angular position of 90° for ALM and 105° for BR). By contrast, the EPTM works in a more averaged but robust way: a lower effective velocity is computed on the T2's extraction plane ($V^*_{T2} < V^*_{T1}$), yielding consistently decreased value of forces and power. The differences in the performance prediction across the three approaches are found to be greater for T2 than for T1, which is caused by the discrepancy in upstream wake reproduction. The EPTM and the ALM overpredicts the drag of T2 by 0.8% and 6%, and the power by 4% and 11%, respectively,

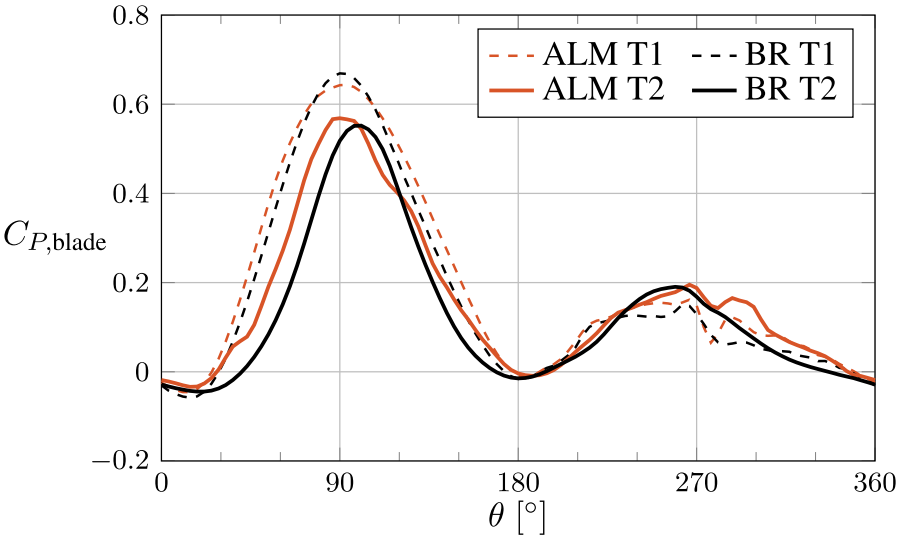

Figure 12: Evolution of C_P of one blade for both turbines in the tandem array scenario (#2), predicted by both unsteady turbine modelling approaches Actuator Line Method (ALM) and Blade-Resolved (BR).

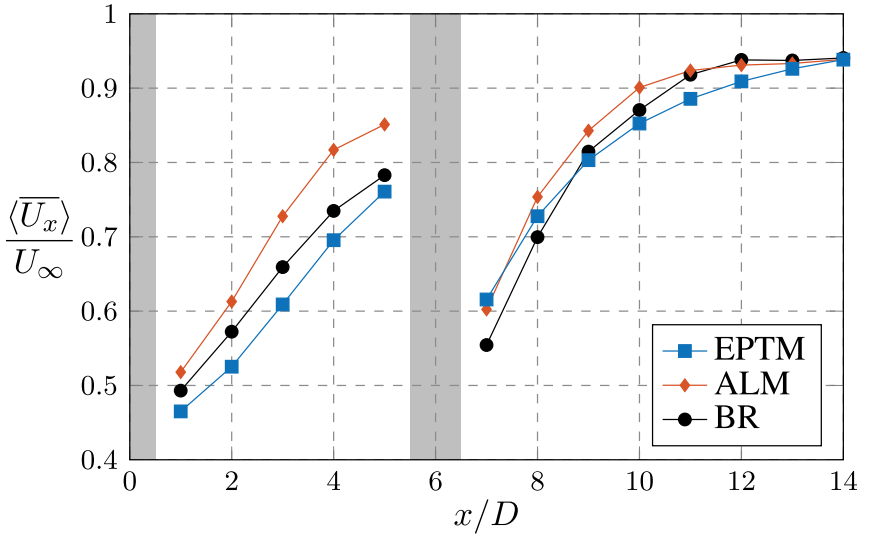

Figure 13: Streamwise evolution of the section-averaged mean streamwise velocity for the tandem array scenario (#2) predicted by the three turbine models. The shaded zones correspond to the streamwise extent occupied by the rotors.

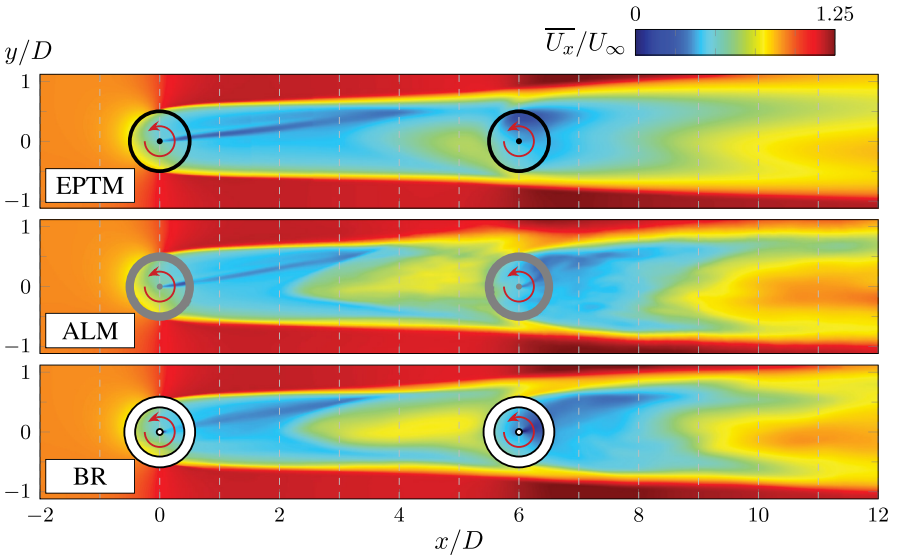

Figure 14: Comparison of the mean wake for the tandem array scenario (#2) generated by the three turbine modelling approaches through contours of mean streamwise velocity on the mid-span plane section.

compared to the BR simulation. Nonetheless, the performance predictions of the simplified models can still be considered consistent to the reference values obtained in the BR simulation, falling into acceptable difference ranges.

Figure 13 and Figure 14 compare the wake recovery for the three simulations of scenario #2. It is found that the T1's wake, almost unaffected by the T2 up to 1D upstream of T2 (i.e., $x/D \leq 5$), shows discrepancies among the three approaches as was noticed for the single turbine (see Section 4.1), which strongly affect the performance prediction accuracy for T2. In fact, the overprediction of power (after correction) of the ALM T2 is related to the excessively recovered upstream wake. Moreover, the fact that the upstream wake recovering centre of the ALM rotor is more toward the positive y direction than that of the BR rotor (as illustrated in the right panels of Figure 9 for $x/D = 4$ and 6) explains the prediction difference for the angular position of the blade extraction peak viewed in Figure 12. Conversely, even with an underestimated inflow velocity, the EPTM overpredicts slightly the power for T2. This arises from the large non-uniformity of the incoming flow in this case, since the EPTM is developed from a single turbine operating in uniform flow, not accounting for the turbine power reduction in wake flows. From another perspective, the EPTM may perform better in other array configurations where one would want to avoid severely sheared inflow for the downstream turbines. The T2's mean wake regenerated by the two simplified models resembles quite closely the mean wake of the BR rotor (see Figure 13 and Figure 14), meaning that the performance prediction accuracy would be good for hypothetic turbines deployed further downstream in the wake.

4.3 Scenario #3: Triangular Cluster

The third scenario consists of three turbines configured into a triangular (staggered) cluster. As illustrated in Figure 5c, two counter-rotating turbines (T1 and T2) are placed side by side with a lateral spacing of 2.24D at $x/D = 0$ into a channel maintaining a constant blockage ratio of 20%. Another turbine (T3) is positioned downstream along the midline between the upstream turbines. Configurations with various longitudinal spacings (s_x) from 1.2D to 6D and two rotation patterns (named "inward" and "outward," as illustrated in Figure 15) are tested using the EPTM. With lateral symmetric planes present, these configurations are practically equivalent to two-row arrays of infinite width, where side-by-side turbines rotate in alternating directions. ALM simulations are conducted only for the best and worst cases predicted by the EPTM simulations (i.e., with the highest and lowest average power extraction). However, high-fidelity BR simulations are not conducted in this triangular cluster scenario since it becomes too expensive.

As expected, the EPTM predicts always an optimal tip-speed ratio close to 3 for the upstream turbines T1 and T2 since their inflow and blockage conditions remain unchanged compared to scenario #1. Larger optimal tip-speed ratios are predicted for T3, with $\lambda_{opt,T3}$ ranging from 3.15 to 3.25 depending on turbine arrangements.

As shown in Figure 16, the EPTM predicts a decreasing trend in the mean power extraction with increasing longitudinal spacing; however,

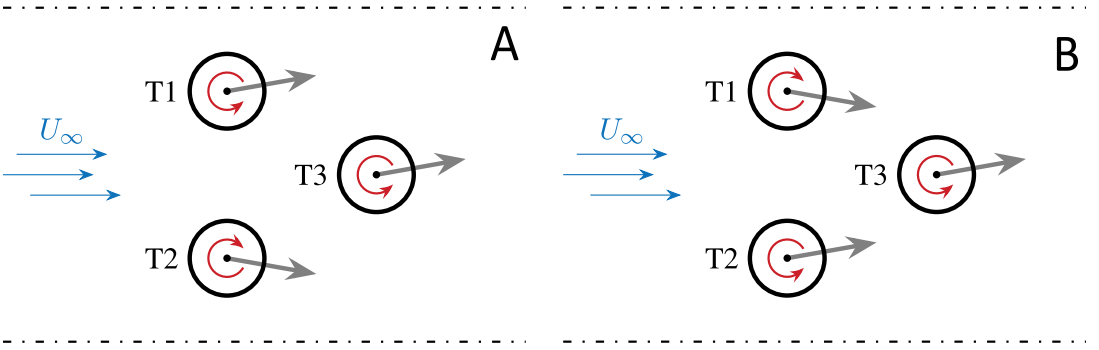

Figure 15: Test configurations of turbine rotation direction in triangular clusters illustrated from top view by red arrows. The grey arrows indicate the anticipated wake deflection direction of each turbine. (a) Inward rotation. (b) Outward rotation.

the cluster average is always higher than the single turbine's mean power. This array performance improvement is attributed to the accelerated bypass flow between the turbines T1 and T2 hitting the turbine T3. In these test configurations, T3 extracts about 10% – 25% more power than the average of the upstream turbines, while the average power production of the upstream row remains quite close to that of the single turbine. The impact of the rotation direction is limited in this case. For the most compact configurations, the inward-rotating upstream turbines produce more power than the outward-rotating ones, whereas this effect diminishes when s_x exceeds $2D$.

For configurations with $s_x/D > 4$, upstream turbines rotating outward (with upstream wakes defecting inward) are more detrimental to T3's power extraction. These above trends jointly determine the best- and worst-performing cases, i.e., the $s_x/D = 1.2$ configuration with inward rotation and the $s_x/D = 6$ configuration with outward rotation, respectively. The two cases are now investigated in more detail and compared with the ALM simulations.

The most pronounced discrepancy between the two cases lies in the performance of the downstream turbine T3. The ALM's power predictions are quite consistent to those of the EPTM (about 1% of difference), except for the downstream turbine T3 in the worst case (9% of difference), as presented in the right panels of Figure 17.

In the best cases, T3 benefits from the accelerated bypass flow between the upstream turbines, resulting in a notably enhanced mean power $\overline{C_{P,\mathrm{T3}}}$ (+25 relative to the single turbine scenario, as predicted by both EPTM and ALM). As predicted by the ALM, the benefit to the blade instantaneous power extraction occurs mainly in the upstream phase of rotation, while the effect on the downstream phase is quite limited (see Figure 18).

In the worst case, the EPTM predicts a much less increase in $\overline{C_{P,\mathrm{T3}}}$ (+13%), whereas the ALM predicts that there is only a small gain of 3% for T3. For one thing, this reduced gain for T3 results from the gradually decelerated bypass flow with the reenergization of the upstream wakes, which explains also the power reduction of T3 with increasing longitudinal spacing as observed in Figure 16. This is further supported by the observation in Figure 18 that the maximum $C_{P,\mathrm{blade}}$ in the worst case, while lower than that in the best case, still exceeds that of

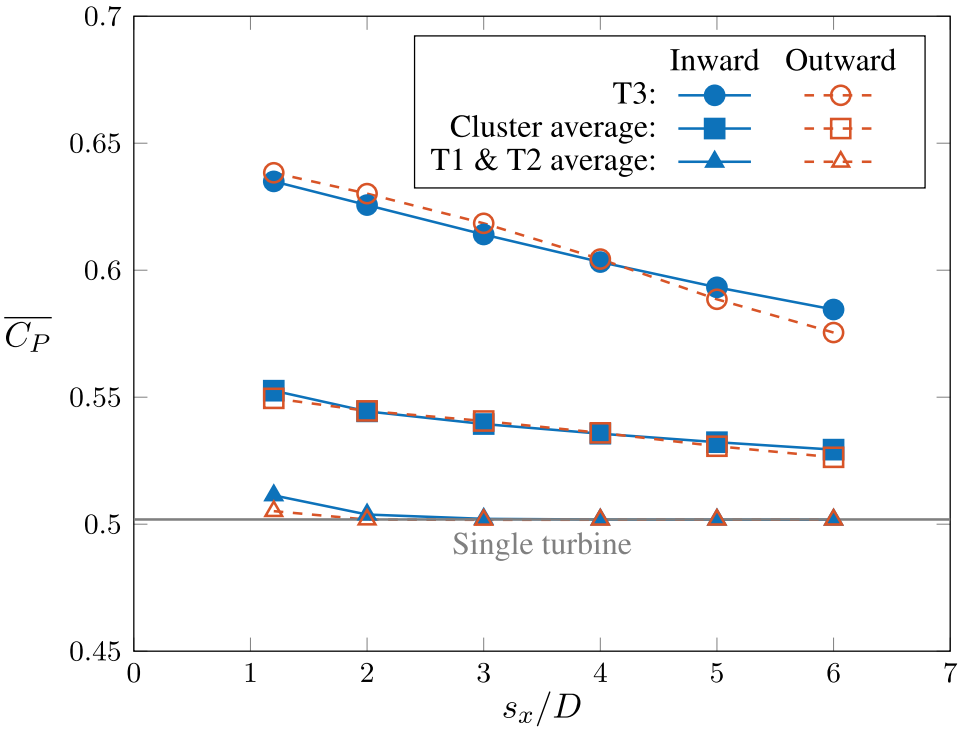

Figure 16: Mean power coefficient $\overline{C_P}$ for the triangular cluster with different longitudinal spacing s_x and rotation patterns, as predicted by the Effective Performance Turbine Model (EPTM).

a single turbine, as predicted by the ALM. For another, in the worst case, due to the inward deflection of the upstream wakes, the velocity deficit penetrates the T3's extraction region (as viewed on the left panels of Figure 17b for both the EPTM and ALM), causing notable wake-turbine interaction and performance degradation for T3, which is also revealed by a decrease in instantaneous power extracted by the single blade around $\theta = 45^\circ$ and 150° (see Figure 18); by contrast, this detrimental effect is well avoided in the best case. The discrepancy between the two approaches in the power prediction of T3 is not such a surprise since the ALM's wake is more diffused, resulting in a slower bypass and a stronger penetration of velocity deficit into the T3's extraction region.

Moreover, minor differences are noted for the two upstream turbines in the compact cluster (best case) compared to the single turbine scenario, which may be marginal for array deployment studies yet meaningful for the purpose of model comparison. Firstly, the upstream turbines, on average, extract 2% more power than the single turbine. Since T3 is placed downstream between the two upstream turbines at a sufficiently short distance, the blockage effect of the upstream row is effectively enhanced by the presence of the closely placed downstream row. Secondly, both EPTM and ALM predict that T1 extracts 6% less power than T2 in the best (compact) configuration, which is caused by the asymmetric upstream deceleration (visible right upstream of T3 in Figure 17 (left)) induced by T3.

In brief, the two simplified turbine models are not only able to predict similar trends in the mean power variation across the clusters in a

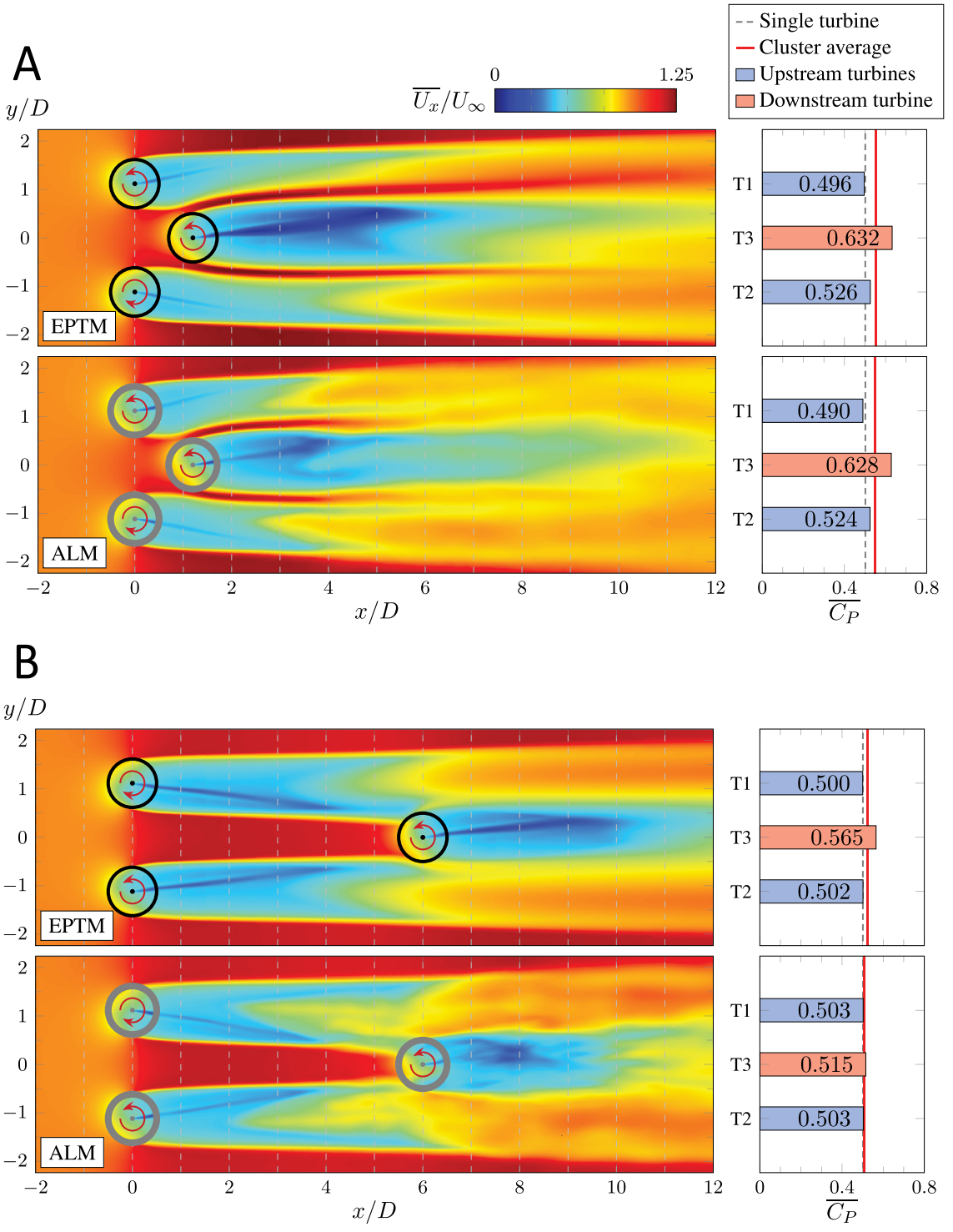

Figure 17: Comparison of the mean wake produced (top) and the mean power prediction (bottom) of the Effective Performance Turbine Model (EPTM) versus Actuator Line Method (ALM) for the two triangular clusters with the best and worst performances. Mean streamwise velocity are shown on the mid-span plane section. (a) Best case: s_x/D = 1.2, inward rotation. (b) Worst case: s_x/D = 6, outward rotation.

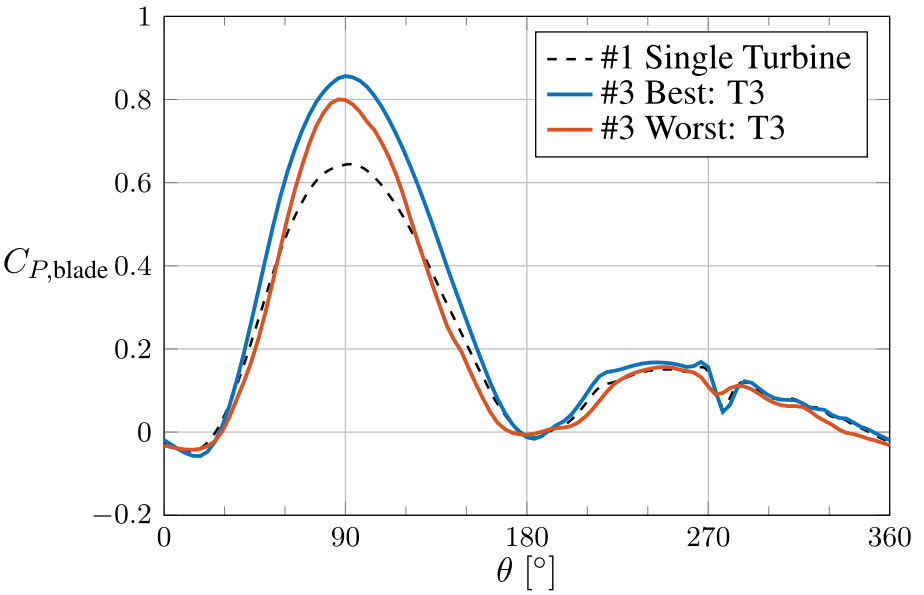

Figure 18: Evolution of C_P of one blade for the downstream turbine T3 in the triangular array scenario (#3), in comparison to the single turbine scenario (#1).

simple manner, but can also reproduce consistent flow phenomena and effects (even minor ones) associated with these observed trends.

4.4 Computational Costs

A comparison of the computational costs required by the three turbine modelling approaches is provided in Figure 19. The EPTM and ALM simulations employ comparable mesh cell counts, roughly five million cells per turbine, which is of the order of 10^{-1} of that used in the BR simulations. However, since the EPTM is a steady-state model, which does not require temporal marching nor time statistics for mean turbine performance, its has always the lowest Central Processing Unit (CPU) time requirement among the three methods. The CPU hour consumption of the EPTM grows with the cell count and also with the complexity of interactions within the turbine array which may require more iterations to converge. For comparison purposes, the CPU time requirements of the two unsteady methods ALM and BR shown in Figure 19 are estimated according to a conservative scenario. It is supposed that a minimum of ten turbine cycles discretized with 360 steps/cycle and five final cycles in 1,000 steps/cycle are required for the single turbine scenario (#1) and the compact triangular cluster (#3 best). Ten more coarsely discretized cycles are required before the final cycles for the tandem array scenario (#2) and the extended triangular cluster (#3 worst) so that the wake from the upstream turbines could be effectively transported to the turbine located far downstream. The ALM consumes on average about 2×10^4 CPU hours per turbine, equivalent to five days of computation on a 192-core compute node, being approximately 1,000 times more than the EPTM demand; nonetheless, the ALM is still about five times faster than the high-fidelity BR simulation.

5. CONCLUSION

This study presented a comparative assessment of two simplified turbine models

(EPTM and ALM) tailored for CFTs. Their performance prediction, wake reproduction, and computational costs were evaluated with three deployment scenarios to determine each model's suitability for turbine farm simulations.

The EPTM was shown to accurately predict the performance of each scenario, with the only minor discrepancy being a slower wake recovery in the near wake, as demonstrated by comparisons with blade-resolved results for the first two scenarios. The main advantage of this method lies in its low computational costs. In fact, it is considerably more cost-effective: $\sim 10^3$ times less CPU hours than the ALM simulations, making it an efficient alternative to unsteady models and ideally suited for large-scale turbine farm simulations. Indeed, this model could be applied to farms with more than 20 turbines while maintaining excellent accuracy in the predicted results.

The ALM was shown to effectively reproduce the overall performance trends and the wake due to its unsteady modelling approach. A systematic correction based on the relative difference in the mean power coefficient of the single turbine scenario was developed to mitigate the overprediction of the C_P. This correction notably enhanced the predictive capability of the ALM. However, the corrected ALM still exhibited a slight overprediction compared with the EPTM, particularly for the downstream turbine in tandem configuration, due to the ALM faster wake recovery. In future work, such a correction could be derived from the flow physics observed in BR simulations (e.g., increased downwash from tip vortices). With this adjustment applied to its performance prediction, the ALM becomes more suitable for simulating small and compact turbine clusters (involving fewer than five turbines to maintain a reasonable computational cost) where near-wake interactions are strong and unsteady effects important.

Future work could focus on comparing and analyzing the models in the context of resource-turbine interactions by modifying the channel bed topography, including a free-surface model, and varying the flow turbulence level to assess the models under more realistic conditions representative of a river or tidal environments.

ACKNOWLEDGMENT

The authors thank the Digital Research Alliance of Canada for providing computational resources, as well as their colleagues at the LMFN especially Sébastian Bourget and Olivier Gauvin-Tremblay, Professor G. Winckelmans of Université catholique de Louvain, and Mr. J. Huang of Natural Resources Canada for all the fruitful discussions.

Authors' Declaration

- Funding: Financial support from the Natural Sciences and Engineering Research Council of Canada (NSERC Discovery Grant No. RGPIN-2024-06374; CGRS M Scholarship) and the Fonds de recherche du Québec (FRQNT BRE Scholarship) is gratefully acknowledged.
- Ethical approval: This paper does not contain any studies with human participants or animals.
- Competing interests: The authors declare that there are no competing interests.
- Availability of data and materials: Datasets used and/or analyzed during the current

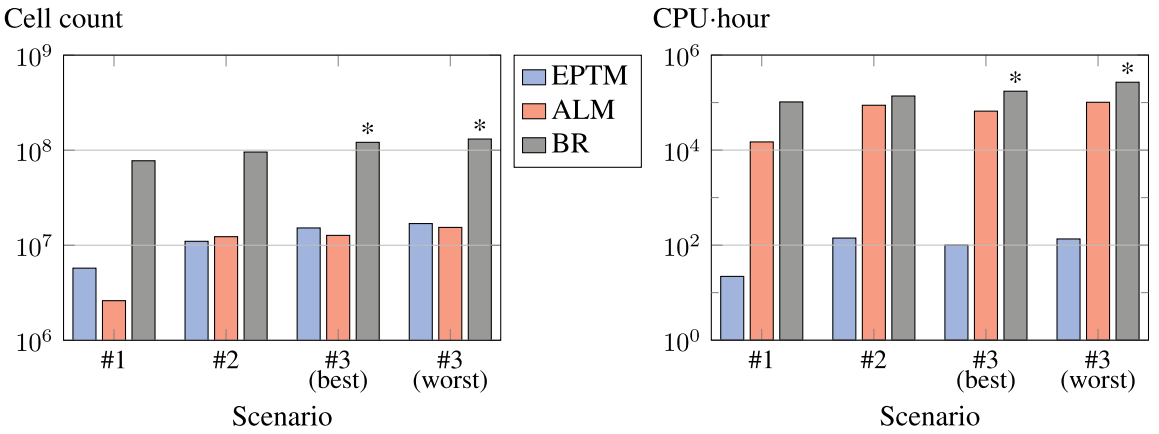

Figure 19: Comparison of the computational costs required by each turbine modelling approaches in terms of mesh cell count (top) and Central Processing Unit (CPU) time (bottom). Cases marked with an asterisk (*) were not performed; the corresponding costs are roughly estimated based on other cases.

study are available from the corresponding author upon reasonable request.

- Artificial intelligence: During the preparation of this work the authors used the ChatGPT tool as a writing assistant, particularly for translation, paraphrasing, as well as spelling and grammar correction. After using this tool, the authors reviewed and edited the content as needed and take full responsibility for the content of the publication.

REFERENCES

[1] I. Paraschivoiu, *Wind Turbine Design: With Emphasis on Darrieus Concept*. Montréal, QC, Canada: Polytechnic International Press, 2002.

[2] D. De Tavernier, C. Ferreira and A. Goude, "Vertical-axis wind turbine aerodynamics," in *Handbook of Wind Energy Aerodynamics*, Cham, Switzerland: Springer Nature, 2022, pp. 1-45.

[3] J. O. Dabiri, "Potential order-of-magnitude enhancement of wind farm power density via counter-rotating vertical-axis wind turbine arrays," *Journal of Renewable and Sustainable Energy*, vol. 3, p. 043104, 2011. doi: 10.1063/1.3608170.

[4] T. Nishino and R. H. Willden, "Two-scale dynamics of flow past a partial cross-stream array of tidal turbines," *Journal of Fluid Mechanics*, vol. 730, pp. 220-244, 2013. doi: 10.1017/jfm.2013.340.

[5] O. Gauvin-Tremblay and G. Dumas, "Hydrokinetic turbine array analysis and optimization integrating blockage effects and turbine-wake interactions," *Renewable Energy*, vol. 181, pp. 851-869, Jan. 2022. doi: 10.1016/j.renene.2021.09.003.

[6] O. Gauvin-Tremblay and G. Dumas, "A numerical study on the interaction between two cross-flow turbines in tandem configuration to support a simplified turbine model approach," *Journal of Renewable and Sustainable Energy*, vol. 12, no. 5, p. 054502, Sep. 2020. doi: 10.1063/5.0018237.

[7] S. Draper and T. Nishino, "Centred and staggered arrangements of tidal turbines," *Journal of Fluid Mechanics*, vol. 739, no. 1, pp. 72-93, Mar. 2014. doi: 10.1017/jfm.2013.593.

[8] T. Kinsey and G. Dumas, "Impact of channel blockage on the performance of axial and cross-flow hydrokinetic turbines," *Renewable Energy*, vol. 103, pp. 239-254, Apr. 2017. doi: 10.1016/j.renene.2016.11.021.

[9] J. I. Whelan, J. M. R. Graham and J. Peiró, "A free-surface and blockage correction for tidal turbines," *Journal of Fluid Mechanics*, vol. 624, pp. 281-291, Apr. 2009. doi: 10.1017/S0022112009005916.

[10] L. Kuang, H. Lei, D. Zhou, Z. Han, Y. Bao and Y. Zhao, "Numerical Investigation of Effects of Turbulence Intensity on Aerodynamic Performance for Straight-Bladed Vertical-Axis Wind Turbine," *Journal of Energy Engineering*, vol. 147, no. 1, p. 04020087, Feb. 2021. doi: 10.1061/(ASCE)EY.1943-7897.0000740.

[11] A. Talamalek, M. C. Runacres and T. De Troyer, "Effect of Free-Stream Turbulence on the Power Performance and Wake Characteristics of Paired Counter-Rotating Vertical-Axis Wind Turbines," *Wind Energy*, vol. 28, no. 2, pp. 1-25, Feb. 2025. doi: 10.1002/we.2968.

[12] J. Thiébot, N. Guillou, S. Guillou, A. Good and M. Lewis, "Wake field study of tidal turbines under realistic flow conditions," *Renewable Energy*, vol. 151, pp. 1196-1208, May 2020. doi: 10.1016/j.renene.2019.11.129.

[13] T. Villeneuve, M. Boudreau and G. Dumas,

"Improving the efficiency and the wake recovery rate of vertical-axis turbines using detached end-plates," *Renewable Energy*, vol. 150, pp. 31-45, May 2020. doi: 10.1016/j.renene.2019.12.088.

[14] T. Villeneuve, G. Winckelmans and G. Dumas, "Increasing the efficiency of vertical-axis turbines through improved blade support structures," *Renewable Energy*, vol. 169, pp. 1386-1401, May 2021. doi: 10.1016/j.renene.2021.01.092.

[15] R. Gosselin, "Analysis and optimization of vertical axis turbines," PhD thesis, Department of Mechanical and Industrial Engineering, Université Laval, Québec City, QC, Canada, 2015.

[16] S. Bourget, "Development and assessment of a modeling method for hydrokinetic turbines operating in arrays," M.Sc. thesis, Department of Mechanical and Industrial Engineering, Université Laval, Québec City, QC, Canada, 2018. [Online]. Available: https://hdl.handle.net/20.500.11794/31588

[17] P. Rochefort, "Modélisation aéro-hydrodynamique de turbines à axe vertical H-Darrieus (VAT) par la méthode des lignes actuatrices (ALM) et caractérisation des effets de courbure," M.Sc. thesis, Department of Mechanical and Industrial Engineering, Université Laval, Québec City, QC, Canada, 2025. [Online]. Available: https://hdl.handle.net/20.500.11794/178663

[18] S. Bourget, O. Gauvin-Tremblay and G. Dumas, "Hydrokinetic turbine array modeling for performance analysis and deployment optimization," *Transactions of the Canadian Society for Mechanical Engineering*, vol. 42, no. 4, pp. 370-381, Jul. 2018. doi: 10.1139/tcsme-2017-0088.

[19] P. Bachant and M. Wosnik, "Effects of Reynolds Number on the Energy Conversion and Near-Wake Dynamics of a High Solidity Vertical-Axis Cross-Flow Turbine," *Energies*, vol. 9, no. 2, p. 73, Feb. 2016. doi: 10.3390/en9020073.

[20] O. Gauvin-Tremblay, "Modeling and optimizing hydrokinetic turbine arrays using numerical simulations," PhD thesis, Department of Mechanical and Industrial Engineering, Université Laval, Québec City, QC, Canada, 2021.

[21] R. Merabet and É. Laurendeau, "Hovering Helicopter Rotors Modeling Using the Actuator Line Method," *Journal of Aircraft*, vol. 59, no. 3, pp. 774-787, May 2022. doi: 10.2514/1.C036314.

[22] F. Trigaux, P. Chatelain and G. Winckelmans, "Investigation of blade flexibility effects on the loads and wake of a 15 MW wind turbine using a flexible actuator line method," *Wind Energy Science*, vol. 9, no. 8, pp. 1765-1789, Aug. 2024. doi: 10.5194/wes-9-1765-2024.

[23] R. J. Stevens, L. A. Martínez-Tossas and C. Meneveau, "Comparison of wind farm large eddy simulations using actuator disk and actuator line models with wind tunnel experiments," *Renewable Energy*, vol. 116, pp. 470-478, Feb. 2018. doi: 10.1016/j.renene.2017.08.072.

[24] M. J. Churchfield, S. J. Schreck, L. A. Martinez-Tossas, C. Meneveau and P. R. Spalart, "An Advanced Actuator Line Method for Wind Energy Applications and Beyond," in *AIAA 2017-1998. 35th Wind Energy Symposium*, Grapevine, TX, USA, Jan. 9-13, 2017. doi: 10.2514/6.2017-1998.

[25] G. Winckelmans, P. Rochefort, T. Villeneuve, F. Trigaux, M. Duponcheel and G. Dumas, "Improved modeling of flow curvature effects on vertical-axis turbines, and actuator line method with aerodynamic moment," *Wind Energy Sciences*, pre- print, Dec. 2025. doi: 10.5194/wes-2025-283.

[26] F. Trigaux, T. Villeneuve, G. Dumas and G. Winckelmans, "Near-tip correction functions for the actuator line method to improve the predicted lift and drag distributions," *Journal of Fluid Mechanics*, vol. 989, p. A1, Jul. 2024. doi: 10.1017/jfm.2024.461.

[27] P. Bachant, A. Goude and M. Wosnik, "Actuator line modeling of vertical-axis turbines," 2018, *arXiv: arXiv:1605.01449*.

[28] R. Zhao, A. C. W. Creech, A. G. L. Borthwick, V. Venugopal and T. Nishino, "Aerodynamic Analysis of a Two-Bladed Vertical-Axis Wind Turbine Using a Coupled Unsteady RANS and Actuator Line Model," *Energies*, vol. 13, no. 4 p. 776, 2020. doi: 10.3390/en13040776.

[29] P. F. Melani, F. Balduzzi, G. Ferrara and A. Bianchini, "Tailoring the actuator line theory to the simulation of Vertical-Axis Wind Turbines," *Energy Conversion and Management*, vol. 243, p. 114422, Sep. 2021. doi: 10.1016/j.enconman.2021.114422.

[30] Siemens Digital Industries Software, *Simcenter STAR-CCM+ version 2406*, 2024.

[31] M.-A. Breault, P. Rochefort and G. Dumas, "On the simulation of a wing with detached end-plates using an actuator line based on an anisotropic Gaussian kernel," *Transactions of the Canadian Society for Mechanical Engineering*, vol. 48, no. 4, pp. 534-542, Jan. 2024. doi: 10.1139/tcsme-2023-009.

[32] M. Boudreau and G. Dumas, "Comparison of the wake recovery of the axial-flow and cross-flow turbine concepts," *Journal of Wind Engineering and Industrial Aerodynamics*, vol. 165, pp. 137-152, June 2017. doi: 10.1016/j.jweia.2017.03.010.

Simulating Complex Energy Systems

Dr. Peter Ogban

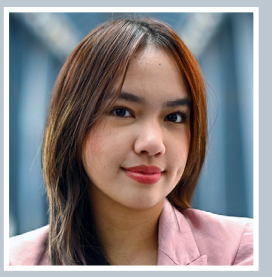

Grace Khatrine

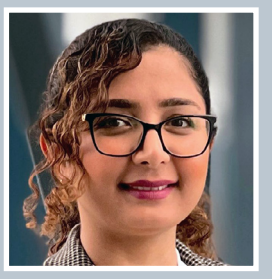

Fatemeh Kafrashi

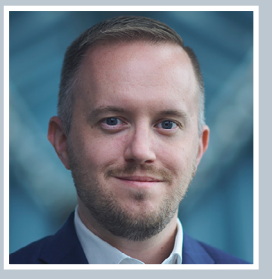

Chad LaFitte

Spatial modelling with techno-economic analysis

Who should read this paper?

This paper should be read by energy policy-makers, offshore wind developers, grid planners, and researchers involved in renewable energy planning, particularly those assessing offshore wind, energy storage integration, and grid readiness in Atlantic Canada. It is also relevant for investors and regulatory bodies seeking early-stage techno-economic insights to support resilient, low-carbon energy system decisions.

Why is it important?

This work is a techno-economic, spatial, and systems level modelling study that evaluates hybrid offshore wind and energy storage configurations using a unified optimization framework. It applies the proprietary Model for Energy Systems Optimization (MESO) platform to simultaneously integrate high-resolution offshore wind data, storage dispatch, emissions impacts, and financial performance in early-stage project assessment. The study advances current practice by coupling artificial intelligence/machine learning-enhanced data processing with scenario-based optimization across multiple designated offshore lease areas. By linking offshore wind, battery storage, and export or local supply pathways within a single modelling environment, the work provides a novel, decision-ready approach for resilient marine energy planning.

This paper demonstrates how offshore wind development can be planned in a way that aligns with marine conditions, environmental protection, and long-term ocean use. It provides evidence-based insights into how site selection, foundation types, and hybrid energy systems interact with offshore environments, helping inform responsible and resilient marine energy development.

The work provides clear, data-driven guidance on where and how offshore wind development can occur while respecting marine conditions, existing ocean uses, and environmental constraints. By quantifying trade-offs between foundation types, energy yield, emissions reduction, and grid integration, the study supports more informed marine spatial planning and reduces uncertainty for stakeholders who depend on healthy and well-managed ocean spaces. The findings also help align offshore renewable energy development with long-term ocean sustainability, economic opportunity, and community confidence in marine decision-making. The technology will be available for commercial application in 2026.

About the authors

Dr. Peter Ogban is a professional engineer with 15 years of experience specializing in wind energy systems, energy storage, and energy systems optimization. His work focuses on techno-economic modelling and integration of offshore and onshore wind with grid and storage solutions to support decarbonization. He has led and contributed to multiple renewable energy and R&D projects involving wind resource assessment, computational fluid dynamics, and transmission system analysis. His work supports efficient grid integration and performance optimization of renewable systems. He holds a PhD in mechanical engineering from Memorial

University of Newfoundland (MUN) and a master's degree in renewable energy from Newcastle University and is registered with Professional Engineers and Geoscientists of Newfoundland and Labrador (PEGNL).

Grace Khatrine is an energy systems engineer-in-training with a multidisciplinary background in Earth sciences and clean energy systems. At Angler Solutions, she supports offshore wind and renewable energy development through energy system modelling, supply chain analysis, and hybrid system design, including energy storage solutions such as compressed air and pumped hydro. Her expertise includes subsurface analysis and offshore basin evaluation, providing a strong foundation for integrated energy planning in offshore environments. She holds a bachelor of engineering from Universitas Trisakti and a master of science in Earth sciences from MUN.

Chad Fowlow

Fatemeh Kafrashi is an electrical engineer-in-training with expertise in renewable and hybrid energy systems. She holds a master of engineering in electrical engineering from MUN, where her research focused on renewable-powered infrastructure and system optimization. Her work includes electrical system modelling, data integration, and energy balance analysis for hybrid systems, including offshore wind applications. She supports development and implementation of MESO-based models for renewable energy projects, contributing to system design and performance validation.

Chad LaFitte is a professional engineer with 13 years of experience in energy systems, with a focus on offshore energy and low-carbon project development. As manager of innovation and opportunities at Angler Solutions, he leads techno-economic analysis and digital modelling for renewable and hybrid energy systems, including offshore wind integration, using the MESO platform. He has supported offshore oil and gas developments in Atlantic Canada and international projects, with experience in reservoir engineering, project delivery, and energy transition initiatives including carbon capture and storage. He has contributed to industry collaborations focused on decarbonization and technology deployment. He holds bachelor's and master's degrees in engineering from MUN and is a certified project management professional and qualified reserves evaluator.

Chad Fowlow is a professional engineer with over 27 years of experience in the energy sector and is the founder and principal consultant of Angler Solutions Inc. He leads strategic initiatives supporting the energy transition, with a focus on offshore electrification, offshore wind integration, hydrogen systems, and carbon capture and storage. He has extensive experience in offshore project development, including subsea construction, concept selection, feasibility studies, and front-end engineering design. He has worked across Canada and internationally on projects ranging from early-stage renewable integration to large-scale offshore developments. His expertise includes techno-economic analysis, R&D program leadership, and stakeholder engagement across industry, government, and academia. He holds bachelor's and master's degrees in engineering from MUN and is a registered professional engineer with PEGNL.

TOWARD RESILIENT HYBRID ENERGY FUTURES: MESO ASSESSMENT OF OFFSHORE WIND, STORAGE, AND GRID READINESS IN NOVA SCOTIA

Peter Ogban*, Grace Khatrine, Fatemeh Kafrashi, Chad LaFitte, Chad Fowlow
Angler Solutions Inc., St John's, NL, Canada
**Corresponding author: peter.ogban@anglersolutions.ca*
DOI: https://doi.org/10.48336/9BSW-QG41

ABSTRACT

The rapid evolution of hybrid energy systems, driven by global decarbonization goals, underscores the urgent need for advanced modelling tools that integrate technological, economic, and environmental dimensions. In response, Angler Solutions Inc. has developed a proprietary Model for Energy Systems Optimization (MESO), a versatile, artificial intelligence/machine learning enhanced platform for simulating and optimizing complex energy systems.

This study highlights MESO's application in assessing hybrid configurations of offshore wind and potential energy storage for three newly prioritized Nova Scotia offshore wind lease areas: French Bank, Middle Bank, and Sydney Bight, which were formally identified in the Joint Strategic Direction Letter from the Governments of Canada and Nova Scotia in September 2025. These configurations can be designed to support high-intensity, continuous loads and to enhance grid-level resilience by supplying power directly to local and regional grids, or by exporting it to other parts of Canada and the United States. MESO models the temporal dynamics between intermittent generation and storage technologies, optimizing system sizing, dispatch strategies, levelized cost of energy, and emissions performance.

The proposed methodology includes three key stages. First, a site-specific assessment of offshore wind potential using high-resolution modelled meteorological data and techno-economic parameters, integrated with spatial layers. Second, environmental constraints are evaluated, focusing on emissions reduction and cost savings. Third, in cases where energy storage is needed, appropriate technologies such as battery energy storage system will be assessed based on techno-economic criteria including capital expenditure, round-trip efficiency, and charge/discharge duration. To frame the study's objective, the current state of grid and transmission readiness, for local integration and export opportunities, will be examined, providing broader context for decision-making.

MESO combines spatial modelling with techno-economic analysis to de-risk early-stage hybrid energy projects. This study will demonstrate how optimized wind storage systems

can reduce emissions, enhance grid resilience, and strengthen regional energy security. Key findings will highlight actionable pathways toward resilient, low-carbon energy futures in Atlantic Canada.

Keywords: MESO, hybrid energy system, offshore wind energy, offshore Nova Scotia, energy storage systems, marine renewables, modelling and optimization tool, artificial intelligence AI, machine learning ML

1. INTRODUCTION

Nova Scotia has reached an important phase in its transition to clean energy. The province has set targets to generate 80% of its electricity from renewables by 2030 and to achieve net-zero carbon emissions by 2050. Nova Scotia's history of offshore activity and strong offshore wind resources have become central to achieving these goals. The recent Regional Assessment of Offshore Wind Development and the government's modular Offshore Wind Roadmap show growing momentum and a clear path toward successful offshore wind development in the province. These efforts highlight the importance of environmental protection, long-term planning, stakeholder engagement, and technical opportunity [1], [2].

In July 2025, four offshore wind zones were officially designated as suitable areas for future development. These areas include Middle Bank, French Bank, Sable Island Bank, and Sydney Bight. These zones were selected through rigorous regulatory analysis, community feedback, seabed and wind resource mapping, and scientific studies. Three of these designated areas, Middle Bank, French Bank, and Sydney Bight, are the focus of this study, as they represent a balance of manageable distances to shore, favourable depths, and strong wind potential [3].

As Nova Scotia prepares to license its offshore wind lease areas, there is an increasing need for energy system modelling tools to evaluate early-stage designs, storage solutions, and grid readiness. Hybrid offshore wind energy and storage systems can support power reliability, reduce curtailment, and support grid resilience. To support these early planning needs, this paper applies the proprietary Model for Energy Systems Optimization (MESO), a web-based techno-economic modelling platform developed by Angler Solutions Inc. In this case, MESO is used to evaluate hybrid offshore wind and battery storage configurations for the three designated areas. This study aims to provide practical, early-stage, techno-economic insights related to the proposed wind development areas. Understanding technical viability and economic feasibility will be crucial as Atlantic Canada begins to lay the foundation for a resilient offshore wind energy industry.

1.1 Background Study

Nova Scotia's interest in offshore wind development is grounded in a combination of favourable natural conditions, a coordinated regulatory framework, and renewable energy goals. The Regional Assessment of Offshore Wind Development provides a comprehensive understanding of the Scotian Shelf

environment, including seabed conditions, wind speeds, ecological considerations, and water depths. It also highlights the need for continuous engagement with the Mi'kmaq and coastal communities, protection of sensitive marine areas, and coexistence with fisheries. This assessment forms the social and scientific foundation for offshore wind planning in the region [1].

Building on this, the Nova Scotia Offshore Wind Roadmap provides the broader development pathway, including community perspectives, regulatory processes, and supply chain readiness. It emphasizes that an offshore wind energy project is both a social and economic opportunity that must reflect environmental responsibility, equitable development, and shared values. This pathway helps ensure that future offshore wind projects meet the expectations of local communities and industry participants and align with provincial goals [2].

The designation of the offshore wind areas in 2025 marked a critical point for Nova Scotia. Sydney Bight, Middle Bank, and French Bank were selected after site mapping and public engagement. French Bank and Middle Bank are the most suitable sites due to their water depths and strong wind conditions, while the Sydney Bight area was adjusted to increase its distance from shore following community feedback. These areas represent the most development ready sites and are considered strong locations for Nova Scotia's first offshore wind licensing [3].

The successful designation of offshore wind areas in Nova Scotia creates a basis for techno-economic assessment of hybrid offshore wind and energy storage. By modelling annual energy production, energy storage requirements, and grid interactions, this study supports Nova Scotia's transition toward low-carbon, resilient energy systems.

1.2 Study Area: Nova Scotia Offshore

The study focuses on the Canada-Nova Scotia Offshore Energy Regulator (CNSOER) leased offshore wind areas in Nova Scotia, named French Bank, Middle Bank, and Sydney Bight (Figure 1) [4] with representative location (Lat, Long) as follows: 44.7°, -61.5°; 44.5°, -60.7°; 46.5°, -60.1°. These regions are characterized by favourable wind conditions and water depths suitable for both fixed and floating wind foundations. Nova Scotia's current energy system relies on a combination of hydroelectric, fossil fuel, and limited wind generation, supplemented by emerging energy storage infrastructure to manage intermittency [5]. Analyzing the spatial distribution, local load demands, and grid connectivity of these lease areas is essential for assessing the feasibility of large-scale offshore wind deployment and hybrid energy system integration in a manner that maximizes local energy security and export potential.

1.3 Technical Background: Offshore Wind Foundation Types

Offshore wind development requires careful consideration of foundation technologies, which are primarily categorized as fixed-bottom and floating systems. Fixed-bottom foundations, such as monopiles, jackets, and gravity-based structures, are most suitable for shallow to intermediate water depths (typically less than 60 metres) and offer robust structural stability with well-established construction

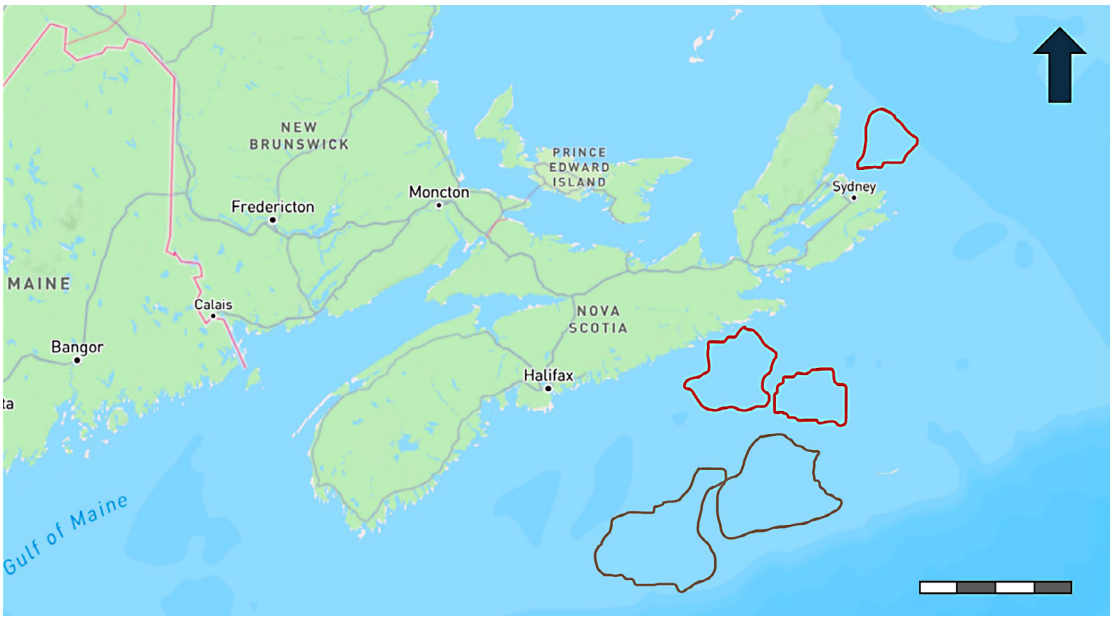

Figure 1: Canada-Nova Scotia Offshore Energy Regulator designated offshore wind areas. Red boundaries show current active leases; grey boundaries show proposed leases that were later deferred.

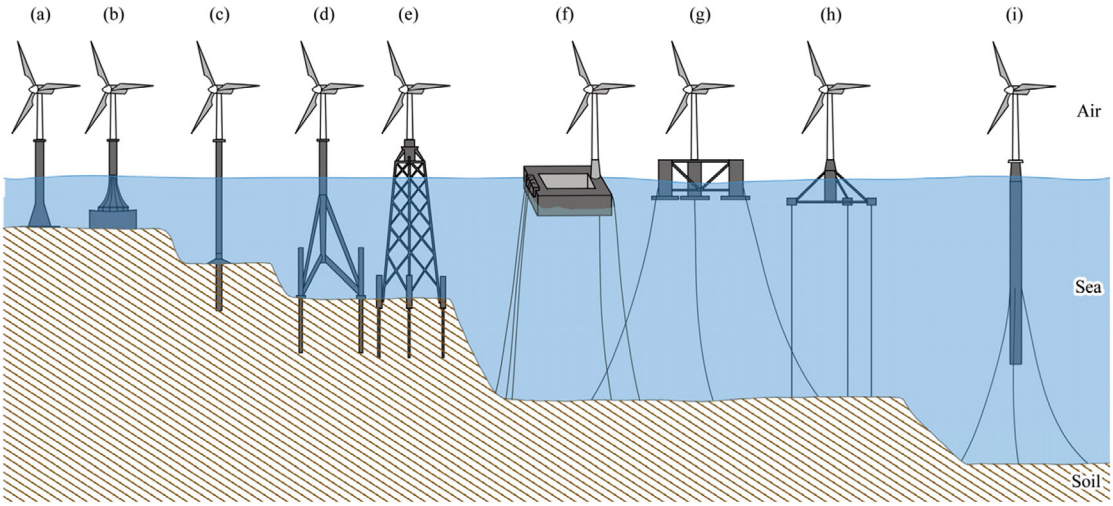

Figure 2: Structural foundation types of existing mainstream offshore wind turbines: (a) gravity-based; (b) bucket; (c) monopile; (d) tripod; (e) jacket; (f) barge; (g) semi-submersible; (h) tension-leg platform; and (i) spar. (Reproduced from [6], under the CC BY 4.0 license.)

practices. In contrast, floating foundations, including semi-submersible, spar buoy, and tension-leg platforms, allow deployment in deeper waters where fixed-bottom installations are impractical (Figure 2) [6], [7]. The choice of foundation type directly influences project costs, installation complexity, and operational performance, and is critical for optimizing offshore wind deployment within the CNSOER lease areas.

2. METHODOLOGY

2.1 MESO Technology Overview

MESO is Angler Solutions' proprietary modelling platform for techno-economic analysis and optimization of energy systems. The platform is designed to evaluate the technical viability, sustainability, and economic feasibility of hybrid energy system development projects. The MESO platform enables investors, policy-makers, researchers, and energy developers to make informed decisions by simulating real-world energy systems for both cost effectiveness and technical performance.

The MESO platform integrates various renewable generation technologies and energy storage solutions, offering the capability of simulating an energy balance where generation technologies are combined with storage solutions and load profiles to model end-to-end systems with the goal of maximizing energy reliability while minimizing levelized cost. MESO also incorporates machine learning for environmental data forecasting, geospatial analysis for wind turbine placement optimization, and carbon emissions analysis for environmental impact assessment.
These combined capabilities result in a comprehensive energy systems modelling platform. The platform enables systematic evaluation of renewable and hybrid energy development concepts, with added capabilities for the optimization of development parameters such as site selection, turbine placement, installed capacities, storage integration, and simulation of multiple scenarios to capture operational risk and uncertainty. By providing data-driven insights, MESO facilitates informed decision-making with the goal of maximizing the technical and economic value of hybrid energy systems.

The modelling methodology, such as those methods used to generate MESO-Artificial Intelligence (AI) predictions or the logic behind hybrid energy modelling, is not discussed in this paper.

2.2 Process Flow

MESO modelling requires rigorous data cleaning and management to ensure model reliability and underpins the sensitivity analysis of MESO's optimization outcomes. This study alone employs multiple datasets, including meteorological observations, techno-economic inputs, and turbine specific power curves, which were cleaned, preprocessed, and formatted for MESO integration (Figure 3). To enhance the predictive accuracy of MESO, the model is calibrated against observed wind speed and energy production data. Missing or inaccurate wind inputs are addressed using MESO's integrated AI/machine learning algorithms, which interpolate and correct anomalies while maintaining consistency with measured meteorological records.

This study runs sensitivity analyses for all designated areas with a variety of turbine models, evaluating the impact of turbine size, spacing, storage integration on overall energy yield, environmental Greenhouse Gas (GHG) analysis, and cost-effectiveness. MESO's scenario-based approach allows for comprehensive assessment of operational and economic trade-offs, informing optimal hybrid energy configurations for the CNSOER lease areas.

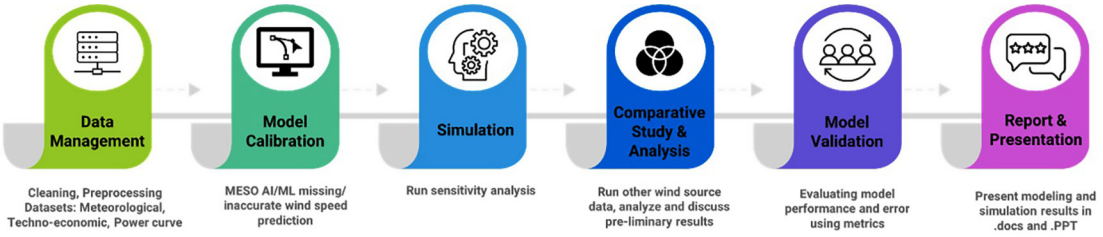

Figure 3: Research methodology.

A comparative analysis is conducted using alternative wind source datasets and scenarios to evaluate MESO's output robustness and identify site-specific performance variations. By comparing results from different datasets, the study examines discrepancies in predicted energy production, storage utilization, and cost metrics, enabling a preliminary assessment of uncertainties and system resilience. Model validation is performed to quantify MESO's predictive reliability and identify sources of error. Performance metrics such as mean absolute error, root mean square error, and correlation coefficients are used to compare simulated outputs against observed data. Validation ensures that MESO's techno-economic predictions are credible, supports confidence in scenario analysis, and provides a benchmark for iterative model refinement and decision-making for offshore wind deployment in Nova Scotia. Results from MESO simulations and analyses are compiled into structured documentation and presentations to facilitate stakeholder communication.

3. SIMULATION INPUTS AND SYSTEM SPECIFICATIONS

This section presents the modelling framework, input datasets, and assumptions used to simulate offshore wind farm performance across three designated areas. The simulations were run as a standalone case and a combined high-resolution wind resource data, turbine-level modelling, and Battery Energy Storage System (BESS) time-of-use analysis. All simulations were performed using a uniform methodology (discussed Section 2) to enable direct comparison between locations.

3.1 Wind Resource and Turbine Performance

3.1.1 Data Sources

In this study, three complementary meteorological datasets were employed to capture both large-scale climatological patterns and high-resolution site-specific wind behaviour across the selected study areas. Datasets including NASA Modern-Era Retrospective analysis for Research and Applications (MERRA-2 atmospheric reanalysis dataset), European Centre for Medium-Range Weather Forecasts Reanalysis 5, fifth generation reanalysis (ERA5), and Meteorological Service of Canada 50-year dataset (MSC50) as the custom data (Table 1).

Comparisons among the three datasets were performed to assess inter-annual variability, extreme wind events, or seasonal patterns that historically occurred. ERA5 and MSC50 showed an alignment, while NASA MERRA-2 tended to under-estimate peak wind velocities, consistent with known resolution limitations.

The MSC50 dataset was specifically developed for the North Atlantic and Canadian offshore regions, making it particularly suitable for regional wind

Table 1: Comparison of wind resource datasets used in the simulation.

Feature	MSC50	ERA5	NASA MERRA-2
Region	North Atlantic & Canadian offshore (regional)	Global	Global
Horizontal Resolution	~0.1° (~10 km)	~0.25° (~30 km)	~0.5° (~50 km)
Temporal Coverage	1954-2005 (extended to 2021)	1950-present	1980-present
Regional Tuning	Yes, blended with local buoy, ship, and coastal data	No, global reanalysis	No, global reanalysis
Wave Model	OWI-3G spectral model optimized for North Atlantic	Bulk wave parameterizations	Bulk wave parameterizations
Strengths	High-resolution regional detail, better extreme event stats, validated for offshore engineering	Global consistency, continuously updated, includes recent satellite data	Global coverage, long-term consistency
Limitations	Regional, not updated in near real time; reliability decreases outside calibration region	Coarse resolution; limited local tuning	Coarse resolution; limited local tuning

and wave studies. Unlike coarse global reanalyses, MSC50 incorporates regional tuning by blending and correcting surface winds with local buoy, ship, and coastal station observations, thereby capturing coastal features, fetch-limited seas, and smaller storm systems more accurately [8], [9]. Its horizontal resolution of ~0.1° (~10 km) is finer than ERA5 (~0.25°, ~30 km) and NASA MERRA-2 (~0.5°, ~50 km), allowing better representation of local wind gradients and mesoscale variability. In addition, MSC50 employs the OWI-3G spectral wave model optimized for North Atlantic storm physics, resulting in more accurate extreme wave statistics and storm climatology. Nevertheless, MSC50 has some limitations: its original temporal coverage was 1954-2005 (later extended to 2021), it is regionally focused and less reliable outside its calibration domain, and it is not updated in near real time. The dataset is based on National Centers for Environmental Prediction/National Center for Atmospheric Research global reanalysis, which is reanalyzed and downscaled to a high-resolution 0.1° grid, using observational data both to adjust the model during reanalysis and to validate hindcast results [9]. Compared to ERA5 and MERRA-2, MSC50 provides higher fidelity for regional offshore wind and wave characterization, particularly in areas where mesoscale features and extreme events are critical.

3.1.2 Turbine Model Specification

All simulations employ the Siemens Gamesa SG 21-276 DD offshore wind turbine, selected due to its proven performance in offshore wind applications and the manufacturer's proximity in the United States, facilitating potential project deployment and maintenance. The turbine's power curve (Figure 4) was applied to site-specific wind speed distributions using standard bin-averaging methods and turbulence-adjusted effective wind speeds, enabling accurate estimation of energy production across the modelled locations. Atmospheric and operational parameters were set according to typical offshore conditions (Table 2).

3.1.3 Turbine Selection and Layout

Based on capacity density of 5 MW/km^2, the

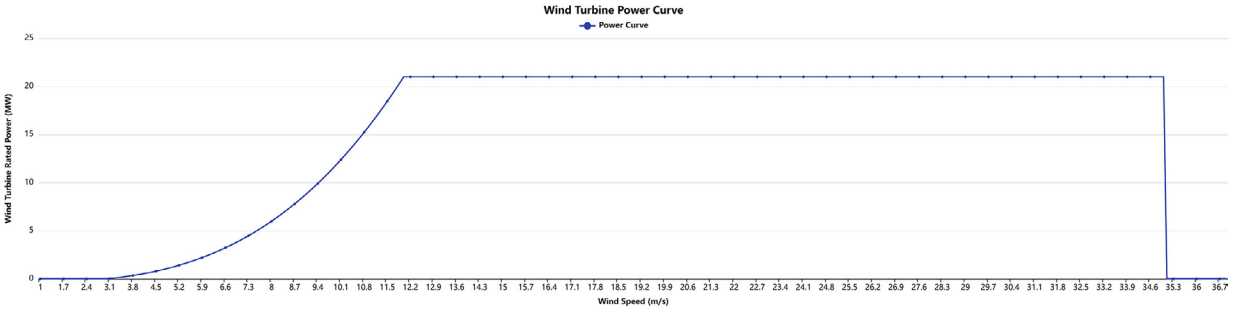

Figure 4: Power curve of the Siemens Gamesa SG 21-276 DD offshore wind turbine applied in this study.

Table 2: Key specifications and operational parameters of the Siemens Gamesa SG 21-276 DD offshore wind turbine.

Parameter	Value
Rated Power	21.5 MW
Rotor Diameter	276 m
Hub Height	140 m
Rated Wind Speed	12 m/s
Operational Wind Speed Range	3–35 m/s
Power Coefficient	0.3
Wind Shear Exponent	0.1
Air Density (Standard temperature and pressure)	1.23 kg/m³
Specific Gas Constant (dry air)	287 J/kg·K
Specific Humidity	0.008 kg/kg

number of turbines selected for assessment is 550 for French Bank, 318 for Middle Bank, and 200 for Sydney Bight. Each site includes a mix of fixed- and floating-bottom turbines, with floating foundations deployed in waters deeper than 100 m. At French Bank, 72 turbines (13%) are fixed, while 478 (87%) are floating. Middle Bank has a higher proportion of fixed turbines, with 210 units (66%) fixed and 108 units (34%) floating. Sydney Bight consists of 34 fixed turbines (17%) and 166 floating turbines (83%). This distribution reflects both water depth constraints and site-specific bathymetric conditions, aimed to maximize energy capture while minimizing installation and operational challenges associated with deep-water foundations.

3.1.4 Loss Factors

Wind farm loss factors represent the difference between the theoretical maximum energy a turbine could produce. These losses arise from aerodynamic, electrical, and operational mechanisms that affect turbine performance throughout its lifetime. To approximate operational performance, a consistent 10% (Table 3) wind-related loss factor was applied to gross energy yield calculations.

Aerodynamic losses occur because real-world conditions differ from idealized power-curve assumptions. Factors such as blade contamination or icing [10], wake interactions between turbines [11], turbulence intensity, and yaw misalignment [12] reduce the effective

Table 3: Wind farm loss assumptions used in the energy yield simulation.

Category	Sub-category	Loss (%)
Aerodynamic	Icing / blade contamination	1%
	Aerodynamic wake	2%
	Environmental turbulence intensity	1%
Electrical	Cable losses	1%
	Transformer losses	1%
	Transmission losses	1%
Operational	Turbine availability / curtailment	2%
	Yaw misalignment	1%

wind speed or alter the inflow angle, leading to lower aerodynamic efficiency.

Electrical losses arise as electricity flows through inter-array or export cables, transformers, and transmission systems before reaching the grid [13], [14]. Resistive heating in cables, conversion losses in transformers, and export system inefficiencies contribute to a predictable, typically small reduction in delivered energy.

Operational and availability related losses include downtime for maintenance, mechanical faults, and grid-imposed curtailment. Even modern turbines with high availability (≥97%) experience short interruptions that reduce annual energy production [15]. Curtailment may also occur during periods of oversupply, grid constraints, or extreme weather events [16] (Table 3).

3.1.5 Economic

The economic assessment of the offshore wind farm is based on key cost, revenue, and financial parameters. The Capital Expenditure (CAPEX) is assumed to be USD$3.9 million per MW, while Operational Expenditure (OPEX) is set at 2.5% of CAPEX per year, reflecting routine maintenance, monitoring, and administrative costs typical for utility-scale offshore wind projects. Energy revenues for export scenarios are estimated using an energy export rate of USD$120 MWh. The project is evaluated over a 25-year payment period, with a construction timeline of three years and a discount rate of 8% to account for the time value of money. Carbon pricing is incorporated at USD$57 per ton of CO_2, capturing the potential financial benefit of avoided emissions. A salvage value of USD$14,350 is assumed at the end of the project lifetime, and plant self-consumption is estimated at 50 MWh per year. These inputs provide the basis for Levelized Cost of Energy (LCOE), Net Present Value (NPV), Internal Rate of Return (IRR), and other key techno-economic metrics used to assess the financial viability of offshore wind deployment under both export and local supply scenarios (Table 4).

3.2 BESS

The BESS component was modelled to evaluate dispatch flexibility, grid compliance, and potential smoothing of variable wind output at each site.

3.2.1 BESS Input to the Simulation

BESS operation is driven by wind farm output, grid requirements, and optimization

Table 4: Economic assumptions used in the wind project financial simulation.

Parameter	Value	Description
CAPEX (fixed-foundation)	3.2 MUSD/MW	Turbine + balance of plant
CAPEX (floating foundation)	3.9 MUSD/MW	Includes hull, moorings, dynamic cables
OPEX	2.5% of CAPEX per year	Includes maintenance and offshore logistics
Energy export rate	USD$120 /MWh	Realized revenue at point of interconnection
Project payment period	25 years	Financial evaluation horizon
Construction time	3 years	Used for staged CAPEX payment
Discount rate	8%	Real, pre-tax
Carbon pricing	USD$57 /$tCO_2$	Applied to displaced emissions benefits
Salvage value	USD$14,350	Residual value at end of project life
Plant energy usage	50 MWh/year	Self-consumption, deducted from gross output

objectives. The BESS was modelled as a modular, utility-scale configuration designed to complement offshore wind generation in Nova Scotia. A Time-of-Use on-grid BESS operational model is used, in which the storage system charges during low-price or high-generation periods and discharges during peak demand or low-wind intervals. The following assumed configuration reflects the scale and cost parameters of existing grid-scale BESS projects deployed in Nova Scotia: 175 MW of renewable firming supported by a 50 MW, 4-hour (200 MWh) BESS with a CAPEX of USD$300 /kWh and OPEX of 2.5%. The firmness metric is defined as the fraction of on-peak hours where total delivered power meets the 175 MW target. This metric mirrors effective load-carrying capability and loss of load expectation methods used by grid operators (e.g., ISO New England, Southwest Power Pool, North American Electric Reliability Corporation) for capacity accreditation of renewable-plus-storage systems in this scenario: any surplus offshore wind generation beyond local demand is also considered for export. Each battery unit has a nominal capacity of 110 Ah and a voltage of 12 V, with individual modules combined to form a battery bank providing a total energy capacity of 36 × 5.644 MWh (Table 5). Charging and discharging were performed at a 0.25 C-rate, with rectifier and inverter efficiencies of 95% and system wiring losses of 3%, resulting in a system voltage of 1,331.2 V. Battery State of Health (SOH) was assumed to degrade at 1.5% per year, representing the gradual loss of capacity and efficiency due to chemical aging, cycle fatigue, and operational stresses over the project lifetime.

LCOE and Levelized Cost of Storage (LCOS) are calculated independently based on capital and operating costs [17]. Revenue analysis differentiates between local firm block sales (valued at on-peak local market prices) and export energy output. The BESS was integrated with a wind farm operating at CAPEX of USD$3,900 /kW and an OPEX of 2.5%, while

Table 5: Key specifications and operational parameters of the 50M2, 4-hour Battery Energy Storage System (BESS) configurations.

Category	Parameter	Value
Economic Input	Wind CAPEX	3900 $/kW
	Wind OPEX	2.5%
	Battery CAPEX	300 $/kW
	Battery OPEX	2.5%
	Battery Replacement Cost	60%
	Battery Replacement Year	15 years
	End of Project Salvage Value	10%
GHG Emission Factor	GHG Emission for Wind	10 $kgCO_2e/MWh$
	GHG Emission for Battery	30 $kgCO_2e/MWh$
	GHG Emission for Local Grid	502 tCO_2e/MWh
System Input Parameters	Rectifier & Inverter Efficiency	95%
	System Wiring Losses	3%
	System Voltage	1331.2 V
	Battery SOH Yearly Degradation	1.5%
Battery Input	Individual Battery Capacity	110 Ah
	Individual Battery Voltage	12 V
	Battery Bank Energy	36 * 5.644 MWh
	Battery Charging & Discharging Efficiency	96%
	Initial SOH for Battery Bank	100%
	State of Change Min, Max	20%, 100%
	Capacity at End of Life	80%
	Number of Cycles	5,000
	Charging & Discharging C-rate	0.25

the battery system had a CAPEX of USD$300 /kWh, with an OPEX of 2.5%. The selected OPEX accounts for routine maintenance, system monitoring, minor component replacement, and ancillary operational costs, consistent with existing utility-scale battery deployments. A replacement cost of 60% in year 15 and an end-of-project salvage value of 10% were assumed to reflect the residual economic value of the system.

To evaluate the environmental benefits of the BESS integration, GHG emissions from battery operation and wind generation were compared to emissions from the local grid. While wind and storage systems produce minimal operational emissions (10 and 30 $kgCO_2e/MWh$, respectively), the local grid in Nova Scotia exhibits significantly higher GHG intensity (502 tCO_2e/MWh). This comparison is critical for quantifying the potential reduction in fossil fuel reliance and validating the decarbonization impact of hybrid offshore wind-BESS systems.

The BESS dispatch algorithm computes the net delivered power to the grid, modified by Round-Trip Efficiency (RTE) and availability factors. Outputs include daily and annual storage utilization, contribution to firm capacity, and impacts on net energy yield.

3.2.2 System Configuration

The Nova Scotia electricity grid provides transmission lines at multiple voltage levels,

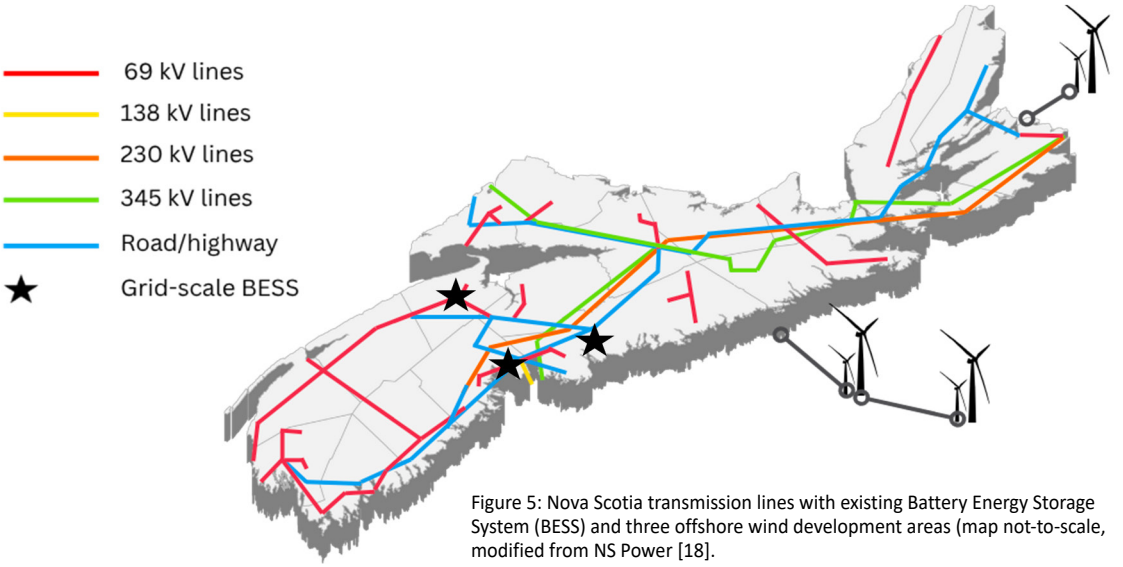

Figure 5: Nova Scotia transmission lines with existing Battery Energy Storage System (BESS) and three offshore wind development areas (map not-to-scale, modified from NS Power [18].

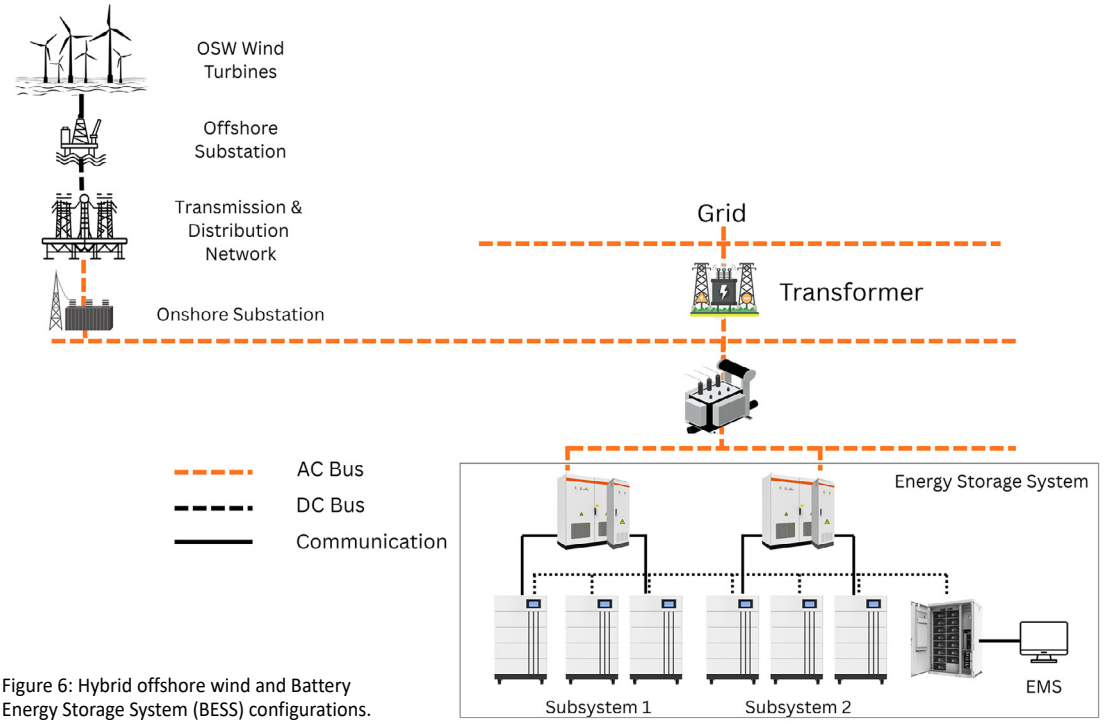

Figure 6: Hybrid offshore wind and Battery Energy Storage System (BESS) configurations.

including 69, 138, 230, and 345 kV [18] (Figure 5). Although suitability can only be confirmed by many factors (such as distance, capacity, cable vs. overhead line, converter requirements, local grid strength, regulations), the higher voltage 230 and 345 kV lines are by design suitable for large-scale offshore wind exports, minimizing transmission losses over long distances, while the 69 and 138 kV lines can support localized integration and distribution [19], [20]. The infrastructure readiness of Nova Scotia's grid to fully support "hybrid offshore wind + storage + export" (Figure 6) depends on upgrades and transmission planning: one

recent assessment indicates that the existing transmission system may not yet fully meet the criteria required for large scale offshore wind development without further upgrades [21]. These configurations are evaluated in the subsequent Results section to assess their impact on local energy supply reliability, utilization of offshore wind resources, and potential for exporting surplus generation.

4. RESULTS

This section presents multilayer outcomes, ranging from wind data source and techno-economic and environmental simulation results for two offshore wind deployment pathways: (1) exporting offshore wind generation and (2) serving local demand within Nova Scotia. The export scenario operates without energy storage, whereas the local supply scenario incorporates a BESS.

4.1 Offshore Wind Model and Simulation

The first scenario evaluates an energy export configuration, in which offshore wind generation is transmitted to external markets in the United States or Western Canada as part of broader Wind West export pathways. Because this scenario assumes no subsidies or financial incentives, three economic cases are examined using different cost structures and export rates:

(1) All fixed-foundation turbines with a CAPEX of USD$3,200 /kW and an export rate of USD$120 /MWh (Figure 7a). The three sites exhibit strong Return on Investment (ROI) across the board, with French Bank and Middle Bank showing the highest ROIs (≈216-217%) and Sydney Bight noticeably lower (166%). IRR values are modest and clustered in the single digits to low teens (≈9.4-11.6%), with Middle Bank showing the highest IRR (11.61%) and Sydney Bight the lowest (9.42%). LCOE ranges from $53 to $74/MWh: French Bank is the cheapest at $53/MWh, Sydney Bight is intermediate at $61/MWh, and Middle Bank has the highest cost at $74/MWh.

Taken together, Middle Bank produces the strongest returns (highest ROI and slightly highest IRR) despite having the highest LCOE, which suggests that its revenue or yield assumptions outweigh its higher unit costs (e.g., greater capacity factor, higher tariff, or favourable financing). French Bank combines high ROI with the lowest LCOE, indicating an efficient cost-to-output balance and attractive project economics. Sydney Bight shows the lowest ROI and IRR with a mid-range LCOE, making it the least attractive of the three under the current assumptions.

(2) All fixed-foundation turbines with a CAPEX of USD$4,500 /kW and an export rate of USD$135 /MWh (Figure 7b). This scenario compares the economic outcomes of three fixed-bottom offshore wind locations using ROI, IRR, and LCOE as key indicators of financial viability. French Bank demonstrates the strongest return performance, with an ROI of 141% and an IRR of 8.27%, accompanied by an LCOE of $75/MWh. Sydney Bight yields a moderate ROI of 102% and the lowest IRR among the three sites at 6.34%, while its LCOE is the highest at $86/MWh. Middle Bank produces an ROI of 106% and an IRR of 6.58%, paired with an LCOE of $75/MWh.

Overall, the results indicate that French Bank offers the most attractive economic profile

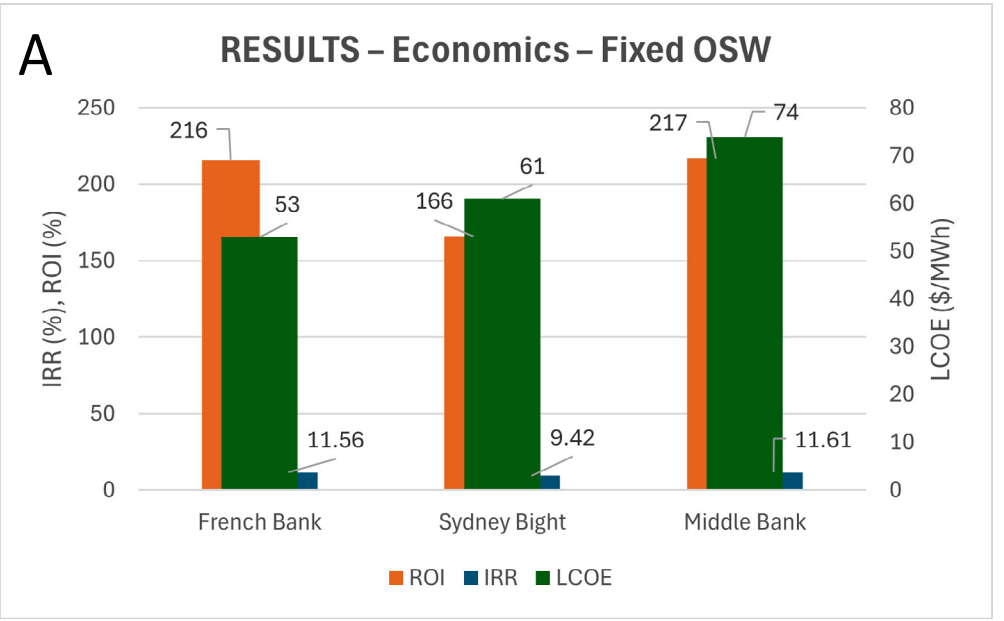

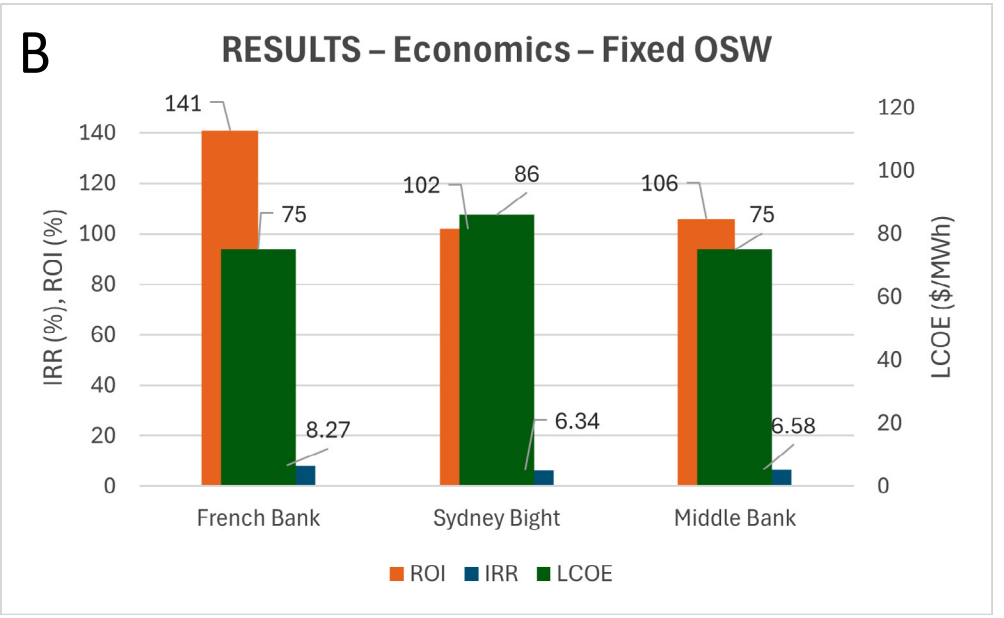

Figure 7: (top) Scenario A; (bottom) Scenario B: Economic performance indicators (Return on Investment (ROI), Internal Rate of Return (IRR), and Levelized Cost of Energy (LCOE)) for three fixed-bottom offshore wind sites. The left axis shows return based metrics (ROI and IRR), while the right axis shows the LCOE.

due to its combination of high returns and competitive LCOE. Sydney Bight performs least favourably, as both its ROI and IRR are the lowest while its LCOE is the highest, suggesting a weaker financial case under the assumed conditions. Middle Bank presents a balanced but less compelling economic outcome: although its LCOE matches French Bank's, its ROI and IRR remain modest. These comparisons highlight how site-specific factors (such as local wind resource quality, CAPEX, and operational costs) materially influence economic performance in fixed offshore wind development.

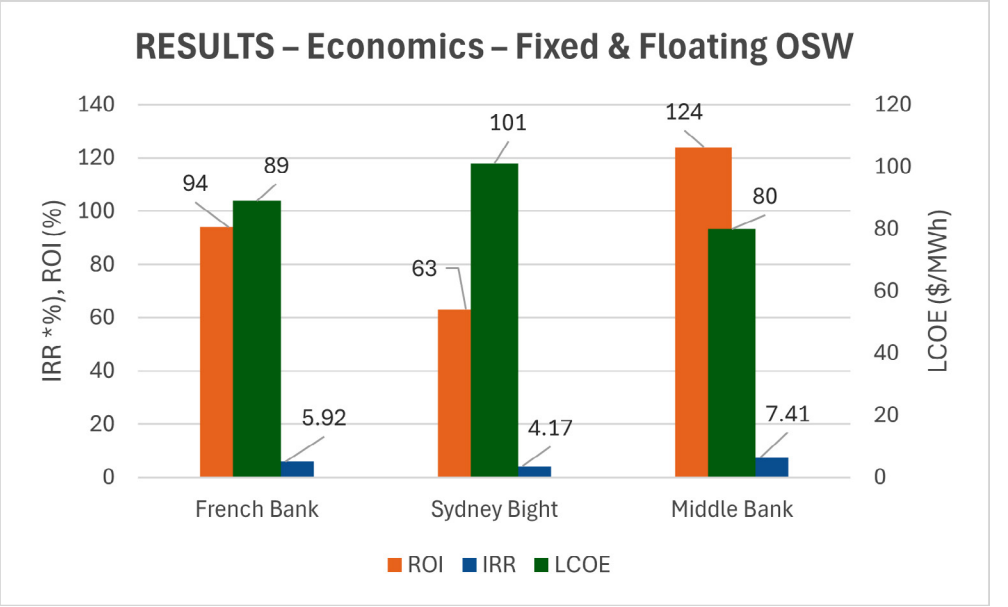

Figure 8: Economic performance metrics for fixed and floating offshore wind scenario sites. Bars represent Return on Investment (ROI, %; orange), Internal Rate of Return (IRR, %; blue), and Levelized Cost of Energy (LCOE, $/MWh; green). ROI and IRR correspond to the left axis, while LCOE corresponds to the right axis.

(3) A mixed configuration with fixed-foundation turbines (CAPEX USD$4,500 /kW) and floating turbines (CAPEX USD$5,500 /kW), using the same export rate of USD$135 /MWh (Figure 8). Mixed fixed-bottom and floating offshore wind foundations introduce higher costs and reduced financial returns compared with installations relying solely on fixed-bottom technology. This outcome aligns with commercial experience, as floating systems require more complex mooring arrangements, dynamic cabling, and deeper-water installation processes that collectively elevate both CAPEX and OPEX. When compared with the earlier fixed-bottom results, several systematic shifts become apparent. LCOE increases across all sites, rising from approximately $53-$86/MWh under fixed-bottom conditions to $80-$101/MWh in the mixed fixed-floating scenario, reflecting the additional technological and logistical demands of operating in deeper bathymetry. Correspondingly, both ROI and IRR decline: fixed-bottom ROI values of roughly 100-217% and IRRs of 6-12% fall to 63-124% and 4-7%, respectively, underscoring the reduced financial attractiveness associated with integrating floating technologies under similar economic assumptions. For fixed-bottom, French Bank consistently performed strongly, while Sydney Bight was the weakest. In the mix fixed-bottom and floating scenario, Sydney Bight remains the least economically favourable but Middle Bank emerges as the strongest performer, benefiting from more advantageous conditions as the depth increases. This shift highlights that deeper-water sites respond differently to floating technology depending on local resource potential and cost drivers.

Overall, the transition from fixed-bottom to mixed fixed-floating offshore wind results in

higher costs and lower returns but also clarifies which locations retain economic viability as depths increase. These insights are essential for informed long-term offshore wind planning in regions with varied bathymetric conditions.

4.2 Hybrid Offshore Wind and BESS

The second scenario focuses on local supply for Nova Scotia, where offshore wind is integrated with energy storage to support provincial demand, increase dispatchability, and enhance system reliability. The simulation operates on an hourly time step over one full year, using site-specific offshore wind data with a capacity factor near 50%, consistent with modern deep-water offshore projects. The dispatch optimization enforces technical and operational limits [22]:

$$SOC_t = SOC_{t-1} + \left(\eta_{Ch} P_t^{Ch} - \frac{P_t^{Disch}}{\eta_{Disch}}\right) \frac{\Delta t}{E^{Cap}} \quad (1)$$

$$SOC_{min} \leq SOC_t \leq SOC_{max} \quad (2)$$

Where SOC_t and SOC_{t-1} represent the state of charge at hour t and previous hour, respectively. P_t^{Ch} is the charging power at hour t (kW), and P_t^{Disch} is the discharging power at hour t (kW). The charging and discharging efficiency of the battery are denoted by η_{Ch} and η_{Disch}, respectively. E^{Cap} represents the total energy capacity of the battery bank. SOC_{min} and SOC_{max} are allowable minimum and maximum State of Change (SOC) limits, which ensure safe and reliable battery operation.

Charging sufficiency is verified each day to ensure off-peak energy availability exceeds the energy discharged (after accounting for RTE = 93%).

Yearly battery shares remain in the 7.8-8.6% range, reflecting modest but meaningful contributions to short-term balancing and grid-support functions. The technical results suggest that hybridization with storage will enable strong operational stability, with average SOC values around 72-76%, well within optimal operational ranges for lithium-ion systems (Figure 9). GHG reduction potential is substantial across all locations, but French Bank exhibits the largest total reduction due to higher energy throughput (Table 6). In terms of economic outcomes (Figure 10, Table 7), Sydney Bight demonstrates the strongest overall economic return, achieving an NPV of roughly $59M and the lowest LCOE (≈$66.9/MWh), supported by relatively low CAPEX requirements compared with French Bank. French Bank's project reaches a higher NPV (~$13.6B), but this is driven by much larger system size and associated CAPEX (~$46B), resulting in a longer payback period despite a high IRR. Middle Bank shows moderate performance with a mid-range NPV and competitive IRR, but slightly higher LCOE relative to Sydney Bight. The comparative analysis indicates that while French Bank may offer the greatest absolute economic value due to scale, Sydney Bight provides the most cost-efficient energy and strongest balance between investment risk and return.

4.3 Wind Data Source Results

Validation against buoy observations indicates that MSC50 wind speed biases are typically within ±0.5 m/s, whereas ERA5 and MERRA-2 can under- or overestimate by 1-2 m/s in coastal and storm affected regions; similarly, MSC50 significant wave height bias is generally below 5%, while ERA5

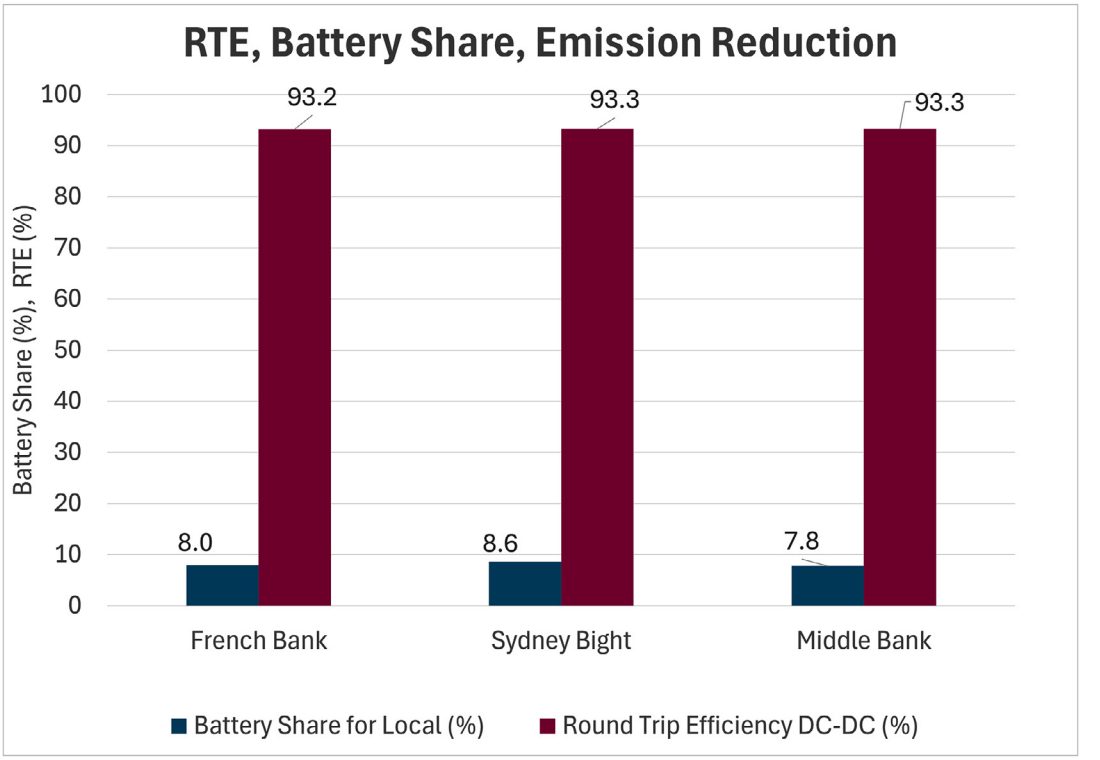

Figure 9: Technical performance assessment for hybrid Battery Energy Storage System (BESS) + offshore wind across Nova Scotia sites.

Table 6: Average SOC and GHG emission reduction for hybrid offshore wind + BESS.

	French Bank	Sydney Bight	Middle Bank
Average SOC %	76.4	72.5	76.3
GHG Emission Reduction (tCO2/MWh)	29,945,412	24,220,836	25,385,409

Table 7: CAPEX, IRR, payback periods, and discounted payback periods for hybrid offshore wind + BESS.

	French Bank	Sydney Bight	Middle Bank
Total CAPEX	46,177 MM	16,830 MM	7,427 MM
IRR (Hybrid)	74.61	58.96	67.77
Payback Period	11	13	12
Discounted Payback Period	15	19	17

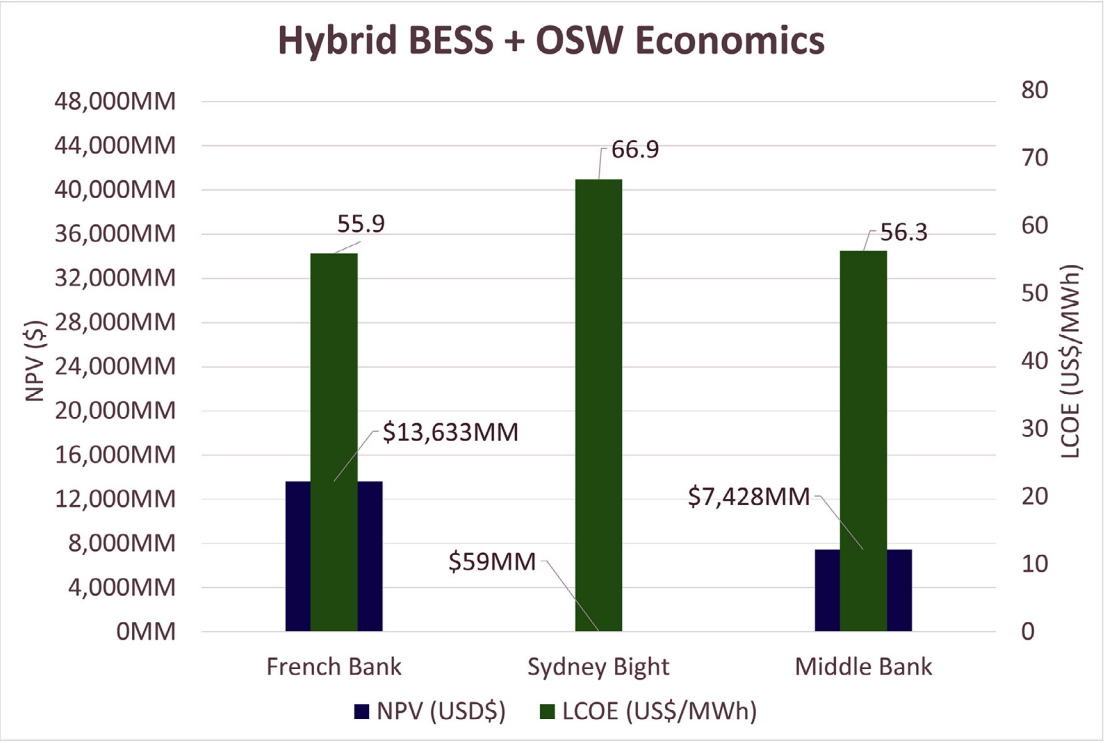

Figure 10: Economic performance of hybrid Battery Energy Storage System (BESS) + offshore wind across Nova Scotia sites.

underestimates extremes in Canadian offshore waters. Temporal variations are shown across all datasets and statistical metrics, such as mean, median, maximum, minimum, and coefficient of variation. They were calculated to quantify differences in wind behaviour. Data completeness was also assessed, with MSC50 providing 100% coverage over the study period. Overall, this multi-dataset comparison highlights the strengths and limitations of each source, demonstrating that MSC50 offers the most consistent and high-resolution representation of local offshore wind conditions for energy production modelling (Figure 11).

To better visualize temporal variations in wind conditions, hourly wind speed heatmaps were generated for both the NASA MERRA-2 and MSC50 datasets, with the x-axis representing hours throughout the year and the y-axis indicating wind speed in metres per second. These heatmaps provide an intuitive view of seasonal and diurnal patterns, highlighting periods of high and low wind availability. Additionally, a delta heatmap (MSC50 minus NASA MERRA-2) was created to identify systematic differences between the datasets, revealing potential biases or discrepancies in wind representation. Such comparisons are critical for offshore wind resource assessment, as they inform the selection of reliable datasets for energy production modelling and help quantify the uncertainty associated with different wind data sources (Figure 12).

5. CONCLUSION

This study demonstrates a compelling technical and economic case for large-scale

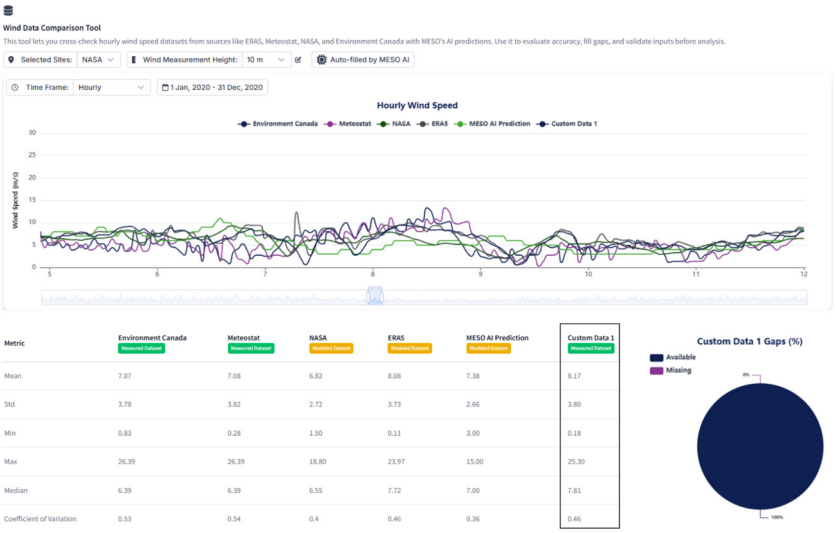

Figure 11: Hourly wind speed comparison between modelled and measured datasets, including Environmental Canada, Meteostat, NASA MERRA-2, ERA5, MESO-AI predictions, and MSC50. Insets show statistical metrics (mean, median, maximum, minimum, and coefficient of variation) and data completeness (percentage of available data).

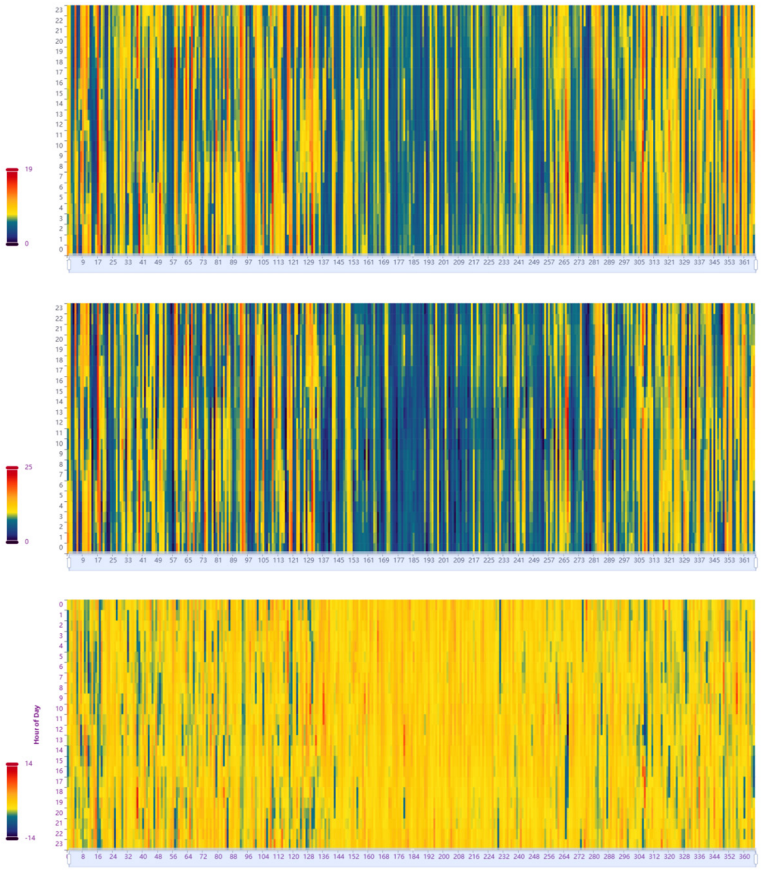

Figure 12: Spatial distribution of average wind speeds from NASA MERRA-2 and MSC50 datasets, and their difference (MSC50 minus NASA MERRA-2) across the study area.

offshore wind development in Nova Scotia. Using the high-resolution MSC50 wind dataset, the assessed sites show significantly higher energy outputs and capacity factors than ERA5 or NASA MERRA-2 data products (average annual generation: 52.8 TWh; CF: 51%). Economic evaluations indicate that both export oriented (US/Canada) and domestic hybrid supply scenarios are financially viable, particularly under subsidy support.

Hybrid offshore wind-BESS systems further improve grid stability and resource utilization, achieving an LCOE of $60 /MWh, LCOS of $123 /MWh, and an IRR of 7%.

Surplus wind generation can be profitably exported to neighbouring jurisdictions such as the US East Coast or Wind West markets. Environmentally, the system yields substantial emission reductions (average 16.9 Mt CO_2e), significantly decreasing reliance on fossil fuel generation. Overall, the findings position Nova Scotia as a potential renewable energy exporter and a strategic clean power hub in Atlantic Canada.

Potential future research could expand on this study by conducting detailed policy sensitivity analyses to evaluate how changes in subsidies, market structures, and regulatory frameworks influence project viability. In addition, further work could investigate advanced hybrid energy export scenarios, including multi-jurisdictional transmission pathways and optimized offshore wind-BESS configurations, to better understand Nova Scotia's long-term role in regional clean energy trade.

ACKNOWLEDGMENT

The authors gratefully acknowledge financial support from the Government of Newfoundland and Labrador and the National Research Council of Canada – Industrial Research Assistance Program, which made this work possible.

Authors' Declaration

- Ethical approval: This study does not involve human participants or animals.
- Competing interests: The authors declare competing interests related to patents and potential commercialization of the tools described.
- Availability of data and materials: The datasets generated and analyzed during this study are available from the corresponding author upon reasonable request.
- Artificial intelligence: During the preparation of this work, the authors used AI-assisted tools to support text refinement and editing. After using these tools, the authors reviewed and revised all content as needed and take full responsibility for the final manuscript.

REFERENCES

[1] G. Daborn, S. Parsons, L. Whitman, A. Wilkie (co-chair), and J. Wooder (co-chair), "Regional Assessment of Offshore Wind Development in Nova Scotia," Regional Assessment Committee Established by the Federal Minister of Environment and Climate Change, Nova Scotia, Canada, Jan. 2025. Accessed: Dec. 10, 2025. [Online]. Available: https://iaac-aeic.gc.ca/050/documents/p83514/160595E.pdf

[2] Government of Nova Scotia, "Nova Scotia Offshore Wind Roadmap- Module 3," Nova Scotia, Canada, Jul. 2025. Accessed: Dec. 10, 2025. [Online]. Available: https://novascotia.ca/offshore-wind/docs/offshore-wind-roadmap-module-3.pdf

[3] Natural Resources Canada, "Designated Offshore Wind Energy Areas," Jul. 2025. Accessed: Dec. 10, 2025. [Online]. Available: https://novascotia.ca/offshore-wind/docs/designated-offshore-wind-energy-areas.pdf

[4] Canada-Nova Scotia Offshore Energy Regulator. "Governments Designated Offshore Wind Energy Areas." CNSOER.ca. Accessed: Dec. 05, 2025. [Online]. Available: https://cnsoer.ca/renewable-energy/lands-management/governments-designated-offshore-wind-energy-areas

[5] Nova Scotia Power. "Clean Energy Sources." nspower.ca. Accessed: Dec. 05, 2025. [Online]. Available: https://www.nspower.ca/cleanandgreen/clean-energy/clean-energy-sources

[6] J. Xie et al., "Dynamics of Offshore Wind Turbine Foundation: A Critical Review and Future Directions," *Journal of Marine Science and Engineering*, vol. 13, no. 10, p. 2016, Oct. 2025, doi: 10.3390/JMSE13102016.

[7] E. Faraggiana, G. Giorgi, M. Sirigu, A. Ghigo, G. Bracco, and G. Mattiazzo, "A review of numerical modelling and optimisation of the floating support structure for offshore wind turbines," *Journal of Ocean Engineering and Marine Energy*, vol. 8, no. 3, pp. 433–456, Jul. 2022, doi: 10.1007/S40722-022-00241-2.

[8] V. R. Swail et al., "The MSC50 Wind and Wave Reanalysis," presented at the 9th International Workshop on Wave Hindcasting & Forecasting, Victoria, BC, Canada, Sept. 24-29, 2006. [Online]. Available: https://www.oceanweather.com/about/papers/The%20MSC50%20Wind%20and%20Wave%20Reanalysis.pdf

[9] Fisheries and Oceans Canada. "MSC50 Wind and Wave Climate Hindcast." dfo-mpo.gc.ca. Accessed: Dec. 05, 2025. [Online]. Available: https://www.meds-sdmm.dfo-mpo.gc.ca/isdm-gdsi/waves-vagues/MSC50-eng.html

[10] F. Caccia and A. Guardone, "Numerical Simulations of Ice Accretion on Wind Turbine Blades: Are Performance Losses Due to Ice Shape or Surface Roughness," *Wind Energy Science*, vol. 8, no. 3, pp. 341–362, Mar. 2023, doi: 10.5194/WES-8-341-2023.

[11] Z. Malecha and G. Dsouza, "Modeling of Wind Turbine Interactions and Wind Farm Losses Using the Velocity-Dependent Actuator Disc Model," *Computation*, vol. 11, no. 11, p. 213, Nov. 2023, doi: 10.3390/COMPUTATION11110213.

[12] E. J. Aju, D. Kumar, M. Leffingwell, M. A. Rotea, and Y. Jin, "The Influence of Yaw Misalignment on Turbine Power Output Fluctuations and Unsteady Aerodynamic Loads Within Wind Farms," *Renewable Energy*, vol. 215, p. 118894, Oct. 2023, doi: 10.1016/J.RENENE.2023.06.015.

[13] E. Gulski et al., "Discussion of Electrical and Thermal Aspects of Offshore Wind Farms' Power Cables Reliability," *Renewable and Sustainable Energy Reviews*, vol. 151, p. 111580, Nov. 2021, doi: 10.1016/J.RSER.2021.111580.

[14] J. A. Pilgrim and S. Kelly, "Thermal and Economic Optimisation of Windfarm Export Cable," Journal of Engineering, vol. 2019, no. 18, pp. 4991–4995, Jun. 2019, doi: 10.1049/JOE.2018.9272.

[15] S. Krohn, P.E. Morthorst, and S. Awerbuch, "The Economics of Wind Energy," European Wind Energy Association, Mar. 2009, Accessed: Dec. 05, 2025. [Online]. Available: https://www.ewea.org/fileadmin/files/library/publications/reports/Economics_of_Wind_Energy.pdf

[16] B. G. Thurber, R. J. Kilpatrick, G. H. Tang, C. Wakim, and J. R. Zimmerling, "Economic Impacts of Curtailing Wind Turbine Operations for the Protection of Bat Populations in Ontario," *Wind*, vol. 3, no. 3, pp. 291–301, Sep. 2023, doi: 10.3390/WIND3030017/S1.

[17] C. Augustine and N. Blair, "Storage Futures Study: Storage Technology Modeling Input Data Report," National Renewable Energy Laboratory, Golden, CO, USA, NREL/TP-5700-78694, doi: 10.2172/1785959.

[18] Nova Scotia Power. "Electricity." nspower.ca. Accessed: Dec. 05, 2025. [Online]. Available: https://www.nspower.ca/about-us/producing

[19] M. K. P, "High-Voltage Direct Current (HVDC) Transmission: Reliability and applications," *World Journal of Advanced Research and Reviews*, vol. 16, no. 02, pp. 1207–1215, Nov. 2022, doi: 10.30574/wjarr.2022.16.2.1074.

[20] B. Gustavsen and O. Mo, "Variable Transmission Voltage for Loss Minimization in Long Offshore Wind Farm AC Export Cables," in *IEEE Transactions on Power Delivery*, vol. 32, no. 3, pp. 1422-1431, June 2017, doi: 10.1109/TPWRD.2016.2581879.

[21] C. Plet. "Will the New Nova Scotia Independent Energy System Operator Advance Coordinated Offshore Grid Planning?" DNV.com. Accessed: Dec. 05, 2025. [Online]. Available: https://www.dnv.com/article/will-the-new-nova-scotia-independent-energy-system-operator-advance-coordinated-offshore-grid-planning/

[22] S. Lamichhane and A. Dubey, "Stochastic Economic Dispatch with Battery Energy Storage considering Wind and Load Uncertainty," 2025, Accessed: Dec. 10, 2025. arXiv:2509.18100.

Digital Stakeholder Engagement

Dr. Khalid Kamhawi

Waterfront application technology

Who should read this paper?

This paper should be read by researchers, practitioners, and policy-makers working in marine spatial planning, offshore wind development, and fisheries management. It is also relevant to technologists and ocean industry stakeholders seeking evidence-based digital solutions for reducing marine sector conflict.

Why is it important?

This work presents a technically detailed examination of Waterfront, a digital, cloud-based, real-time stakeholder engagement platform designed to mitigate conflicts between offshore wind projects and commercial fisheries. Waterfront replaces fragmented, low-fidelity communication channels with an integrated architecture that fuses Automatic Identification System telemetry, geospatial analytics, metocean forecasting, and secure bidirectional messaging. It introduces advanced functionalities such as automated vessel speed compliance monitoring, geofenced risk detection, ghost gear retrieval, and multitask machine learning models that predict spatial conflict hotspots.

Digital stakeholder engagement technologies can address long-standing communication failures between marine sectors, a barrier repeatedly identified in global case studies and stakeholder interviews. The research provides empirical evidence that such tools improve situational awareness, reduce gear interaction risks, and support coexistence in increasingly crowded ocean spaces. By operationalizing multi use and coexistence principles through real-time data exchange, the work offers a scalable model for sustainable ocean governance amid accelerating offshore wind deployment.

The technology is available for commercial application. As a SaaS product, it is in continuous development and there are periodic updates with new features and functionalities.

About the author

Dr. Khalid Kamhawi is the founder of Ithaca Clean Energy where he leads the development of digital technologies that support marine sustainability and cleantech by leveraging artificial intelligence and machine learning solutions. He holds a PhD in mathematics from Imperial College London and a B.Sc. in mechanical engineering from Carnegie Mellon University.

FACILITATING COEXISTENCE BETWEEN FISHERIES AND OFFSHORE WIND THROUGH DIGITAL STAKEHOLDER ENGAGEMENT TECHNOLOGY

Khalid Kamhawi
Ithaca Clean Energy (a.k.a. Manifoldz Inc.), New Bedford, MA, USA
Corresponding author: khalid.kamhawi@ithacacleanenergy.com
DOI: https://doi.org/10.48336/WQ24-VQ46

ABSTRACT

The global expansion of offshore wind energy is a cornerstone of climate mitigation strategies, yet it introduces spatial conflicts with traditional marine sectors, particularly commercial fisheries. These conflicts arise from overlapping operational zones, gear entanglement risks, and navigational risks; all due to an underlying barrier of insufficient communication between stakeholders. This paper examines the Waterfront Application (or "Waterfront"), a digital stakeholder engagement platform designed to enable coexistence and multi-use of ocean space by providing real-time, location-based information exchange between offshore wind developers and fisheries. Drawing on empirical insights from stakeholder interviews, technical development milestones, and deployment data, the paper details Waterfront's architecture, functionalities, and risk mitigation strategies. The platform's features – including dynamic notifications, vessel speed compliance, gear pinning, ghost gear tagging, ecological observation logging, and secure messaging – address critical challenges in marine spatial planning. Results from field implementation demonstrate improved situational awareness, reduced operational conflicts, and enhanced trust among marine stakeholders. Waterfront exemplifies how digital innovation can support sustainable ocean governance and facilitate colocation of offshore wind and fisheries within integrated marine spatial planning frameworks.

Keywords: Offshore wind, fisheries, marine spatial planning, coexistence, multi-use, digital engagement, stakeholder communication, gear pinning, ecological monitoring, ocean governance

1. INTRODUCTION

Offshore wind energy has emerged as a critical component of global decarbonization efforts, with projections indicating that installed capacity will exceed 400 gigawatts (GW) by 2040 [1]. Recent data from the International Energy Agency show that global offshore wind capacity reached 64 GW in 2024, with an expected annual growth rate of 18%, positioning offshore wind as one of the fastest-growing renewable technologies [1]. This expansion is essential for reducing greenhouse gas emissions, as each GW of offshore wind can power approximately 1 million households and offset 3.5 million metric tons of CO_2 annually [1], [3].

Despite these benefits, offshore wind development introduces complex spatial challenges in marine environments. Offshore wind farms occupy extensive sea areas traditionally used by commercial fisheries, creating potential conflicts over access, navigation, and operational safety. Studies indicate that up to 15% of prime fishing grounds in the US Northeast overlap with proposed offshore wind lease areas, potentially displacing fishing effort and increasing operational risk [2], [9]. These conflicts are compounded by the dynamic nature of offshore activities, where vessel movements, construction schedules, and maintenance operations intersect with fishing patterns [2].

Conventional communication mechanisms – such as email notifications and static notices to mariners – are inadequate for managing these interactions in real time. Consequently, there is a growing need for technological solutions that enable proactive, transparent, and evidence-based engagement between offshore wind developers and marine stakeholders to support coexistence and multi-use of ocean space [3].

2. BACKGROUND AND RATIONALE

Marine Spatial Planning (MSP) has emerged as a critical governance tool for balancing competing uses of ocean space, particularly in regions experiencing rapid offshore wind development. The European Union's MSP Directive (2014/89/EU) mandates member states to implement integrated planning frameworks that promote coexistence among sectors such as energy, fisheries, and conservation [4]. However, practical implementation remains uneven, and case studies reveal persistent challenges in reconciling offshore wind expansion with commercial fisheries.

In Denmark, one of the earliest adopters of offshore wind, coexistence strategies have included turbine spacing adjustments and cable burial standards to accommodate certain fishing activities. Danish projects such as Horns Rev have demonstrated that pot fisheries can operate within wind farm boundaries under specific conditions, though trawling remains largely incompatible due to gear interaction risks [5]. Similarly, the Netherlands has advanced multi-use concepts through its North Sea 2050 Spatial Agenda, which explores the colocation of offshore wind with aquaculture and passive fisheries. Pilot projects have tested mussel and seaweed cultivation within wind farm zones, highlighting opportunities for synergistic uses while underscoring the need for robust monitoring and stakeholder engagement [6].

In the United Kingdom, the Crown Estate's leasing rounds have accelerated offshore wind deployment, yet fisheries organizations have raised concerns about cumulative spatial impacts. The National Federation of Fishermen's Organisations emphasizes that without proactive planning and transparent communication, offshore wind expansion risks displacing fisheries and eroding coastal livelihoods [2]. Scotland's sectoral marine plan for offshore wind incorporates coexistence principles, but floating wind technologies introduce new complexities. Trials at Hywind Scotland, the world's first floating wind farm, revealed that dynamic mooring systems pose significant challenges for mobile gear fisheries, necessitating research into alternative mooring configurations such as tension-leg systems to enhance compatibility [7].

Beyond Europe, Japan's offshore wind strategy under the "Vision for Offshore Wind Power" includes provisions for stakeholder engagement and coexistence with fisheries, reflecting cultural and economic reliance on marine resources. Pilot projects in Akita and Chiba Prefectures have integrated fisheries liaison committees into planning processes, though technological solutions for real-time communication remain limited [8]. The United States Bureau of Ocean Energy Management (BOEM) has issued draft Fisheries Mitigation Guidance recommending digital platforms to disseminate survey and construction schedules, which, as will be discussed, aligns with the functional objectives of Waterfront [9].

Collectively, these global experiences underscore that coexistence is not merely a regulatory aspiration but a technical and operational challenge requiring innovative solutions. While policy frameworks advocate for multi-use, their success depends on tools that provide transparency, traceability, and responsiveness in stakeholder engagement. Waterfront addresses these gaps by operationalizing coexistence principles through real-time data exchange, spatial awareness, and risk mitigation, complementing international best practices and advancing the discourse on sustainable ocean governance.

2.1 Offshore Wind Policy Shifts: The United States as an Example

In the United States, BOEM has played a central role in advancing offshore wind leasing and permitting. As of late 2024, BOEM had issued over 30 active offshore wind leases, primarily along the Atlantic Outer Continental Shelf, representing a technical potential of 2,000 GW – nearly double current US electricity demand [9]. However, recent policy developments have introduced significant delays and cancellations. In 2023-2024, several high-profile projects, including portions of the New York Bight and Gulf of Maine lease areas, experienced permit suspensions or work order cancellations due to concerns over cumulative environmental impacts, stakeholder opposition, and escalating costs.

The US Department of the Interior cited impacts on ocean users, including commercial fisheries and maritime navigation, as key factors in these decisions. Fisheries organizations have argued that offshore wind development could displace up to 15-20% of prime fishing grounds in the Northeast, affecting sectors that contribute $4.8 billion annually in landings value [2]. These spatial conflicts, combined with inflationary pressures

and supply chain constraints, have led to renegotiations of power purchase agreements and, in some cases, project terminations. In late 2024, two major developers withdrew from planned projects in New Jersey and Massachusetts, citing "unresolved coexistence challenges and regulatory uncertainty" [10].

BOEM's Draft Fisheries Mitigation Guidance (2022) acknowledges these challenges and recommends digital platforms for real-time communication of survey and construction schedules, aligning with the functional objectives of Waterfront [9]. This reflects a broader recognition that coexistence is not merely a regulatory aspiration but a technical and operational necessity requiring innovative solutions.

However, with the onset of 2025, the Trump Administration repeatedly delayed offshore wind development by suspending permits and issuing broad stop work orders that halted construction on multiple major projects along the East Coast [11]. In December 2025, the Interior Department ordered all work on five large-scale offshore wind farms – including Revolution Wind, Vineyard Wind 1, Empire Wind 1, Sunrise Wind, and the Coastal Virginia Offshore Wind project – to stop for at least 90 days, citing unspecified national security concerns such as radar interference, despite earlier federal reviews that had already addressed these issues. Developers and state officials criticized the move as arbitrary and politically motivated, noting that many of the projects were more than 80% complete and had undergone years of consultation with the Department of Defense, which had previously approved mitigation measures [12].

2.2 Offshore Wind Impacts on Fishing Effort

Offshore wind development can significantly disrupt commercial fisheries by reducing access to traditional fishing grounds, increasing operational risks, and introducing financial uncertainty. These impacts occur throughout the offshore wind project life cycle – from site surveys and construction to operation and maintenance – due to vessel traffic, safety exclusion zones, and subsea infrastructure hazards [2], [5].

Specific disruption factors include:

- Potential damage or loss to gear, nets, and other equipment caused by offshore wind vessel activities, introducing financial risk for fishers.
- Increased marine traffic and the risk of collision in wind farm areas, resulting in a reduction in fishing effort.
- Elevated collision risk for fishing vessels operating near wind farm boundaries during construction and maintenance phases.

A study by Bonsu et al. [13] documented a 30% increase in near-miss incidents in Danish waters during peak construction periods. Studies in the North Sea indicate that offshore wind farms can displace up to 10-20% of trawl fishing effort within designated lease areas [6]. Danish projects such as Horns Rev and Anholt demonstrated that while pot fisheries (e.g., lobster and crab) can operate within turbine arrays under controlled conditions, mobile gear fisheries remain largely excluded because of snagging risks on subsea cables and rock armouring [5]. Similarly, pilot projects in the Netherlands tested mussel and

seaweed cultivation within wind farm zones, highlighting opportunities for aquaculture but confirming persistent challenges for traditional trawling [6]. Floating wind technologies introduce additional complexities. Trials at Hywind Scotland revealed that dynamic mooring systems pose significant hazards for mobile gear fisheries, with snagging incidents reported during early deployment phases [7]. Research into alternative mooring configurations, such as tension-leg systems, is ongoing to enhance compatibility.

Industry reports indicate that gear loss incidents associated with offshore wind activities can cost individual fisheries $10,000-$50,000 per event [2]. Delays in conflict resolution and compensation claims have been cited as contributing factors to project permitting challenges, increasing development costs by 5-10% in some US projects [9].

In the United States, the National Marine Fisheries Service estimates that commercial fisheries in the Northeast generate $4.8 billion annually in landings value, supporting over 40,000 jobs [2]. BOEM's environmental impact assessments suggest that proposed lease areas in the New York Bight and Gulf of Maine overlap with 15–20% of prime fishing grounds [9]. These spatial conflicts have been cited as contributing factors in recent permit delays and cancellations.

2.3 Impacts of Delaying Offshore Wind Deployment

Delays in offshore wind development have significant economic repercussions, affecting both project viability and broader decarbonization targets. These delays often stem from regulatory uncertainty, stakeholder opposition, and supply chain constraints, with coexistence challenges frequently cited as contributing factors [9]. As projects are required to avoid, minimize, or compensate for their marine impacts, developers face political and financial challenges from ocean stakeholders that delay acquiring permits, decrease vessel utilization, and interfere with maintenance campaigns. For the wind developer, this results in lost green energy generation, avoidable carbon emissions, pre-emptive fishery mitigation compensation costs, and high insurance spending.

Recent analyses indicate that permitting delays of 12-18 months can increase capital expenditure (CAPEX) by 5-15%, primarily due to extended vessel charter periods, inflationary pressures, and contractual penalties [1]. For large-scale projects exceeding 1 GW, this translates into additional costs of $150-$300 million per project. Furthermore, developers face increased insurance premiums and pre-emptive compensation obligations to fisheries, which can add $10-$50 million depending on the scale of spatial conflicts [2].

Operational delays reduce the time turbines are generating electricity, resulting in lost revenue and deferred climate benefits. A one-year delay for a 1 GW offshore wind farm can forgo approximately 4 TWh of clean energy generation, equivalent to avoiding 1.4 million metric tons of CO_2 emissions [1]. In 2023-2024, several US projects experienced cancellations or renegotiations due to escalating costs and unresolved coexistence issues. Developers cited "unanticipated regulatory delays" as primary drivers,

with some projects withdrawing after cost projections exceeded $12 billion [10]. At a national level, these delays threaten the achievement of renewable energy targets; US goals of 30 GW by 2030 could be reduced by 30-40% due to permitting bottlenecks [1].

2.4 Barriers to Coexistence: Lack of an "Evidence Based Relationship"

Through customer discovery, fishers have identified specific hazards to marine coexistence, such as gear snagging on subsea cables, collisions with turbines, and depleted wildlife populations. In 2020, Ithaca Clean Energy participated in the National Science Foundation (NSF) Innovation Corps (I-Corps) program at Cornell University. As NSF I-Corp team #1799, Ithaca Clean Energy held over 140 customer discovery interviews with marine stakeholders, particularly from the offshore wind and fisheries industries.

These interviews revealed that offshore wind developers do not have effective ways to share real-time information, leading to poor communication, disjointed coordination, and a lack of accountability. Key consensus points included:

- No streamlined automated way to share information between fisheries and developers.
- Fisheries will not share information willingly; they will usually only react to provided information.
- Data exchange is limited and not used to avoid or minimize impacts.
- Fisheries need to know offshore wind vessel activities beforehand for waterfront decisions.
- Communication via email notifications is ineffective, static, and not traceable.

Stakeholder testimonials highlighted these gaps:

"There is no streamlined way to share information ... There is a definite need to do so." Scientist, NOAA
"Fisheries need to know activities of offshore wind vessels beforehand to take optimal waterfront decisions." Director, seakeeper.org
"Fisheries will not share information willingly; they will only react to information provided to them." FLO, Major US Offshore Wind Developer

The underlying structural barriers stem from long standing disconnects between offshore wind developers and the fishing community. Data fragmentation remains a core issue, as both groups operate on separate, often incompatible digital systems, preventing real-time visibility, shared situational awareness, or coordinated decision-making. This separation leads to misunderstandings, duplicated efforts, and missed opportunities for proactive planning. Compounding this is a deep trust deficit, shaped by years of fishers feeling excluded from early planning phases and skeptical that coexistence efforts genuinely account for their operational realities. This historical tension makes collaboration harder and slows the adoption of new tools, even when they are beneficial. Finally, regulatory gaps persist – while agencies such as BOEM recommend digital engagement and transparency enhancing technologies, their adoption remains largely voluntary. Without enforceable standards or incentives, uptake varies widely across developers, preventing

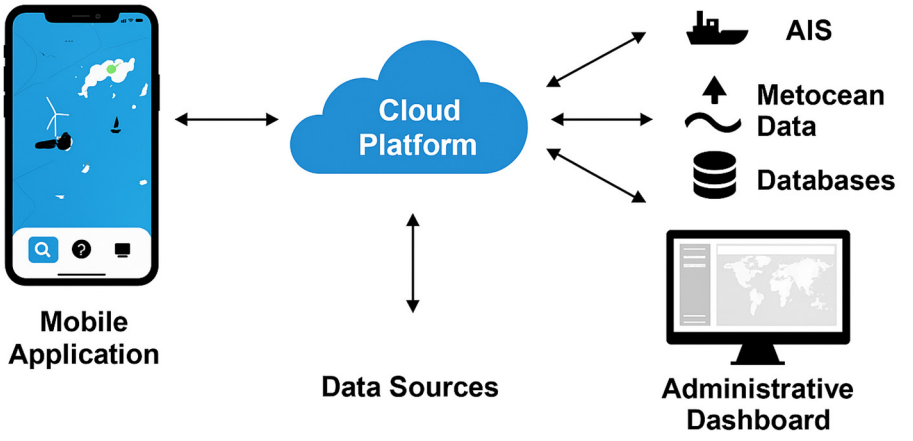

Waterfront Architecture and Data Flow

Figure 1: Waterfront architecture and data flow. The diagram illustrates the integration of mobile applications (iOS and Android), cloud-based services, Automatic Identification System (AIS) data streams, metocean forecasting, and secure messaging channels. It highlights the bidirectional flow of information between offshore wind developers and fisheries stakeholders, enabling real-time situational awareness and proactive conflict mitigation. Source: Adapted from Ithaca Clean Energy internal architecture documentation.

consistency and limiting the effectiveness of industry wide coexistence frameworks.

3. DIGITAL MARINE STAKEHOLDER ENGAGEMENT APPLICATION: WATERFRONT

Waterfront provides marine stakeholders with a comprehensive, real-time information feed that selectively streamlines activity logistics and environmental conditions. It eliminates the need to access multiple platforms (email, mariner updates, project postings) by combining them into a single mobile application. This supports an evidence-based framework to mitigate impacts on fisheries and helps developers meet federal stakeholder engagement guidance. By disseminating location-based marine information, the technology addresses opposition that leads to project delays and increased costs. It allows fishing vessels to avoid collisions and gear snagging, diffusing tensions and removing permitting roadblocks. This enables faster and more sustainable deployment of offshore wind, supporting decarbonization strategies and reversed economic hardship for coastal communities.

3.1 Waterfront Technology Architecture

Waterfront is composed of a native mobile application (iOS and Android) with a desktop/web admin dashboard, powered by cloud computing data repository web services (Figure 1). The mobile app is free to download and use and constitutes a map-based interface that streamlines relevant project information pertaining to marine activities, site specific metocean data, bathymetry, weather forecasting, and Automatic Identification System (AIS) marine traffic based on the user's location and preferences. The desktop/web admin dashboard provides the customers with access to data governance settings, control panels, integration functionalities, data analytics, and reporting features.

Waterfront is both a data provider and a data aggregator, facilitating the logging,

gathering, and sharing of marine activity and data (subject to data governance and privacy restrictions) alongside integrated external environmental, weather, and marine traffic inputs and third-party Application Programming Interfaces (APIs).

Waterfront combines machine learning, cloud-based data, and a mobile user interface into an information-sharing platform. It is a multi-partner system that facilitates real-time digital communication and data exchange.

The machine learning, data driven Waterfront platform enables offshore wind developers to optimize marine activity planning and decision-making, reducing operational risks and CAPEX. At its core, the platform offers several proprietary capabilities designed to streamline communication, enhance situational awareness, and strengthen collaboration between offshore wind projects and the fishing community. Its Marine Update Engagement feature allows users to tag and raise a "case" on any project marine update, triggering a dedicated workflow and opening a private communication channel with the offshore wind farm to resolve issues efficiently. Waterfront also provides robust offline data gathering tools, including gear pinning and unpinning – which records gear type, location, and time to help prevent loss and damage – and ecological observation logging, enabling users to capture fisheries related sightings with GPS precision. A multi task supervised machine learning model predicts spatial hotspots where conflict or interaction between fisheries and offshore wind activity is likely, generating proactive planning and navigational alerts. User participation is further strengthened through reinforcement learning based incentives, rewarding frequent information sharing with tokens, perks, and enhanced access. To ensure interoperability across the marine industry, Waterfront is also developing APIs that allow its mapped intelligence to integrate seamlessly with various vessel plotter and navigation software systems.

Key architectural components include:

- **Cloud-based Services Layer:** Functions as the core processing hub for data integration and forecasting.
- **Geospatial Analytics and AIS Data:** Integrates vessel position and movement streams for dynamic mapping and collision avoidance.
- **Metocean Forecasting Module:** Provides predictive insights into oceanographic and meteorological conditions.
- **Secure Messaging:** Facilitates bidirectional communication using AES-256 encryption and multi-factor authentication.
- **Offline Data Caching:** Maintains functionality in low-bandwidth offshore environments.

Recognizing connectivity limitations offshore, Waterfront incorporates offline data caching and synchronization protocols to maintain functionality in low-bandwidth offshore environments. Risk mitigation strategies include strict data governance protocols, interoperability with vessel navigation systems, and redundancy through distributed cloud architecture to ensure service continuity. By enabling transparent, real-time communication and spatial awareness, Waterfront reduces the likelihood of gear damage, navigational hazards, and operational disputes. The platform

supports proactive conflict avoidance, fosters trust, and aligns with regulatory guidance for stakeholder engagement, thereby facilitating colocation of offshore wind and fisheries within shared marine spaces [9].

The mobile application layer serves as the primary user interface for fisheries stakeholders and offshore wind operators, providing real-time notifications, gear pinning functionality, and ecological observation logging.

The cloud-based services layer functions as the system's core processing hub, hosting geospatial analytics, AIS data integration, and metocean forecasting modules. This layer employs distributed architecture to ensure redundancy and resilience, while leveraging scalable computing resources to support high-volume data exchange during peak operational periods.

AIS data streams are integrated to deliver vessel position and movement information, enabling dynamic mapping of marine traffic and proactive collision avoidance. These data streams are processed in real time and synchronized with user-defined "Areas of Interest" to generate targeted alerts for fisheries stakeholders. The metocean forecasting module provides predictive insights into oceanographic and meteorological conditions, supporting safe navigation and operational planning. By combining historical datasets with real-time sensor inputs, the system enhances situational awareness and reduces risk during construction and maintenance activities.

Finally, the secure messaging subsystem facilitates bidirectional communication between developers and marine stakeholders, incorporating AES-256 encryption and multi-factor authentication to ensure confidentiality and compliance with ISO/IEC 27001 standards. This component underpins trust and accountability, enabling transparent engagement and traceable decision-making across the project life cycle.

3.2 Waterfront Distinguishing Features

Waterfront offers a suite of distinguishing features designed to enhance safety, efficiency, and environmental stewardship across the maritime community. It provides secure private and group chat, enabling fishers to communicate confidentially while identifying vessels via Maritime Mobile Service Identify numbers to form effective collaborative groups. Its gear pinning function allows users to mark the live location of equipment such as trawl nets or lobster pots, reducing gear loss and simplifying compensation claims. The platform also records detailed vessel paths on a dynamic map, giving fishers a verifiable history of their traditional fishing areas for use in displacement related compensation processes. In support of marine conservation efforts, Waterfront includes ecological observation logging so users can record sightings of wildlife and hazards for biodiversity monitoring. Stakeholders can further define Areas of Interest and receive alerts when vessels enter those zones. Additionally, Waterfront's ghost gear functionality enables fishers to locate missing or lost gear and retrieve it safely, helping reduce marine debris and clear plastics from the ocean.

Waterfront's Vessel Speed Compliance functionality transforms a previously slow, manual, and error prone reporting workflow

into a fully automated, real-time solution aligned with the strict requirements of the Incidental Harassment Authorization and the North Atlantic Right Whale Strike Management Plan. Under these regulations, project vessels must adhere to seasonal 10 knot restrictions, with speed exceedances permitted only in limited zones or under specific exceptions such as emergency response or manoeuvrability related safety needs. Waterfront continuously monitors vessel transits through high risk areas – including Woods Hole, Quicks Hole, and Muskeget Channel – where challenging oceanographic conditions often require brief speed increases for safe manoeuvring. As soon as a vessel exceeds 10 knots in these regions, the system flags the event instantly, supporting the mandated 24 hour reporting requirement to US Bureau of Safety and Environmental Enforcement (BSEE).

A major technical advancement of the Waterfront platform is its ability to unify AIS feeds with its own vessel tracking engine and apply real-time geofenced speed compliance logic. Unlike legacy workflows that required offshore wind projects up to six days to manually process AIS data, identify potential speed deviations, and verify conditions across an entire week of vessel activity, Waterfront executes the entire process in seconds. It analyzes live AIS transmissions, computes vessel speed at sub minute intervals, and checks compliance against any geofence shape or boundary, whether large zones like Narragansett Bay or irregular manoeuvre restricted corridors like Woods Hole. This enables instant detection when a vessel enters or exits a regulated region at >10 knots, delivering precise metadata – including coordinates, timestamps, and duration of exceedance – to compliance managers immediately.

Prior systems triggered inconsistent notifications and lacked contextual information such as where the exceedance occurred or how long it lasted. This forced compliance managers to manually inspect 24 hour AIS histories, creating inefficiencies and increasing the risk of missing BSEE's strict reporting window. Waterfront replaces all of this with continuous, automated processing: vessels travelling above 10 knots outside allowed seasonal zones are flagged instantly, while vessels navigating inside the three manoeuvre restricted corridors are treated differently, recognizing that exceedances there typically fall under safety exceptions but still require rapid review. By merging AIS, custom geofences, and real-time analytics, Waterfront ensures full regulatory compliance and eliminates weeks' long data delays – delivering a step change improvement over historical practices.

Waterfront's ghost gear functionality is built around a simple but powerful idea: when fishers can precisely tag and geolocate lost or found gear, the entire marine community becomes part of a coordinated recovery network. Waterfront's ghost gear retrieval module was developed in close collaboration with crabbers in Humboldt Bay, who experience firsthand the environmental and financial impact of lost pots, buoys, and lines that become plastic debris in the water.

Each time a fisher encounters gear in the water, they can log it in the system with a detailed tag

– selecting the gear type, adding a description, attaching photos, and including optional tag IDs. The platform automatically captures GPS coordinates and timestamps, creating a clear, time anchored record of when and where the gear was identified. This structured data ensures that even gear discovered in rough conditions or remote areas is documented with accuracy, giving owners the information they need to determine whether the item belongs to them and how to retrieve it safely.

Once logged, the information is shared securely across the Waterfront community, instantly notifying nearby users and allowing the rightful owner to take action. Push alerts inform fishers when gear is found near their typical fishing grounds, while protecting anonymity for those reporting gear and supports efficient communication between finders and owners. A built in chat feature enables direct but secure communication between the finder and the owner, coordinating pickup whether the gear remains in place, has been moved, or has been brought on board. By combining tagging, geolocation, timestamps, and real-time alerts, Waterfront transforms what used to be chance encounters and costly losses into a collaborative, transparent system that quickly reconnects fishers with their gear and reduces plastic waste in the ocean.

4. IMPLEMENTATION AND RESULTS

The deployment of the Waterfront platform was executed progressively across multiple offshore wind projects in the US Northeast and California, with pilot engagements extending to fisheries communities in Massachusetts, Rhode Island, Connecticut, Humboldt Bay, New Jersey, and New York. Strategic partnerships with major developers such as Orsted, RWE, Avangrid, and Vineyard Offshore, alongside fisheries organizations including the Commercial Fisheries Center of Rhode Island and the Massachusetts Lobstermen's Association, facilitated targeted onboarding and adoption. The rollout coincided with critical operational phases of offshore wind development, including survey campaigns and early construction activities, ensuring that the platform addressed real-time coexistence challenges.

4.1 Data Sources

Data presented in this section is derived from Google Analytics and iOS Apple Analytics, collected over three consecutive quarters (Q1-Q3 2024). This multi-quarter dataset provides a robust basis for evaluating user acquisition, engagement, and feature utilization trends, as well as interpreting the platform's impact on stakeholder coordination and operational efficiency. The data used in this paper is limited by the accuracy of the source systems, updates, corrections, or system errors. The data has been processed to adhere to Ithaca Clean Energy's Privacy Policy requirements. The performance metrics of the application are subject to variations based on factors such as load, user behaviour, network conditions, updates, and other environmental factors. Therefore, these metrics should not be used as the sole basis for making decisions about the overall health or performance of the application. Finally, the analysis and interpretations in this report are based on the data available at the time of writing and do not constitute a definitive or complete interpretation of the overall performance of the application.

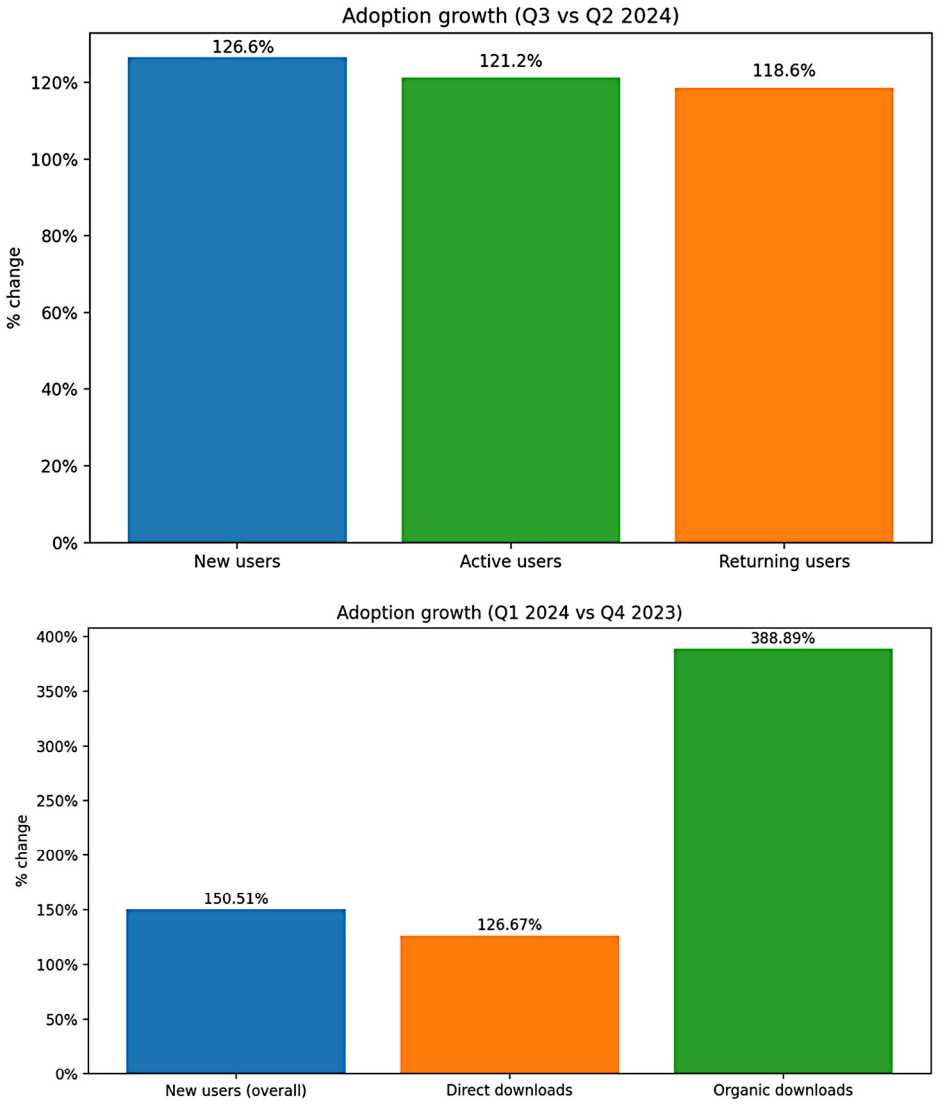

Figure 2: (top) Waterfront adoption percentage growth rates Q3 vs. Q2 2024. (bottom) Waterfront adoption channel percentage growth rates Q1 2024 vs. Q4 2023.

4.2 Results: User Adoption

Between 2023-2025, Waterfront experienced substantial momentum across all major user and engagement metrics (Figure 2). Early baseline comparison (Q1 vs. Q4 2023) for adoption has new users (overall) +150.51%, direct +126.67%, organic +388.89%. From 2024, new user registrations rose by 126.6%, while active user engagement increased by 121.2% over the same period. Returning users grew by 118.63%, reflecting strengthening platform loyalty.

In California, adoption continued to build through targeted on water workflows (e.g., ghost gear retrieval) and a mobile first footprint. In the US Northeast, adoption gains were broad based across core coastal states.

Note that in contrast to US average phone platform use, where iOS (Apple iPhones) exceeds Android usage dominating the market share at approximately 60%, Waterfront users are overrepresented by Android users at 83%

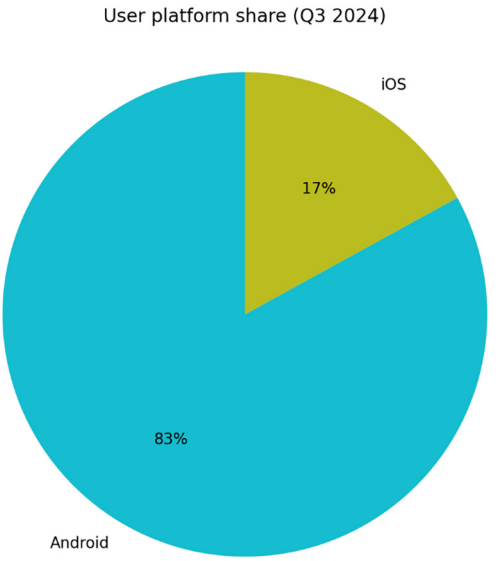

Figure 3: Waterfront mobile platform split Q3 2024.

vs. iOS at 17% (Figure 3). At closer inspection, this actually demonstrates that many of the users are ocean goers as fishers tend to buy the "cheaper" phones to take offshore.

4.3 Results: User Engagement

Engagement baseline (Q1 vs. Q4 2023): users +51.41%, sessions +8.21%, engaged sessions +17.77%, event count +104.26%, and key events +150.51% – showing early momentum that carried into Q3 (Figure 4). Engagement strengthened alongside adoption, with views +27%, event interactions +70%, sessions +60.63%, and engaged sessions +47.73%. Event based interactions grew by 70%, with gear pinning and ecological logging ranking as the most utilized features. Notably, analysis confirms that increased use of the gear pinning feature correlates with a 40% reduction in gear loss claims compared to baseline incident rates.

Regional adoption patterns underscore Waterfront's penetration in the US Northeast, with concentrated uptake in Massachusetts and Rhode Island and emerging engagement in Connecticut and New York. Secondary adoption clusters were observed in Northern California and the Mid-Atlantic, reflecting the platform's scalability beyond its initial deployment zone.

Event driven and community engagement was also reflected regionally. In the Northeast US, digital updates and community activities coincided with elevated in app engagement (e.g., higher views and events), while in California, fishers reinforced usage of recovery and safety support features – contributing to consistent week over month participation. (Metrics above reflect the percent changes for the relevant period.)

4.4 Results: Stickiness Ratios

Waterfront also achieved a Weekly Active Users/Monthly Active Users (WAU/MAU) ratio of 35% (Figure 5), indicating strong platform stickiness – WAU measures how many unique users engage with the platform each week, while MAU measures the number of unique users active over a month. A higher WAU/MAU ratio signals that users are returning frequently and finding recurring value and underscores frequent repeat usage during the month. Trend view Q1 to Q3 stickiness; Q1 vs. Q4 baseline Stickiness (WAU/MAU) rose from 31% in Q1 to 35% in Q3, indicating a steady increase in weekly return behaviour within the monthly cohort.

5. DISCUSSION AND FUTURE WORK

This study positions the Waterfront platform as a substantive technological advance over legacy communication modalities in coastal

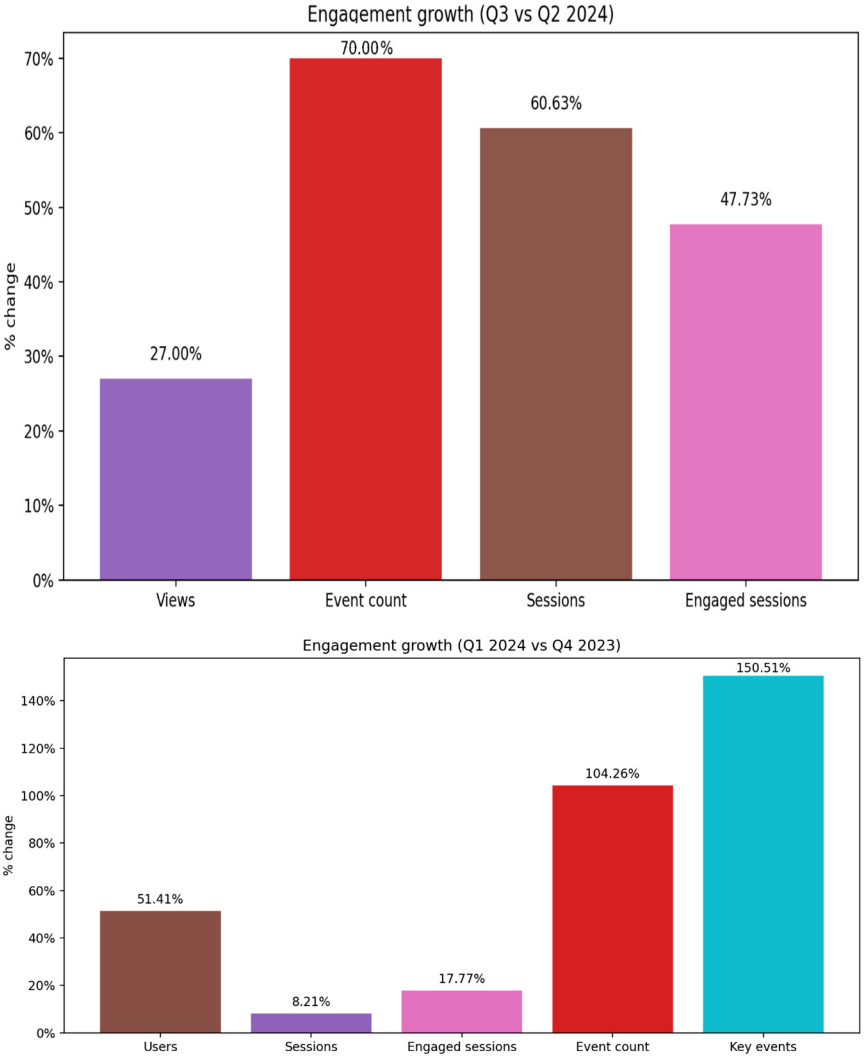

Figure 4: (top) Waterfront engagement percentage growth rates Q3 vs. Q2 2024. (bottom) Waterfront engagement percentage growth rates Q1 2024 vs. Q4 2023.

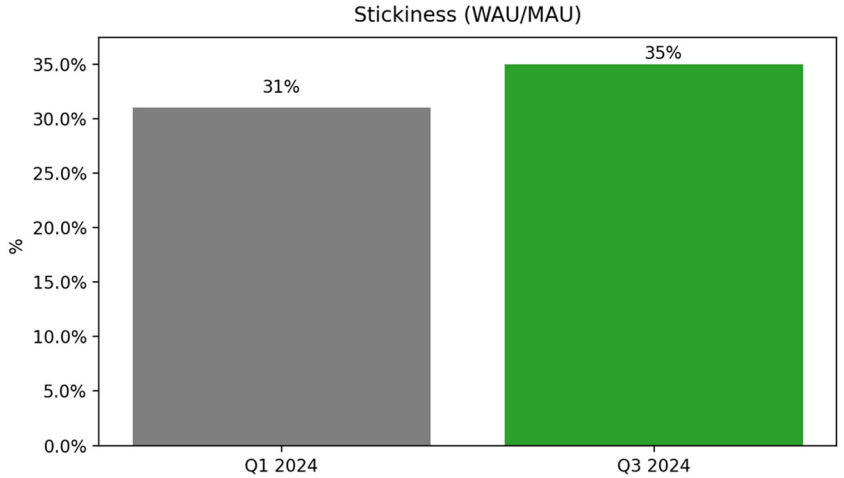

Figure 5: Waterfront stickiness Weekly Active Users/Monthly Active Users (WAU/MAU) ratios for Q3 2024 vs. Q1 2024.

and offshore operations. Conventional practices – principally VHF radio exchanges, disparate email lists, port office postings, and retrospective manual logs – are neither temporally granular nor interoperable enough to support contemporary decision-making demands. In contrast, Waterfront implements an integrated, event driven architecture that fuses AIS telemetry, user generated operational events (e.g., gear interactions and ecological observations), and geofenced policy logic into a coherent, low latency information environment. By unifying communication and spatial analytics within a single operational picture, the platform reduces coordination friction, improves the precision of situational awareness, and provides a reproducible digital record suitable for compliance verification and post hoc analysis. The resultant socio-technical system replaces ad hoc, point to point communication with structured, auditable, and persistently available data flows that are resilient to individual actor availability, radio congestion, or transcription errors.

Observed adoption and usage dynamics further indicate that the technology confers practical value to end users. Quarter over quarter increases in new, active, and returning accounts, coupled with a sustained weekly to monthly active user ratio indicative of routine re-engagement, suggest that the platform has transitioned from trial to incorporation in day to day workflows. Feature level engagement patterns – particularly recurring interactions with the map interface, event logging (e.g., gear pinning, ecological sightings), and area of interest alerts – demonstrate that users mobilize the system's geospatial and communication capabilities to meet operational needs rather than treating the application as a passive information repository. From a human factors standpoint, these behaviours imply that Waterfront's combination of real-time data capture, context aware notifications, and private or group messaging effectively substitutes for, and improves upon, historically fragmented channels by lowering cognitive load, shortening feedback cycles, and enhancing transparency across heterogeneous stakeholders.

Future work will extend Waterfront's capabilities through additional advanced artificial intelligence and machine learning modules designed for maritime contexts. First, multi modal predictive modelling will couple mesoscale weather forecasts, oceanographic fields (e.g., wave height, currents, and tides), and historical vessel traffic patterns to produce risk adaptive routing recommendations, probabilistic congestion surfaces, and hazard nowcasts. Second, personalized planning services will leverage supervised and reinforcement learning to co-optimize navigation and fishing activities under user defined objectives (e.g., fuel efficiency, safety margins, gear conflict avoidance), constrained by regulatory closures and dynamic management areas. Third, anomaly detection pipelines will monitor AIS kinematics and event streams to flag atypical behaviours (e.g., prolonged loitering in restricted zones, unexpected speed profiles), enabling proactive compliance checks and targeted outreach. Fourth, on vessel, low latency audio agents will provide hands free access to critical information – weather windows, regulatory conditions, port status, mariner updates – via natural language interfaces resilient to noisy marine environments. Finally, stakeholder specific

decision support dashboards will synthesize these forecasts and detections into interpretable, role tailored outputs (e.g., route advisories for vessel operators, deconfliction suggestions for fleet managers, environmental indicators for monitoring teams), accompanied by uncertainty quantification to support risk aware decisions.

Methodologically, these extensions will require attention to data governance, model generalizability, and evaluation under operational constraints. Privacy preserving mechanisms (e.g., differential privacy, secure aggregation) will be necessary where user contributed data are employed for model training. Domain adaptation and transfer learning will mitigate performance degradation across regions with differing traffic compositions, bathymetry, and weather regimes. Robustness will be assessed through backtesting against historical scenarios and prospective A/B evaluations that measure decision quality (e.g., near miss reductions, route efficiency gains) and user centric outcomes (e.g., task time, alert precision/recall). Interpretability techniques – such as feature attribution maps for spatial predictions and counterfactual explanations for alert generation – will be incorporated to support user trust and post incident review. Collectively, these research directions position Waterfront not merely as a communication upgrade but as an extensible, intelligent operations platform capable of advancing safety, efficiency, and environmental stewardship in complex marine systems.

5.1 Operational and Economic Implications

The observed engagement trends have direct implications for offshore wind project economics and stakeholder relations. Increased use of real-time notifications and gear pinning functionalities mitigates operational conflicts, reducing the likelihood of permitting delays and associated cost overruns. Economic modelling suggests that Waterfront's ability to streamline communication and pre-empt disputes can lower construction vessel idle time by 10-15%, translating into potential savings of $1.5-$3 million per project phase. Furthermore, improved coordination of inspection and maintenance activities minimizes turbine downtime, enabling recovery of up to 50 GWh annually in lost generation for large-scale projects. This recovered output equates to powering approximately 12,500 households and avoiding 17,500 metric tons of CO_2 emissions, reinforcing the platform's contribution to climate mitigation objectives.

Beyond project-level benefits, enhanced stakeholder engagement supports broader socioeconomic outcomes. By reducing friction between offshore wind developers and fisheries, Waterfront accelerates project timelines, safeguarding job creation in coastal economies. Each GW of offshore wind capacity supports 4,000-5,000 jobs during construction and 150-200 permanent operation and maintenance positions; thus, delays avoided through improved coexistence mechanisms have material implications for regional employment and supply chain stability.

6. CONCLUSION

The coexistence of offshore wind and fisheries is fundamental to sustainable ocean governance and the achievement of climate targets. Waterfront demonstrates that digital

stakeholder engagement can operationalize multi-use principles, mitigate spatial conflicts, and enhance safety in shared marine environments. Its scalability and adaptability position it as a critical enabler of integrated MSP in an era of accelerating offshore energy development. Continued investment in digital innovation and collaborative governance will be pivotal to harmonizing the interests of diverse marine stakeholders and ensuring that the transition to renewable energy does not compromise the resilience of traditional marine industries.

ACKNOWLEDGMENT

Author Declaration

- Funding: The author did not receive financial support from any organization for the submitted work.
- Ethical approval: This paper does not contain any studies with human participants or animals.
- Competing interests: The author declares that he has no competing interests.
- Availability of data and materials: Datasets used and/or analyzed during the current study are available from the corresponding author upon reasonable request.
- Artificial intelligence was not used in this work.

REFERENCES

[1] International Energy Agency, "World Energy Outlook 2024." Paris, France: IEA, 2024. Available: https://www.iea.org/reports/world-energy-outlook-2024

[2] D. Rodmell, "Can Fisheries Co-exist with Offshore Wind in the Race to Carbon Net Zero?" NFFO.org.uk. Accessed: Nov. 30, 2025. [Online]. Available: https://www.nffo.org.uk/can-fisheries-co-exist-with-offshore-wind-in-the-race-to-carbon-net-zero

[3] M. F. Schupp, A. Kafas, B. H. Buck, G. Krause, V. Onyango, V. Stelzenmüller, I. M. Davies, and B. E. Scott, "Fishing within offshore wind farms in the North Sea: Stakeholder perspectives for multi-use from Scotland and Germany," Journal of Environmental Management, vol. 279, Art. no. 111762, Feb. 2021. doi: 10.1016/j.jenvman.2020.111762.

[4] European Parliament and the Council of the European Union, Directive 2014/89/EU of the European Parliament and of the Council of 23 July 2014 establishing a framework for maritime spatial planning. [Online]. Available: http://data.europa.eu/eli/dir/2014/89/oj

[5] V. Stelzenmüller, A. Gimpel, J. Letschert, C. Kraan, and R. Döring, "Impact of the use of offshore wind and other marine renewables on European fisheries," Policy Dept. for Structural and Cohesion Policies, European Parliament, Oct. 2020. Available: https://www.europarl.europa.eu/RegData/etudes/STUD/2020/652212/IPOL_STU(2020)652212(SUM01)_EN.pdf

[6] S. W. K. van den Burg, P. Kamermans, M. Blanch, D. Pletsas, M. Poelman, K. Soma, and G. Dalton, "Business case for mussel aquaculture in offshore wind farms in the North Sea," Marine Policy, vol. 85, pp. 1–7, 2017, doi: 10.1016/j.marpol.2017.08.007.

[7] Equinor, "Collaboration to trial safe fishing within floating wind farms," 29 July 2021. Accessed: Jan. 12, 2026. [Online]. Available: https://www.equinor.com/news/uk/collaboration-trial-safe-fishing-within-floating-wind-farms

[8] Japan Wind Power Association, "JWPA Wind Vision 2023: Contribution of wind power toward the realization of a safe, stable and sustainable society," JWPA, May 29, 2023. Accessed: Jan. 12, 2026. [Online]. Available: https://jwpa.jp/en/information/7754

[9] U.S. Bureau of Ocean Energy Management, "Draft Fisheries Mitigation Guidance." Washington, DC: U.S. Department of the Interior, June 23, 2022. Accessed: Jan. 12, 2026. [Online]. Available: https://www.boem.gov/sites/default/files/documents/renewable-energy/DRAFT%20Fisheries%20Mitigation%20Guidance%20062320222_0.pdf

[10] Power Technology, "Empire Wind receives temporary suspension," 2023. Accessed: Jan. 12, 2026. [Online]. Available: https://www.power-technology.com/news/empire-wind-temporary-suspension

[11] A. Kuffner, "Trump administration orders halt to offshore wind projects. What it means," The Providence Journal (USA TODAY Network),

Dec. 22, 2025. Accessed: Jan. 12, 2026. [Online]. Available: https://www.usatoday.com/story/news/politics/2025/12/22/trump-halts-offshore-wind-projects-again-including-revolution-wind/87882097007

[12] A. Kuffner, "Revolution Wind seeks to overturn Trump administration stop-work order," The Providence Journal (USA TODAY Network), Jan. 2, 2026. Accessed: Jan. 12, 2026. [Online]. Available: https://www.usatoday.com/story/news/environment/2026/01/02/revolution-wind-seeks-court-injunction-to-lift-stop-work-from-trump/87990935007

[13] P. O. Bonsu et al., "Co-location of fisheries and offshore wind farms: current practices and enabling conditions in the North Sea," *Marine Policy*, vol. 159, art. no. 105941, 2024. doi: 10.1016/j.marpol.2023.105941.

Organizing Data for Regulatory Needs

Dr. Andrea Copping

Dr. Lenaïg Hemery

Dr. Lysel Garavelli

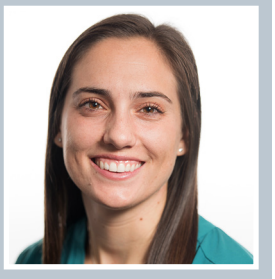

Mikaela Freeman

Tidal energy data collection and analysis

Who should read this paper?

This paper should be read by the community of researchers, Marine Renewable Energy (MRE) device and project developers, regulators, and stakeholders with an interest in MRE. The nature of the data collection and analysis has strong overlap with oceanographic data collection including the interpretation of underwater active acoustics and underwater video.

Why is it important?

This paper lays out a process for dealing with data that are collected to address the potential risk of marine animals colliding with rotating tidal turbines. It seeks to make sense of the potential DRIP – data rich, information poor – aspect of many different groups collecting data of marine animals around tidal turbines and organize those data so that they are accessible and helpful for enabling the permitting process needed to deploy tidal turbines.

The tidal energy industry cannot move forward efficiently until the concern around collision risk of marine animals with turbines is settled. There are many data collection efforts underway, but the industry and regulators have no clear path forward, and the research community needs guidance to ensure their work in this area is focused on the most important questions. This paper documents the work of a large international group of scientists working on a common goal.

MRE project developers can use the results of this paper to organize and seek information they will need for permitting processes, while the regulators will become aware of the resources available to help interpret the incoming information. The research community, who work closely with the authors, will continue to have direct access to the most recent and timely information needs of the industry.

About the authors

Dr. Andrea Copping is an oceanographer and senior advisor at Pacific Northwest National Laboratory (PNNL), and a faculty member at the University of Washington. She focuses on the environmental effects of marine energy and offshore wind development and the role that these effects play in technology development and project initiation. She has led international projects that share information on environmental effects of wave and tidal (Ocean Energy Systems-Environmental) around the world. She also leads research and development for the use of marine energy devices to power Blue Economy applications, including ocean thermal energy conversion and seawater air conditioning. Dr. Copping serves as an associate editor of *Coastal Management Journal*, on the editorial board for *International Marine Energy Journal*, and as an advisor to marine energy consortia in Ireland, Chile, Australia, and France.

Dr. Lenaïg Hemery is a research scientist in the Coastal Sciences Division of PNNL, located at the Marine and Coastal Research Laboratory in Sequim, Washington. As a marine ecologist with a multidisciplinary background, her work mostly focuses on the potential effects of climate solutions (such as marine energy,

offshore wind, and marine carbon dioxide removal) on the marine environment and novel monitoring approaches to study these effects. In addition, Dr. Hemery thrives on disseminating the scientific knowledge generated from her research to various audiences to help advance these marine industries in a sustainable way.

Dr. Lysel Garavelli holds a PhD in biological oceanography and is a research scientist at PNNL in Seattle, Washington, US. Her research focuses on the effects of anthropogenic activities on the marine environment. Particularly, she works across several scientific disciplines to determine the implications of MRE and offshore wind development on marine resources. Dr. Garavelli works closely with the international community to understand environmental effects of MRE development and share environmental effects information to benefit from progress made around the world.

Mikaela Freeman is a research scientist in PNNL's Coastal Science Division in Seattle, Washington, US. She undertakes interdisciplinary research to understand the environmental and socioeconomic effects of marine activities, mainly MRE, and the potential for co-location of aquaculture with MRE. She focuses on addressing human dimensions, permitting and regulatory aspects, and outreach and engagement to work towards sustainable ocean solutions.

PROGRESSING TIDAL ENERGY THROUGH ORGANIZED DATA APPROACHES

Andrea Copping, Lenaïg Hemery, Lysel Garavelli, Mikaela Freeman
Pacific Northwest National Laboratory, Seattle, WA, USA
Corresponding author: andrea.copping@pnnl.gov
DOI: https://doi.org/10.48336/VXJT-9C60

ABSTRACT

As the tidal energy industry reaches commercial status in parts of Europe and pre-commercial status in North America, more environmental data are being collected, and research studies continue to address the most difficult questions around risks to marine life and environment. Collision risk of fish and marine mammals, as well as diving seabirds and sea turtles, remain the most challenging tidal turbine interactions and the focus of extensive studies in many parts of the world. At the same time, questions around animal disturbance from acoustic output of turbine or electromagnetic fields from power export cables, as well as alterations of benthic and pelagic habitats need to be addressed to achieve regulatory permission to deploy and operate tidal farms. In addition, as marine energy projects scale up to large arrays, interactions like displacement of marine animals or entanglement in mooring lines will need to be investigated.

Working with 15 other nations, Ocean Energy Systems-Environmental has developed tools and frameworks to assist in organizing and applying data and information on potential risks from tidal turbines to permitting, mitigation, and licensing. Tools have been developed that organize data to match regulatory needs including risk retirement, data transferability, management measures, and guidance documents. This paper will discuss the application of these tools and frameworks.

Keywords: Tidal energy, environmental effects, collision risk, international cooperation, organizing data and information

1. INTRODUCTION

Development of tidal energy is progressing from early demonstration projects toward commercial status in parts of Europe and pre-commercial status in North America. Despite this progress, regulatory processes continue to be prolonged and complicated by a lack of certainty around potential effects of tidal devices on marine animals, habitats, and ecosystem processes [1]. Collision risk of fish and marine mammals, as well as diving seabirds and sea turtles, remain the most challenging tidal device interactions and remain the focus of extensive studies in many parts of the world [2]. After almost two decades of deployments and demonstrations of tidal devices in the ocean, data have been collected in close proximity to at least 42 tidal devices and numerical models have been generated to explain potential interactions and deleterious effects of rotating tidal blades on marine animals [3]. Challenges of collecting data in fast moving waters in close proximity to devices, lack of knowledge about populations and behaviour of marine mammals and fish at greatest risk, and a lack of standard approaches to gathering and analyzing data combine to create a challenge for regulators who evaluate potential risks, as well as device and project developers who seek approval for development [4], [5], [6]. The research community continues to address the key questions around collision risk but has little guidance on what data are needed to describe, minimize, and eliminate the risk from tidal turbines to marine animals.

With many independent research groups globally pursuing answers to collision risk and other concerns around tidal devices, as well as data collection by consultant teams at the request of device and project developers, a uniform means of collecting, collating, analyzing, interpreting, and reporting data is elusive. As tidal demonstration and commercial projects increase, there is an exponential increase in the number of datasets and outputs. This expansion has the potential to lead to DRIP – data rich, information poor – situation [7]. We have lots of data but what does it mean? Compounding this situation is the fact that almost all the data that have been collected around tidal devices comes from deployments of single devices or very small arrays [3]. Extrapolating these findings to larger arrays remains challenging, even while these large installations are under development [8].

The research community has used stressors and receptors to describe and measure interactions between marine renewable energy devices and the marine environment [9]. Stressors are those aspects of tidal energy that might cause stress, injury, or death to the receptors – marine animals, habitats, or ecosystem processes. When considering the interaction of marine animals and tidal turbines, the terms “avoid” has become commonly used to indicate that the animal can sense the turbine blade at a distance and take action to not come into close proximity, while “evade” is used when an animal does not sense the turbine until it is within a few body lengths of the blade and takes immediate evasive action.

While collision risk to marine animals remains the most difficult stressor-receptor interactions to address for tidal turbines, other key stressor-

receptor interactions are also of importance in reaching regulatory permission to deploy devices. In particular, effects on marine mammals and certain fish species from the noise generated underwater by tidal devices, effects of electromagnetic fields from power export cables and energized portions of turbines, changes in benthic and/or pelagic habitats, displacement of animal populations from their normal routes or habitats, and potential changes in oceanographic conditions from the removal of energy and disruption of tidal flows must all be evaluated and assessed for risk to the marine environment [10].

International efforts to standardize engineering and power generation aspects of marine renewable energy devices are underway [11], but to date there has been no success in standardizing protocols for data collection and analysis of parameters of importance to marine animals, with the exception of the measurement of underwater noise [12]. It may not be possible to impose strict standard protocols for data collection and analysis globally in the near future, nor require the use of only certain instruments for obtaining the data; however, there is a clear need to standardize the way we look at the existing datasets, how they are used to inform regulatory processes, and how the collective tidal energy community interprets and mitigates potential risks. Numerical models are an important tool in furthering our understanding of the mechanics, the biology, and the outcomes of marine animals swimming in the vicinity of an operating turbine.

As additional environmental effects of tidal energy data have become available, there continues to be a disconnect between what the researchers and consultants collect and analyze and the inputs needed by regulators to assess risks. These risks help drive requirements for permitting, as well as mitigation conditions determined for development. These challenges remain the most difficult barriers to overcome to understand collision risk around tidal turbines and potentially retire the risk for each new project.

Ocean Energy Systems-Environmental (OES-Environmental) is a task under the International Energy Agency's Ocean Energy Systems (OES) Technology Collaboration Programme. Fifteen countries and the European Commission have signed onto OES-Environmental with the goal of understanding the potential environmental effects of marine renewable energy, including tidal energy, development, and operation, as they may affect regulatory processes for moving the marine renewable energy industry forward. OES-Environmental is led by the United States Department of Energy and implemented under the leadership of the authors of this paper at Pacific Northwest National Laboratory. OES defines the marine renewable energy industry as those devices that harvest energy from the movement of ocean water (tides, waves, persistent ocean current) or gradients in the ocean (temperature, salinity). This paper reports on the activities under OES-Environmental that have organized methods to handle data on the environmental effects of marine renewable energy development to maximize the utility and accessibility of those data to create information that informs and assists with the regulatory process. This paper focuses on those pathways and examples in support of the tidal energy industry.

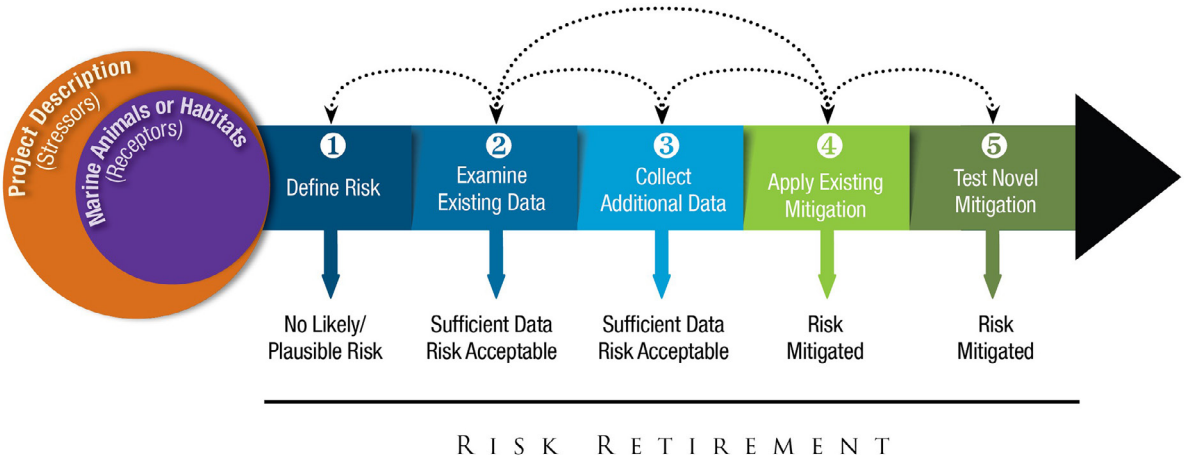

Figure 1: Schematic of the steps in the risk retirement process. Developed by OES-Environmental.

2. OES-ENVIRONMENTAL'S ORGANIZED DATA APPROACHES

In order to address the need for information for permitting marine renewable energy devices, OES-Environmental has developed the risk retirement process [13]. This process applies existing and newly collected data in an organized manner that will be useful for developers interacting with the regulatory process (Figure 1). This process is useful only as far as the data are accessible, of high quality, and consistent.

The approach that has been developed by OES-Environmental revolves around examining potential effects that may occur from the interaction of specific portions of a tidal energy system, as well as deployment, operation, or maintenance procedures that might affect the risk of collision with marine animals, notably marine mammals, fish, diving seabirds, and sea turtles. The interactions detail the stressor (that aspect of tidal energy that might cause stress, injury, or death to an animal) and receptors (the specific animal species), commonly known as stressor-receptor interactions.

The system of interlocking methods that has been developed by OES-Environmental fits into a framework of risk retirement – the concept that, for all new tidal projects, not all stressor-receptor interactions must be fully investigated, but should rely on information from existing permitted projects, surrogate industries, and research studies. The risk retirement process was described in [14]. The process assists developers in determining what data they might need to present for regulatory purposes, where they might find those data (existing data or data that must be collected), and how existing data might be applied.

Evaluating the relative risk of each stressor-receptor interaction within the risk retirement process requires the best available knowledge generated by other projects or studies. OES-Environmental has assembled the most relevant high-quality papers and reports for each of the stressor-receptor interactions and made them available as evidence bases (https://tethys.pnnl.gov/risk-retirement-evidence-bases). OES-Environmental adds to these evidence bases annually as new studies are completed and datasets become available. The

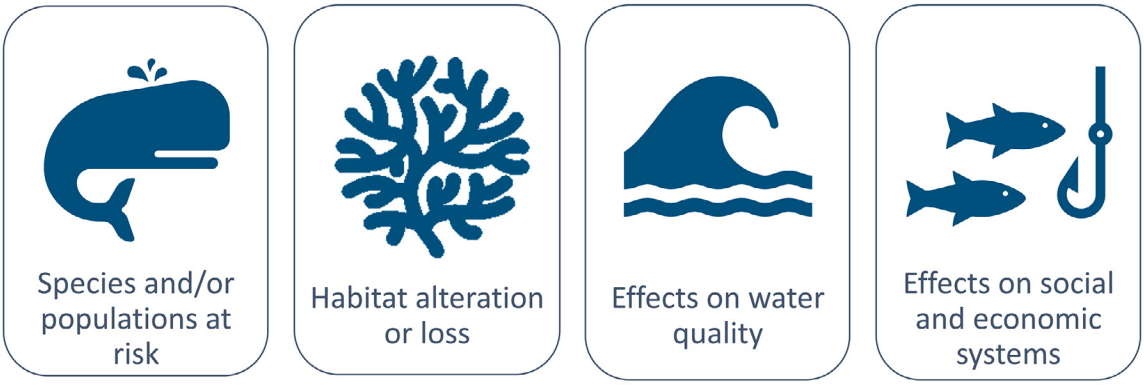

Figure 2: Four categories of legal and regulatory focus for permitting and licensing of tidal projects. Developed by OES-Environmental.

collision risk evidence base consists of 40 peer-reviewed journal papers, conference papers, and reports (https://tethys.pnnl.gov/collision-risk-evidence-base).

Coupled with the evidence bases for key stressor-receptor interactions is the need to determine effective mitigation measures, should they be needed. The management measures tool developed by OES-Environmental (https://tethys.pnnl.gov/management-measures) documents over 300 mitigation measures that have been required, tested, or suggested for permitting tidal or wave energy projects. These studies, field trials, and models are applied to the steps in the risk retirement process that indicates risk is still present after collection and analysis of data and comparisons with existing marine renewable energy projects.

OES-Environmental has addressed the disconnect between the data needed for tidal energy permitting and what is being collected in many monitoring programs through the development of guidance documents that relate the stressor-receptor interactions of marine energy (including tidal) devices to groupings of laws and regulations that govern permitting and licensing. Through an assessment within OES-Environmental member countries, it was determined that all regulations pertaining to marine energy fall into one of four groupings (Figure 2). All OES nations protect marine species and populations through a series of laws and regulations, most often focused on endangered species or species at risk. Habitat alteration or loss is often associated with determining the aerial extent and location of seabed leases or shoreline cable landings. Water quality effects are not as commonly used for marine energy permitting, but with the increased interest in using ocean temperature and salinity gradients for energy, as well as the application of antifouling coatings and paints to marine energy devices, water quality risks are being increasingly scrutinized. The potential effects and benefits of marine renewable energy development on local and regional communities is also taken into account in the regulatory process in most nations.

Guidance documents were created based on these groupings and consist of pathways that are useful internationally (Figure 3). In addition to the generalized guidance documents, stressor-specific guidance documents are available, as well as a series of

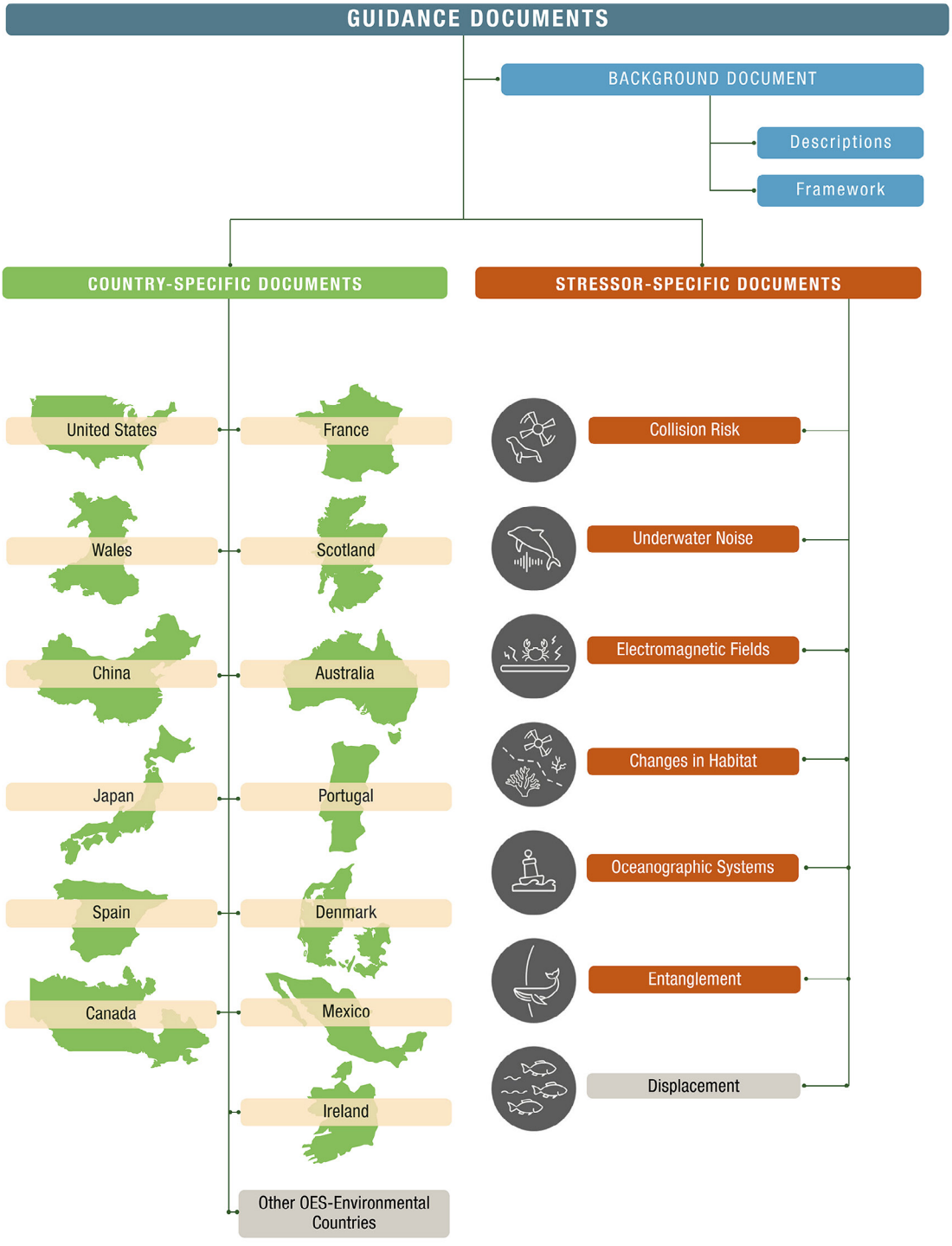

Figure 3: Guidance documents that help organize scientific information for use in permitting applications for marine (including tidal) energy. The background documents describe the process, while the stressor-specific documents bring together information that addresses each part of a tidal system. The country-specific documents provide more detail that is particular to the nation, while the best management practices for risk retirement help guide the user through the process. Developed by OES-Environmental.

country-specific guidance documents that demonstrate the nuances of regulation in each of the OES-Environmental nations (Figure 3). More detailed information is found at https://tethys.pnnl.gov/guidance-documents.

The final step in making data available and accessible was developed as a set of Best Management Practices (BMPs) for applying the risk retirement methods and models. The BMPs consist of guidelines for handling data and assessing data sufficiency and are written in a manner that is accessible and actionable for the marine renewable energy industry, regulators and advisors, and other stakeholders.

A use case consisting of a tidal turbine deployed in the Bay of Fundy, Canada, is analyzed using the risk retirement process and the results reported here. This process, as outlined in this paper, will be most useful to a device or project developer who seeks to gain regulatory permission to deploy a tidal device in the Bay of Fundy.

3. APPLICATION OF APPROACHES THROUGH A USE CASE

The risk retirement process developed by OES-Environmental consists of six steps: defining the risk; examining existing data; collecting additional data as needed; applying existing mitigation measures; testing novel mitigation measures; and finally, determining what can be done if residual unacceptable risk remains.

To demonstrate how the risk retirement process comes together to support the development of tidal energy, a realistic but not real-world tidal project in the Bay of Fundy was used in this paper to apply the risk retirement process to collision risk. Information that should be collected at each of these steps is applied to the tidal project. We begin by describing the project and identifying the animals and habitats potentially at risk. Here we use a floating tidal turbine anchored in 40 m of water. The floating body is held in place with three anchor lines, two lines at the bow and one at the stern. The floating body supports three two-bladed turbines that can be lowered for energy generation and raised for maintenance. Each rotor is 16 m in diameter; when lowered, the rotor swept area reaches a depth of approximately 22 m. Key receptors of concern in the area of the Bay of Fundy include Atlantic salmon, striped bass, white sharks, and harbour porpoise [15]. The risk retirement pathway was applied for the use case by examining each step in the process.

3.1 Define the Risk

For Atlantic salmon, striped bass, white sharks, and harbour porpoise in the Bay of Fundy, a collision with the rotating blades clearly defines a plausible risk as each species frequents the water column where the blades are deployed during energy generation [15]. Regulators may request additional baseline data collection to verify that the marine animals of concern are present at the planned tidal deployment location. Deploying at test sites and other well-characterized sites may help lessen this baseline collection need.

By comparing similar potential encounters found in the collision risk evidence base (https://tethys.pnnl.gov/collision-risk-evidence-base), this risk must be considered plausible rather than likely as many additional

factors must align for a collision to occur, as discussed in the following section [2]. Based on the potential risk, the developer must continue to gather information to evaluate the risk of collision.

3.2 Examine Existing Data

The additional factors that must be considered for a collision to occur include the need for the fish (salmon, bass, and shark) or marine mammal (porpoise) to be swimming at the particular depths of the turbine, in order to be struck while the blades are rotating, which only occurs during part of each tidal cycle. In addition, the animals must have little to no ability to detect and avoid or evade the blades. Existing data from laboratory studies, field observations, and numerical models demonstrate a reasonable likelihood that many species of fish will pass close to or even through the rotor swept area of a turbine without harm [16], [17], [18], [19]. Some fish species appear to avoid or evade an underwater device such as a tidal turbine, while others may be subject to hydrodynamic forces that prevent them from being struck by the blades [20]. Similar studies support the ability of marine mammals, including harbour porpoise, to detect and avoid/evade a collision [5], [6], [21]. Existing datasets from the United Kingdom and elsewhere could help provide insight into the likelihood of collision with the tidal turbine blades for fish and marine mammals in the Bay of Fundy. These datasets can be gleaned from the data transferability process, through providing the key parameters of the project (e.g., tidal device, depth envelope, channel width; https://tethys.pnnl.gov/monitoring-datasets-discoverability-matrix).

While there are considerable indications in published literature that the risk of collision with a tidal turbine blade is likely to be very low, this risk cannot be ruled out. Hence, the developer must consider the need to collect additional data.

3.3 Collect Additional Data

The goal of open communication between researchers and developers in the tidal energy community is to ensure that sufficient information is developed to meet the needs of permitting specific tidal projects. This should include sufficient information to understand and mitigate effects of collision risk universally, but must also be tailored to different deployment sites, water bodies, and species, as well as the specific tidal device proposed for deployment. However, variable ocean conditions, differing latitudes and weather conditions, and regional differences in species distributions will require that local conditions be considered, most commonly with the collection of additional data.

Regulators in the Bay of Fundy region are likely to require that site-specific information be compiled to determine the level of risk that will guide their decisions on permitting and licensing the tidal project. The tidal developers and their consultants can anticipate this need by examining the guidance document that pertains to collision risk [22]. While standardized collection and analysis methods continue to evade the marine renewable energy research community, the data transferability process provides the first steps in designing an effective field effort to collect those data through the data collection consistency table (https://tethys.pnnl.gov/data-transferability).

The developer and their consultants should be prepared to design and implement a monitoring campaign that consists of sufficient data collection before deployment to ensure that the presence, movement, behaviour, and seasonality of the marine animals of concern are known for the planned deployment area. In addition, a post-deployment collision risk monitoring campaign may be required for the operational phase of the project, which can best be designed using information from other tidal projects and research studies (e.g., [5], [23], [21]) as well as the results of numerical models that simulate encounters of marine animals with turbines (e.g., [16], [24]).

Despite these data collection efforts, regulators and stakeholders may continue to be concerned about potential collisions and may require investigations into mitigation measures. Collision risk cannot be considered "retired" or set aside, unlike other stressor-receptor risks for single devices [10] (such as underwater noise and electromagnetic fields).

3.4 Apply Existing Mitigation

As tidal energy projects continue to expand in the UK and Europe, there have been investigations into how any remaining risk of collision might be lessened for marine animals by implementing mitigation measures. The management measures tool developed by OES-Environmental (https://tethys.pnnl.gov/management-measures) is a searchable database that will allow a tidal developer to examine the range of proposed or implemented measures, filtering by the project phase (installation, operation, maintenance, decommissioning), and the receptor group (fish, marine mammals, etc.). It is important to note that many of these mitigation measures have never been enacted, largely because they were found to be unnecessary or unfeasible. Some of the mitigations that might make sense in the Bay of Fundy include the use of acoustic deterrent devices that create a sound that alerts marine mammals and fish with hearing capabilities to the presence of the turbine, enhancing their ability to avoid or evade the blades. This has been proposed in the UK, drawing on experience with keeping seals away from aquaculture pens [25] [26]. Coloured blades have been used successfully in shallow water applications at the European Marine Energy Centre to assist marine animals in seeing the turbine [27]. Soft start procedures for slowly bringing the turbine up to speed have also been suggested as a way to make the animals aware of the turbine and move out of the area before it reaches full operational speed [27].

Should mitigation be considered necessary, and existing measures not be deemed sufficient, the development and testing of new mitigation measures may become the purview of the research community.

3.5 Test Novel Mitigation

There is room for new and different collision risk mitigation measures to be tested either as a direct obligation under a regulatory process or in forward-thinking research. Mitigation measures that have been discussed as part of permitting and licensing procedures in the UK, Europe, Australia, Canada, and the US but never tested include decreasing the tip speed of the turbine blades to make the reaction time for animals less urgent, and the ability to stop the turbine in real time with a

detection system, triggered when sensitive species are present.

3.6 Changes to Tidal Project

Eventually, if the tidal developer, working with the regulators, determines that the risk retirement process steps (i.e., examining existing data, collecting new data, evaluating existing mitigation strategies, and testing novel mitigation strategies) are not sufficient to avoid significant risk to the marine animals of concern, there is cause to re-examine the tidal project itself. Modifications to the design of the project might include changing the planned deployment location, making alterations in the design and/or operation of the turbine, or modifying the installation or maintenance procedures. If none of these actions can reduce the risk sufficiently, the project in its proposed form may need to be abandoned.

4. DATA COLLECTION, ANALYSIS, STORAGE, AND ACCESSIBILITY

True standardization and universally accepted protocols for collecting data on animal behaviour and tidal blade encounter around tidal energy projects is challenging. These fast-moving and often turbid environments have been the location of an increasing number of research studies. The use of underwater cameras and video, as well as a range of active acoustic instruments, appears to provide the best data [3], [10]. Underwater still and video cameras are limited to shallow, clear water for the most part, although the use of strobe lights triggered by the movement of animals can extend their use into deeper water and/or nighttime. Acoustic cameras, echosounders, and a series of other sonar devices all provide useful data about nearfield encounters and potential collisions with tidal turbines [28]. In addition to the challenges of collecting the data, video and acoustic instruments collect vast amounts of data that must be analyzed, often slowing or requiring frequent subsampling, and needing vast human and financial resources [8]. The best professional judgement gathered by OES-Environmental recommends the development of more open-source data collection approaches as a community [10]. These approaches should include:

- A means to lower the “data mortgage” with smart systems that record data only when movement of marine animals occurs around a turbine.
- Increased use of existing video and acoustic datasets near turbines to understand the movement and mechanisms of potential harm to animals.
- Improvements to our ability to recognize species using acoustic data.
- Use of animal-mounted tracking devices to gather data, where feasible.
- Use of numerical model outputs to design and interpret field data.
- Improvements to understanding marine animal use of an area before a tidal project is initiated.

In addition, ensuring that collision risk studies and associated data are made accessible to all users is key to solving the collision risk puzzle. Researchers must be responsible for quality assurance of their data, but common repositories with strong capabilities for curation and long-term storage as well as active outreach to ensure accessibility are

necessary. One such example is the integrated PRIMRE system in the US that houses data and information on all aspects of marine renewable energy development (https://openei.org/wiki/PRIMRE), allowing for comparison and integration of environmental information and data that are stored in the environmental knowledge hub Tethys (https://tethys.pnnl.gov/) with engineering, modelling, geospatial, and guidance data that can be used to assist in understanding and mitigating potential harm to marine animals [29].

5. USE OF MODELS IN COLLISION RISK

Collision risk and encounter risk models have been in use for more than a decade [16], [30], [31], although many have been adapted from collision and encounter risks for birds around wind turbines and continue to need refinement and parameterization that is more appropriate for tidal turbines and marine animals. Newer modelling approaches include agent-based models that are organized around individual animals [32]. While there is general consensus that there is a need to improve the working of all the existing models, the greatest need is for more field data for calibration and validation that will increase the realism of the models [24], [10]. As these models improve and are validated with additional data, they can be used to plan field campaigns by optimizing sampling locations and timing. The goal of these models is to ensure that they are sufficiently robust to use in most tidal energy locations and begin to replace most, if not all, monitoring of interactions between marine animals and tidal turbines. However, that time has yet to come.

6. SCALING UP TIDAL ARRAYS

The knowledge that has been gained on the potential for marine animals to collide with rotating tidal turbine blades comes largely from monitoring around single deployed devices, small arrays such as those of Ampeak Energy, formerly SAE Renewables, (MeyGen, in Pentland Firth, Scotland) and Nova Innovations (Blue Mull Sound, in the Shetland Islands, Scotland), as well as from models and research studies. As the tidal energy industry seeks to scale up to larger commercial arrays, much of what has been learned at the smaller scale will be applicable but how those potential effects will extrapolate is not clear [34]. Monitoring around multiple tidal devices will be needed to ensure that our understanding of collision risk scales as anticipated, and, in some locations, additional site-specific monitoring may be needed as well.

7. CONCLUSION

In order for the tidal energy industry to become firmly established as a renewable energy source, the risk of collision with marine animals must be well understood and the information must be made widely available to regulators and stakeholders. The state of our knowledge is not yet there, and the circular problem of not having enough permitted tidal turbines in the water around which to gather data to improve our state of knowledge remains as a considerable barrier. The tidal energy community as a whole – developers, researchers, regulators and advisors, and other stakeholders – must collectively push for more research to narrow the uncertainty around collision risk [10]. That

research can only move forward efficiently if there are deployed devices around which monitoring can take place.

Frameworks such as OES-Environmental's risk retirement process and associated tools can help organize and increase the value from data and information that is available, help identify the gaps in knowledge that will drive research studies toward decreasing the uncertainty, and anticipate the use of new information.

The tidal energy industry continues to be most affected by the lack of comprehensive knowledge about collision risk, and the research community seeks to focus available public funds on answering the most pressing questions. Regulators suffer from this uncertainty as well, torn between the need for reliable renewable energy sources and their mandates to protect natural resources. Other stressor-receptor interactions also feature in the regulatory processes and must be shown to be acceptable. Through the risk retirement process, questions around animal disturbance from acoustic output of turbines and electromagnetic fields from power export cables as well as alterations of benthic and pelagic habitats have been "retired" for small tidal deployments [14], [33]. As new information becomes available with an increase in deployed arrays, this information will need to be revisited. In addition, as tidal energy projects scale up to large arrays, interactions like displacement of marine animals or entanglement in mooring lines will need to be investigated [8], [4].

The use of strategies such as the risk retirement process outlined here will not completely solve the DRIP problem nor settle all concerns about collision risk to marine animals from rotating tidal blades. However, with continued open communication, sharing of data, and broad accessibility of information among the marine renewable energy community, collision should become a manageable risk for device and project developers, regulators and advisors, and stakeholders.

ACKNOWLEDGMENT

The authors thank the US Department of Energy Hydropower and Hydrokinetics Office and Ocean Energy Systems for their support of and encouragement for this work. We are also grateful for the consistent collaborations with the analysts representing the OES-Environmental countries. We also want to acknowledge all the hard work of the OES-Environmental team at Pacific Northwest National Laboratory (Hayley Farr, Debbie Rose, Kristin Jones, Jacob McGrath, Amy Woodbury).

Authors' Declaration

- Funding: The authors received financial support under a contract to Pacific Northwest National Laboratory, operated by Battelle for the United States Department of Energy under contract DE-AC05-76RL01830.
- Ethical approval: This paper does not contain any studies with human participants or animals.
- Competing interests: The authors declare that they have no competing interests.
- Availability of data and materials: Datasets used and/or analyzed during the current

study are available from the corresponding author upon reasonable request.

- Artificial intelligence was not used in this work.

REFERENCES

[1] L. Garavelli, D. Rose, M. Freeman, L. Hemery, H. Farr, and A. Copping, "Minimizing environmental risks to progress the marine renewable energy industry," *Proceedings of the European Wave and Tidal Energy Conference*, vol. 16, Sep. 2025, doi: 10.36688/ewtec-2025-1193.

[2] A. E. Copping, D. J. Hasselman, C. W. Bangley, J. Culina, and M. Carcas, "A Probabilistic Methodology for Determining Collision Risk of Marine Animals with Tidal Energy Turbines," *Journal of Marine Science and Engineering*, vol. 11, no. 11, p. 2151, Nov. 2023, doi: 10.3390/jmse11112151.

[3] A. E. Copping, M. L. Martínez, L. G. Hemery, I. Hutchison, K. Jones, and M. Kaplan, "Recent Advances in Assessing Environmental Effects of Marine Renewable Energy Around the World," *Marine Technology Society Journal*, vol. 58, no. 3, pp. 70–87, Sep. 2024, doi: 10.4031/mtsj.58.3.2.

[4] L. G. Hemery et al., "Animal displacement from marine energy development: Mechanisms and consequences," *Science of The Total Environment*, vol. 917, pp. 170390–170390, Jan. 2024, doi: 10.1016/j.scitotenv.2024.170390.

[5] L. Palmer, D. Gillespie, J. D. J. MacAulay, C. E. Sparling, D. J. F. Russell, and G. D. Hastie, "Harbour porpoise (*Phocoena phocoena*) presence is reduced during tidal turbine operation," *Aquatic Conservation: Marine and Freshwater Ecosystems*, vol. 31, no. 12, pp. 3543–3553, Nov. 2021, doi: 10.1002/aqc.3737.

[6] D. Gillespie, L. Palmer, J. Macaulay, C. Sparling, and G. Hastie, "Harbour porpoises exhibit localized evasion of a tidal turbine," *Aquatic Conservation: Marine and Freshwater Ecosystems*, vol. 31, no. 9, pp. 2459–2468, Jul. 2021, doi: 10.1002/aqc.3660.

[7] T. A. Wilding et al., "Turning off the DRIP ('Data-rich, information-poor') – rationalising monitoring with a focus on marine renewable energy developments and the benthos," *Renewable and Sustainable Energy Reviews*, vol. 74, pp. 848–859, Jul. 2017, doi: 10.1016/j.rser.2017.03.013.

[8] D. Hasselman et al., "2020 State of the Science Report, Chapter 10: Environmental Monitoring Technologies and Techniques for Detecting Interactions of Marine Animals with Turbines," Pacific Northwest National Laboratory (PNNL), Richland, WA, USA, PNNL--29976CHPT10, Sep. 2020, doi: 10.2172/1633202.

[9] G. W. Boehlert and A. B. Gill, "Environmental and ecological effects of ocean renewable energy development: A Current Synthesis," *Oceanography*, vol. 23, no. 2, pp. 68–81, Jun. 2010, [Online]. Available: https://www.jstor.org/stable/24860713.

[10] L. Garavelli, L. Hemery, D. Rose, H. Farr, J. Whiting, and A. Copping, "2024 OES-Environmental 2024 State of the Science Report, Chapter 3: Marine Renewable Energy: Stressor-Receptor Interactions," Pacific Northwest National Laboratory (PNNL), Richland, WA, USA, PNNL--36020CHPT3, Aug. 2024, doi: 10.2172/2438589.

[11] "PRIMRE/Telesto/Standards | Open Energy Information." Openei.org. Accessed: Jan. 05, 2026. [Online]. Available: https://openei.org/wiki/PRIMRE/Telesto/Standards

[12] "IEC TS 62600-40:2019." Webstore.iec.ch. Accessed: Jan. 05, 2026. [Online]. Available: https://webstore.iec.ch/en/publication/31031#additionalinfo

[13] A. E. Copping, M. C. Freeman, A. M. Gorton, and L. G. Hemery, "Risk Retirement – Decreasing Uncertainty and Informing Consenting Processes for Marine Renewable Energy Development," *Journal of Marine Science and Engineering*, vol. 8, no. 3, p. 172, Mar. 2020, doi: 10.3390/jmse8030172.

[14] A. Copping, M. Freeman, A. Gorton, and Lenaig Hemery, "2020 State of the Science Report, Chapter 13: Risk Retirement and Data Transferability for Marine Renewable Energy," Pacific Northwest National Laboratory (PNNL), Richland, WA, USA, PNNL--29976CHPT13, Jun. 2020, doi: 10.2172/1633208.

[15] "FORCE." Fundyforce.ca. Accessed: Jan. 05, 2026. [Online]. Available: https://fundyforce.ca/document-collection/environmental-effects-monitoring-program-quarterly-report-july-september-2025

[16] J. I. Peraza and J. K. Horne, "Quantifying conditional probabilities of fish-turbine encounters and impacts," *Frontiers in Marine Science*, vol. 10, Nov. 2023, doi: 10.3389/fmars.2023.1270428.

[17] A. Bender et al., "Imaging-sonar observations of salmonid interactions with a vertical axis instream turbine," *River Research and Applications*, vol. 39, no. 8, pp. 1578–1589, Jun. 2023, doi: 10.1002/rra.4171.

[18] M. B. Courtney, A. J. Flanigan, M. Hostetter, and A. C. Seitz, "Characterizing Sockeye Salmon Smolt Interactions with a Hydrokinetic Turbine in the Kvichak River, Alaska," *North American Journal of Fisheries Management*, vol. 42, no. 4, pp. 1054–

1065, Jul. 2022, doi: 10.1002/nafm.10806.
[19] T. Yoshida et al., "Experimental study of fish behavior near a tidal turbine model under dark conditions," *Journal of Marine Science and Technology*, vol. 27, no. 1, pp. 541–548, Mar. 2022, doi: 10.1007/s00773-021-00850-w.
[20] M. Grippo, G. Zydlewski, H. Shen, and R. A. Goodwin, "Behavioral responses of fish to a current-based hydrokinetic turbine under multiple operational conditions," *Environmental Monitoring and Assessment*, vol. 192, no. 10, Oct. 2020, doi: 10.1007/s10661-020-08596-5.
[21] J. Onoufriou, D. J. F. Russell, D. Thompson, S. E. Moss, and G. D. Hastie, "Quantifying the effects of tidal turbine array operations on the distribution of marine mammals: Implications for collision risk," *Renewable Energy*, vol. 180, pp. 157–165, Dec. 2021, doi: 10.1016/j.renene.2021.08.052.
[22] OES-Environmental. "Stressor-Specific Guidance Document: Collision Risk." tethys.PNNL.gov. Accessed Jan. 05, 2026. [Online]. Available: https://tethys.pnnl.gov/publications/stressor-specific-guidance-document-collision-risk
[23] K. Smith, "Subsea Monitoring Report- Shetland Tidal Array (as extended) – Bluemull Sound, Shetland – 06642/00009110." marine.gov.scot. Accessed: Jan. 05, 2026. [Online]. Available: https://marine.gov.scot/data/subsea-monitoring-report-shetland-tidal-array-extended-bluemull-sound-shetland-0664200009110
[24] K. E. Buenau, L. Garavelli, L. G. Hemery, and G. García Medina, "A Review of Modeling Approaches for Understanding and Monitoring the Environmental Effects of Marine Renewable Energy," *Journal of Marine Science and Engineering*, vol. 10, no. 1, p. 94, Jan. 2022, doi: 10.3390/jmse10010094.
[25] Tidal Lagoon Power. "Swansea Bay Environmental Statement: Chapter 23 Mitigation and Monitoring." tethys.PNNL.gov. Accessed: Jan. 05, 2026. [Online]. Available: https://tethys.pnnl.gov/publications/swansea-bay-environmental-statement-chapter-23-mitigation-monitoring
[26] THETIS Energy. "Proposed Torr Head Tidal Scheme Environmental Scoping Report." tethys.PNNL.gov. Accessed: Jan. 05, 2026. [Online]. Available: https://tethys.pnnl.gov/publications/proposed-torr-head-tidal-scheme-environmental-scoping-report
[27] Xodus Group, "EMEC Billia Croo Test Site: Environmental Appraisal." tethys.PNNL.gov. Accessed: Jan. 05, 2026. [Online]. Available: https://tethys.pnnl.gov/publications/emec-billia-croo-test-site-environmental-appraisal
[28] E. Cotter and G. Staines, "Observing fish interactions with marine energy turbines using acoustic cameras," *Fish and Fisheries*, vol. 24, no. 6, pp. 1020–1033, Jul. 2023, doi: 10.1111/faf.12782.
[29] H. Farr, "2024 OES-Environmental 2024 State of the Science Report, Chapter 8: Marine Renewable Energy Data and Information Systems," Pacific Northwest National Laboratory (PNNL), Richland, WA, USA, PNNL—36020CHPT8, 2025, doi: 10.2172/2438597.
[30] N. Horne et al., "Collision risk modelling for tidal energy devices: A flexible simulation-based approach," *Journal of Environmental Management*, vol. 278, p. 111484, Jan. 2021, doi: 10.1016/j.jenvman.2020.111484.
[31] L. Hammar et al., "A Probabilistic Model for Hydrokinetic Turbine Collision Risks: Exploring Impacts on Fish," *PLOS ONE*, vol. 10, no. 3, p. e0117756, Mar. 2015, doi: 10.1371/journal.pone.0117756.
[32] K. Rossington and T. Benson, "An agent-based model to predict fish collisions with tidal stream turbines," *Renewable Energy*, vol. 151, pp. 1220–1229, May 2020, doi: 10.1016/j.renene.2019.11.127.
[33] L. G. Hemery, D. J. Rose, M. C. Freeman, A. E. Copping, "Retiring Environmental Risks of Marine Renewable Energy devices: the 'habitat Change' Case," in *Proceedings of the 14th European Wave and Tidal Energy Conference*, Sep. 2021.
[34] D. Hasselman et al., "'Scaling up' our understanding of environmental effects of marine renewable energy development from single devices to large-scale commercial arrays," *Science of the Total Environment*, 904, 166801, 2023, doi: 10.1016/j.scitotenv.2023.166801.

Understanding Ground Conditions

Dr. Trevor King

Dr. Luke Griffiths

Dr. Maarten Vanneste

Risks and challenges of offshore wind projects

Who should read this paper?

Stakeholders interested in the seafloor and sub-seafloor conditions across proposed wind energy development areas and how they impact the location, installation, and design of project facilities (i.e., turbines, sub-stations, cables) will find this paper of value. This will include energy regulators, data acquisition companies, offshore wind developers, local communities, and other marine industries (e.g., shipping, fishing, tourism).

Why is it important?

There is a large body of public domain literature and data on the ground conditions offshore Nova Scotia, most of which has been generated by the Geologic Survey of Canada. This paper integrates this information in the context of offshore wind development and summarizes the ground-related risks and uncertainties that face future offshore wind projects. It draws on industry-leading expertise in geological and geotechnical site characterization, and specifically from key players in successful offshore wind projects around the globe. Two of these projects are presented as case studies, providing an expectation of things to come and a basis to predict potential future complications, plan for process improvements, and generate efficiencies.

Nova Scotia is poised for a rapid transition in energy supply and much of its generation capacity lies off the Atlantic coast where conditions are right for large-scale offshore wind development. As outlined in its roadmap for offshore wind development, including the Wind West project, the next decade will see a significant increase in ocean activities. This will include metocean surveying, marine site investigation, and port developments, but this is all predicated on the technical and commercial success of the first few projects. This success will require a tremendous degree of collaboration and aligned effort across all stakeholders, and this paper could help develop the necessary line of sight.

Much of this paper builds from a Desktop Study that was completed in August 2025 (and updated in November 2025), the lead for which is also the lead author in this paper. The study – both a full report and a digital project – is available at https://info.tgs.com/nova-scotia-desktop-study.

About the authors

Dr. Trevor King is lead principal geoscientist at NGI with over 25 years of experience in technical, project management, and strategic planning roles that span the range of geologic settings and operational environments. Recent work has included the integrated interpretation of geoscience and geotechnical data to generate ground models in the Americas and Europe, the development of machine learning algorithms to estimate glauconite content in soils, and leading a desktop study to understand wind and ground conditions offshore Nova Scotia. Prior to NGI he worked for Vår Energi, Imperial Oil, and ExxonMobil on offshore projects across the globe, living in Canada, UK, Norway, Nigeria, and USA. He is a technical expert in seismic interpretation, site characterization, data science, and geographical information systems.

Dr. Luke Griffiths is a senior geophysicist at NGI specializing in geophysics, subsurface characterization, inversion, and data science. With a PhD in experimental geophysics and extensive experience in both laboratory and field studies, he leads and contributes to ground model development projects integrating geological, geophysical, and geotechnical data for major offshore wind developments. His skills in numerical analysis, inverse methods, and data science allow him to process, integrate, and present complex and heterogeneous geoscientific datasets to provide new and robust understanding of challenging geological environments. He has served as geoscience lead on large offshore wind projects, including Arklow Bank Wind Farm and Bałtyk II and III, has authored over 20 peer-reviewed publications and conference proceedings, and is a regular reviewer for international journals in geophysics.

Dr. Maarten Vanneste is a technical expert at NGI with more than 25 years of experience from both academia and consultancy. At NGI since 2006, his work includes offshore geohazard and risk assessment, integrated site characterization, geophysical mapping techniques, multi-component seismics, quantitative seismic interpretation, fluid flow phenomena, and the development of data-driven ground models with particular focus on offshore renewables. He is a leading member of the ISO Technical Panel 19901-10 on Marine Geophysical Investigations; chairman of the bi-annual conference series Applied Shallow Marine Geophysics, initiated in 2014, under the umbrella of the EAGE Near-Surface Geoscience Division; and Scientific Committee member of the EAGE Energy Transition Conferences. He has overseen and guided most of the integration and geoscience activities for various large offshore wind projects (e.g., Empire Wind, Dogger Bank South, Bałtyk II and III, Arklow Bank, Ten noorden van de Waddeneilanden, IJmuiden Ver, Mona, Morgan, Morven), and has authored or co-authored over 50 peer-reviewed publications and conference proceedings.

OFFSHORE WIND SITE CHARACTERIZATION: EXAMPLES FROM NOVA SCOTIA, AMERICA, AND EUROPE

T. A. King[1*], L. Griffiths[2], M. Vanneste[2]
[1]NGI USA, Houston, TX, USA
[2]NGI Norway, Oslo, Norway
** Corresponding author: trevor.king@ngi.no*
DOI: https://doi.org/10.48336/JAAX-NT79

ABSTRACT

The technical and commercial success of offshore wind farms requires a robust understanding of ground conditions so that facilities can be optimally located and designed, and then successfully installed and operated. At the outset, a desktop study can provide an initial assessment of the ground conditions (i.e., geohazards, engineering constraints, and soil/rock properties) that are expected across potential project sites. This can aid screening-level decisions around project feasibility and concept selection and, where outcomes are positive, additional site investigation data are acquired. An understanding of the spatial variability in ground conditions is then developed as a ground model. As a project matures toward final investment and uncertainties are further reduced, the ground model can become increasingly quantitative and may include probabilistic predictions of properties in 3D.

This paper summarizes the ground-related risks and challenges that offshore wind projects will face in Nova Scotia, many of which result from glacial processes that were active over ten thousand years ago. We discuss how to maximize the value of new geophysical, geotechnical, and geological data and illustrate the importance of collaboration across these technical disciplines. Case studies from developments in formerly glaciated regions demonstrate how robust site characterization can optimize engineering decisions and reduce development timeframes. We conclude with a look to the future and suggest steps that may help Nova Scotia realize its bold offshore wind vision.

Keywords: Nova Scotia, offshore wind, site investigation, site characterization, desktop study, ground model, geohazards, engineering constraints, geotechnical properties, seismic inversion, machine learning, value of information

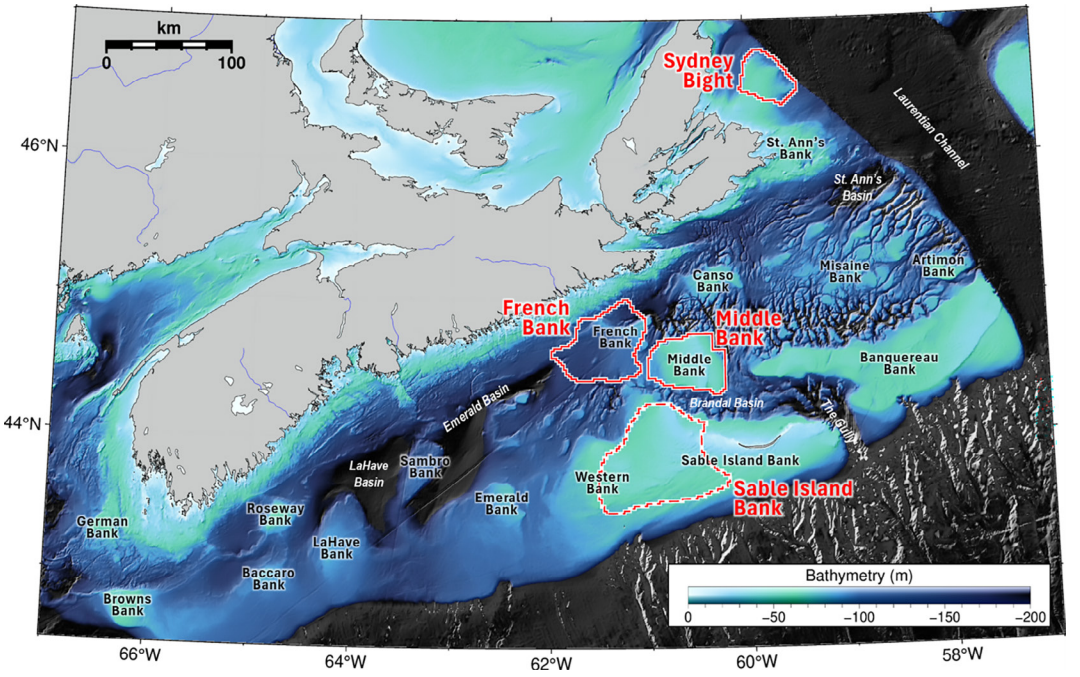

Figure 1: Bathymetry map (colour bar clipped to 200 m water depth; data from [2]), showing the shallower banks (black labels) and deeper basins (white labels) across the continental shelf. Solid red polygons show the three Wind Energy Areas (WEAs) that will be the focus of Nova Scotia's first offshore wind licensing round; Sable Island Bank WEA is expected to be included in future rounds.

1. INTRODUCTION

Nova Scotia is preparing for the large-scale development of its significant offshore wind resource. This will initially focus on three of four designated Wind Energy Areas (WEAs; Figure 1) – French Bank, Middle Bank, Sydney Bight – which cover a combined area of 6,700 km^2, and where water depths range between 30 and 220 m. At anticipated nacelle elevations, mean annual wind speeds exceed 9.5 m/s [1], which is more than sufficient for commercial-scale development. Licensing activities are under way and the expectation is that several parcels across the three WEAs will be available for bidding in a first round that will conclude in 2026.

By 2030, the province is aiming to have wind farm licenses in place for 5 Gigawatts (GW) of generation capacity, and successful bids from the 2026 round may account for up to 3 GW of this. For 15 Megawatt (MW) Offshore Wind Turbines (OWTs) spaced at 1 nautical mile, 3 GW requires around 200 OWTs spread across 685 km^2. This represents ~10% of the area within the three WEAs. While commercial-scale offshore wind farms can range in size, Nova Scotia is expecting the first licensing round to initiate three or four projects.

This represents the beginnings of the larger Wind West Atlantic Energy project that plans for 15 GW of operational capacity by 2040 [3], [4]. This may require the installation of around 1,000 turbines over the next ~15 years covering over 3,000 km^2 of the banks and basins shown in Figure 1. The Wind West project sees an ultimate potential of over 60 GW of generation capacity in Nova Scotia.

Offshore wind development at this pace, which historically has only been sustained and exceeded in China, is predicated on the assumption that Nova Scotia's initial projects demonstrate both technical feasibility and

commercial viability [5]. A critical factor for this is the presence of safe and stable ground conditions that can support a range of project facilities, including fixed-bottom turbine foundations, floating turbine anchors, and power cables both within licenced areas and for export to shore.

This paper uses some of the Desktop Study (DTS) results from [1], which includes in-depth discussion on the wind conditions and shallow geology offshore Nova Scotia. The study goes on to describe ground conditions, maps their variability across the offshore region, and quantifies their impacts on development concepts within each WEA.

2. NOVA SCOTIA GEOLOGIC SETTING

2.1 Glaciation

Offshore wind farm planning typically requires an understanding of the upper 50 to 100 m of the seabed. For example, some of the deepest OWT foundations to date were installed offshore Scotland at the 1.1 GW Seagreen wind farm that penetrate up to 59 m below the seafloor [6]. Across the Nova Scotian shelf, the shallow geology is heavily influenced by Quaternary glaciation, especially the most recent Wisconsinan phase that lasted from around 75 to 11 thousand years (kyr) ago.

At its maximum extent around 20 kyr ago – the so-called Last Glacial Maximum (LGM) – the Laurentide Ice Sheet covered all of Nova Scotia and extended as far out as the current shelf-slope break [7]. Fast-flowing ice streams within the sheet carved deep channels that persist today as distinct bathymetric features, including “The Gulley” between the Sable Island Bank and Banquereau Bank and the U-shaped Laurentian Channel between Nova Scotia and Newfoundland (Figure 1). Thick sequences of mounded till were deposited in terminal moraines across the outer Scotian Shelf (Figure 2).

Complex patterns of sediment deposition and erosion occurred across Nova Scotia as the ice sheet cycled through periods of advancement and retreat that, combined with sea level fluctuations, generated significant geologic heterogeneity. This includes glacial till and boulders from sub-glacial and moraine deposition, glacial outwash sands and muds from meltwater streams, mud and silt from meltwater plumes outboard of the ice sheet, and dropstone boulders. In beach and subtidal areas, deposits were reworked into cleaner sands. Additional complexity results from tunnel valleys formed by sub-glacial streams of high-pressure water, glaciotectonic deformation within grounding zones (e.g., push moraines), and freeze-thaw weathering.

Nova Scotia has been ice-free for the last 10 kyr and the shelf became progressively submerged as sea level rose through the Holocene. Today, only Sable Island remains above the waves (Figure 3) and the last remnants of the great Laurentide Ice Sheet are seen as ice caps over 2,000 km away in Nunavut.

2.2 Shallow Geology

The Geological Survey of Canada (GSC) has undertaken numerous studies across the areas being considered for offshore wind development (e.g., [9], [10], [11], [12], [13]).

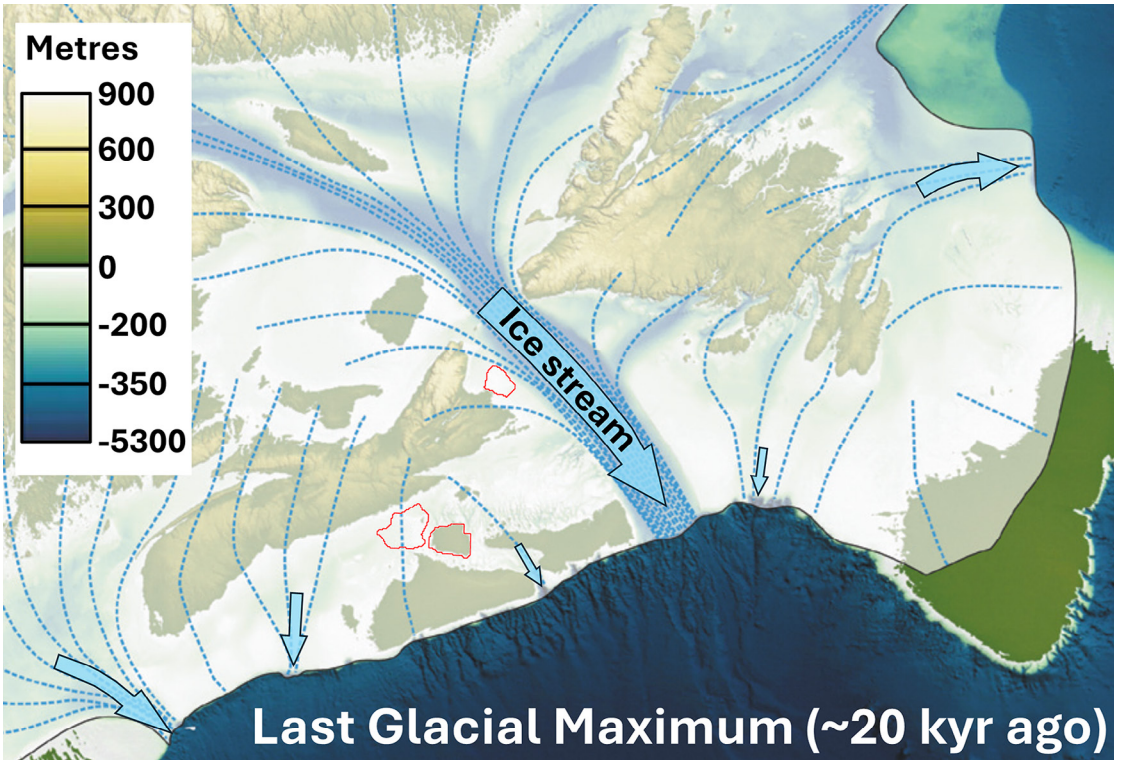

Figure 2: The extent of the Laurentide Ice Sheet at the Last Glacial Maximum (modified from [7]). Colour bar represents ground elevation 20 kyr ago, dashed blue lines are generalized ice flow lines, and blue arrows indicate major ice streams. Red polygons show the four designated Wind Energy Areas (WEAs).

Figure 3: Aerial photograph of Sable Island [8]. The crescent-shaped island is about 40 km long and 1 km wide, with sand dunes up to 30 m high.

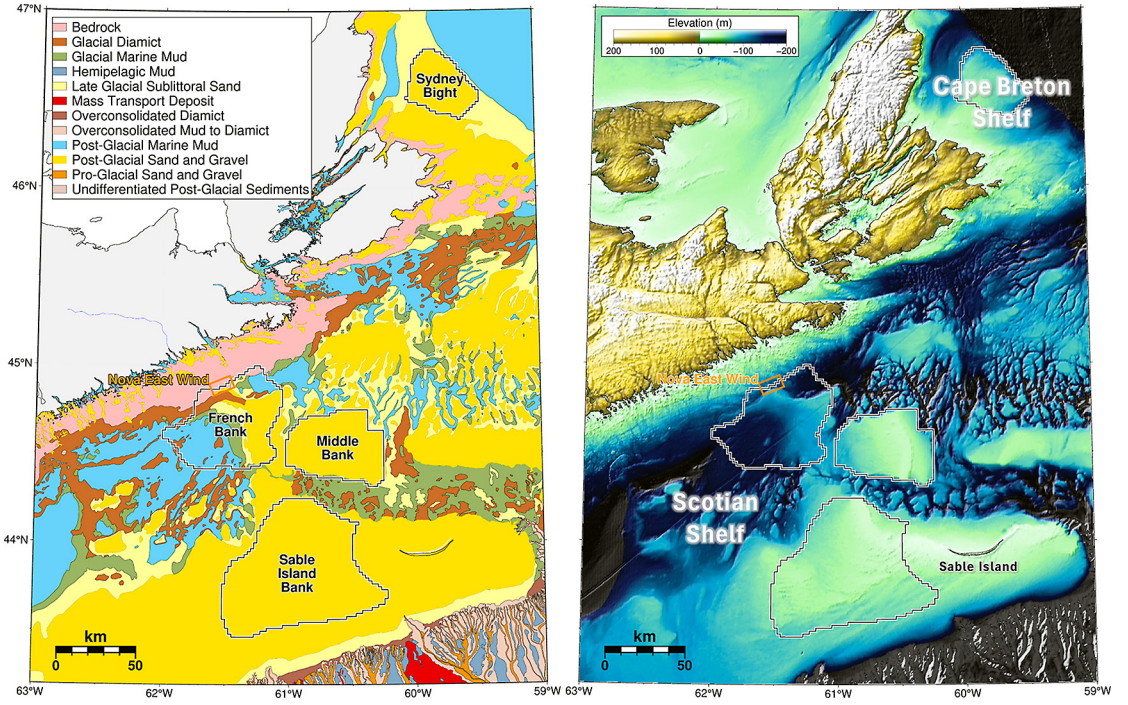

Figure 4: Seafloor geology (left [12]) and bathymetry (right [2]). Black polygons show the designated Wind Energy Areas (WEAs), of which three are on the Scotian Shelf (French Bank, Middle Bank, Sable Island Bank) and one on the Cape Breton Shelf (Sydney Bight). Orange polygon shows the approximate location of a planned floating wind development called Nova East Wind [14].

Table 1: Seafloor lithologies across the shelf (adapted from [9], [11], [12]). Lithology column colours correspond to those across shelfal areas in Figure 4. "Glacial" and "Post-glacial" refer to the Wisconsinan glaciation event.

Lithology		Description	Depositional environment
Post-glacial	Sand & gravel	Sand with gravel; often with mobile bedforms, coarse lags & boulders	Coarse fraction from reworked till and outwash deposits in high energy waves / currents
	Mud	Soft clay & silty clay; weakly stratified, with some organic layers and fine sand	Fines from reworked glacial sediment, widespread deposits in low energy marine basins
Glacial	Sand	Muddy sand, fine sand & silt; little gravel	Reworked till in shallow water, seen mostly as bands around bank edges
	Mud	Silty clay with dropstones; stratified, with varying amounts of sand & gravel	Marine glacial outwash deposits i.e., meltwater plumes outboard of ice sheet
	Till	Poorly sorted conglomerates of boulders, gravel, sand & mud (i.e., diamict)	Sub-ice and moraine deposits
Bedrock	Various	Variable lithologies e.g., Cambro-Ordovician metamorphics, Devonian granites, Carboniferous clastics & coals, Mesozoic-Cenozoic (pre-Wisconsinan) clastics	

Based on its studies, the seafloor geology can be grouped into post-glacial, glacial, and bedrock lithologies (Figure 4; Table 1). Across the entirety of two WEAs (Middle Bank, Sydney Bight), "post-glacial sand and gravel" is exposed at the seafloor, whereas the seafloor geology across the French Bank WEA is more variable and all of the lithologies described in Table 1 are present.

Currently, limited information is available on the sub-seafloor geology within the WEAs.

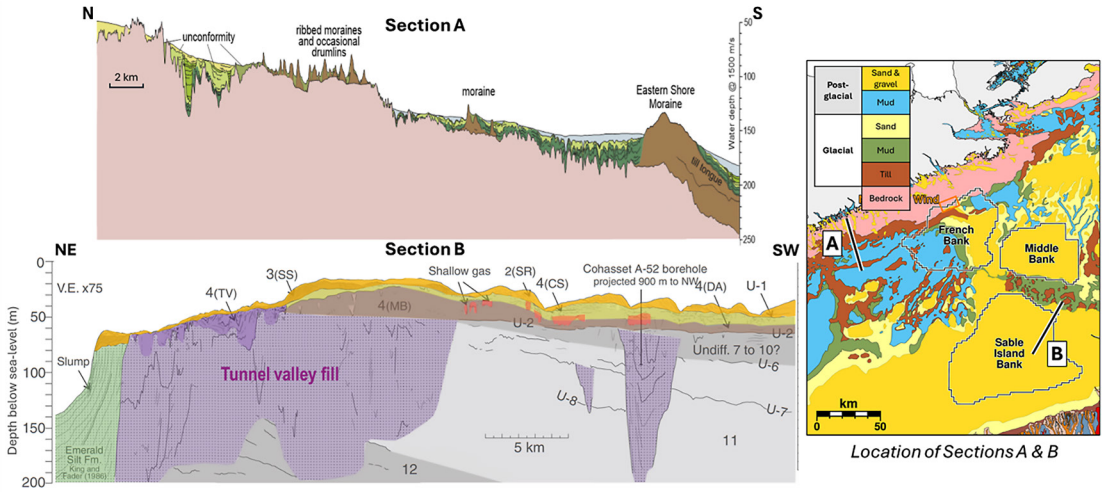

Figure 5: Two published cross sections [10], [21], locations shown on geologic map (modified from [12]). Sections are shown at the same vertical and horizontal scale, with a vertical exaggeration of 75.

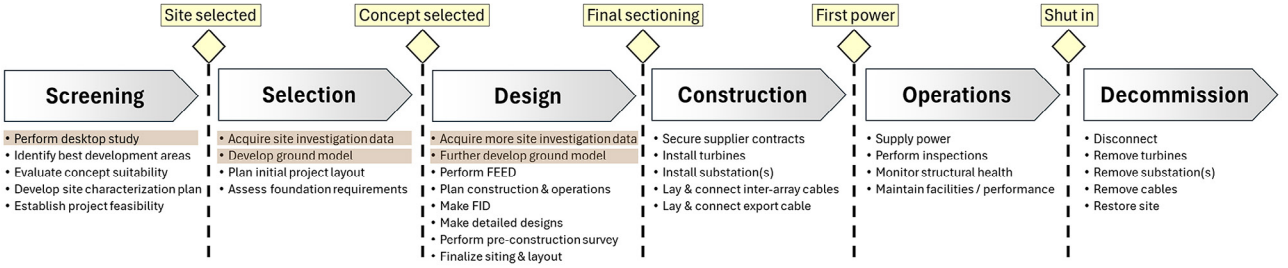

Figure 6: General offshore wind project cycle, with decision gates (yellow) separating development stages. Lists show typical activities, brown shading indicates those for site characterization. FEED: front-end engineering design. FID: final investment decision.

From a general understanding of glacial processes (e.g., [15], [16], [17], [18], [19], [20]), we expect a complex layering and interfingering of glacial and post-glacial lithologies with rapid variations in thickness. This is supported by published seismic cross sections and their interpretations (e.g., Figure 5).

3. SITE CHARACTERIZATION

3.1 General Workflow

A generalized offshore wind project development workflow is shown in Figure 6, where capital and risk are managed through a series of stages separated by decision gates.

Site characterization aims to understand the ground conditions across a development area, which can be grouped into three broad categories:

- **Geohazards:** dynamic or geologic processes that risk project safety and integrity e.g., mobile bedforms, slope instability, earthquakes
- **Engineering Constraints:** static features that impact facility location and design e.g., anomalously soft soils, boulders, existing infrastructure
- **Properties:** geologic and geotechnical parameters e.g., lithology, density, shear strength

At the outset, a DTS of publicly available data can provide an understanding of the ground conditions to facilitate Screening decisions such as project feasibility, site selection, and

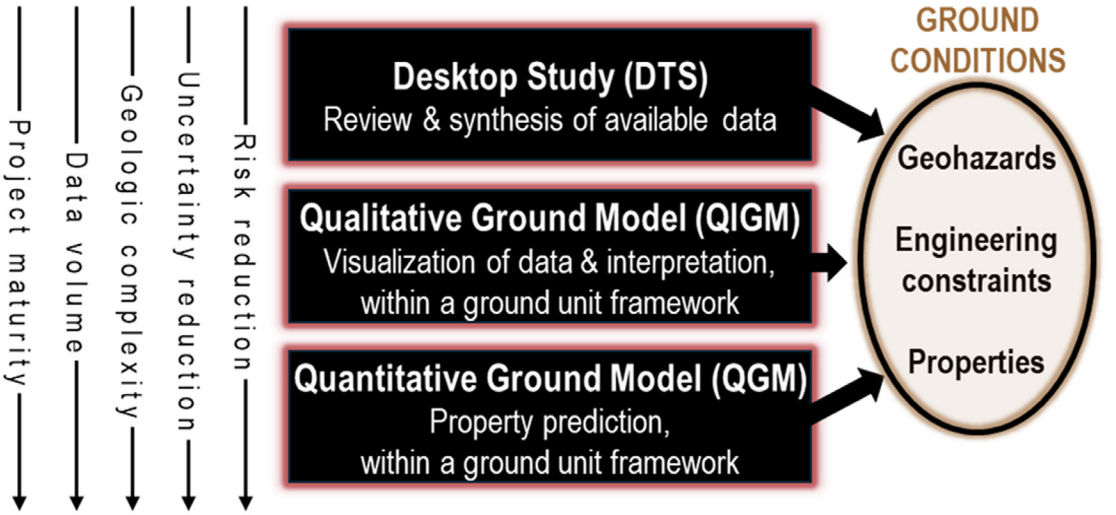

Figure 7: Ground model level of detail, generally increasing from Desktop Study (DTS) to Qualitative Ground Model (QlGM) to Quantitative Ground Model (QGM). More detail may be necessary for higher ground complexities and later project decisions. (Ground unit framework is discussed in Section 3.3.)

the suitability of specific foundation concepts. Where outcomes are positive, additional data are acquired and interpreted, and the spatial variability in ground conditions is represented as a ground model. Several phases of site investigation and ground model generation can occur through the project Selection and Design stages (Figure 6).

We note that while this workflow is generally applicable, different regulatory bodies may award project licenses at different stages. For example, the US Bureau of Ocean Energy Management (BOEM) has held licensing rounds during the Screening stage (e.g., Section 4.1), and the Netherlands Enterprise Agency (RVO) holds licensing rounds in the Design stage (e.g., Section 4.2).

The level of detail in a ground model increases with project maturity as more data are acquired and should ultimately scale with geologic complexity. Where this complexity is modest, a Qualitative Ground Model (QlGM) based on widely spaced data may be adequate for project development. For areas of higher complexity, a Quantitative Ground Model (QGM) based on large volumes of high-resolution data may be necessary to reduce uncertainties and risks to acceptable levels (Figure 7).

Whether due to local regulations or final design requirements, a Cone Penetration Test (CPT), Borehole (BH), or Vibrocore (VC) may ultimately be acquired at most (and maybe all) foundation locations. While this may cause some to speculate "*if we're going to measure properties, why model them?*", the following value propositions should be considered:

- **DTS:** An early and accurate understanding of the expected ground conditions and their levels of complexity can generate significant efficiencies by enabling robust decisions around project feasibility, licensing strategy, and initial site investigation.
- **QlGM:** Where ground complexity is modest, qualitative models showing the geologic and geotechnical variability across a site may be sufficient to proceed

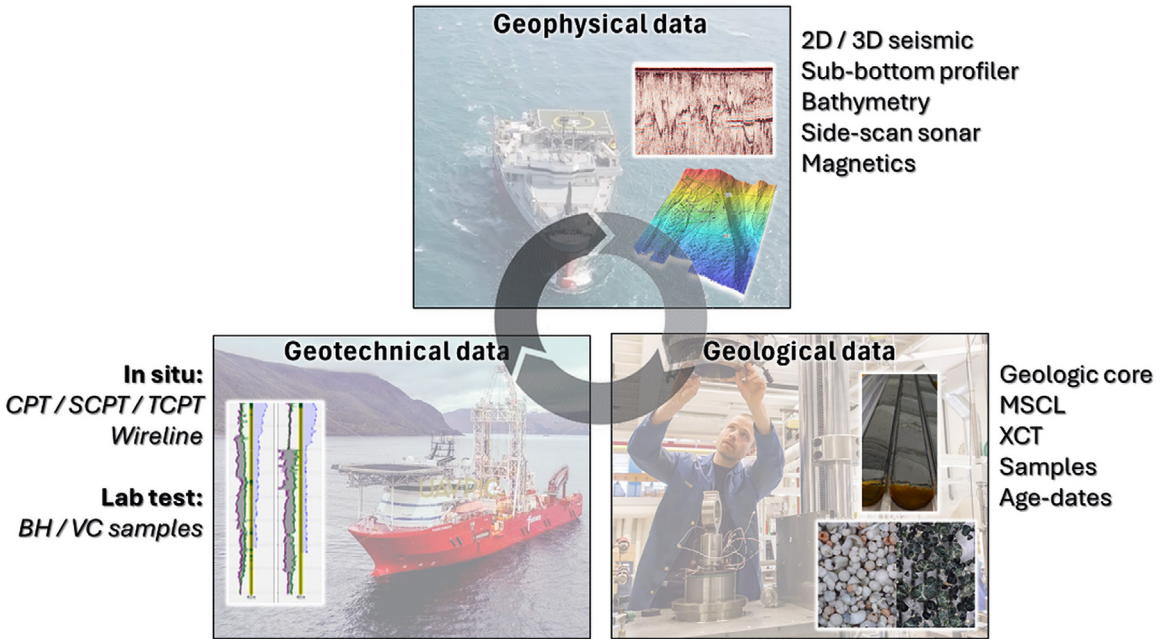

Figure 8: Site investigation data typically required to understand ground conditions across an offshore wind site. CPT: Cone Penetration Test. SCPT: Seismic CPT. TCPT: Thermal CPT. BH: Borehole. VC: Vibrocore. MSCL: Multi-Sensor Core Logging. XCT: X-ray Computed Tomography.

to the Construction and Operations stages. In more heterogeneous regions, the model can identify areas of high complexity and critical uncertainty that require further investigation.

- **QGM:** The ability to predict geotechnical properties (and their uncertainties) at any location across a site can provide flexibility and guard against unforeseen complications, especially in areas of high geologic complexity. If the geotechnical data at a planned foundation location is poor (e.g., early refusal, low recovery) or absent (e.g., only one CPT acquired across several floating anchor locations), a predictive model may provide a design basis with the required level of confidence. In addition, where there is some uncertainty in the final deployed location (e.g., anchors, torpedo piles), a predictive model may identify large enough target areas where geotechnical variability remains within tolerance limits. If a foundation location needs to be optimized (i.e., micro-siting) or changed (e.g., clearance requirement, installation failure), a location that is further from geotechnical measurement may be selected on the basis of predicted parameters.

Ultimately, the value of a ground model is measured by its ability to reduce uncertainties and risks to levels that enable the project to progress to the Construction and Operations stages in an efficient and cost-effective manner. This is returned to in the case studies presented in Section 4.

3.2 Site Investigation

Several types of data are required to understand ground conditions for a project to develop and operate successfully. These generally fall into three categories: geophysical, geotechnical, and geological

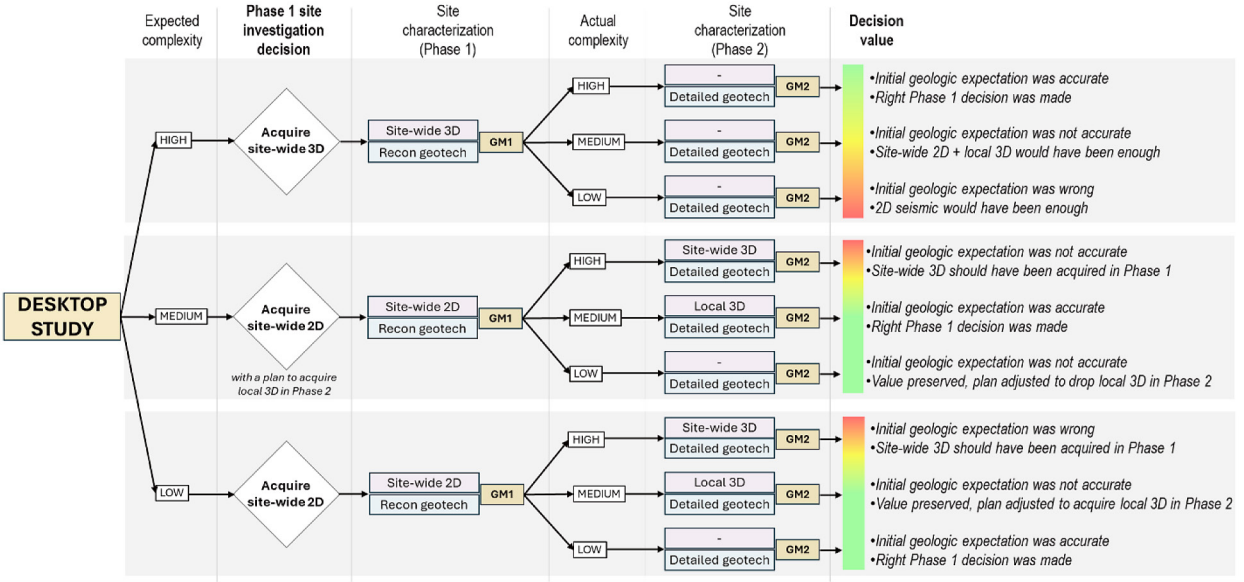

Figure 9: Value creation (green) or erosion (red) related to the decision to acquire site-wide 2D or 3D seismic data early in site characterization. Assumes "low" geologic complexity is adequately resolved on 2D, "medium" complexity requires some local 3D, and "high" complexity requires site-wide 3D seismic. GM1 and GM2 refer to ground model iterations.

(Figure 8). Maximizing the value of these data requires coordinated acquisition plans that continually refer to the evolving ground model to target the reduction of project-critical uncertainties.

3.2.1 Geophysical Data

Ultra High-Resolution (UHR) or extremely high-resolution multi-channel seismic reflection data [22] are probably the most important geophysical data for accurate characterization of offshore wind sites. The higher the frequency content, the higher the resolution, although there is a natural trade-off with imaged depth as higher frequencies are preferentially attenuated. In general, sub-metre vertical resolution to depths of at least 50 m is desired.

Deciding whether, where, and when to acquire 3D seismic should consider the value of information given the expected level of geologic complexity (although additional factors may be important [23]). Early and site-wide 3D seismic may add value in highly complex areas, enabling the migration of energy to its true point of reflection and allowing detailed geologic mapping. Alternatively, where geology is less complex, it may be better to acquire site-wide 2D seismic, and later – when ground conditions are better understood – acquire 3D in areas of highest uncertainty and risk (e.g., [24]). Figure 9 illustrates how a good and reliable DTS can be a significant factor in making the right decision.

Understanding the seafloor and the first few metres of the seabed often requires the acquisition of additional geophysical data such as Sub-Bottom Profiler (SBP), Multibeam Echosounder (MBES) bathymetry, Side Scan Sonar (SSS), and Magnetics (MAG). These data are typically acquired along with high-resolution seismic (Figure 10; [25]), and integrated interpretations are critical to

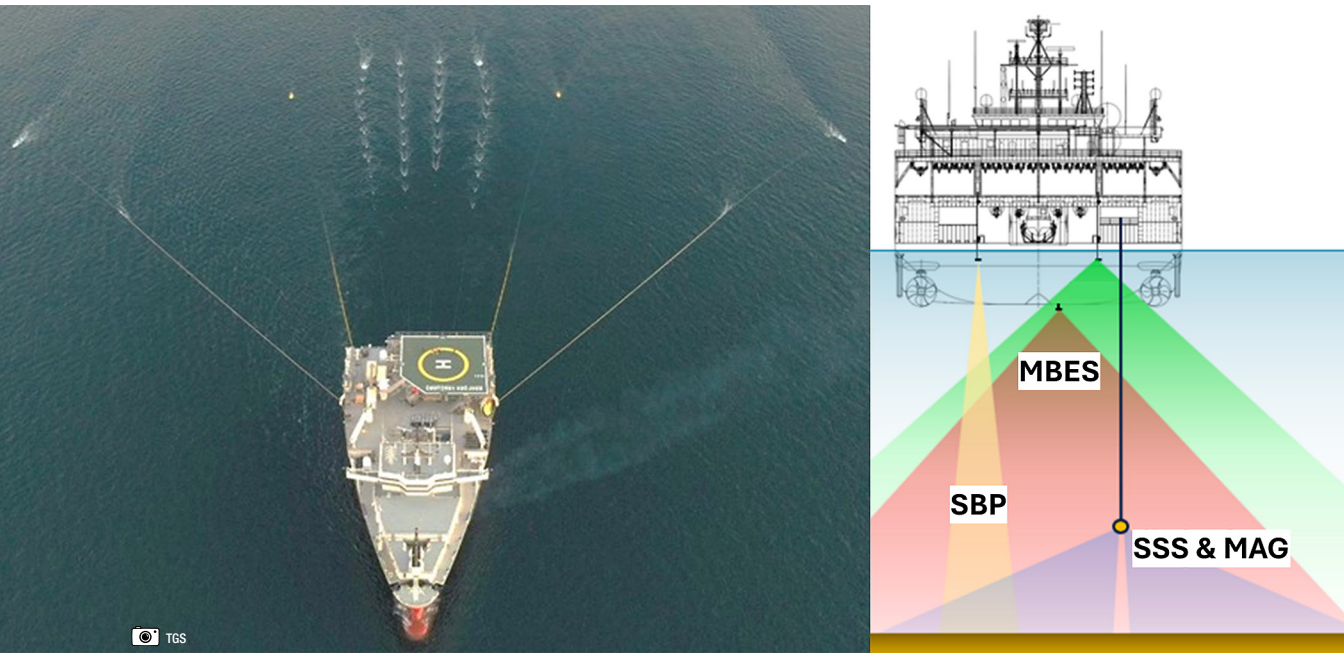

Figure 10: Integrated acquisition of Ultra High-Resolution (UHR) seismic and other geophysical data. MBES=Multibeam Echosounder. SBP=Sub-Bottom Profiler. SSS=Side Scan Sonar. MAG=Magnetics.

Figure 11: Geotechnical laboratory testing.

accurately identify, characterize, and map geohazards and engineering constraints in the ground model.

3.2.2 Geotechnical Data

Geotechnical data are obtained through CPTs, BHs, VCs, and wireline log measurements. Subsequent analyses, including basic and advanced laboratory testing (Figure 11), generate depth profiles of the geotechnical properties that are critical to engineering design and installation. These properties are

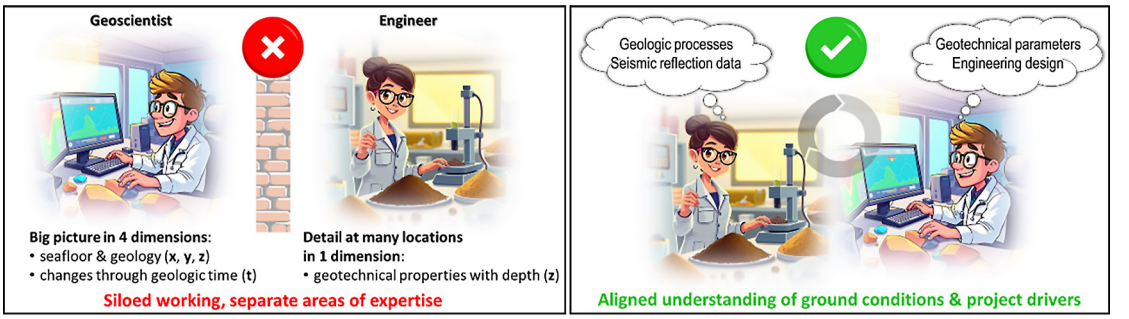

Figure 12: Effective integration of geoscience and engineering expertise requires mutual understanding of disciplines with an aligned view of ground conditions and project drivers.

expected to vary significantly across formerly glaciated regions. As site characterization progresses, it is typical to see multiple site investigation campaigns e.g., an initial "reconnaissance" phase followed by "detailed" phases that target critical uncertainties identified in the evolving ground model (see Figure 9). In general, locating geotechnical data precisely on seismic lines can reduce uncertainty in their integrated interpretation and generate more accurate ground models.

3.2.3 Geological Data

Geological data come from tests performed on samples obtained from the seafloor, BHs, and VCs. The most fundamental of these is a core description – often integrating high-resolution photography, Multi-Sensor Core Logging (MSCL), X-ray Computed Tomography (XCT), CPT, and wireline data – to describe the vertical succession of geologic facies at a single location. This includes grain types, grain sizes, sedimentary features and fossil assemblages and, when integrated with seismic/SBP data, can help understand the lithologic variability across a site. This is often enhanced by performing radiocarbon and biostratigraphic age-dating at key locations and depths to understand the depositional history across the project site and establish a robust, chronostratigraphic ground unit framework.

3.3 Ground Model Generation

Overly conservative engineering of offshore wind structures is undesirable, and accurate ground models are needed to generate optimal and lowest-cost geotechnical designs. This begins with the interpretation of a 3D "ground unit framework" (sometimes called a "structural framework," "stratigraphic framework," or "geologic ground model"), a succession of chronostratigraphic layers whose boundaries correspond to seismic reflection events (i.e., "horizons") and to measured changes in geotechnical/geological properties. The spatial variability in the properties of a single unit may then be understood by considering the distribution of environments and processes that were present during (and maybe also following) its deposition.

Seismic interpretation is typically performed in the Two-Way Time (TWT) domain and tying ground unit boundaries to geotechnical data generates interval velocities. These can be used in conjunction with other velocity information (e.g., seismic, wireline, Seismic Core Penetration Test (SCPT), MSCL) to generate a ground unit framework in depth.

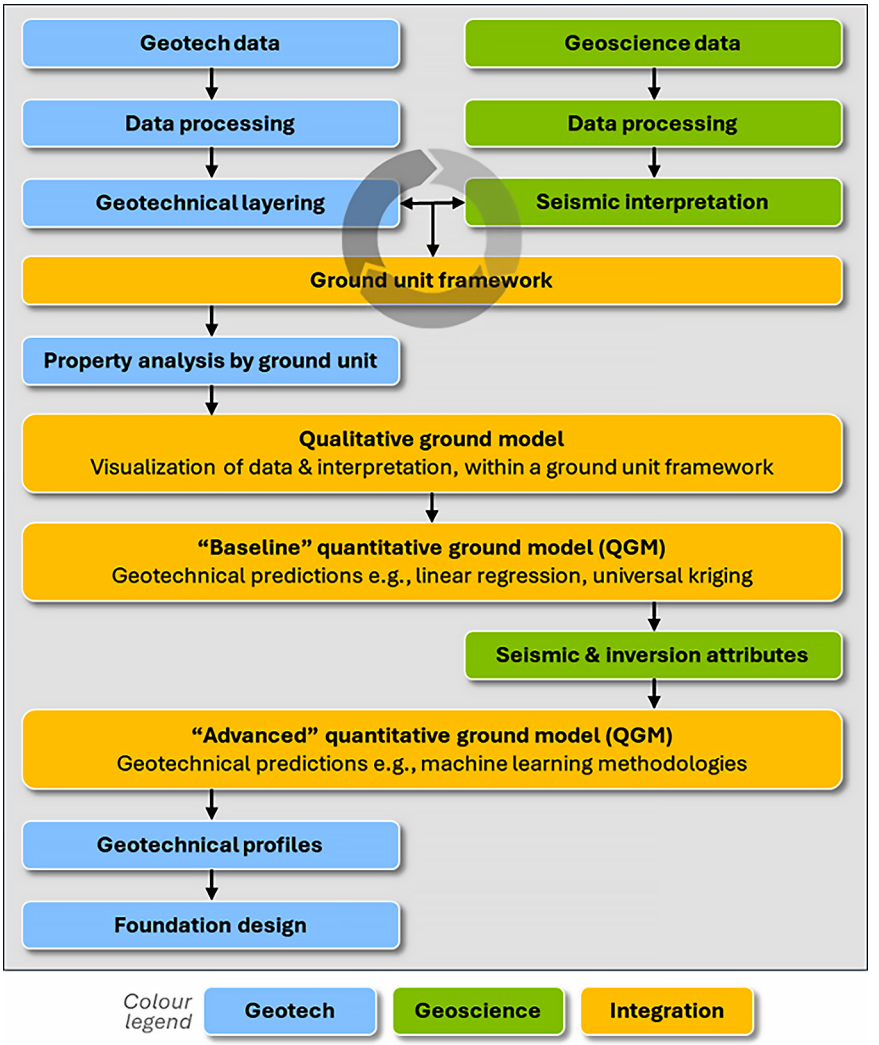

Figure 13: General workflow for qualitative and quantitative ground models. After site investigation data have been acquired and processed, geoscientists and geotechnical engineers define and map a ground unit framework in 3D. Geotechnical measurements are then analysed, understood, and – if required – predicted across a project site within that framework.

As more data are acquired, it is often necessary to update this framework – such as adding/sub-dividing units and refining their top and base depths – requiring close collaboration between geoscientists and geotechnical engineers (Figure 12).

As a project matures toward the Construction and Operations stages, more targeted data are acquired to address critical uncertainties and the level of detail in the ground model increases (see Figure 7). Ground models may become more quantitative and include probabilistic prediction of properties in 3D (Figure 13). The simplest predictions involve linear regression and geostatistical interpolation to predict properties within each ground unit. If combinations of seismic and inversion attributes are shown to correlate with geotechnical measurements, then machine learning techniques can be used to make predictions [26].

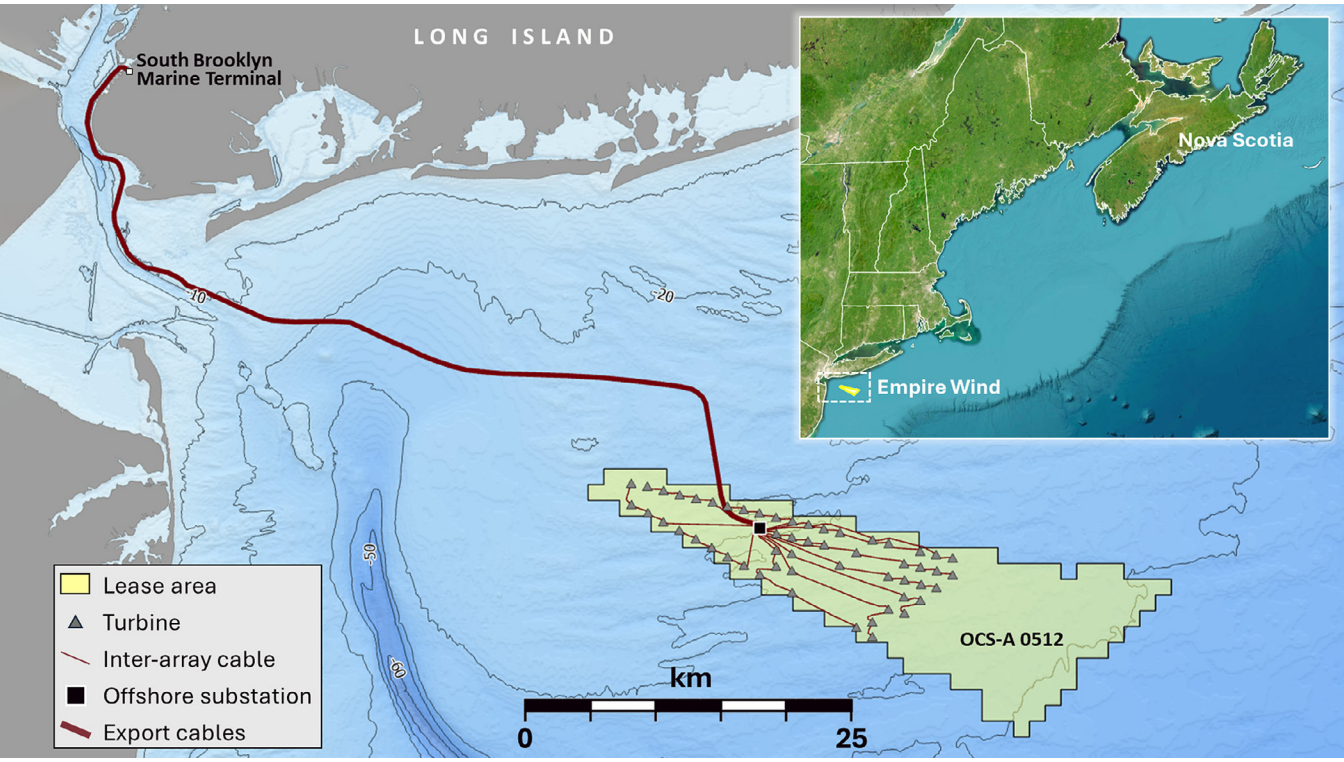

Figure 14: Empire Wind location map. The project includes 54 turbines in water depths of 23-36 m, and 150 km of export cable connecting the substation to the South Brooklyn Marine Terminal.

4. CASE STUDIES

The approach described in the previous section is being followed at offshore wind projects in formerly glaciated regions including the US Atlantic, the North Sea, the Irish Sea, the Barents Sea, and the Baltic Sea. We highlight two case studies where ground conditions are analogous to those present offshore Nova Scotia: Empire Wind (USA) and Ijmuiden Ver (IJV; Netherlands).

4.1 Empire Wind, USA

4.1.1 Project Summary

Empire Wind is located in the New York Bight about 30 km south of Long Island, where water depths range between 23 and 36 m (Figure 14). The 320 km^2 offshore lease area (OCS-A 0512) was awarded to Statoil (now Equinor) in a December 2016 licensing round. Site investigation began in 2018 with BOEM's approval of the site investigation plan, and the final Construction and Operations Plan was approved in February 2024. The development includes 54 OWTs (15 MW capacity) on monopile foundations for a total project capacity of 810 MW. Over 150 km of inter-array cables will connect these to an offshore substation, and two 75 km long export cables will connect to a terminal in south Brooklyn at the western tip of Long Island. Front-End Engineering Design (FEED) commenced in February 2021, construction began in April 2024, monopile installation began in September 2025, and first power is expected by the end of 2026, ten years after the licensing round.

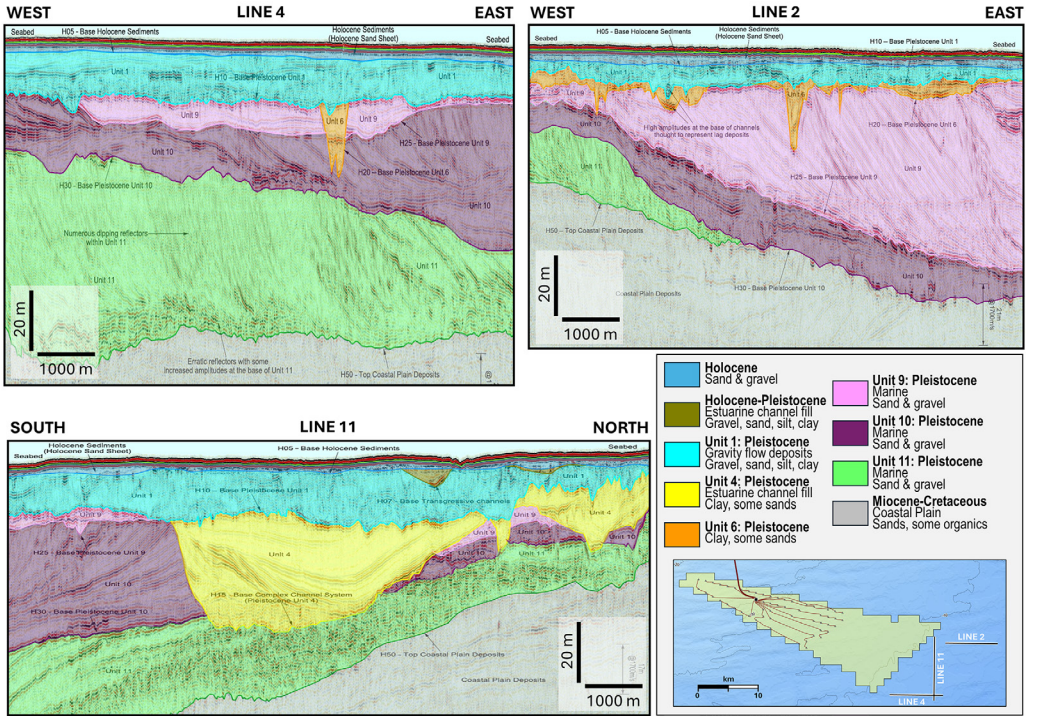

Figure 15: Seismic cross sections located immediately east of the Empire Wind lease (modified from [31], vertical exaggeration ~50), illustrating geologic complexities across the area. Interpretations are consistent with an initial ground unit framework that was developed across the Empire Wind site, which became increasingly more detailed with time to account for the spatial variability in measured geotechnical properties and seismic reflection characteristics.

4.1.2 Geologic Summary

The Quaternary geology across the New York Bight is diverse. This reflects depositional and erosional processes related to cycles of glaciation and sea level fluctuation through the Pleistocene (2.58 Myr to 11.7 kyr ago) and Holocene (11.7 kyr ago to present day) epochs.

At the maximum of the Wisconsinan glaciation around 20 kyr ago, the Laurentide Ice Sheet extended as far south as Long Island, marked by the Harbor Hill and Ronkonkoma moraines [27], [28]. The Empire Wind site is located 50 km south of the maximum ice extent, in what would have been a periglacial environment (i.e., where the ground is perennially or seasonally frozen) through the Wisconsinan cycle. We, therefore, expect the shallow geology to show a high degree of spatial variability [29], although absent of the complexities that occur at the base and edges of ice sheets (e.g., tunnel valleys, eskers, drumlins, ground moraine, terminal moraine).

The export cable route remains to the east of the present-day Hudson channel axis (Figure 14) where surficial sediment is dominantly sand, but some regions of till and boulder fields exist. Across the lease area, seafloor gradients are generally less than 1 degree. A 1 to 2 m cover of Holocene (i.e., post-LGM) sand with some gravels has been reworked into broad ridge-and-swale bedforms (<1 m height, up to 2 degrees slope), indicating a degree of sediment mobility. These sediments are underlain by the Pleistocene estuarine, marine and gravity flow deposits comprising gravels, sands, silts, and clays in varying proportions. Rapid thickness changes, channel incisions, and complex cross-cutting geometries occur, and these continue into the region to the immediate east of the lease area (Figure 15).

Table 2: Offshore site investigations performed at Empire Wind. Early Export Cable Routes (ECR) surveys included four routes to potential landfall sites in New York and New Jersey. Excludes metocean, benthic, wildlife, and archaeological surveys. Compiled from several public sources; may not be entirely accurate or complete. TCPT=Thermal Core Penetration Test

Year	Type	Location	Data
2018	Geophysics	Lease	MBES, SSS, MAG, SBP, 2D UHRS multi-channel
	Geophysics	ECR	MBES, SSS, MAG, SBP
	Geotech	Lease	VC, CPT, seafloor samples
	Geotech	ECR	VC, CPT, seafloor samples
2019	Geotech	Lease	BH, CPT, SCPT
	Geotech	ECR	VC, CPT, TCPT
	Geotech	ECR	Seafloor samples
2020	Geophysics	ECR	MBES, SSS, MAG, SBP, 2D UHRS single channel
	Geotech	Lease	VC, CPT, TCPT
	Geotech	Lease	BH, CPT
	Geotech	ECR	BH, VC, CPT
2021	Geotech	Lease	BH, CPT
2023	Geophysics	Lease & ECR	SSS, MAG (UXO clearance)
	Geotech	ECR	VC

This is underlain by partially lithified Miocene-Cretaceous coastal plain deposits, comprising coarse to medium sand with occasional gravel and organic matter [30].

4.1.3 Site Characterization

It is likely that some studies on the ground conditions were performed before the 2016 licensing round and, although details are not available, information may have been similar to that in regional and desktop studies that are now in the public domain (e.g., [30], [32], [33], [34], [35]). These describe the regional geology and highlight the geohazards (e.g., mobile bedforms) and engineering constraints (e.g., boulders, soft soils, communication cables) that future developments would likely encounter.

From 2018 to 2023, several proprietary geophysical and geotechnical surveys were performed across the lease area and along Export Cable Routes (ECRs) (Table 2). High-resolution geophysical data were acquired early on – including SBP and UHR seismic – which enabled the generation of a ground unit framework to understand the variability measured at geotechnical locations. Although no 3D seismic data were acquired, the 2D lines were closely spaced at ~30 m (with perpendicular tie-lines every 500 m). Geotechnical data were acquired in several phases, beginning with reconnaissance acquisition in 2018 and becoming more detailed and targeted as project plans matured. This ultimately included the acquisition of CPT, BH, and VC data at several hundred locations.

Early results identified the presence of glauconite in Pleistocene and Cretaceous units, an iron potassium mica that can form in shallow marine environments. When stressed, glauconite grains can crush and degrade into clay-like material and change the soil's strength, compressibility, and drainage characteristics. This can lead to increased pile-driving resistance and premature refusal [36],

Figure 16: Monopile installation using a semi-submersible crane vessel, driving the piles to sub-seafloor depths of 50 m (left). Installed 15 MW turbines with a rotor diameter of 260 m, with tips reaching 290 m above sea level (middle). Cable laying along the 75 km route from south Brooklyn to the offshore substation (right).

[37]. In 2019 and 2020, detailed geotechnical data were acquired to understand glauconite distributions and the potential impacts on Empire Wind foundation location, design, and installation. In 2021, recognizing the need for a greater and more regional level of understanding, the Piling in Glauconitic Sand Joint Industry Project was established [38].

Several ground model iterations were performed across the lease area and export cable routes, becoming more detailed as development plans matured and the subsurface complexities became apparent. More ground units were defined and mapped to understand the varying glauconite levels seen in the geotechnical and geological data, and to capture the stratigraphic complexities associated with periglacial environments and fluctuating sea level. A QlGM that was developed toward the end of the Design phase included 46 ground units [39], and the results factored into the project's decision to install monopiles using a semi-submersible crane vessel (Figure 16).

4.2 IJV Gamma Wind Farm Zone, Netherlands

4.2.1 Project Summary

The Dutch offshore wind energy roadmap aims to grow offshore wind capacity to 21 GW by 2032 and 50 GW by 2040. The IJV area was identified in 2019 as one of the development areas, and the 278 km^2 "Gamma" portion is located about 60 km offshore where water depths range between 23 and 35 m (Figure 17). A licensing round is being planned that includes the development of two wind farms (Gamma-A, Gamma-B), each with a generation capacity of 1 GW.

4.2.2 Geologic Summary

The upper 100 m of ground is comprised of Pleistocene and Holocene sediments with a complex layering that records three cycles of glaciation [40]. The deepest layers of interest were deposited over 500 kyr ago in systems flowing in from the east. These deposits include cycles of deltaics coarsening up to fluvial sands, with regional unconformities and deep channel cuts.

Glaciation cycles intensified from the mid-Pleistocene, and ice advanced across the IJV Gamma site during the Elsterian glaciation (500-421 kyr ago), carving deep tunnel valleys that were filled by a succession of till and marine mud. As the ice retreated, a network of braided rivers cut fluvial channels that were filled by a mix of clastic lithologies

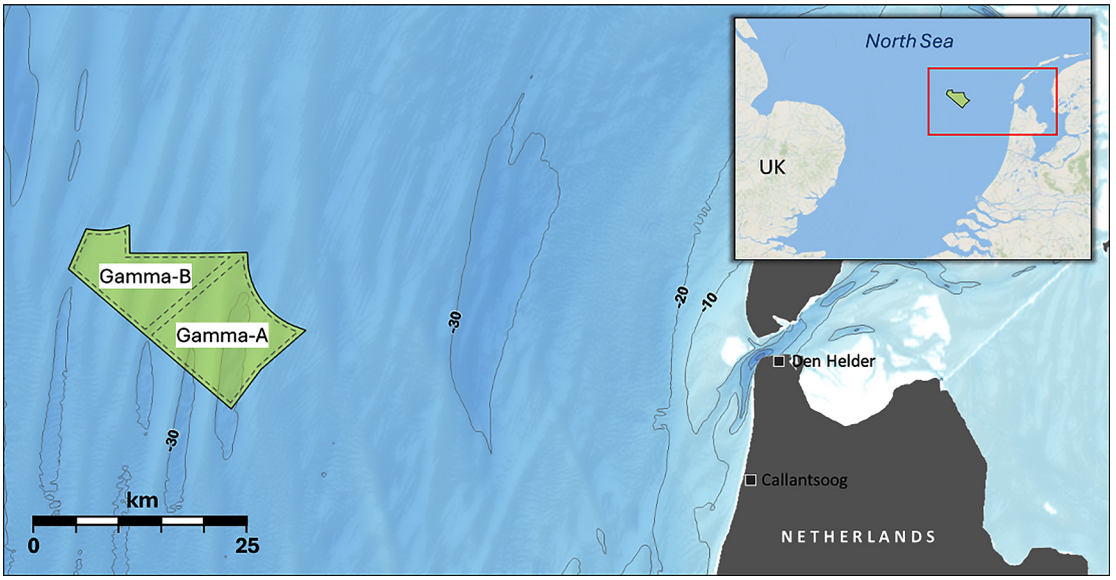

Figure 17: Location of the IJV Gamma wind farm zone, where two projects are planned (Gamma-A, Gamma-B). The ~60 km long export cable route to shore is not yet defined.

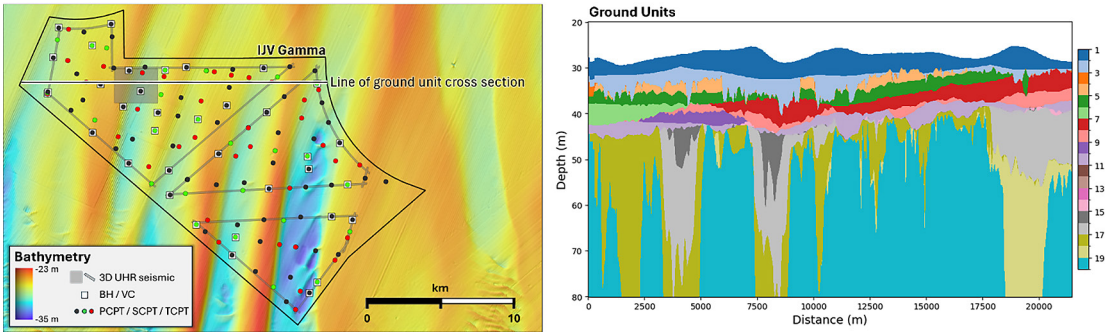

Figure 18: Bathymetry map showing location of geophysical and geotechnical site investigation data; 2D seismic not shown but was acquired across the entire IJV Gamma site (left). West-east geologic cross section showing 19 ground units (right).

until rising sea level saw the deposition of open marine fine-grained sand, silt, and clay.

During the Saalian glaciation (395-130 kyr ago), sea level fell again, and the environment transitioned from marine, to coastal, and ultimately to terrestrial periglacial conditions. Sediments include cycles of terrestrial, shallow marine, and meltwater plume deposits. Ice advanced to within ~50 km of the site from where it began to retreat, and the rising sea levels again resulted in transgressive erosion and deposition in a succession of fluvial, coastal, and marine environments.

The maximum extent of glacial ice during the Weichselian phase (115-12 kyr ago; equivalent to the Wisconsinan in North America) lies ~100 km from IJV Gamma, and the associated low sea level exposed the site again and periglacial conditions returned. With glacial retreat during the early Holocene, sea level rise created a marine transgressive surface with a complex system of channels filled with lagoonal, littoral, and fluvial sediments. On top of these we see high energy open marine deposits that form the waves and ripples of today's seafloor (see Figure 18).

Table 3: Offshore site investigations performed at IJV Gamma, in chronological order. Excludes metocean, benthic, wildlife, and archaeological surveys.

Year	Type	Location	Data
2021	Geotech	Lease	BH, CPT (reconnaissance, 12 locations)
	Geophysics	Lease	MBES, SSS, MAG, SBP, 2D UHRS multi-channel
2022	Geophysics	Lease	3D UHRS (7 km^2 area)
	Geotech	Lease	VC, CPT, TCPT, seafloor samples
	Geophysics	Lease	MBES, 3D UHRS corridors (3 loops, 110 m wide, 125 km)
2023	Geotech	Lease	Seafloor / shallow samples
	Geotech	Lease	CPT, SCPT, TCPT (shallow phase)
2023-4	Geotech	Lease	BH, CPT, SCPT, wireline (deep phase)

4.2.3 Site Characterization

A DTS was completed in 2019 that formed the basis for initial site investigation plans. After a reconnaissance geotechnical survey in 2021 (12 locations, to depths of 80 m), 2D seismic data – both SBP for shallow imaging and multi-channel UHR to image down to 100 m – were acquired across the entire lease, with 70 m inline spacing (oriented NNE-SSW) and 420 m crossline spacing for a total of 5,700 line km. The detailed geotechnical campaigns were planned so that CPTs, BHs, and VCs were located precisely on geophysical survey lines. In total, core samples were retrieved from 36 locations and CPTs were acquired at 115 locations (includes piezo, seismic, and thermal CPTs) with penetrations down to 80 m (Table 3; Figure 18).

Understanding and interpreting the features associated with the glaciation cycles and sea level fluctuations was critical to the development of the ground unit framework. This comprised of 19 units mapped on the UHR seismic data (in TWT) which, when converted to depth, lined up with geotechnical changes seen on the CPT data. This effectively segmented a highly variable distribution of lithologies, across which we see sharp contrasts resulting from different depositional environments, regional erosion, and steep-sided channels.

With the framework in place, visualizing data in a QlGM generated an understanding of the ground conditions critical to early design decisions. For inter-array cables, measured variability in sediment cohesiveness and thermal conductivity was related to the presence of specific ground units, notably channel systems and periglacial landforms mapped within the Holocene. For OWT foundations, the ground model enabled the identification of areas with higher risk of sediment remobilization (e.g., related to differential compaction above tunnel valley margins) and greater likelihoods of encountering constraints caused by the presence of boulders, organic matter, and free gas.

RVO required a QGM that could generate geotechnical design profiles with uncertainty envelopes. A 3D grid was generated from the ground unit framework with over 1.3 billion cells, each measuring 25 m by 25 m in map view and 0.1 m in thickness. Each cell was initially attributed with its depth below the seafloor and with one of the 19 ground units.

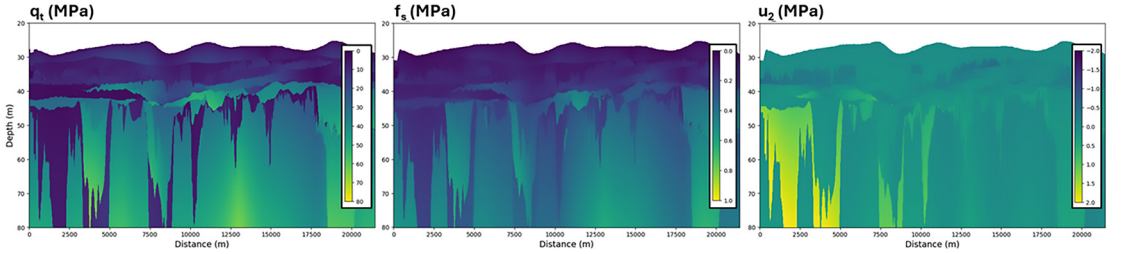

Figure 19: Example results from geostatistical prediction of Core Penetration Test (CPT) properties q_c, f_s, and u_2. Results capture the spatial variability in depth trends within each unit. The line of section is shown in Figure 18.

The simplest predictions involved defining depth trends, with both global linear (i.e., a single gradient and intercept per unit) and geostatistical (i.e., spatially varying trends per unit) approaches. This underscores the importance of an accurate ground unit framework as these will bracket intervals of low variability and thus highest predictability. Figure 19 shows geostatistical predictions for three CPT properties (corrected cone tip resistance, q_t; sleeve friction, f_s; pore pressure response, u_2). Benefits of these baseline methods (see Figure 13) are that they are computationally fast, produce predictions that are closely aligned with engineering best practices, account for lateral variability (in the case of the geostatistical approach), and can be readily applied from early-phase through to final site characterization.

More advanced machine learning methods were also tested and applied, including using Artificial Neural Networks (ANNs) with seismic inversion parameters to predict both CPT and engineering properties along all 2D seismic lines. First, pre-stack elastic inversion generated 2D sections of acoustic impedance (Z_p), shear impedance (Z_s), bulk density (ρ), and seismic quality factor (Q_p). From these, the small-strain shear modulus (G_{max}) was estimated (i.e., Z_s^2/ρ), and ANNs were trained to predict CPT and other geotechnical parameters (e.g., undrained shear strength, s_u; peak friction angle, φ). This machine learning workflow was probabilistic, using an ensemble of ANNs to capture and propagate uncertainties from the seismic inversion and training data into the final predictions.

A final step involved interpolating the predictions from the 2D seismic lines to populate the entire 3D model. This interpolation was guided by a "stratigraphic index," a fine-scale subdivision of each ground unit that assigned one of over 3,500 relative geologic ages to each model cell based on the unit's depositional model. This approach allowed property prediction to be guided by grouping synchronous deposits, across which variability is expected to be most predictable. Figure 20 shows results along the same west-east cross section used in Figure 18 and Figure 19.

In the future, companies will be invited to bid for the Gamma-A and Gamma-B licenses. The QGM results have generated a good understanding of the spatial variability in ground conditions that will allow developers to quickly build robust project plans and may eliminate the need for further site investigations. The associated cycle time reduction should lead to higher value projects.

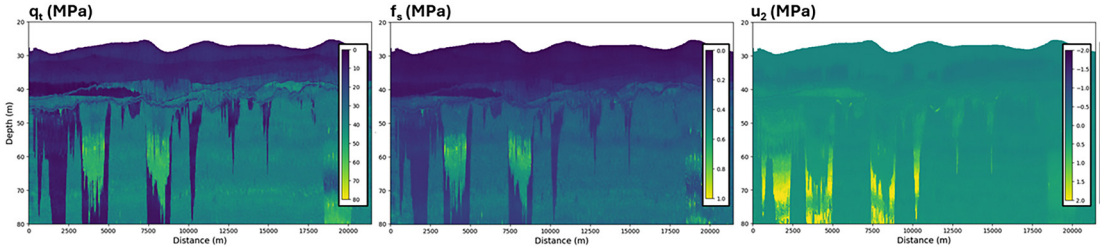

Figure 20: Example results from Artificial Neural Network (ANN) prediction using seismic inversion properties trained on Core Penetration Test (CPT) data. Results capture the variability in seismic impedance (and other seismic and inversion properties) within each unit. The line of section is shown in Figure 18.

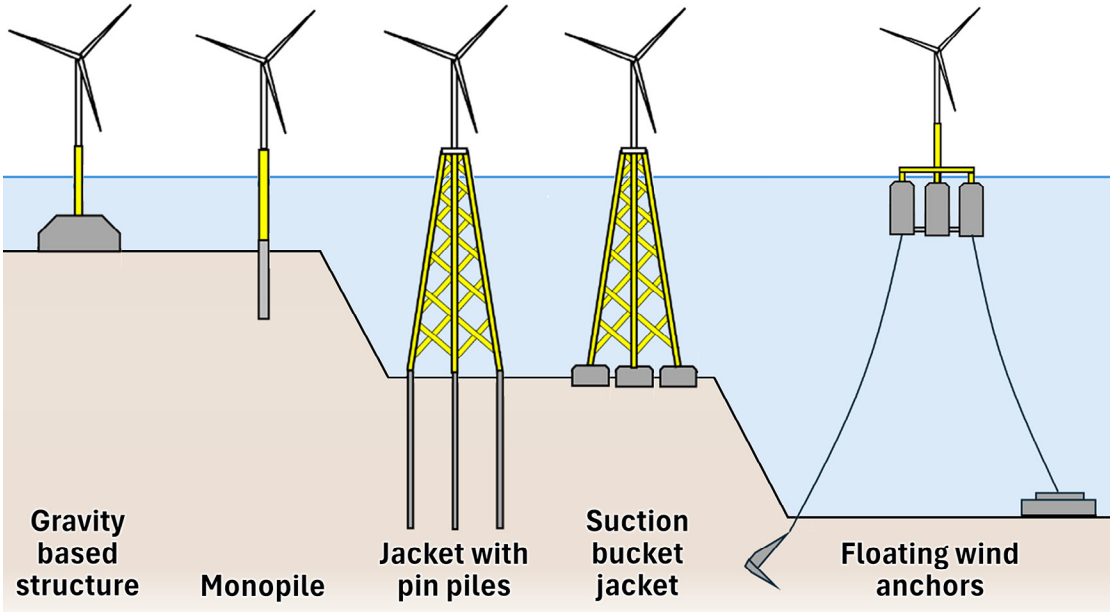

Figure 21: Offshore Wind Turbine (OWT) foundation concepts that are likely in play offshore Nova Scotia.

5. NEXT STEPS FOR NOVA SCOTIA

A recent DTS [1] integrated public-domain research and data to describe the shallow geology across the shelfal areas of Nova Scotia. While confidentiality prevents us from including detail, the study concludes that suitable ground conditions likely exist and indicates where a range of fixed and floating concepts (Figure 21) may be best suited (Figure 22).

The DTS may help potential developers with Screening decisions ahead of planned licensing rounds, the first of which is expected to conclude in 2026 with the issuance of three or four Submerged Land Licences. Additional data will also become available, including survey results from GSC expeditions and legacy oil and gas data that may be repurposed to provide information on near-surface ground conditions (e.g., [41]). The value of these data will likely be highest when integrated with DTS results.

A significant amount of new data will be needed across acquired leases and along their potential export cable corridors. Project value will likely be generated from high-resolution

Geohazards	Potential impacts
Mobile bedforms	Sediment build-up around foundations; cable damage e.g., burial, uncovering
Sediment scour	Foundation stability; cable damage e.g., uncovering, freespan
Fluid expulsion	Methane release; seafloor instability; foundation integrity; cable damage
Slope instability	Slumps & gravity flows; foundation & cable damage
Earthquakes	Ground shaking; liquefaction; fluid expulsion; slope instability; tsunamis
Tsunamis	High wave loads; sediment scour; foundation weakening; cable damage
Salt movement	Seafloor movement; foundation integrity
Coal mine collapse	Seafloor collapse; foundation integrity & cable damage
Engineering constraints	**Potential impacts**
Heterogeneous properties	High geotechnical variability; sub-optimal location & design decisions
Abnormal properties	Extreme geotechnical conditions; sub-optimal location & design decisions
Boulders	Surface & buried obstacles to foundations and cables
Shallow bedrock	Foundation refusal / damage, poor cable trenching / protection
Shallow gas	Reduced foundation capacity; gas release
Rugged / steep seafloor	Foundation & cable laying challenges; cable freespan
Existing infrastructure	Foundation & cable laying obstacles / challenges
Shipwrecks, debris, UXO	Foundation & cable laying obstacles / challenges

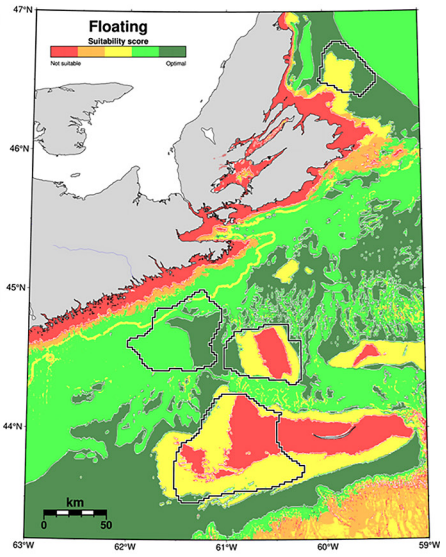

Figure 22: Geohazards and engineering constraints identified and mapped across the Wind Energy Areas (WEAs; left). Map shows the suitability of a single Offshore Wind Turbine (OWT) foundation concept to water depths and ground conditions (right). UXO=Unexploded Ordnance

geophysics and, in areas of high geologic complexity, we expect the acquisition of 3D seismic to be desirable in the first phase of site characterization.

Early alignment between geoscientists and engineers should be established through the development of a ground unit framework, generating a common understanding of project critical uncertainties and the data/analyses required to reduce them. As more geophysical and geotechnical data are acquired, the ground model should be updated to serve as the basis for site investigation, project layout, and engineering design decisions.

In some areas, we anticipate that QGMs will be needed to predict geotechnical design parameters (and their uncertainty envelopes) at locations where additional geotechnical acquisition may be cost prohibitive. Recent advancements in seismic acquisition, data processing, seismic inversion, and machine learning may generate reliable predictions, enabling detailed design and installation away from points of geotechnical measurement. These surveys will need to be planned, acquired, and processed with care to maximize data quality and retain amplitude variation with offset compliance.

Success will require a high level of coordination and aligned effort across regulators, local communities, manufacturers, suppliers, and developers, as well as experts in geoscience and engineering. Nova Scotia may also benefit from the experiences and lessons learned at offshore wind developments located in formerly glaciated regions, such as those discussed in this paper.

6. CONCLUSION

Around 20 kyr ago, the areas being considered for offshore wind development in Nova Scotia lay beneath the great Laurentide Ice Sheet. We expect the upper 100 m of the seabed to present a complex mosaic of

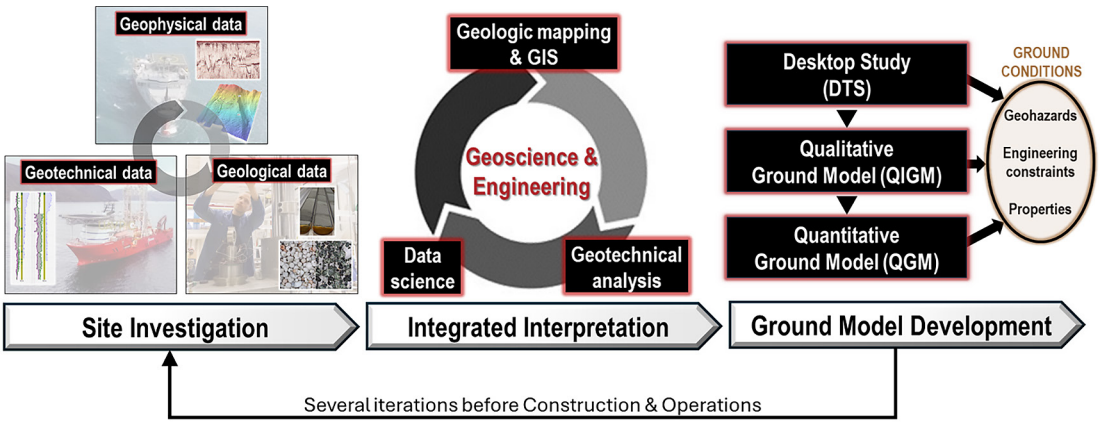

Figure 23: General site characterization workflow. Several cycles of integrated data acquisition and interpretation are typically performed through project Screening, Selection, and Design (see Figure 6). As a project matures and the volume of data grows, the level of detail in its ground model increases from a Desktop Study (DTS) to a Qualitative Ground Model (QlGM), and areas of high geologic complexity may ultimately require a Quantitative Ground Model (QGM).

geohazards, engineering constraints, interfingering lithologies, and heterogeneous geotechnical properties. This is supported by a recent DTS [1] and by site characterizations for offshore wind developments on geologically analogous terrains.

The ultimate success of an offshore wind development is enhanced by accurate site characterization (Figure 23), which enable stakeholders to:

- **Select the Best Project Sites:** In the absence of detailed data, an integrated analysis of publicly available information can be critical to Screening decisions. A DTS that accurately represents the nature and expected complexity of ground conditions can lead to the identification of feasible concepts and favourable areas and, therefore, to good licensing decisions.
- **Maximize the Value of Data:** Site investigation is generally phased over the first few years of development. Significant project value can be generated when the level of detail in the initial phase matches the complexity of ground conditions. This may especially apply to decisions concerning the acquisition of high-resolution 3D seismic data. Geophysical and geotechnical surveys need to be carefully designed and considered in partnership with the wider project objectives, targeting areas of critical subsurface uncertainty that are recognized in the evolving ground model.
- **Optimize Infrastructure Location and Design:** As more geophysical, geotechnical, and geological data are acquired, their integrated interpretation generates a 3D representation of ground conditions (i.e., geohazards, engineering constraints, and soil/rock properties) as a ground model. A critical step is the establishment of a robust ground unit framework – this requires geoscientists and geotechnical engineers to develop a common understanding of the nature and consequences of ground heterogeneity, and to define and map the minimum number of units that adequately capture

it. In early stages of development, QlGMs may be used to make high-level project decisions and to identify areas of critical uncertainty for more focused site investigation. As the development matures, the ground model can become increasingly more detailed with more ground units. In areas where variability is not adequately captured by geotechnical measurements, it may be necessary to predict properties with a QGM for final infrastructure location and design decisions.

Nova Scotia has a bold vision for offshore wind, and successful projects from its early licensing rounds are needed for the journey that lies ahead. Accurate site characterizations will be critical to reducing the time needed to ensure the right project facilities with the right designs are installed at the right locations. The result will be shorter payout times and increased profitability, which will encourage long-term investment and the continued development of Canada's vast offshore wind resource.

ACKNOWLEDGMENT

We thank NGI for supporting the development of this paper, and TGS for allowing us to discuss elements of the NGI-TGS "Nova Scotia Offshore Wind: Wind and Ground Conditions" DTS [1]. We also thank Gregory Lampman at New York State Energy Research and Development Authority for providing information on the New York Bight area, and RVO for allowing us to include information from offshore wind development zones in the Netherlands.

Authors' Declaration

- Funding: The authors did not receive financial support from any organization for the submitted work.
- Ethical approval: This paper does not contain any studies with human participants or animals.
- Competing interests: The authors declare that they have no competing interests.
- Availability of data and materials: Datasets used and/or analyzed during the current study are available from the corresponding author upon reasonable request.
- Artificial intelligence was not used in this work.

REFERENCES

[1] T. A. King, F. Pisanò, S. Halder and S. Eichelberger, "Nova Scotia offshore wind desktop study: wind and ground conditions," NGI & TGS, 2025. [Online]. Available at: https://info.tgs.com/nova-scotia-desktop-study

[2] GEBCO Compilation Group, "GEBCO 2025 Grid," International Hydrographic Organization (IHO) & Intergovernmental Oceanographic Commission (IOC), 2025. [Online]. Available at: https://www.gebco.net/data-products-gridded-bathymetry-data/gebco2025-grid

[3] Government of Nova Scotia, "Wind West: a nation-building energy project," Province of Nova Scotia, 2025. [Online]. Available at: https://novascotia.ca/wind-west/docs/wind-west-strategic-plan-en.pdf

[4] Government of Nova Scotia, "Offshore wind," 2025. Accessed: Dec. 1, 2025. [Online]. Available at: https://novascotia.ca/offshore-wind

[5] T. A. King, L. Griffiths and M. Vanneste, "Offshore wind site characterization: examples from Nova Scotia, America & Europe," in Marine Renewables Canada (MRC) 2025 Conference & Exhibition, Halifax, Nova Scotia, 2025.

[6] NGI, "This is what the foundation of the world's deepest offshore wind park looks like. The technology is Norwegian," 23 June 2023. Accessed: Dec. 1, 2025. [Online]. Available at: https://www.ngi.no/en/news/this-is-what-the-foundation-of-the-worlds-deepest-offshore-wind-park-looks-like.-the-technology-is-norwegian

[7] J. Shaw, "Deglaciation and postglacial sea-

level changes in Atlantic Canada: science driven by technology," in Voyage of Discovery: 50 years of science at the Bedford Institute of Oceanography, M. Latremouille, D. C. Gordon, C. F. M. Lewis and D. N. Nettleship, Eds., 2014, pp. 325-329. [Online]. Available at: https://www.researchgate.net/publication/280879237_Deglaciation_and_postglacial_sea-level_changes_in_Atlantic_Canada_science_driven_by_technology

[8] A. Pope, "Sable Island, N.S. as you've never seen it before," Canadian Geographic, 17 April 2020. [Online]. Available at: https://canadiangeographic.ca/articles/sable-island-n-s-as-youve-never-seen-it-before

[9] L. H. King and G. B. J. Fader, Wisconsinan glaciation of the Atlantic continental shelf of southeast Canada, Geological Survey of Canada, Bulletin 363, 1986, p. 72. [Online]. Available at: https://ostrnrcan-dostrncan.canada.ca/entities/publication/acb99f3a-5ce1-440f-907f-e010c8b537da

[10] E. L. King, "Surficial geology and features of the inner shelf of eastern shore, offshore Nova Scotia," Geological Survey of Canada, Open File 8375, 2018. [Online]. Available at: https://ostrnrcan-dostrncan.canada.ca/entities/publication/41efb71b-9f4e-4f13-9f17-f71a89c6eab6

[11] J. B. R. Eamer, J. Shaw, E. L. King and K. MacKillop, "Seabed conditions on the inner shelves of Atlantic Canada," Geological Survey of Canada, Open File 8731, 2020. [Online]. Available at: https://ostrnrcan-dostrncan.canada.ca/entities/publication/5d7a17f9-58dd-425b-8e9f-f92223830e29

[12] G. Philibert et al., "Updated surficial geology compilation of the Scotian Shelf bioregion, offshore Nova Scotia and New Brunswick, Canada," Geological Survey of Canada, Open File 8911 (revised), 2024. [Online]. Available at: https://osdp-psdo.canada.ca/dp/en/search/metadata/NRCAN-GEOSCAN-1-330474

[13] G. Philibert, J. Eamer, E. L. King and M. Z. Li, "Geological model of parameters relevant for offshore wind-energy infrastructure in Atlantic Canada," Geological Survey of Canada, Open File 9253, 2025. doi: 10.4095/pv67z56149.

[14] Nova East Wind, "Nova East Wind: Canada's first offshore wind farm," 2025. Accessed Dec. 1, 2025. [Online]. Available at: https://novaeastwind.ca

[15] M. R. Bennett and N. F. Glasser, Glacial geology: ice sheets and landforms, Wiley-Blackwell, 2009, p. 450.

[16] J. S. Griffiths and C. J. Martin, Engineering Geology and Geomorphology of Glaciated and Periglaciated Terrains – Engineering Group Working Party Report, vol. 28, J. S. Griffiths and C. J. Martin, Eds., Geological Society of London, Engineering Geology Special Publications, 2017, p. 953.

[17] B. Kurjanskia, B. R. Rea, M. Spagnoloa, D. G. Cornwella, J. Howella and S. Archer, "A conceptual model for glaciogenic reservoirs: from land systems to reservoir architecture," Marine and Petroleum Geology, vol. 115, 2020. doi: 10.1016/j.marpetgeo.2019.104205.

[18] D. J. A. Evans and I. S. Evans, "Glacial processes and landforms," in The History of the Study of Landforms or the Development of Geomorphology, T. Burt, A. Goudie and H. Viles, Eds., Geological Society, London, Memoir No. 58, 2022, pp. 333-377. [Online]. Available at: https://www.lyellcollection.org/doi/full/10.1144/M58-2021-17

[19] K. R. Johnson, N. Dakin, G. D. O. Carter and E. Phillips, "Geo-challenges for ground model development in previously glaciated and periglaciated terrains," in Offshore Site Investigation Geotechnics 9th International Conference Proceeding, London, UK, 2023. [Online]. Available at: https://onepetro.org/SUTOSIG/proceedings/OSIG23/OSIG23/SUT-OSIG-23-095/650467

[20] B. Bellwald et al., "Marine Geohazards and Geo-Engineering Constraints on the Glaciated European Margins," Submitted to Earth-Science Reviews, 2025. [Online]. Available at: https://eartharxiv.org/repository/view/9135

[21] E. L. King, "A glacial origin for Sable Island: ice and sea-level fluctuations from seismic stratigraphy on Sable Island Bank, Scotian Shelf, offshore Nova Scotia," Natural Resources Canada, 2001. [Online]. Available at: https://ostrnrcan-dostrncan.canada.ca/entities/publication/0e2db9b5-7463-4ca6-930e-ddeae7ef206c

[22] A. W. Hill, G. Nicol and M. R. Cook, "A proposed standard seismic frequency nomenclature for geophysical site investigation surveys in the offshore energy sector," First Break, vol. 42, no. 11, pp. 37-41, 2024. doi: 10.3997/1365-2397.fb2024092.

[23] V. Catterall, L. Arlott, J. Clarke, L. Cottee and J. Morris, "Drivers for acquiring 3D UHRS data across offshore wind farms," in Proceedings of the 5th International Symposium on Frontiers in Offshore Geotechnics (ISFOG) 2025, Nantes, France, 2025. [Online]. Available at: https://www.issmge.org/uploads/publications/132/133/ISFOG2025-40.pdf

[24] B. Bellwald, G. Wood, S. A. Smith, A. Kvamsdal and M. Vanneste, "Extremely high resolution 3D seismic data: a requirement for offshore wind along glaciated margins," in 6th EAGE Global

Energy Transition Conference & Exhibition, Rotterdam, Netherlands, 2025. doi: 10.3997/2214-4609.202521193.
[25] A. McKay et al., "Accelerating offshore wind site characterisation with integrated 3D UHR geophysical and hydrographic survey," First Break, vol. 43, pp. 63-69, 2025. doi: 10.3997/2214-4609.202575012.
[26] M. E. Vardy, M. A. Clare, M. Vanneste, C. F. Forsberg and J. K. Dix, "Seismic inversion for site characterization: when, where and why should we use it?" in Offshore Technology Conference, Houston, USA, 2018. [Online]. Available at: https://onepetro.org/OTCONF/proceedings/18OTC/18OTC/D021S027R005/179738
[27] USGS, "Long Island topography," New York Water Science Center, 7 June 2017. Accessed: Dec. 1, 2025. [Online]. Available: https://www.usgs.gov/centers/new-york-water-science-center/science/long-island-topography
[28] Hofstra University, "Glacial Geology of Long Island," 10 July 2021. Accessed: Dec. 1, 2025. [Online]. Available: https://www.youtube.com/watch?v=vP86xg3x5ag
[29] D. P. Giles, J. S. Griffiths, D. J. A. Evans and J. B. Murton, "Geomorphological framework: glacial and periglacial sediments, structures and landforms," in Engineering Geology and Geomorphology of Glaciated and Periglaciated Terrains – Engineering Group Working Party Report, vol. 28, J. S. Griffiths and C. J. Martin, Eds., Geological Society, London, Engineering Geology Special Publications, 2017, pp. 59-368. doi: 10.1144/EGSP28.3.
[30] NYSERDA, "Area for consideration for the potential locating of offshore wind energy areas," New York State Energy Research and Development Authority, 2017. [Online]. Available at: https://www.nyserda.ny.gov/-/media/Project/Nyserda/Files/Programs/Offshore-Wind/Potential-Locating-OSW-AreaConsideration.pdf
[31] NYSERDA, "Hudson North Study Area (Subarea A): geophysical survey interpretative report," New York State Energy Research and Development Authority, 2021. [Online]. Available at: https://www.nyserda.ny.gov/-/media/Project/Nyserda/Files/Programs/Offshore-Wind/21-08-Hudson-North-Subarea-A-Geophysical-Interpretive-Report-redacted-acc.pdf
[32] NYSERDA, "Analysis of multibeam echo sounder and benthic survey," New York State Energy Research and Development Authority, 2017. [Online]. Available at: https://www.nyserda.ny.gov/-/media/Project/Nyserda/Files/Publications/Research/Biomass-Solar-Wind/Master-Plan/17-25a-MBES-and-Benthic-Survey-Data.pdf
[33] NYSERDA, "Cables, pipelines and other infrastructure," New York State Energy Research and Development Authority, 2017. [Online]. Available at: https://www.nyserda.ny.gov/-/media/Project/Nyserda/Files/Publications/Research/Biomass-Solar-Wind/Master-Plan/17-25f-Cables-Pipelines-and-Other-Infrastructure.pdf
[34] NYSERDA, "Geotechnical and geophysical desktop study to support offshore wind energy development in the New York Bight," New York State Energy and Research Development Authority, 2019. [Online]. Available at: https://www.nyserda.ny.gov/-/media/Project/Nyserda/Files/Programs/Offshore-Wind/19-19-Geotechnical-and-Geophysical-Desktop-Study-to-Support-Offshore-Wind-Energy-Development.pdf
[35] BOEM, "Geological and geotechnical overview of the Atlantic and Gulf of Mexico Outer Continental Shelf," Bureau of Ocean Energy Management, 2022. [Online]. Available at: https://www.boem.gov/sites/default/files/documents/BOEM-GG-DTS.pdf
[36] D. J. DeGroot, Z. J. Westgate and T. I. Yetginer-Tjelta, "Geological and geotechnical challenges of the East Coast United States for offshore energy transition," in Offshore Site Investigation Geotechnics 9th International Conference Proceeding, London, UK, 2023. doi: https://onepetro.org/SUTOSIG/proceedings/OSIG23/OSIG23/SUT-OSIG-23-002/650498.
[37] Z. J. Westgate et al., "Effect of degradation on geotechnical behavior of glauconite sands from the U.S. Mid-Atlantic Coastal Plain," Ocean Engineering, vol. 283, p. 19, 2023. doi: 10.1016/j.oceaneng.2023.115081.
[38] Z. Westgate et al., "The Piling in Glauconitic Sand (PIGS) JIP: insights from site characterisation and laboratory testing," in 5th International Symposium on Frontiers in Offshore Geotechnics (ISFOG), Nantes, France, 2025. [Online]. Available at: https://www.issmge.org/uploads/publications/132/133/ISFOG2025-75.pdf
[39] M. Vanneste et al., "Data integration tailored to assess spatial variability for jack-up clearance zone assessment – application to offshore renewables," in Offshore Site Investigation Geotechnics 9th International Conference Proceeding, London, UK, 2023. doi: 10.3723/EGIM6139.
[40] NGI, "How geology shapes offshore wind: IJmuiden Ver Gamma ground model animation," 26 September 2025. Accessed: Dec. 1, 2025. [Online]. Available at: https://www.ngi.no/en/news/how-geology-shapes-offshore-wind
[41] A. B. Hart et al., "Reprocessing and repurposing of historical O&G data for offshore renewable projects," in Offshore Site Investigation Geotechnics 9th International Conference Proceeding, 2023. doi: 10.3723/NSFH3383.

Informative

Cutting Edge

Provocative

Challenging

Informative

International

thejot.net

Large Drum Centrifuge

Dr. Tim Newson

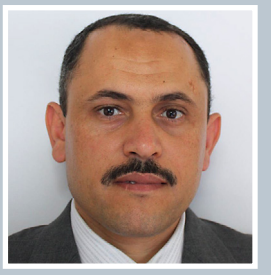

Dr. Aly Ahmed

Dr. Paul Ibanez

Boaz Norton

Modelling wave-induced forces

Who should read this paper?

The findings have practical implications for reducing uncertainty, cost, and risk across offshore energy projects, with relevance to engineers, researchers, regulators, and insurers working in ocean and coastal environments.

Why is it important?

The paper addresses critical technical challenges that currently limit the reliable deployment of offshore wind energy, a priority issue as marine renewable developments accelerate. The work is applied, experimental research aimed at improving the design, assessment, and risk management of offshore wind energy infrastructure in Atlantic Canada. It focuses on addressing critical technical challenges associated with coupled wave loading and soil-structure interaction that currently limit reliable offshore wind deployment.

The research uses a unique drum centrifuge-based wave flume, enabling realistic scaling of both geotechnical stresses and hydrodynamic forcing within a single experimental framework. This capability provides more accurate, industry-relevant evidence than conventional laboratory approaches, reducing uncertainty, lowering costs, and supporting better-informed engineering and investment decisions. Improved wave generation and reflection control in a drum centrifuge enable more reliable assessment of wave-induced loads, seabed response, and foundation performance for safer, more cost-effective offshore wind and coastal developments.

The centrifuge discussed in this paper is fully commissioned and the wave flume will be operational following proof testing toward the end of 2026.

About the authors

Dr. Tim Newson is a professor and research director in the Geotechnical Research Centre at the University of Western Ontario (UWO). He has 30+ years' experience of industry and academic projects in civil engineering for the oil/gas, mining, and renewable energy sectors, and has conducted both consulting and research in Europe, Australasia, Asia, and the Americas. He is a former vice president for North America for the International Society for Soil Mechanics and Geotechnical Engineering. His research interests and consulting activities include in-situ testing, constitutive modelling of soils, wind engineering, buried structures, centrifuge and laboratory testing techniques, dynamic and cyclic soil-structure interaction, contaminant transport through soils, and offshore foundations. He was responsible for the key technological developments for the Canada Foundation for Innovation-funded project "Enhancing the Resilience and Sustainability of Critical Geotechnical Infrastructure," which has developed one of the most sophisticated geotechnical drum centrifuge facilities in the world. He has published 200+ peer-reviewed journal papers and conference papers.

Dr. Aly Ahmed is the facility manager for the UWO drum centrifuge. His expertise covers laboratory testing of soils and waste materials, underground structures and foundations, and physical modelling of various geotechnical structures.

Dr. Paul Ibanez and Boaz Norton of ANCO Engineers, Inc. have worked with UWO to design and construct the drum centrifuge wavemaker. They have also been involved with the design of two degrees of freedom earthquake shake tables installed in two large beam centrifuges in the PRC, and the construction of small university research beam centrifuges. Both authors have decades of experience in providing dynamic testing systems such as single and multi-axis shake tables worldwide and performing force vibration testing of full-scale civil structures to investigate structural dynamics and soil structure interaction.

NOVEL SCALED PHYSICAL MODELLING OF WAVE LOADING OF OFFSHORE WIND TURBINE TOWERS AND FOUNDATIONS USING CENTRIFUGE TECHNOLOGY

T. Newson[1*], A. Ahmed[1], P. Ibanez[2], B. Norton[2]
[1]Geotechnical Research Centre, Department of Civil and Environmental Engineering, University of Western Ontario, London, ON, Canada
[2]ANCO Engineers Inc., Boulder, CO, USA
**Corresponding author: tnewson@eng.uwo.ca*
DOI: https://doi.org/10.48336/SABD-6D75

ABSTRACT

Experimental studies of wave loading on offshore structures are often conducted in 1 g flumes. For full-scale relevance, very large flumes are needed, but when investigating soil-structure interaction with a model seabed, scaled-down flumes face difficulties in accurately reproducing soil responses. Geotechnical centrifuge experiments using scaled models under high-gravity conditions overcome this limitation, enabling correct soil stress replication while also allowing fluid wave modelling. Conventional beam centrifuges have been used to generate solitary, standing, and progressive waves to study coastal erosion, offshore loading, pipeline instability, and wave-induced seabed liquefaction. However, their limited test-box length restricts wave characteristics and complicates reflection attenuation. Drum centrifuges provide significant advantages, offering a longer effective testing channel around the drum circumference, which improves fluid wave generation. Wave generation devices must account for high centrifugal accelerations and elevated wave frequencies. To achieve high-quality data, incident waves must be dissipated without reflection. Passive absorbers, such as slotted caissons or beaches, have been employed with varying success. An alternative is an active paddle wavemaker system, which minimizes wave re-reflections by modifying the control signal, a process known as reflection compensation. This paper presents the principles of wave generation in a geotechnical centrifuge and describes the new active fluid wave system in the large drum centrifuge at the University of Western University. Its application to physical modelling of wave-induced forces on offshore wind turbine towers and pile foundations in shallow water is discussed.

Keywords: Offshore wind, pile foundations, scaled laboratory models, wave loading, current

Table 1: Comparison of major large-scale wave flumes around the world.

Affiliated Country or Institution	*Length (m)*	*Width (m)*	*Depth (m)*	*Max Wave H_{max} (m)*	*Wave Period (s)*
a. Tianjin Research Institute for Water Transport Engineering, M.O.T., China	456	5.0	8–12	3.5	2–10
b. Coastal Research Center (Large wave flume, FZK), Hannover, Germany	330	5.0	7.0	2.5	2–8
c. Deltares, De Voorst, Netherlands	233	5.0	7.0	2.5	1–15
d. Tainan Hydraulics Laboratory, National Cheng Kung University, Taiwan	300	5.0	5.0	1.5	2.5–4.3
e. Central Research Institute of Electric Power Industry, Tokyo, Japan	180	3.4	6.0	2.0	-
f. Large Hydro – Geo Flume Port and Airport Research Institute, Japan	185	3.5	12	3.5	6–8
g. Institut National De La Recherche Scientifique, Canada	120	5.0	5.0	1.8	3–10
h. State Hydrodynamics Institute, St. Petersburg, Russian	110	4.0	7.5	2.0	-
i. "Super tank," Oregon State University, USA	104	3.7	4.6	1.3	0.8–12
j. Ciem flume, Polytechnic University of Catalonia, Spain	100	3.0	5.0	1.6	-

1. INTRODUCTION

1.1 Experimental Modelling of Offshore Structures with Flumes

1.1.1 Large 1 g Flume Systems

Offshore and coastal structures are exposed to complex and variable loads from wind, waves, currents, tides, ice floes, and a range of seabed geohazards. One-dimensional wave flumes are essential tools in ocean and coastal engineering, enabling controlled study of wave and current dynamics, fluid-structure interactions, load transfer to the seabed, and related environmental effects. Hydraulic stress changes or structural loads from large waves can induce seabed shear failure or liquefaction, threatening the stability of pipelines, cables, offshore platforms, and wind turbines. Flumes and large tanks reproduce these interactions under laboratory conditions, providing theoretical insights, experimental data, and technical guidance for design. However, conventional 1 g flume experiments face limitations in replicating seabed responses accurately, since the soil behaviour is highly stress dependent. Scale effects can distort results, reducing their applicability to full-scale prototypes [1], [2], [3].

Extremely large wave flumes (length >100 m) address these challenges by accommodating larger experimental models, mitigating scale effects, and improving reliability. Such facilities enable physical model experiments that more closely resemble prototype conditions, allowing results to be directly applied to engineering practice. Several research institutions worldwide have established these large-scale flumes, advancing the study of realistic marine environments and improving the understanding of wave-current-structure-seabed interactions [4], [5], [6]. The geometry and wave generation characteristics of these large facilities are summarized in Table 1.

Large-scale wave flumes are widely used to investigate coastal processes, wave-structure interactions [7], sediment transport, breakwater performance [8], scour protection, offshore foundation stability [9], wave-float dynamics, and ecological protection strategies [10]. Equipped with advanced wave generation and measurement systems, these facilities enable detailed studies of complex hydrodynamic processes and interactions, benefiting from institutional expertise in large-scale physical modelling. In contrast, conventional wave flumes (typically 50-100 m in length) require highly scaled-down models, introducing significant similitude challenges. Discrepancies in Reynolds and Froude numbers compromise dynamic scaling, while small models amplify surface tension effects, affecting wave-breaking patterns and sediment transport. These geometric constraints limit wave generation characteristics, making it difficult to reproduce representative ocean wave states and corresponding structural responses.

Standard flumes also struggle to produce long-period or large-amplitude waves, and shallow water depths often result in reflected waves that interfere with desired propagation and interactions. This restricts the simulation of high-energy events such as storm surges, typhoons, or tsunamis, and associated phenomena including non-linear wave breaking, long-distance attenuation, and seabed scour. Larger-scale flumes address many of these limitations, providing realistic ocean-like conditions for wave-current-structure and fluid-sediment interaction studies. However, the high costs of constructing and operating such facilities have limited their global number. Even in these large setups, reproducing the stress-dependent behaviour of seabed soils remains challenging due to limited soil profile depths for modelling large offshore structures such as foundation piles. Despite these constraints, large-scale wave flumes remain essential for accurate, physically representative offshore and coastal engineering research.

1.1.2 Centrifuge-based Flume Systems

Geotechnical centrifuge experiments using scaled physical models under enhanced gravitational fields are widely recognized as the most effective method for reproducing prototype stress conditions and the associated non-linear soil behaviour [11], [12]. This approach is particularly suitable for investigating gravity-driven and time-dependent seabed phenomena. Within this framework, fluid wave simulation in centrifuges plays a key role in offshore geotechnical research, providing improved similitude and more accurate modelling of soil-structure interactions. Early work at the University of Cambridge used a 2.2 m drum centrifuge with a water-immersed rectangular float to generate tsunami solitary waves, providing insights into fluid wave generation and propagation under enhanced gravity [13]. Later, conventional beam centrifuges at Kyoto University enabled the creation of standing and progressive waves in model boxes [14]. Sekiguchi et al. [15] applied this technique to study soil liquefaction in loose seabeds beneath fluid layers using a piston-type wavemaker. However, limited container length required a slotted vertical partition as a wave absorber, whose effectiveness was strongly wavelength dependent, restricting the range of wave frequencies that could be applied. Baba et al. [16] later developed a plunger-type

Figure 1: (a) Centrifuge paddle generated fluid waves and (b) soft cliff erosion models showing wave damage (after [17]).

system capable of generating regular waves with moderate amplitudes, but this system could not produce irregular or high-intensity waves necessary to induce liquefaction. An over-sized rectangular model box (3 m long) was used with a paddle wave system by [17] to investigate the erosion of soft granular soil cliffs, allowing further runup of waves and longer wavelengths, as well as an extended structural model section. The created model waves (at 30 g) and the eroding cliff structure are shown in Figure 1a, b.

In contrast, drum centrifuges offer a longer effective testing length around the drum circumference, providing advantages for fluid-wave generation and soil-structure interaction studies [18]. Miyamoto et al. [19] developed a piston-type wave generation system within a drum centrifuge capable of forming irregular

waves, simulating storm sequences with amplitudes increasing from moderate to high. This enabled realistic sea states to be applied to models, including studies on offshore pipeline flotation during wave-induced seabed liquefaction. Over the same period, centrifuge modelling has become increasingly important for examining fluid-soil-structure interaction and wave-induced seabed state changes, contributing significantly to both coastal and offshore geotechnical engineering research [20], [21].

2. CENTRIFUGE SCALING LAWS FOR WAVE LOADING OF OFFSHORE STRUCTURES

2.1 Fluid Wave and Seabed Scaling

2.1.1 Model Similitude for Wave and Seabed Modelling in a Centrifuge

For fluid waves that have a free surface, gravitational forces will dominate the governing dynamics, while the influences of viscosity, surface tension, and any related effects are typically minor and can often be ignored. It is generally accepted that for fluid models, both Reynolds and Froude number similitude cannot be satisfied simultaneously. Consequently, the simulation of gravity fluid waves commonly adopts only Froude scaling, with the associated variations in Reynolds number accepted as a limitation [22]. The Froude number (F_r), which represents the ratio of inertial to gravitational forces, can be defined using:

$$F_r = \frac{U_m}{\sqrt{aD}} \quad (1)$$

where U_m is maximum water particle velocity, a is centrifugal acceleration, and D is a convenient characteristic length or dimension. In accordance with Froude's law of similitude, the following scaling relationship must be satisfied:

$$\frac{\lambda_{U_m}}{\sqrt{\lambda_a \lambda_D}} = 1 \quad (2)$$

where the parameter λ represents the ratio of the model to prototype (full scale) parameters. For centrifuge model tests, any geometric length L = 1/N and the centrifugal acceleration a = Ng, where N is the centrifugal g-level and g is the Earth's gravitational acceleration.

Hence,

$$\lambda_{U_m} = 1 \quad (3)$$

Consequently, this allows the wave-period scale to be found:

$$\lambda_T = \frac{\lambda_D}{\lambda_{U_m}} = \frac{1}{N} \quad (4)$$

where T is the period of the wave. Further similarity laws for fluid waves in a centrifuge environment based on Froude scaling can be found in Table 2, where the wave velocity c = L/T and scales at 1:1.

The primary advantage of centrifuge modelling for small-scale soil and structural models is its ability to reproduce stress and strain conditions identical to those in full-scale prototypes. This is critical because the mechanical behaviour of granular materials, such as soils, is highly non-linear and stress dependent. By accelerating a 1/Nth scale model in a centrifuge to N times Earth's gravity, the vertical stress profile due

Table 2: Scaling laws for fluid wave and soil modelling in a centrifuge.

Aspect	*Variable*	*Generic Units*	*Scale Factor (I)*
General	Centrifugal acceleration (a)	LT^{-2}	N
Fluid	Froude number (F_r)	1	1
	Water depth (d)	L	1/N
	Wavelength (L_w)	L	1/N
	Wave period (T)	T	1/N
	Wave velocity (c)	LT^{-1}	1
	Water particle velocity (U)	LT^{-1}	1
	Fluid (water) density (r_w)	ML^{-3}	1
	Wave pressure on seabed (P_o)	$ML^{-1}T^{-2}$	1
Soil & structure	Geometric length (L)	L	1/N
	Stress (s)	$L^{-1}MT^{-2}$	1
	Strain (e)	-	1
	Density (r)	ML^{-3}	1
	Force (F)	MLT^{-2}	$1/N^2$
	Bending moment (M)	ML^2T^{-2}	$1/N^3$
	Flexural stiffness (EI)	ML^3T^{-2}	$1/N^4$
	Time – dynamic excitation (T_d)	T	1/N
	Time – consolidation/diffusion (T_c)	T	$1/N^2$
	Time – creep (T_{cr})	T	1
	Pore fluid velocity (V)	LT^{-1}	N
	Velocity – dynamic (V_d)	LT^{-1}	1
	Frequency (F_n)	1/T	N

to self-weight closely matches that of the prototype [12], capturing realistic soil stiffness, strength, and failure mechanisms that cannot be replicated in 1 g tests. This enables the study of complex boundary value problems and non-linear soil-structure interactions, including foundation response, tunnel arching, slope stability, and seismic liquefaction, under representative field conditions. Centrifuge scaling laws also accelerate time-dependent processes, such as consolidation, which scales with the square of the gravitational field (N^2). This allows phenomena that take months at full scale to be modelled in hours, facilitating the investigation of long-term processes like storm loading. Additionally, centrifuge testing is more cost-effective and time-efficient than large-scale laboratory or field experiments. Scaled models can be modified and repeatedly tested under controlled conditions, producing robust datasets for a wide range of scenarios. The high-fidelity experimental data are invaluable for calibrating and validating numerical and analytical models, reducing reliance on unverified assumptions, and enhancing predictive accuracy in geotechnical engineering.

2.1.2 Wave Generators

Wave generation in laboratory flumes is typically achieved using two primary types of wavemakers: paddles (flaps) and pistons. Paddle wavemakers are generally employed to generate deep-water waves, where orbital particle motion decays rapidly with depth, resulting in negligible seabed motion. Consequently, they are well-suited for studies involving floating structures and fundamental investigations of ocean wave physics. In such systems, the paddle hinge is often positioned on a ledge slightly above the flume base. Piston wavemakers, in contrast, are more appropriate for shallow water conditions, where the water depth is small relative to the wavelength. In these scenarios, orbital particle

motion is compressed into an elliptical path, generating significant horizontal motion at the base, making piston wavemakers suitable for studies of coastal structures, harbours, and shore-mounted wave energy devices. A key objective in wavemaker design is to closely match the motion of the generator to the required water particle motion, minimizing the production of evanescent waves immediately in front of the device. These unwanted waves decay with distance but reducing their initial amplitude maximizes the effective flume length. Each wavemaker has an optimal operating frequency at which its horizontal motion closely follows the water motion, minimizing the effective inertia, or added mass of the water. At higher frequencies, discrepancies between the wavemaker and fluid motion increase the added mass.

High-frequency wave generation generally requires low power but can impose substantial inertial loads. Conversely, at low frequencies, wave height is limited by the volume of displaced water. A piston displaces approximately twice the water volume of a paddle for a given stroke, producing roughly twice the wave height. Although structural loads are lower at low frequencies, design considerations focus on accommodating large strokes and preventing leakage. These performance and power considerations have contributed to the preference for paddle wavemakers in centrifuge studies. Paddle motion can be controlled to generate waves with specified amplitude, frequency, and form. A key challenge is managing waves reflected from downstream structures. Ideally, the experiment should replicate waves arriving from infinity, passing the structure, and continuing unobstructed. Passive absorption, such as sloping beaches or perforated vertical baffles, mitigates reflected waves downstream. Active absorption addresses waves returning to the paddle, using instrumentation to detect reflections and adjust paddle motions to cancel them without disturbing the incident wave, ensuring realistic wave conditions within a finite flume.

2.1.3 Theoretical Conditions for a Paddle Wavemaker

For gravity-driven ocean waves, the fluid may be idealized as a homogeneous, inviscid, incompressible material undergoing irrotational motion. Under these assumptions, the fluid motion can be represented by a velocity potential, which satisfies Laplace's equation [23]. Simple regular harmonic waves are often employed to investigate the fundamental physics of fluid-structure interaction. According to wave generation theory [24], within the water domain defined by $0 \leq y \leq -d$, as shown in Figure 2, the free-surface elevation $h(x,t)$ of a sinusoidal wave generated by a paddle wavemaker is given by:

$$h(x,t) = \frac{2S\sinh(kd)}{\sinh(2kd)+2kd}\left[\sinh(kd) + \frac{1-\cosh(kd)}{k(d-d_s)}\right] e^{i(kx-\omega t)} \quad (5)$$

where S is the paddle stroke at the water surface, ω is the wave angular velocity ($\omega = 2\pi/T$), d is water depth, d_s is vertical distance from the seabed to the paddle hinge, k is the wave number ($= 2\pi/L_w$), and L_w is the fluid wavelength. The wave dispersion equation [25] is given by:

$$\omega^2 = Ngk.\tanh(kd) \quad (6)$$

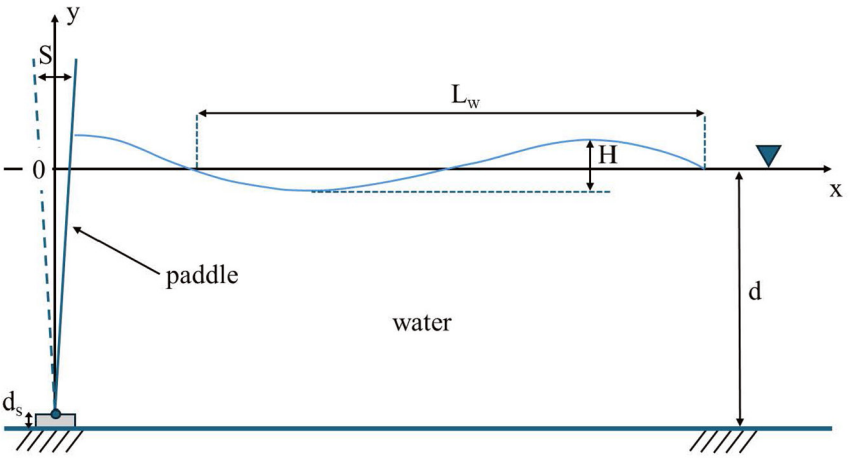

Figure 2: Sketch of paddle type wavemaker (after [25]).

where g is the acceleration due to gravity and N is the centrifugal scaling ratio.

Hence using Equation (5), the wave height H can be found from:

$$H = \frac{4Ssinh(kd)}{\sinh(2kd)+2kd}\left[\sinh(kd) + \frac{1-\cosh(kd)}{k(d-d_s)}\right] \quad (7)$$

3. UNIVERSITY OF WESTERN ONTARIO DRUM CENTRIFUGE WAVE FLUME

3.1 University of Western Ontario Drum Centrifuge Test Environment

The University of Western Ontario (UWO) recently commissioned a Broadbent drum centrifuge for scaled physical modelling of geotechnical processes and structures, supported by a major grant from the Canada Foundation for Innovation. The centrifuge features a 360° drum channel 0.4 m deep and 0.7 m wide, with a diameter of 2.2 m, capable of holding up to 3.5 t of soil (see Figure 3a). Mounted on a central pedestal and powered by a 35-kW motor, it can generate hyper-gravity conditions up to 249 g, creating one of the largest scaled-model soil environments globally (see Figure 3b). The equivalent soil body corresponds to ~13.3 million m³, with a scaled depth of 80 m, a plan area of 0.08 km², and a length of 0.7 km. A centrally located coaxial tool-table system provides direct access to the spinning drum. It includes an independent motor allowing the tool-table to be stopped while the drum remains in-flight, enabling safe installation or adjustment of actuators and sensors. The tool-table can then be re-accelerated, locked to the drum, and precisely indexed at low speed for controlled interaction with the model. A three-axis robotic system mounted on the tool-table permits precise positioning and load application in X, Y, and Z directions, both stationary and in-flight. The robot can apply loads up to ±10 kN or displacements of 0-5 mm/s under various profiles, including monotonic, cyclic, or stepped sequences, allowing realistic site investigation, structural loading, and instrumentation studies on soil bodies and geotechnical structures.

Twin high-speed data acquisition systems for the drum environment and the tool-table are capable of simultaneous interrogation

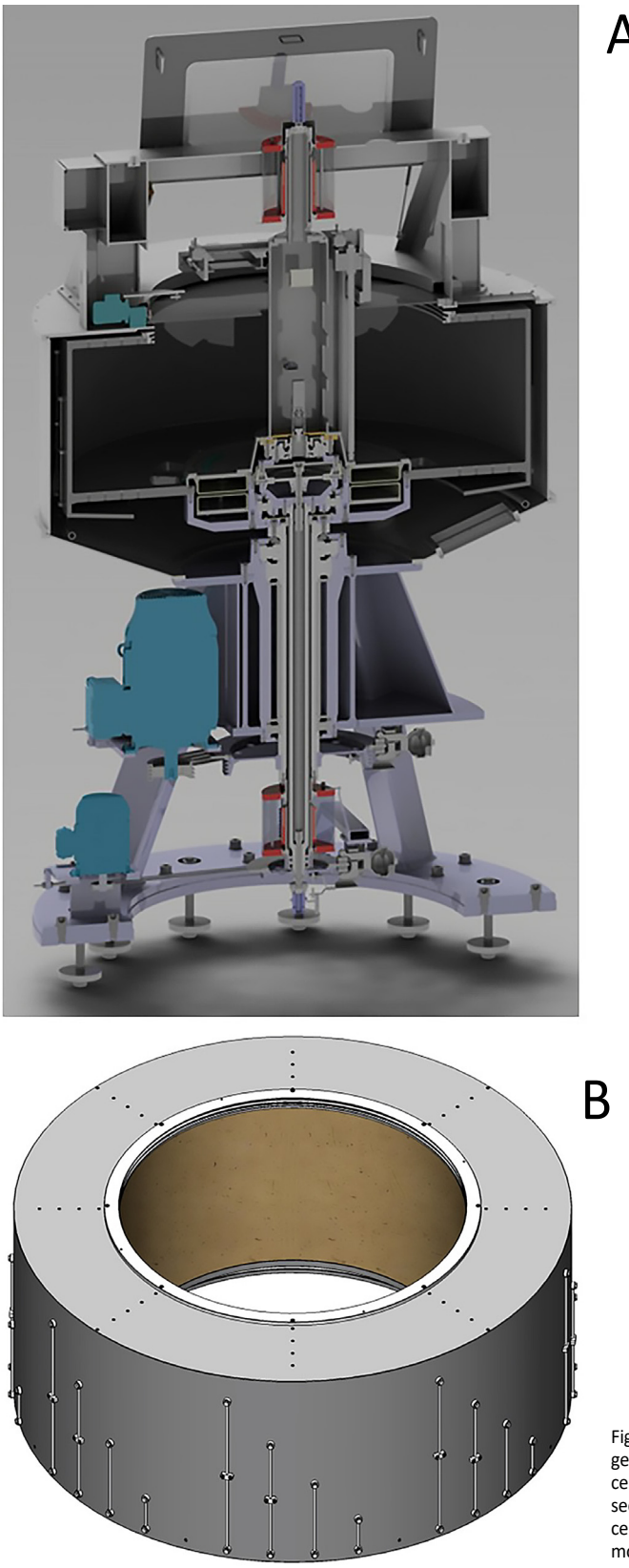

Figure 3: Basic geometry of drum centrifuge: a) cross-section of drum centrifuge and b) drum model environment.

of 64 channels of experimental instrument data with additional onboard digitization, network acquisition, and control. Computer controlled two axis in-flight placement/pouring is used for preparation of soil layers with controlled density and strength. A profile actuator permits the creation, changing, and monitoring of model soil surfaces in-flight. A range of miniature instrumentation allows the measurement of stresses, forces, and movements of soil sediments and structures in the models. Miniature site investigation devices comprise of a piezocone penetrometer and a shear vane. Additional tools are available for T-bar and plate penetrometer testing.

Of the 100+ geotechnical centrifuges in the world, only 10 of these are drum centrifuges and these are located in Japan, Brazil, Australia, UK, China, Switzerland, and USA; the nearest to UWO being located at University of California Davis. Drum centrifuges have advantages of being able to operate at higher 'g' levels, giving greater scaling gains and providing longer continuous lengths of soil compared to more traditional beam systems. Hence, drums can model long, single geotechnical structures, e.g., a slope, pipeline, or embankment, or can be used to simulate a long site with soil that has a common geological history, enabling comparison of different structures or replication of tests in the same material. Due to their structural differences (compared to fixed beams), drum centrifuges have far more lateral space available for instrumentation and actuators within the drum, but less space available in the centre of the centrifuge for data acquisition systems (although this is somewhat accommodated by the ability to quickly change devices in-flight).

3.2 The Drum Centrifuge Wave Flume

3.2.1 Overall Flume Design

The wave flume concept consists of a 360° fluid filled channel placed on the inside circumference of the UWO centrifuge drum. In the rest of this paper, the fluid is referred to as water, but under certain testing circumstances, it may be silicone oil or other types of fluid that can be utilized to balance scaling incompatibility [26] and may be used for achieving similitude with different processes. At one position in the channel there is a wave generator, which consists of an electric actuator outside the channel connected to a movable paddle moving in the fluid channel. This actuator is a programmable, high-torque, electric-servo motor attached to the hinge shaft of the paddle, which penetrates the side wall. An arm connected to the hinge shaft allows the servo motor to operate outside of the channel. The paddle rotates about its hinge approximately ±6° from paddle upright position. This mechanism generates a water wave that travels down the channel and impinges on a test object (simulating the water/soil embedded structures of interest). Typically, this wave channel will be operated at a centrifuge enhanced acceleration between 30-100 g. Therefore, all components are designed to operate up to 100 g. The purpose of this testing will be to investigate the dynamic response of the model structure and soil caused by the incident waves.

3.2.2 Overall Design and Features

The UWO centrifuge drum has an internal diameter of 2.2 m (circumference 6.92 m) and a vertical depth of 70 cm. Due to the presence of the three-axis robot, the radial distance

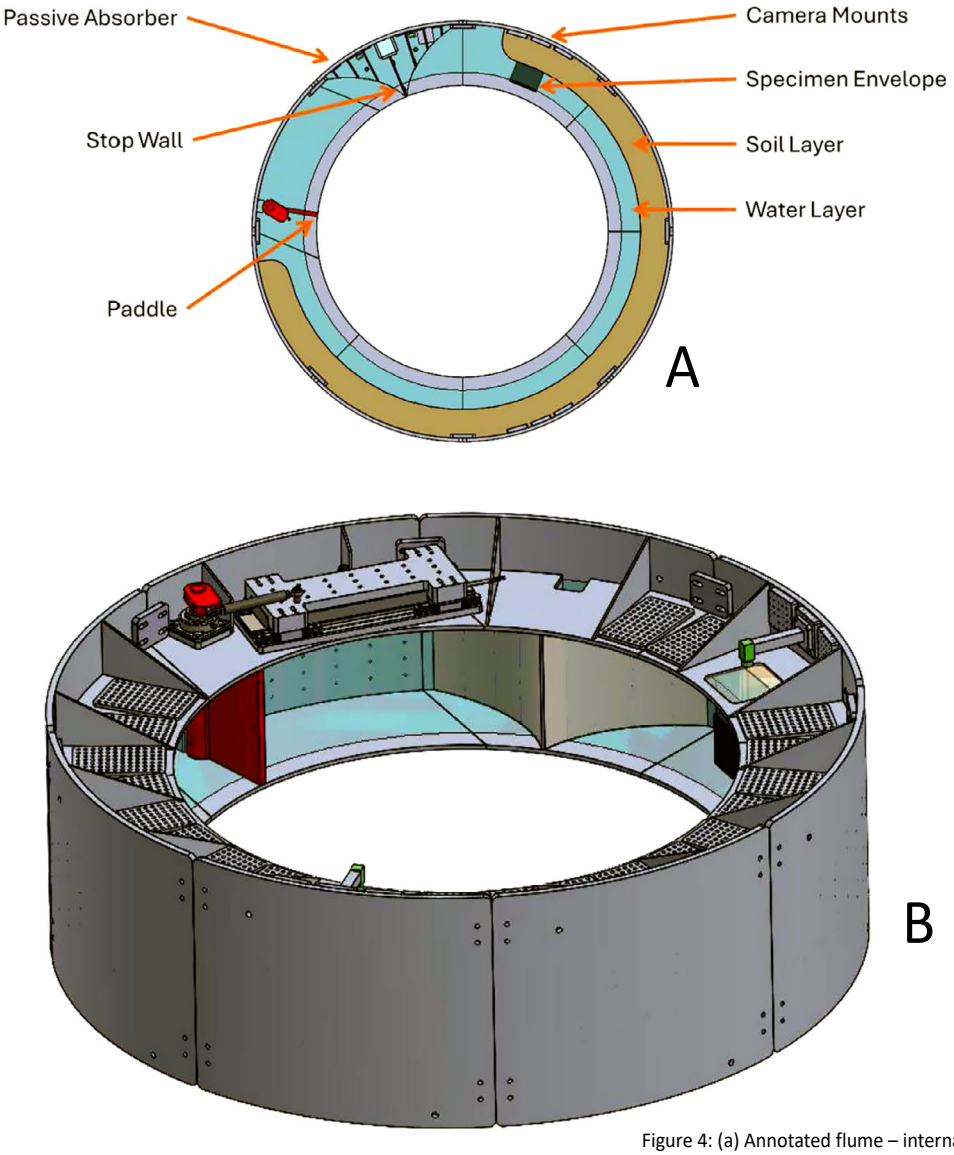

Figure 4: (a) Annotated flume – internal view and (b) flume overall design – solid view.

from the drum surface toward the centre of the centrifuge is limited to 35 cm, defining the usable flume width. The flume floor consists of a 20 mm aluminum plate, yielding a channel depth of 32 cm and leaving a 1 cm clearance between the flume wall and the robot envelope. Lateral viewing windows allow high-speed cameras to monitor fluid waves and model behaviour through the flume walls. The channel contains a soil layer up to 15 cm deep overlaid by a water layer up to 25 cm deep, with wave height controlled to remain below 20% of the water depth. Water is added or removed via ports distributed along the flume circumference (see Figure 4a, b).

The 6.92 m circumference is divided into eight segments of approximately equal length, each

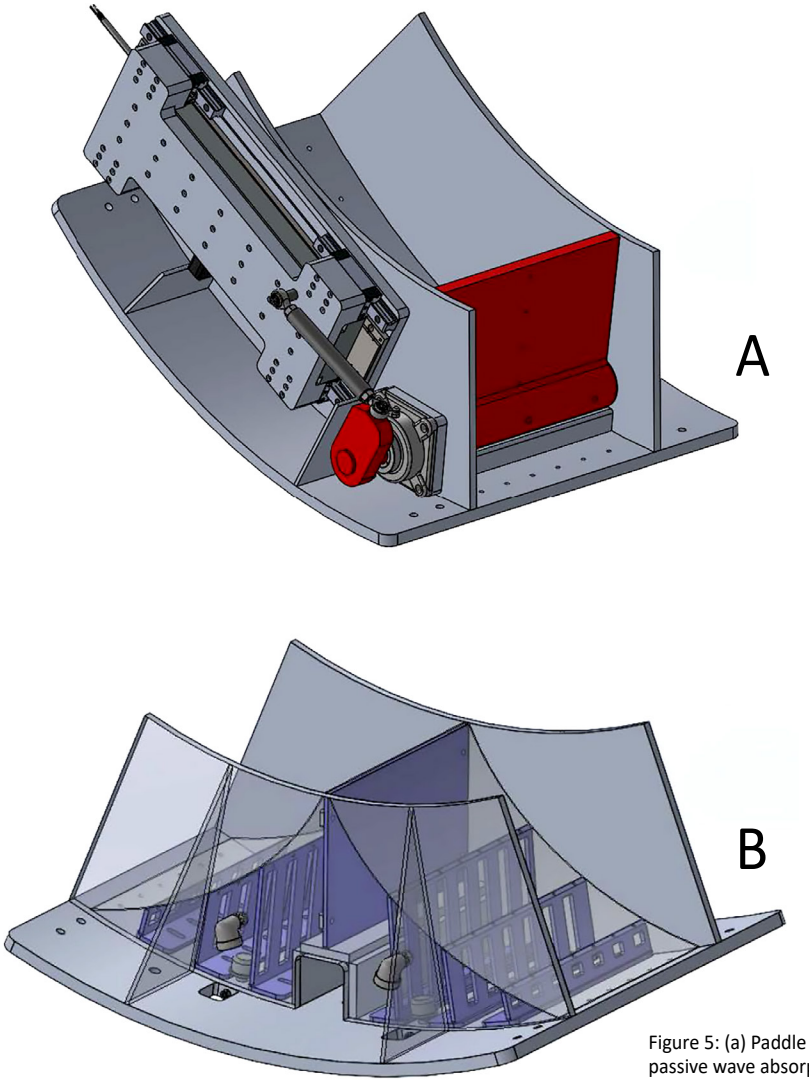

Figure 5: (a) Paddle segment and (b) passive wave absorption segment.

serving a specific function. This segmentation maximizes the wave travel distance before reaching the test structure. Except for the paddle and absorber segments (see Figure 5a, b), which must remain adjacent, the sequence of segments can be rearranged as needed. The paddle segment, constructed from aluminum, pivots on a shaft passing through the channel walls. Bearings support the shaft, and penetrations are sealed with rubber gaskets. The wave dissipation segment is designed to absorb waves passing the test model and any reflected waves generated by the paddle, ensuring controlled and repeatable wave conditions throughout the flume. This configuration allows precise laboratory simulation of wave-soil-structure interactions under realistic scaled conditions. Wave generation should be a harmonic, continuous train of waves, although transient waves and multi-frequency spectral sea states can also be created with advanced configurations and testing. Waves will likely be periodic and near sinusoidal (i.e., Linear Airy Model [27]). Wavelengths of 0.25-1.0 m are possible under scaled conditions with a 100:1 scale factor. Wave periods as low as approximately 0.1 seconds and wavelengths as large as half

the drum circumference are possible. This means wave frequencies up to approximately 10 Hz can be created. The maximum wave amplitude allowable will be ±5 cm (or 20% of fluid depth) or a scaled 5 m wave (at 100 g). The design of the UWO paddle and actuator concentrate on providing the ability to program sinusoidal, non-sinusoidal, and multi-frequency motions of the paddle. This not only allows a variety of experiments but also allows for the required iterative wave correction algorithm.

3.2.3 Passive Wave Energy Absorbing Structures

Prior researchers have used two major types of passive systems: a) beach forms and b) caissons (plates). Beach forms require long distances of gravel-like structures. The caisson forms use slots or mesh covered systems and seem to work well with shorter distances. Gao and Randolph [25] created an interesting hybrid with a porous mesh covered plate and this type of design has been used to create the passive energy absorbing structure for the flume and includes two features: a) a caisson wall mainly intended to prevent the transmission of the waves coming from the backside of the wave generating paddle and b) an extended section of baffles intended to dissipate the energy of the waves that have passed beyond the test model to ensure that they are not significantly reflected to again impinge on the model. The wall divides the energy absorbing section into two parts. One part, called the baffle section, tackles the waves passing the model, and the other part, which consists of the wall itself, takes care of the waves generated from the backside of the paddle moving in the opposite direction. This wall is removable, enabling various porous, perforated, or non-porous walls to be used. Below the wall is a dry channel for passing cables through between the top and bottom of the wave channel. Figure 5b shows the passive wave absorbing segment.

3.2.4 Active Wave Absorption Technique

Active absorption techniques have been used previously to reduce reflected waves in physical wave flume experiments, allowing accurate generation of incident waves for model testing [28], [29]. These methods typically rely on feedback from wave height measurements in the far field or pressure measurements near the paddle. Signals from these sensors are processed and filtered to adjust paddle motion in real time, selectively absorbing reflected waves while maintaining the desired incident wave. Frigaard and Brorsen [28] demonstrated a time-domain approach with digital filtering, exploiting the phase shift between incident and reflected waves to absorb energy efficiently. Using two far-field displacement transducers and several approximations and correction routines, the reflected wave energy was reduced from 30% to 3% of the incident wave energy in experimental cases, although performance varied across wave parameters. The UWO wave flume employs a proprietary iterative algorithm, WAVE, developed by the authors, which builds on principles used in active control of earthquake shake tables and wind-affected building simulations. WAVE allows users to define tests, configure wave channel capabilities, collect and display data, and generate drive signals for the paddle. Its primary objective is to achieve paddle motion that produces wave profiles closely matching

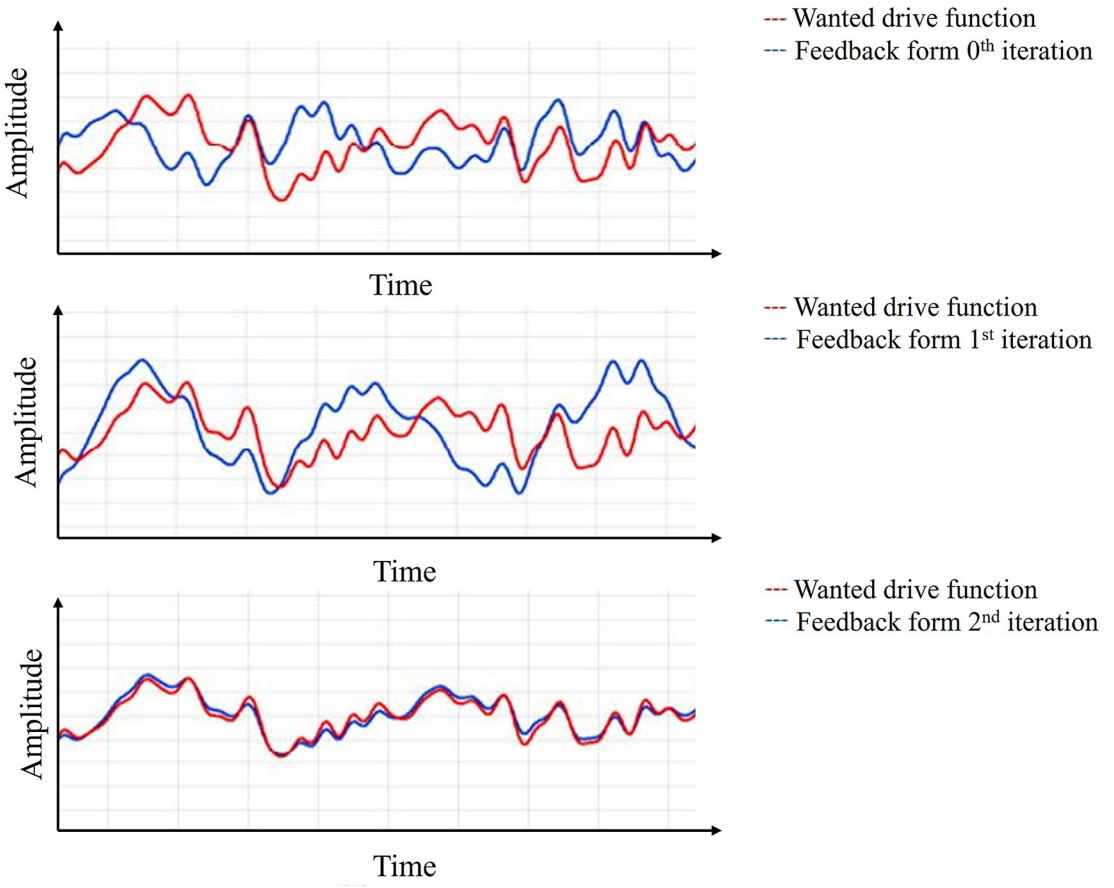

Figure 6: Iterative improvement of wave forms using the WAVE algorithm.

the desired incident wave while minimizing contamination from reflected waves (see Figure 6). WAVE uses an iterative learning approach: initial test waves are analyzed, and deviations caused by paddle limitations, servo control non-linearities, reflected wave dynamics, channel properties, and signal noise are compensated. Through repeated adjustments, WAVE progressively refines paddle motion, reducing the influence of reflected waves and producing final wave motion that more accurately replicates the operator-defined target waveform, enhancing experimental fidelity in wave-structure interaction studies.

3.2.5 Wave Displacement and Pressure Instrumentation

The flume system must allow measurements of various transducers for test documentation and use some of these transducers to implement the reflected wave active absorption algorithm (WAVE). Key to implementing this algorithm is the estimation of the wave height and water pressure as a function of distance and time along the channel and down the front face of the paddle. Based on a review of various displacement measurement systems [30], including resistive sensors, radar, laser triangulation, and video-edge-detection, the best approach has been found to be a

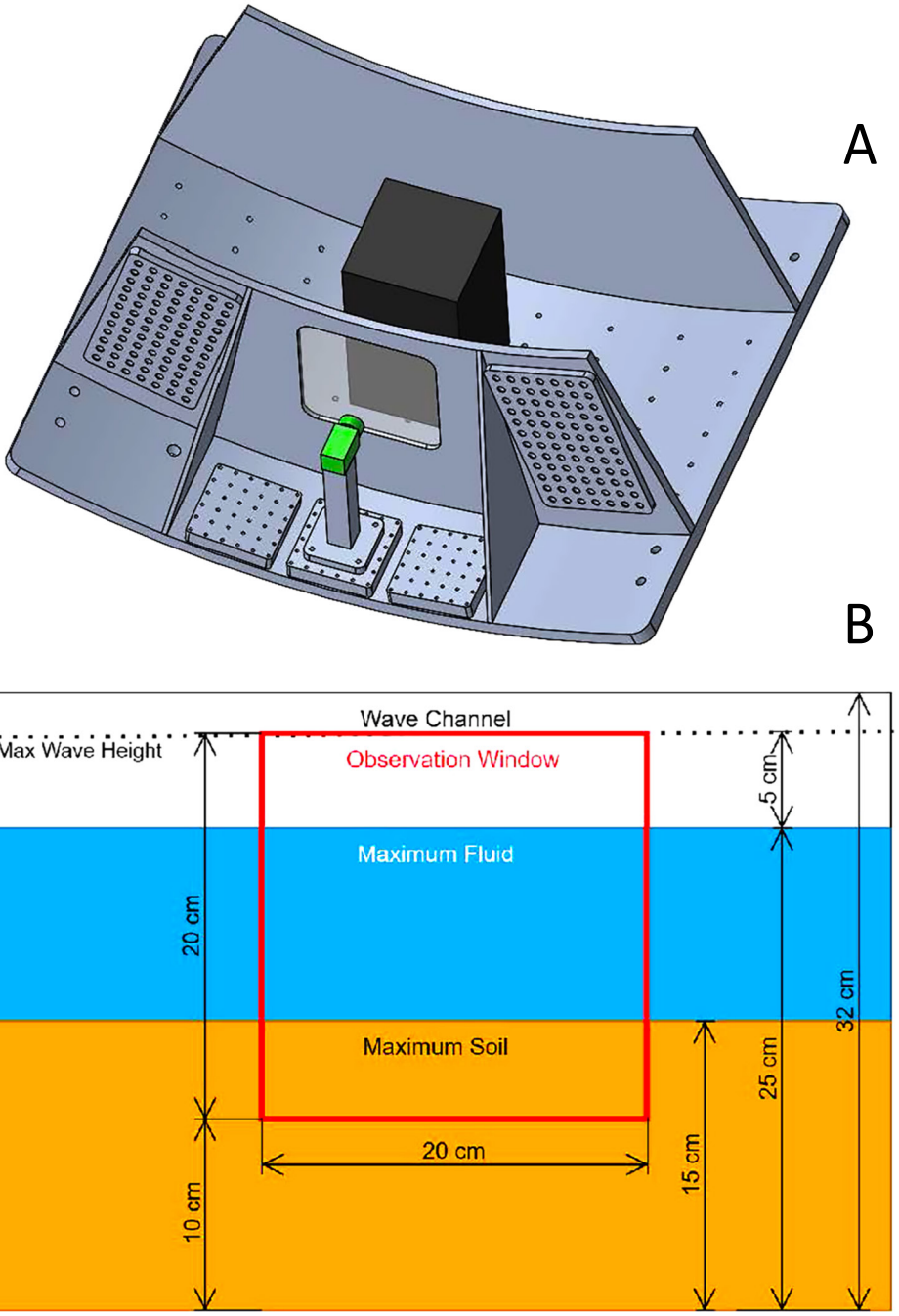

Figure 7: (a) Structure and viewing window segment and (b) channel cross-section showing water and soil thicknesses (model dimensions).

combination of ultrasonic sensors and pressure transducers along the flume and in the face of the paddle. Further information is provided using video tracking techniques in the wave flume. Two high speed video cameras (>100 fps) are used, one located between the wave paddle and the test item, and one at the test item. The model test segment and camera arrangement is shown in Figure 7. Video detection for displacement measurement involves taking a video image of a wave's edge of finite length through the transparent window

on one side of the wave channel, with special lighting to enhance the contrast of the water to air interface. An edge detection algorithm is then used to measure the direct displacement of the entire recorded wave by tracking pixels at the edge boundary to support the other wave front estimation systems [31].

4. FUTURE TESTING WITH THE UWO WAVE FLUME

4.1 Offshore Energy Foundations and Atlantic Canada

4.1.1 Offshore Wind Turbine Foundations

Renewable energy technologies, including hydroelectric, wind, and solar power, are central to global strategies for reducing dependence on fossil fuels and promoting environmental sustainability. Recent advances have enabled the development of much larger offshore wind turbines, with capacities now reaching 16 MW [32]. The deployment of these larger turbines necessitates correspondingly larger and deeper foundations, which can constitute up to 40% of total project costs [33]. A variety of foundation solutions exist – including shallow foundations, monopiles, suction caissons, and buoyant fixed structures – selected based on local experience, plant availability, seabed conditions, metocean loading, and water depth [34]. Monopiles are among the most common solutions due to prior experience from the oil and gas industry, which has informed many early offshore wind deployments. Their design typically involves the widely used p-y method [35], [36]. Significant challenges arise when applying conventional p-y approaches to large-diameter monopiles with relatively low length-to-diameter (L/D) ratios. Studies by [35], [37], [38] have highlighted limitations including the neglect of diameter effects, the restricted number of loading cycles in early experiments, and the direct transfer of design recommendations developed for oil and gas platforms. In response, recent research has sought to improve p-y formulations. The PISA project, for example, proposed enhanced modelling frameworks incorporating additional resistance mechanisms, such as side-shear and base resistance, extending the applicability of p-y methods to large-diameter monopiles [35], [38]. Despite these advances, knowledge gaps remain regarding the long-term behaviour of large monopiles subjected to combined waves, wind, current, tidal, and ice loading over millions of cycles. To address these gaps, various approaches have been explored for evaluating lateral capacity and displacement behaviour, including physical model (see Figure 8) and field testing, numerical finite element modelling, and analytical or semi-empirical methods. Continued research in this area is essential for developing reliable design methodologies for next-generation offshore wind pile foundations.

4.1.2 Developing Offshore Wind Farms in Atlantic Canada

Offshore wind energy has experienced rapid growth, particularly in Europe and Asia, where decades of operational experience now exist. In the United States, offshore wind is emerging, with one small-scale production farm operational and several hundred megawatts in the development pipeline. In contrast, Canada, despite substantial onshore wind capacity, currently lacks operating offshore turbines. Nevertheless, significant

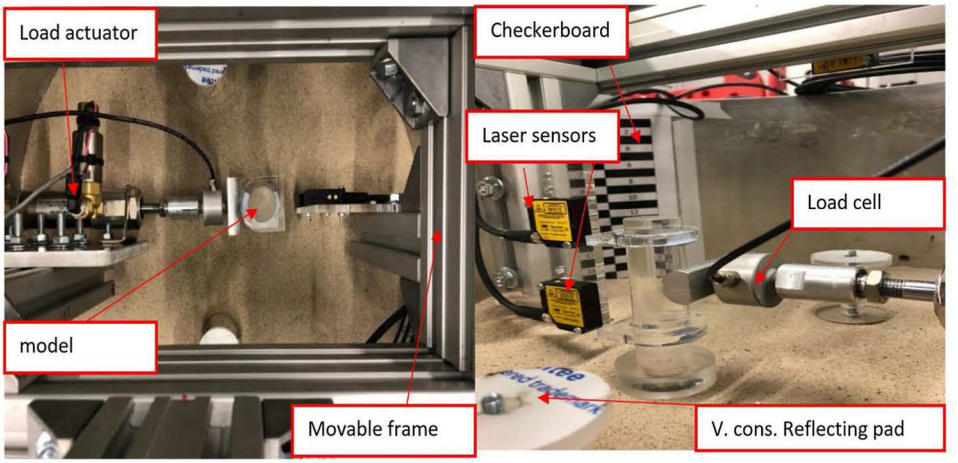

Figure 8: Laterally loaded pile centrifuge setup in sand soil showing load actuators and instrumentation (after [33]).

development plans exist for the wind-resource-rich Atlantic Canadian region. Offshore sites typically experience higher wind speeds than onshore locations due to reduced surface roughness, with mean wind speeds up to 90% stronger than onshore sites [39]. Water depth (bathymetry) is a critical determinant of suitable foundation types for offshore wind turbines. Fixed foundations are generally feasible in shallower waters (<40-60 m), although pile flexibility introduces technical challenges as depth increases. Beyond these depths, the construction of larger substructures renders fixed foundations less viable, and floating systems become more practical, although no commercial floating offshore wind farms currently operate globally.

The Atlantic Canadian inner shelf presents substantial geological constraints. Its Quaternary evolution, shaped by glaciation and postglacial sea level transgression, has influenced seafloor morphology, sediment distribution, and near-surface stratigraphy. While bearing some similarities to the North Sea and northern US Atlantic coast, the region's geology differs sufficiently to preclude straightforward analogues. Limited thicknesses of Quaternary sediments constrain the deployment of conventional bottom-fixed foundations, in contrast with the deeper sediment layers existing in the North Sea and US Atlantic [40]. Consequently, suitable sites for monopiles are rare, with Sable Bank identified as one of the few locations with sufficiently deep sand. Elsewhere, the seabed is dominated by bedrock and bouldery till, favouring floating turbine anchoring, while shallow water areas may accommodate gravity bases, scour effects present a significant concern. Hydrodynamic conditions further complicate potential development; Atlantic Canada experiences some of the world's most extreme tidal ranges, exceeding 16 m in certain locations, driven by coastal funneling and resonance effects, generating strong, rapidly reversing currents. Sea ice is another operational constraint, occurring periodically at many favourable sites. Turbines must withstand ice coverage of at least 30% and ice floes up to 15 cm thick and 100 m long, which can reach velocities up to 4 m/s under tidal and wind forcing [41], [42]. Comprehensive investigation of tidal currents and ice

interactions in these offshore areas is essential to inform turbine design. The development of ice-resistant offshore wind technology would enable deployment in Atlantic Canada and also support wind development in global regions with similar energetic tidal flows and sea ice conditions [43].

4.2 Planned Flume Studies and Gaps to be Addressed

While the potential for significant wind energy capture from offshore locations in Atlantic Canada exists, the technical challenges appear to require additional research and development to occur to optimize the successful exploitation of this rich resource. This section discusses some of the potential uses of the drum-based wave flume to acquire knowledge and develop techniques suitable for industry.

4.2.1 Wave Loading with Combined Tides and Currents

Three primary cyclic loading scenarios are considered in offshore geotechnical pile design: seismic events, short-duration extreme storms (e.g., 1.5 day, 50-year return period for ultimate limit state assessment), and long-term operational loading over the service life of offshore wind turbines. Seismic and storm loads are typically idealized as undrained cyclic loading, with limited drainage in highly permeable strata, resulting in conservative design. Operational loading, however, poses greater complexity. While individual load amplitudes are relatively small, they act over millions of cycles, and their cumulative effect on permanent pile rotation and deformation is often neglected or treated with simplified approaches. Standards such as DNV-RP-212 [44] require consideration of lifetime loading but provide limited guidance on appropriate analysis methods. Most existing cyclic soil models are formulated for undrained conditions [45], [46], rendering them poorly suited for operational loading in sandy soils, where drained or partially drained conditions prevail. These models also often omit the accumulation of permanent shear strain. Experimental evidence from small-scale and centrifuge tests has demonstrated that cyclic loading in drained sands induces progressive pile rotation and permanent deformation, known as soil ratcheting [47], highlighting the need to incorporate these mechanisms into offshore foundation design. Centrifuge studies of cyclic lateral monopile loading have generally applied sinusoidal, equal-amplitude cycles, with variable loading introduced in piecewise form [33]. The use of spectrally consistent irregular wave states would allow more realistic assessment of fatigue and ultimate limit state responses, as well as pore pressure development and volumetric soil changes under partially drained conditions during storm events. Drum centrifuge testing further enables simulation of combined loading from waves, tidal water level variations, and current flows via integrated fluid recirculation systems capabilities not currently achievable in conventional centrifuge or wave flume facilities.

4.2.2 Scour Protection and Particle Transport

Scour erosion around marine foundations is a well-established phenomenon, primarily driven by local hydrodynamic effects caused by the presence of the structure, which alters flow patterns, wave characteristics, and sediment transport processes [48], [49]. For offshore wind turbines supported by piles, scour

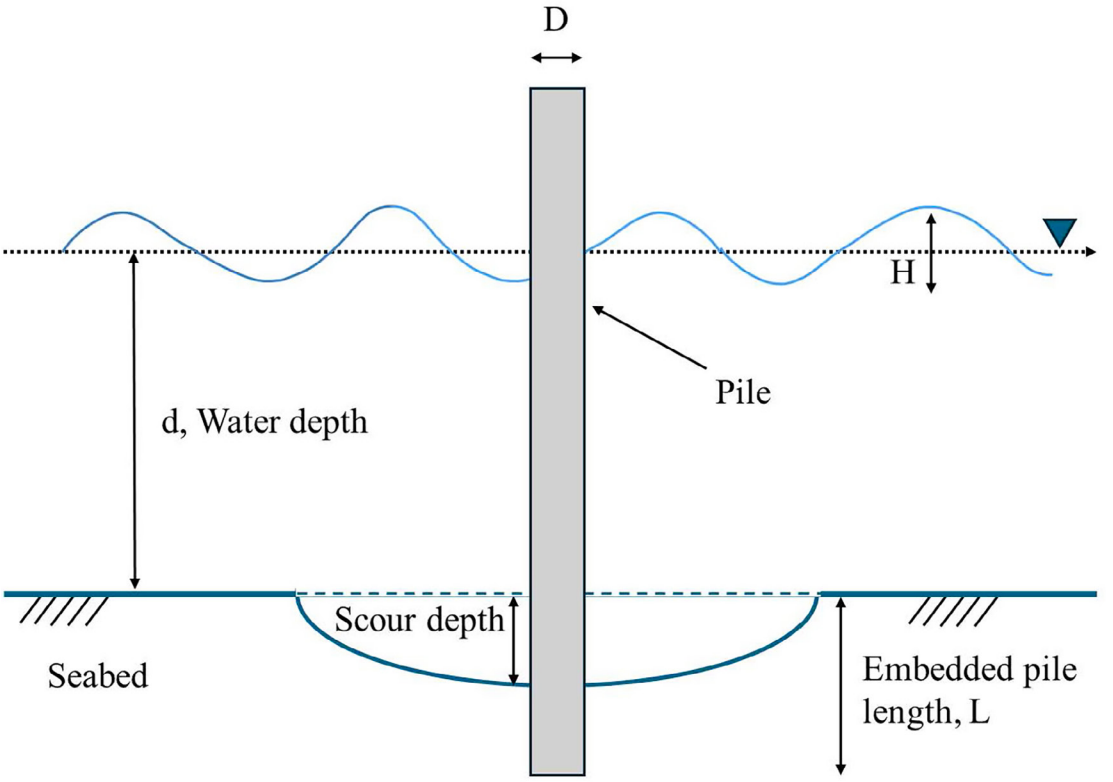

Figure 9: Wave and current induced scour around monopile.

represents a critical design concern, as it can substantially reduce foundation stiffness and bearing capacity, affecting structural dynamics, long-term stability, and fatigue performance [50]. The development and depth of scour holes depend strongly on seabed soil conditions. Experimental studies in sandy deposits report average scour depths (see Figure 9) of approximately 1.3 x the pile diameter (D), with mean values 0.7 D, while cohesive clay deposits typically exhibit depths of 0.75-1.0 D [51], [52]. To mitigate these effects, scour protection systems are routinely employed. Common measures include rock armour, rubble filter layers, solidified slurry, and geotextile bags, which dissipate hydrodynamic energy and stabilize the seabed [49]. Despite extensive research, important knowledge gaps remain. Scour processes are highly sensitive to seabed stratigraphy, yet many studies focus on homogeneous sand deposits. Further investigation is needed to assess scour development and protection effectiveness in heterogeneous soils, particularly regarding pile lateral response under cyclic loading, including scenarios where protection is installed remedially after scour formation. Physical modelling of these processes is challenged by sediment scaling under fluid transport. Dong et al. [53] reviewed scaling laws for high-g modelling of soil transport in turbulent flows, identifying key dimensionless groups such as the Reynolds number, densimetric Froude number, and ratios of soil to water density and characteristic lengths to particle size. Strict similitude requires sediment particle sizes to match geometric scaling – a condition often impractical for small models. Alternative

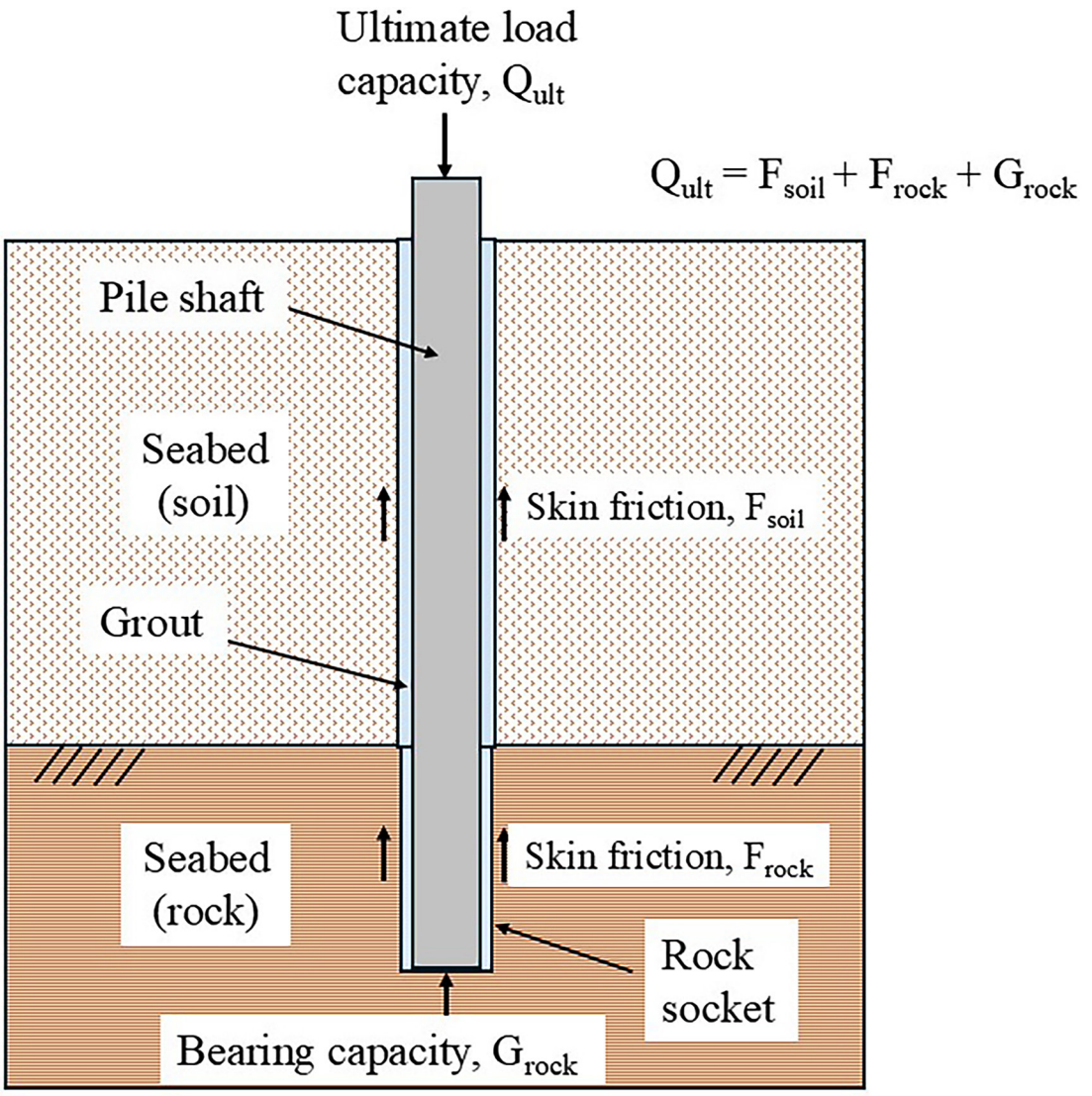

Figure 10: Rock socketed pile cross-section and generalized design equations.

approaches, including lower-density surrogate materials to adjust the densimetric Froude number, offer a practical means to partially compensate for departures from exact similitude, enabling more realistic simulation of scour initiation, progression, and mitigation strategies under representative hydrodynamic conditions.

4.2.3 Rock Socketed Piles

Offshore rock sockets are drilled holes in rocky seabeds (often with shallow overlying sediments), slightly larger than a pile, filled with grout to create a stable foundation. This technique, known as rock socket grouting, can be essential for offshore structures such as wind turbines and oil platforms, where piles cannot be driven through solid rock and do not have access to deep layers of sediment. By bonding the steel pile, grout, and surrounding rock, the method anchors a pile against uplift and lateral forces, effectively transferring loads into the rock mass (see Figure 10). Traditionally, the design of rock socketed piles has relied on empirical formulae (e.g., [54]), although advanced analytical

solutions using finite element methods have also been developed [55], albeit at higher cost and complexity. Centrifuge testing offers a cost-effective alternative, allowing small-scale models subjected to high g-levels to replicate prototype loads. Comparisons with conventional tests demonstrate that centrifuge experiments are particularly suitable for studying rock socketed piles, since shaft resistance development is stress dependent. Previous centrifuge tests [56] show that peak shaft resistance is mobilized at small pile settlements before decreasing slightly to a residual value, while no peak base resistance is observed even at large pile displacements. The ultimate unit shaft resistance and maximum base resistance mobilized at a 10% settlement ratio align closely with existing field-based design methods. When planar weaknesses exist beneath the pile base, capacity is reduced proportionally to the area of weakness. These findings underscore the importance of considering both shaft and base contributions in the presence of sub-base discontinuities and demonstrate the utility of centrifuge testing for understanding the complex behaviour of rock socketed offshore piles. The addition of realistic loading conditions from waves and currents with this form of turbine monopile support system will provide excellent information for future design usage in areas such as Atlantic Canada.

4.2.4 Ice Floe Modelling

Over the past decade, interactions between surface waves and sea ice have been recognized as a critical factor in wave and ice dynamics [57], [58]. International research has focused on wave-ice interactions in the marginal ice zone, where these processes are most pronounced. Recent advances emphasize incorporating wave-ice interactions into numerical wave models and sea ice models [59], [60]. Despite these developments, significant gaps remain, particularly concerning wave-induced ice breakup and associated loads on marine structures. Theoretical approaches generally assume ice fractures when wave-induced stress or strains exceed critical thresholds [61]. Extensions incorporate ice fatigue, probabilistic wave amplitudes, irregular wave spectra, three-dimensional effects and viscoelastic behaviour. Laboratory-scale physical modelling complements theory and field observations, employing 1 g wave basins to study wave attenuation, transmission, and reflection by plastic or wooden floes, freshwater ice, and model ice [60], [62]. However, few experiments have directly investigated wave-induced ice breakup, and none have incorporated centrifuge modelling. Introducing model ice floes into a drum centrifuge (see Figure 11) will enable novel studies of (i) the spatial and temporal evolution of wave-driven ice breakup, (ii) wave attenuation through ice transitioning from continuous to broken states, and (iii) ice-induced loads on turbine piles and consequent soil-structure interactions. The resulting dataset will support improved validation of coupled theories of wave attenuation and ice breakup, addressing a critical gap in understanding wave-ice-structure interactions and informing the design of offshore structures in ice-affected waters.

5. CONCLUSION

While Atlantic Canada possesses substantial potential for offshore wind energy development, the successful exploitation of this resource is contingent upon addressing a range of technical challenges that necessitate

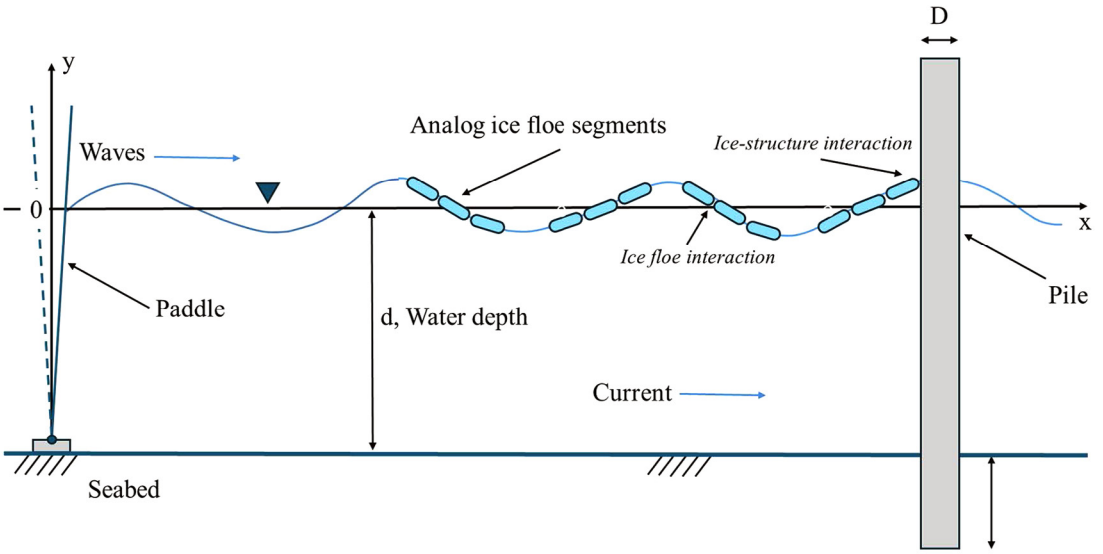

Figure 11: Ice floe-wave-structure interaction modelling.

further research and development. The unique drum centrifuge-based wave flume at the UWO offers a valuable experimental platform for generating the necessary knowledge base and methodological advances required to support industry-relevant design and assessment. The outcome of this research is expected to reduce costs for asset owners and operators, as well as for the insurance sector, while enhancing the competitiveness of consultants and contractors. Moreover, the work will support stakeholders engaged in risk assessment for Canada's geotechnical energy infrastructure by enabling more informed decision-making, strategic planning, and targeted investment. Failure to address these challenges in a timely manner is likely to constrain the near-term growth of Canada's renewable energy portfolio and significantly impede the development of offshore wind energy, with broader implications for Atlantic Canada's productivity and competitiveness.

Specific findings from this work are given below.

- Experimental investigation of wave loading on offshore structures in conventional 1 g flumes is generally constrained by scale effects, particularly when soil-structure interaction is involved, as reduced-scale seabed cannot accurately reproduce prototype soil stress conditions.
- Geotechnical centrifuge modelling overcomes these limitations by enabling scaled physical models to be tested under elevated gravitational fields, thereby achieving correct stress and strain similitude in the soil (seabed), while still permitting realistic fluid wave simulation.
- Traditional beam centrifuges have demonstrated the feasibility of generating solitary, standing, and progressive waves for studies of offshore problems; however, their relatively short test-box lengths limit achievable wave characteristics and complicate the attenuation of reflected waves.
- Drum centrifuges offer substantial advantages for wave modelling, as the

circumferential geometry provides a significantly longer effective testing channel, facilitating improved wave generation and propagation, and allowing much larger model structures to be used.
- Wave generation systems in centrifuge environments must be specifically designed to operate under high centrifugal accelerations and elevated wave frequencies, while maintaining stable and repeatable wave conditions.
- Accurate measurement of wave-induced responses requires effective dissipation of incident waves to prevent re-reflection; passive absorption systems have shown mixed performance under centrifuge conditions and active paddle wavemaker systems with reflection compensation provide a robust alternative, minimizing wave re-reflections through adaptive control of the wavemaker signal.
- The active fluid wave generation system developed for the large drum centrifuge at the UWO demonstrates the practical implementation of these principles and enables advanced physical modelling of wave-induced forces on offshore wind turbine towers and pile foundations in shallow water conditions.

ACKNOWLEDGMENT

Authors' Declaration

- Funding: The authors acknowledge the financial support of the Natural Sciences and Engineering Research Council (Grant: RGPIN-2015-06062) and the Canadian Foundation for Innovation (Grant: #33263).
- Ethical approval: This paper does not contain any studies with human participants or animals.
- Competing interests: The authors declare that they have no competing interests.
- Availability of data and materials: Datasets used and/or analyzed during the current study are available from the corresponding author upon reasonable request.
- Artificial intelligence was not used in this work.

REFERENCES

[1] Y. Sun, Y. Song and S. Bian, "Scour Process Around the Pile Foundation of Marine Platforms and Analysis of Scour Mechanics," *Periodical of Ocean University of China*, pp. 636-640, 2007. doi: 10.16441/j.cnki.hdxb.2007.04.022.

[2] Q. Xiang, Y. Li, Y. Wei, K. Wang and C. Yao, "Review of bridge foundation scour," *Journal Southwest Jiaotong University*, vol. 54, pp. 235-248, 2019. [Online]. Available at: https://jsju.org/index.php/journal/article/view/269

[3] Y. Li, C. Zhang, S. Chi, Y. Yang, J. Shi, and T, "Numerical test of scale relations for modelling coastal sandbar migration and inspiration to physical model design," *Journal of Hydrodynamics*, vol. 34, pp. 700-711, 2022.

[4] K. Shimosako, S. Takahashi, K. Suzuki and Y. Kang, "Large hydro-geo flume and its use for coastal engineering research," *Technical note of National Institute for Land and Infrastructure Management*, vol. 41, pp. 81-89, 2002. [Online]. Available at: https://www.pwri.go.jp/eng/ujnr/joint/33/paper/34suzuki.pdf

[5] T. Yoshii, S. Tanaka and M. Matsuyama, "Tsunami deposits in a super-large wave flume," *Marine Geology*, vol. 391, pp. 98–107, 2017. doi: 10.1016/j.margeo.2017.07.020.

[6] R. Yang, C. Wang, C. Huang, C. Chung, C. Chen and C. Huang, "The 1:20 scaled hydraulic model test and field experiment of barge-type floating offshore wind turbine system," *Ocean Engineering*, vol. 247, 110486, 2022. doi: 10.1016/j.oceaneng.2021.110486.

[7] G. Fromant et al. "Wave boundary layer hydrodynamics and sheet flow properties under large-scale plunging-type breaking waves," *Journal of Geophysical Research: Oceans*, vol. 124, pp. 75-98, 2019. doi: 10.1029/2018JC014406.

[8] G. Van and R. Marcel, "The new Delta flume for

large-scale physical model testing," *Proceedings of the 36th IAHR World Congress*, The Hague, the Netherlands, pp. 1-8, 2015. [Online]. Available at: https://deltares-deltares-p01-website.s3.eu-central-1.amazonaws.com/app/uploads/2015/02/THE-NEW-DELTA-FLUME-FOR-large-scale-testing.pdf

[9] W. Wang, J. Yan, S. Chen, J. Liu, F. Jin., and B. Wang, "Gridded cemented riprap for scour protection around monopile in the marine environment," *Ocean Engineering*, vol. 272, 113876, 2023. doi: 10.1016/j.oceaneng.2023.113876.

[10] H. Oumeraci, *More than 20 Years of Experience Using the Large Wave Flume (GWK) - Selected Research Projects*, Die Küste, pp. 179–239, 2010.

[11] A. Schofield, "Cambridge geotechnical centrifuge operations," *Géotechnique*, vol. 30, no. 3, pp. 227-268, 1980. doi: 10.1680/geot.1980.30.3.227.

[12] R. Taylor, *Centrifuges in modelling: Principles and scale effects. Geotechnical Centrifuge Technology*, Blackie Academic & Professional, pp. 19-33, 1995.

[13] H. Sekiguchi and R. Phillips, "Generation of water waves in a drum centrifuge," *Proceedings of the International Conference CENTRIFUGE 91*, Colorado, pp. 343-350, 1991.

[14] H. Sekiguchi, K. Kita, S. Sassa and T. Shimamura, "Generation of Progressive Fluid Waves in a Geo-Centrifuge," *Geotechnical Testing Journal*, ASTM, vol. 21, no. 2, pp. 95-101, 1998.

[15] H. Sekiguchi, S. Sassa, K. Sugioka and J. Miyamoto, "Wave induced liquefaction, flow deformation and particle transport in sand beds," *Proceedings of the International Conference GeoEng2000*, Lisbon, Portugal: International Society for Rock Mechanics, 2000.

[16] S. Baba, M. Miyake, K. Tsurugasaki and H., Kim, "Development of wave generation system in a drum centrifuge," *Proceedings of the International Conference on Physical Modelling in Geotechnics (ICPMG '02)*, pp. 265-270, 2002, Rotterdam, Netherlands: A.A. Balkema.

[17] T. Newson, P. Sentenac, P. Dong, X. Wu and M. Davies, "Modelling failure mechanisms of soft cliff profiles," *International Conference on Protection and Restoration of the Environment VIII*, pp. 1-8, 2006. [Online]. Available at: https://strathprints.strath.ac.uk/8552/6/strathprints008552.pdf

[18] D. Stewart, R. Boyle and M. Randolph, "Experience with a new drum centrifuge," *Proceedings of the International Conference CENTRIFUGE 98*, Tokyo, pp. 35-40, 1998.

[19] J. Miyamoto, S. Sassa and K. Tsurugasaki, "Wave-induced liquefaction and floatation of pipeline buried in sand beds," *Proceedings of the 9th International Conference on Physical Modelling* in Geotechnics 2018 (ICPMG 2018), pp. 571-576, 2018, London: CRC Press.

[20] M. Sumer, "Liquefaction around marine structures," *Advanced series on ocean engineering*, Singapore: World Scientific, vol. 39, 2014, ISBN10: 9789814329316.

[21] S. Sassa, Y. Takahashi, S, Morikawa and D. Takano, "Effect of overflow and seepage coupling on tsunami-induced instability of caisson breakwaters," Coastal Engineering, vol. 117, pp. 157-165, 2016. doi: 10.1016/j.coastaleng.2016.08.004.

[22] S. Chakrabarti, *Offshore Structure Modeling*, 1994, JBW Printers & Binder Pte. Ltd., ISBN-10: 9810 215134.

[23] M. White, *Viscous Fluid Flow*, 2006, McGraw-Hill, ISBN10: 1264423101.

[24] S. Hughes, "Laboratory wave generation," *In: Physical Models and Laboratory Techniques in Coastal Engineering*, World Scientific Publishing Co., pp. 333–457, 1993.

[25] F. Gao and M. Randolph, "Progressive ocean wave modelling in drum centrifuge," *Frontiers in Offshore Geotechnics: ISFOG 2005* – Gourvenec & Cassidy (eds.) Taylor & Francis Group, London, ISBN 0 415 39063 X, pp. 583-588, 2005.

[26] M. Dewoolkar, H. Ko and R. Pak, "Centrifuge modelling of models of seismic effects on saturated earth structures," *Géotechnique*, vol. 49, no. 2, pp. 247-266, 1999. doi: 10.1680/geot.1999.49.2.247.

[27] A. Craik, "The Origins of Water Wave Theory," *Annual Review of Fluid Mechanics*, vol. 36, pp.1-28, 2004. doi: 10.1146/annurev.fluid.36.050802.122118.

[28] P. Frigaard and M. Brorsen, "A Time-Domain Method for Separating Incident and Reflected Irregular Waves," Coastal Engineering, vol. 24, pp. 205-215, 1995. doi: 10.1016/0378-3839(94)00035-V.

[29] T. Andersen, M. Clavero, P. Frigaard, M. Losada and J. Puyol, "A New Active Absorption System and Its Performance to Linear and Non-Linear Waves," *Coastal Engineering*, vol. 114, pp. 47-60, 2016. doi: 10.1016/j.coastaleng.2016.04.010.

[30] S. Bourdier, K. Dampney, H. Fernandez, G. Lopez and J. Richon, "Non-Intrusive Wave Field Measurement," *WP4: Research to Innovate and Improve Infrastructures, Technologies and Techniques*, Marinet Marine Renewables Infrastructure Network, p. 53, 2014. [Online]. Available at: https://tethys.pnnl.gov/sites/default/files/publications/D4_05_Final.pdf

[31] K. Viriyakijjaa and C. Chinnarasria, "Wave Flume Measurement Using Image Analysis," *Aquatic Procedia*, vol. 4, pp. 522-531, 2015. doi:

10.1016/j.aqpro.2015.02.068.
[32] D. Lombardi, S. Bhattacharya and D. Muir Wood, "Dynamic soil–structure interaction of monopile supported wind turbines in cohesive soil," Soil Dynamics and Earthquake Engineering, vol. 49, pp. 165-180, 2013. doi: 10.1016/j.soildyn.2013.01.015.
[33] Y. Alsharedah, T. Newson, H. El Naggar and J. Black, "Lateral ultimate capacity of monopile foundations for offshore wind turbines: effects of monopile geometry and soil stiffness properties," *Applied Science*, vol.13, no. 22:12269, 2023. doi: 10.3390/app132212269.
[34] B. Byrne and G. Houlsby, Foundations for Offshore Wind Turbines, Philosophical Transactions Royal Society London Series A, vol. 361, pp. 2909–2930, 2003. [Online]. Available at: https://royalsocietypublishing.org/rsta/article/361/1813/2909/51795/Foundations-for-offshore-wind-turbines
[35] B. Byrne et al., "Field testing of large diameter piles under lateral loading for offshore wind applications," *Proceedings of XVI European Conference on Soil Mechanics and Geotechnical Engineering*, Edinburgh, pp 255–1260, 2015.
[36] P. Jeanjean, "Re-assessment of P-Y curves for soft clays from centrifuge testing and finite element modeling," *Offshore Technology Conference*, Houston, Texas, 2009. doi: 10.4043/20158-MS.
[37] Y. Lai, L. Wang, Y. Hong and B. He, "Centrifuge modeling of the cyclic lateral behavior of large-diameter monopiles in soft clay: effects of episodic cycling and reconsolidation," *Ocean Engineering*, vol. 200: 107048, 2020. doi: 10.1016/j.oceaneng.2020.107048.
[38] B. Zhu, Z. Zhu, T. Li, J. and Y. Liu, "Field tests of offshore driven piles subjected to lateral monotonic and cyclic loads in soft clay," *Journal of Waterway, Port, Coastal, and Ocean Engineering*, vol. 143, no. 5:5017003, 2017. doi: 10.1061/(ASCE)WW.1943-5460.0000399.
[39] C. Archer and M. Jacobson, "Evaluation of global wind power," *Journal of Geophysical Research: Atmospheres*, 110, D12110, 2005. doi: 10.1029/2004JD005462.
[40] J. Eamer, J. Shaw, E. King and K. MacKillop, *Seabed conditions on the inner shelves of Atlantic Canada*, Geological Survey of Canada Open File 8731, 2020, 162p. doi: 10.4095/326514.
[41] M. Shokr, Z. Wang and T. Liu, "Sea ice drift and arch evolution in the Robeson Channel using the daily coverage of Sentinel-1 SAR data for the 2016–2017 freezing season," *The Cryosphere*, vol. 14, pp. 3611–3627, 2022. doi: 10.5194/tc-14-3611-2020.
[42] R. Sanders and R. Baddour. *Documenting ice in the Bay of Fundy Canada*, Contractor Report (National Research Council of Canada. Institute for Ocean Technology), no. CR-2006-01, 2006. doi: 10.4224/8896108.
[43] R. Branch, T. Wang, J. Whiting, Z. Yang and G. Caria-Medina. *Sea Ice Collision Risk Assessment for Tidal Turbine Siting in Cook Inlet, Alaska*. Report Prepared for the U.S. Department of Energy Under contract DE-AC05-76RL01830, 2021. [Online]. Available at: https://www.pnnl.gov/main/publications/external/technical_reports/PNNL-32329.pdf
[44] DNV (Det Norske Veritas), *Offshore soil mechanics and geotechnical engineering*, DNV-RP-C212, 2009. [Online]. Available at: https://www.dnv.com/energy/standards-guidelines/dnv-rp-c212-offshore-soil-mechanics-and-geotechnical-engineering
[45] K. Andersen, "Cyclic soil parameters for offshore foundation design," *Frontiers in Offshore Geotechnics III*, 2015, vol 1, pp. 1097-1102.
[46] C. Akdag and F. Rackwitz, "Model test and finite element analysis results of a monopile in very dense sand under unidirectional horizontal cyclic loading," *Ocean Engineering*, vol. 288, 116053, 2023. doi: 10.1016/j.oceaneng.2023.116053.
[47] S. Bayton, J. Black and R. Klinkvort, "Centrifuge modelling of long term cyclic lateral loading on monopiles," *In: Physical modelling in geotechnics*, 1, CRC Press, pp. 689-694, 2018.
[48] A. Stride, *Offshore Tidal Sands*, vol. 237, 1982, Chapman and Hall.
[49] R. Whitehouse, Scour at Marine Structures, Thomas Telford, London, p. 216, 1998.
[50] L. Prendergast, K. Gavin and P. Doherty, "An investigation into the effect of scour on the natural frequency of an offshore wind turbine," Ocean Engineering, vol. 101, pp. 1–11, 2015. doi: 10.1016/j.oceaneng.2015.04.017.
[51] M. Sumer, J. Fredsøe and N. Christiansen, "Scour around vertical pile in waves," *Journal of Waterway, Port, Coastal, and Ocean Engineering*, vol. 118, no. 1, pp. 15–31, 1992.
[52] Y. Kishore, S. Rao and J. Mani, "Influence of the scour on laterally loaded piles," *12th International Conference of International Association for Computer Methods and Advances in Geomechanics*, Goa, pp. 1-6, October, 3283–3288, 2008.
[53] P. Dong, T. Newson, M. Davies and P. Davies, "Scaling laws for centrifuge modelling of soil transport by turbulent fluid flows," *International Journal of Physical Modelling in Geotechnics*, vol. 1, no. 1, pp. 41-45, 2001.
[54] A. Williams and P. Pells, "Side resistance rock sockets in sandstone, mudstone and shale," *Canadian Geotechnical Journal*, vol. 18, pp. 502-513, 1981. doi: 10.1139/t81-061.
[55] R. Rowe and H. Armitage, "Theoretical solutions

for axial deformation of drilled shafts in rock," *Canadian Geotechnical Journal*, vol. 24, pp. 114-125, 1987. doi: 10.1139/t87-010.

[56] C. Leung and H. Ko, "Centrifuge model study of piles socketed in soft rock," *Soils and Foundations*, vol. 33, no. 3, pp. 80-91, 1993. doi: 10.3208/sandf1972.33.3_80.

[57] V. Squire, "Past, present and impendent hydroelastic challenges in the polar and subpolar seas," *Philosophical Transactions, The Royal Society*, A369, pp. 2813–2831, 2011. doi: 10.1098/rsta.2011.0093.

[58] K. Golden et al., Modeling sea ice. *Notices of the American Mathematical Society*, vol. 67, pp. 1535–1555, 2020. doi: 10.1090/ noti2171.

[59] W. Rogers, M. Meylan and A. Kohout, "Estimates of spectral wave attenuation in Antarctic sea ice, using model/data inversion," *Cold Regions Science and Technology*, vol. 182, 103198 2021. doi: 10.1016/j.coldregions.2020.103198.

[60] L. Bennetts, S. O'Farrell and P. Uotila, "Impacts of ocean wave-induced breakup of Antarctic sea ice via thermodynamics in a stand-alone version of the CICE sea-ice model," *The Cryosphere*, vol. 11, pp. 1035–1040, 2017. doi: 10.5194/tc-11-1035-2017.

[61] G. Vaughan and V. Squire, "Wave induced fracture probabilities for Arctic sea-ice," *Cold Regions Science and Technology*, vol. 67, pp. 31–36, 2011. doi: 10.1016/j.coldregions.2011.02.003.

[62] F. von Bock und Polach, M. Klein and M. Hartmann, "A new model ice for wave-ice interaction," *Water*, vol. 13, no. 23, 3397, 2021. doi: 10.3390/w13233397.

Species Recognition using Artificial Intelligence

Mariya Krestyanska Summerfield

Supporting offshore wind farms

Who should read this paper?

This paper is intended for offshore wind practitioners, marine ecologists, regulators, and technology developers involved in biodiversity monitoring and environmental management. It will also be relevant to researchers and policy-makers working at the interface of marine science, digital monitoring, and governance.

Why is it important?

The rapid expansion of offshore wind is creating a growing mismatch between the scale of development and the capacity of traditional biodiversity monitoring approaches. This paper addresses that gap by critically examining how real-time Artificial Intelligence (AI) species recognition can support more responsive, transparent, and credible marine monitoring without overstating current capabilities. It offers a balanced perspective that integrates ecological science, operational reality, and governance considerations, which are increasingly central to ocean management decisions.

This is a synthesis and perspective paper grounded in peer-reviewed literature, emerging offshore wind practice, and practitioner experience. Rather than presenting AI as a standalone solution, the paper reframes real-time species recognition as a screening and prioritization tool embedded within hybrid human-AI monitoring systems. By focusing on how AI outputs are interpreted, validated, and used, the paper moves the discussion beyond algorithm performance toward decision-relevant application.

It provides a practical framework for deploying AI-enabled monitoring in ways that enhance learning without undermining scientific or regulatory credibility. It helps practitioners and regulators distinguish between exploratory signals and evidence suitable for decision-making, reducing the risk of misinterpretation or over-claiming. More broadly, it supports the development of monitoring approaches that can keep pace with offshore renewable energy expansion while maintaining trust and ecological rigour.

About the author

Mariya Krestyanska Summerfield is an environmental consultant at WSP UK specializing in offshore wind consenting, marine biodiversity monitoring, and stakeholder engagement. Her work sits at the interface of marine ecology, environmental governance, and emerging monitoring technologies. She has extensive experience supporting offshore wind projects across the UK and Europe, including fisheries liaison, monitoring strategy design, and nature-inclusive design approaches. Her current interests include hybrid AI-human monitoring systems and how digital tools can be responsibly integrated into marine environmental management.

REAL-TIME ARTIFICIAL INTELLIGENCE SPECIES RECOGNITION FOR MARINE BIODIVERSITY MONITORING: A TRANSFORMATIVE APPROACH FOR OFFSHORE WIND MANAGEMENT

Mariya Krestyanska Summerfield
WSP UK, Bristol, UK
Corresponding author: mariya.summerfield@wsp.com
DOI: https://doi.org/10.48336/ZSVM-2Y98

ABSTRACT

The rapid global expansion of offshore wind is critical for meeting net-zero targets but presents distinct ecological management challenges. Effective biodiversity monitoring around marine renewable installations traditionally involves intermittent, costly methods with significant data gaps, limiting robust ecological assessments and adaptive management responses. Recent advancements in real-time Artificial Intelligence (AI) species recognition technology represent a transformational shift, providing continuous, high-resolution biodiversity data. This research highlights practical applications and validations of AI-driven underwater monitoring systems within offshore wind farms. Notably, initiatives such as The Rich North Sea Program (Netherlands) and RWE's SeaMe project have successfully implemented AI monitoring technologies, significantly enhancing our understanding of ecological interactions and biodiversity outcomes associated with marine structures. Canadian initiatives, including those by Ocean Networks Canada and Fundy Ocean Research Centre for Energy, further validate the role of AI monitoring in ecological understanding and adaptive management of marine renewable projects.

Real-time AI monitoring fosters unprecedented stakeholder engagement through live-streaming biodiversity data, creating transparency and enhancing public support and education, particularly within local communities and educational institutions. This approach is critical for generating social licence and community collaboration in marine renewable developments.

By harnessing the power of real-time AI monitoring, marine renewable projects substantially improve ecological outcomes, effectively meet regulatory demands, and authentically engage communities. This paper discusses the scalability of AI-driven monitoring solutions, integration into adaptive management frameworks, and their role in shaping policy and operational decisions within the offshore wind sector.

Keywords: AI species recognition, adaptive management, ecological impact, marine artificial structures, offshore wind, real-time biodiversity monitoring, stakeholder engagement

1. INTRODUCTION

Offshore wind is expanding at a pace and scale unprecedented in the marine environment. Across European, North American, and Asia-Pacific waters, projects are moving rapidly from single-site developments to large, multi-array offshore wind farms, often in ecologically complex and socially contested seascapes. This acceleration is driven by climate and energy security imperatives, yet it has also intensified scrutiny of offshore wind's environmental footprint, particularly in relation to biodiversity impacts, cumulative effects, and long-term ecosystem change. Regulators, developers, and stakeholders are increasingly required to demonstrate not only compliance with environmental conditions, but credible evidence that monitoring and management approaches are keeping pace with the operational realities of offshore infrastructure [1], [2].

Marine biodiversity monitoring has long relied on a combination of diver surveys, vessel-based observations, fisheries data, and periodic remote sensing. While these methods remain scientifically robust, they are constrained by cost, spatial coverage, temporal resolution, and human availability. As offshore wind arrays extend further offshore, into deeper waters, traditional monitoring approaches are increasingly stretched beyond their practical limits. Monitoring programs are often episodic rather than continuous, spatially restricted rather than system-wide, and slow to translate data into operational decision-making. This mismatch between the tempo of industrial activity and the tempo of ecological observation has become one of the defining challenges of contemporary marine environmental management [3], [4].

Recent advances in Artificial Intelligence (AI), particularly in computer vision and machine learning, have been proposed as a means to address this growing monitoring gap. In aquatic and marine sciences, AI-enabled approaches are increasingly applied to species identification and automated image analysis, with reviews highlighting substantial gains in processing speed and classification accuracy for visually detectable taxa compared to manual methods [5]. At the same time, studies focused on underwater imagery demonstrate that performance remains strongly constrained by environmental conditions such as turbidity, variable lighting, and imbalanced training datasets, particularly for rare or visually difficult-to-detect species [6].

Within the offshore wind sector, interest in real-time or near real-time AI-based monitoring has grown rapidly. Fixed and mobile camera systems, Autonomous Underwater Vehicles (AUVs), and Remotely Operated Vehicles (ROVs) increasingly generate volumes of visual data that far exceed the capacity of human analysts to process manually. Automated species recognition offers an apparent solution: continuous monitoring at scale, rapid detection of ecological signals, and the potential to inform adaptive management

measures within operational timeframes. However, conservation literature cautions that the use of AI in ecological monitoring carries risks of overconfidence, bias, and inappropriate application if deployed without sufficient oversight, particularly in complex ecological systems [7].

Crucially, the application of AI in marine monitoring is not a purely technical challenge. Decisions about what is monitored, how data are interpreted, and how outputs are used carry governance implications that extend beyond model performance. In offshore wind contexts, where monitoring data may inform licensing compliance, mitigation triggers, or stakeholder trust, the legitimacy of AI-derived evidence becomes as important as the accuracy of the underlying technology.

This paper sets out how real-time AI species recognition can support offshore wind biodiversity monitoring when embedded within ecological study design and human decision-making processes. Rather than replacing established methods or expert judgement, AI is positioned as a screening and prioritization tool that enhances human capacity while retaining expert oversight, consistent with emerging concepts of hybrid intelligence [8].

Drawing on peer-reviewed literature and emerging offshore practice, the paper examines how AI-enabled species recognition can contribute to more adaptive and transparent monitoring, while explicitly addressing technical constraints and uncertainty, and asking under what conditions real-time detection meaningfully improves ecological understanding, regulatory confidence, and environmental outcomes [7], [9].

2. THE MONITORING GAP IN OFFSHORE WIND

The rapid expansion of offshore wind has exposed structural limitations in how marine biodiversity is currently monitored, assessed, and governed. While monitoring requirements have increased in scope and ambition – driven by cumulative impact assessment, biodiversity policy, and stakeholder expectations – the underlying methods and delivery models have remained largely unchanged. This has created a widening gap between what monitoring is expected to achieve and what it can realistically deliver under existing paradigms [10], [11].

2.1 Temporal Mismatch: Episodic Surveys in Dynamic Systems

Marine ecosystems are inherently dynamic. Species distributions, behaviours, and interactions vary across daily, seasonal, and interannual timescales, and can respond rapidly to anthropogenic pressures such as noise, vessel activity, and habitat alteration. Conventional offshore monitoring programs, however, are typically structured around survey windows, often constrained to a small number of campaigns per year. These surveys provide valuable snapshots, but they may not capture short-term dynamics needed for adaptive management.

As a result, monitoring outputs are frequently retrospective. Data are collected, processed, quality-assured, and reported months after the ecological conditions of interest have occurred.

By the time evidence reaches regulators or project operators, opportunities for adaptive management – such as modifying operational timing or testing mitigation measures – have often passed. This temporal lag can limit the utility of traditional monitoring in fastmoving industrial contexts.

2.2 Spatial Constraints

Offshore wind farms occupy large spatial footprints, often spanning tens to hundreds of square kilometres. Yet monitoring effort within these areas is necessarily selective, constrained by vessel time, weather windows, and cost. Survey designs typically prioritize statistically representative sampling over comprehensive coverage, leaving substantial portions of project areas unobserved at any given time.

This uneven spatial coverage is particularly problematic when monitoring aims to detect rare events, low-abundance species, or localized ecological responses to infrastructure. For visually detectable taxa, such as demersal fish or mobile invertebrates, detection probability is strongly influenced by survey timing, visibility conditions, and observer effort. Studies in aquatic biology have repeatedly highlighted that nondetections should be interpreted cautiously.

2.3 Cost and Logistical Constraints

Marine surveys are resource intensive. Vessel day rates, specialist equipment, and the need for trained personnel limit how frequently monitoring can be undertaken. As offshore wind projects move further offshore and into more challenging environments, costs increase without necessarily delivering proportionate gains in ecological understanding. In practice, monitoring effort may change postconstruction, even as processes such as colonization, attraction, or displacement continue to develop [12].

The result is that monitoring data may be too infrequent or delayed to meaningfully inform management decisions. From a practitioner perspective, this raises practical questions about whether existing monitoring approaches remain appropriate for the scale and pace of offshore renewable energy development.

2.4 Monitoring as Evidence in Decision-making

Beyond its scientific role, biodiversity monitoring underpins how offshore wind projects are assessed, regulated, and discussed. Monitoring data are used to demonstrate compliance with licence conditions, inform regulatory decisions, and support engagement with fisheries stakeholders and the wider public. Where evidence is perceived as incomplete, outdated, or difficult to interpret, confidence in monitoring outcomes can be undermined, even where substantial effort has been invested [9], [13].

Research on marine governance highlights that monitoring systems shape how information is accessed, interpreted, and communicated, rather than functioning as neutral data pipelines [9]. In offshore wind contexts, this places emphasis on monitoring approaches that are transparent, interpretable, and proportionate to the decisions they are expected to inform.

3. REAL-TIME AI SPECIES RECOGNITION: TECHNICAL FOUNDATIONS AND CONSTRAINTS

Real-time AI species recognition refers to the application of machine learning models – most commonly deep learning-based computer vision – to detect and classify organisms in visual data streams as imagery is collected. In marine settings, this typically involves underwater cameras deployed on fixed infrastructure (such as turbine foundations or scour protection), mobile platforms including ROVs and AUVs, or hybrid systems combining visual sensors with acoustic or environmental metadata. The defining feature of real-time application is not automation alone, but the ability to move more quickly from observation to interpretation, allowing ecological signals to be identified within operationally relevant timeframes.

3.1 Core Technical Approach

Most AI-based species recognition systems are trained to identify organisms in images by learning recurring visual features such as shape, contrast, and movement. In aquatic biology, these approaches have been shown to work best for visually distinctive and frequently observed species, including many fish, crustaceans, and larger mobile fauna. Reviews of AI applications in aquatic biology show that automated classification can be useful in suitable conditions, particularly where large volumes of imagery need to be processed [5].

In offshore wind monitoring, the primary value of these systems lies in their ability to process continuous image streams that would be impractical to analyze manually. Automated detection provides an initial screening layer, allowing species presence or unusual activity to be flagged quickly and directing human effort to where it is most needed.

3.2 Environmental Constraints

Underwater imagery is highly sensitive to environmental conditions. Turbidity, suspended sediments, biofouling, variable light conditions, and camera orientation all influence image quality and, by extension, model performance. Even modest changes in these conditions can reduce detection probability or increase false positives. As a result, some species or size classes may be detected more readily than others, rather than reflecting true ecological patterns.

Training datasets are often dominated by common, easily observed species, while rarer or protected taxa are underrepresented. Automated detection may be less reliable for rare or visually cryptic species [5].

Performance can also vary between locations. Models trained in one area may not transfer well to different habitats or conditions, making site-specific testing and cautious interpretation essential in offshore wind monitoring.

3.3 Real-time Detection and Decision-making

For offshore wind practitioners, it is important to distinguish between real-time detection and decision-ready evidence. Automated outputs indicate possible presence, not confirmed ecological conclusions. Without context – such as monitoring effort, visibility conditions, or environmental variability – detections, and equally non-detections, can be misinterpreted.

Effective use of AI, therefore, relies on combining automation with expert review. Automated systems can screen large volumes of imagery and flag material of interest, but human expertise remains essential to verify detections, interpret ecological relevance, and judge whether evidence is sufficient to inform management or regulatory reporting [8]. Used in this way, AI improves efficiency and responsiveness without removing accountability or ecological understanding.

3.4 Implications for Offshore Wind Monitoring Design

For offshore wind practitioners, the technical foundations of AI species recognition bring both opportunity and responsibility. Continuous automated monitoring can greatly increase the amount of data collected and improve temporal coverage, but it also introduces new sources of uncertainty that need to be managed consciously. Choices about where and how cameras are deployed, what species the system is trained to recognize, how outputs are checked, and when results are reviewed all affect how reliable and useful AI-derived evidence will be.

Recognizing these constraints does not weaken the case for AI-enabled monitoring. On the contrary, it clarifies the conditions under which such systems add value. When deployed as part of a structured monitoring framework – rather than as a standalone technological solution – real-time AI species recognition can support more responsive, transparent, and informative biodiversity monitoring around offshore wind infrastructure. The following sections build on this foundation, examining how hybrid intelligence workflows, governance arrangements, and complementary tools are required to translate technical capability into credible environmental evidence.

4. HYBRID INTELLIGENCE

The practical value of real-time AI species recognition in offshore wind monitoring depends less on algorithmic sophistication than on how automated outputs are integrated into human decision-making. Environmental monitoring and decision-support literature cautions against fully automated approaches in complex ecological settings, emphasizing instead the value of hybrid systems in which automation supports, rather than replaces, expert interpretation and accountability [8].

4.1 Hybrid Intelligence in Marine Monitoring

Marine biodiversity monitoring presents conditions that favour combined human and automated approaches. Ecological signals are variable, detection depends on environmental conditions, and many species of regulatory concern are rare or difficult to identify visually. Automation performs well at scale and speed but is limited in contextual interpretation and accountability. Human expertise remains essential for assessing ecological significance, resolving uncertainty, and supporting defensible decisions.

Hybrid intelligence literature emphasizes allocating tasks according to these strengths: automated systems handle high-volume screening, while human experts retain responsibility for validation, interpretation, and action [8]. In offshore wind monitoring, this

positions AI as a screening and prioritization tool, rather than an autonomous decision-making system.

4.2 Hybrid Use, Uncertainty, and Interpretation

AI-enabled monitoring produces early signals that require validation and context before being used for management or regulatory purposes. In offshore wind monitoring, where outputs may influence compliance assessments or stakeholder confidence, it is important to distinguish clearly between exploratory observations and evidence that has been reviewed and interpreted.

Combining automation with expert review helps manage uncertainty rather than eliminate it. Automated outputs reflect limits in training data and environmental conditions, while human interpretation introduces judgement and potential bias. Being explicit about how outputs are reviewed and used allows projects to benefit from automation without overstating certainty or undermining credibility [8].

4.3 Implications for Offshore Wind Practitioners

For offshore wind developers and regulators, adopting hybrid intelligence approaches has practical implications for resourcing, governance, and expectations. Automation does not remove the need for human expertise; instead, roles shift toward validation and decision support, with associated cost and capacity considerations that need to be recognized early in project design.

At the same time, hybrid systems provide a pathway to scale monitoring without sacrificing credibility. By combining automated screening with expert oversight, projects can increase temporal coverage, respond more rapidly to emerging issues, and communicate evidence more transparently. In offshore wind contexts, hybrid intelligence should be understood as a deliberate design choice that reflects the realities of marine ecosystems and environmental governance, rather than a compromise between technology and expertise.

5. EVIDENCE FROM EMERGING OFFSHORE PRACTICE

The application of real-time or near real-time AI species recognition in offshore wind is no longer purely conceptual. While few projects yet rely on AI-derived outputs as primary decision-grade evidence, a growing number of monitoring programs are using automated image analysis to augment traditional surveys, increase temporal coverage, and improve situational awareness. These early applications provide important lessons about what AI-enabled monitoring can realistically deliver, and under what conditions it adds value.

5.1 Fixed Infrastructure and Continuous Observation

One of the most promising emerging applications of AI species recognition in offshore wind involves the use of fixed camera systems on turbine foundations, substations, and associated scour protection. These installations provide relatively stable viewpoints and long operational lifetimes, making them well suited to continuous or high-frequency observation where monitoring objectives justify it.

Across a small number of European offshore wind projects and research-led trials, fixed cameras have been used to document fish and invertebrate presence around foundations, offering insights into colonization and localized use of structures that are difficult to capture through periodic surveys alone. In most cases, analysis has relied primarily on manual review, reflecting both the exploratory nature of these deployments and the need for caution in interpreting results.

Where AI tools have been trialled alongside fixed camera systems, they have generally been framed as supporting data screening rather than automated reporting. In these cases, automated methods are used to identify imagery that may warrant further attention, while interpretation and reporting remain subject to expert review.

5.2 Mobile Platforms and Operational Monitoring

AI-enabled species recognition has also been explored on mobile platforms, including ROVs and AUVs used for inspection, maintenance, and environmental surveys. These platforms generate large volumes of video footage during routine operations, much of which has historically been underutilized for ecological analysis due to the effort required for manual review.

In offshore wind, interest has focused on whether automated screening could support opportunistic biodiversity monitoring from inspection footage, allowing ecological observations to be extracted without dedicated survey time. This approach remains limited in scope and is not yet widespread and has so far been explored primarily through research-led initiatives and the opportunistic use of inspection footage, including programs such as SeaMe.

Where considered, the appeal lies in closer alignment between engineering and environmental activities: inspections undertaken for asset integrity may also provide ecological insight, provided that data quality, metadata, and validation requirements are addressed. However, footage collected on mobile platforms varies substantially in camera angle, speed, lighting, and proximity to structures. This variability introduces additional uncertainty for automated detection and reinforces the need for cautious interpretation and expert review.

5.3 Regional Initiatives and Collaborative Programs

Beyond individual projects, there is growing interest in whether AI-enabled monitoring could support learning at broader spatial scales. In European waters, research consortia and offshore renewable energy test sites have begun to explore combinations of fixed sensors, automated analysis, and shared data approaches to better understand habitat use and potential cumulative effects. These efforts remain exploratory, reflecting recognition that single project monitoring is often insufficient to capture broader ecological patterns.

Practical examples of this approach are already emerging within European offshore wind. The Rich North Sea Programme in the Netherlands has applied long-term, camera-based ecological monitoring around offshore energy infrastructure to support learning on habitat use and ecological

function at program scale. Similarly, RWE's SeaMe initiative integrates underwater camera systems and digital monitoring tools across offshore wind assets to improve understanding of species-structure interactions and to inform adaptive environmental management. In both cases, AI-assisted analysis has been explored to support data screening and interpretation [14], [15].

Such initiatives highlight both the potential and the challenges of scaling AI-enabled monitoring. Shared datasets improve model training and benchmarking, but raise questions about data ownership, access, and standardization. Moreover, while regional analyses can reveal trends not apparent at site level, they also amplify the consequences of bias or error if validation is inconsistent. Early experience suggests that governance arrangements are as critical as technical capability in determining the success of these approaches.

5.4 What Practice Reveals about Limits

Across these emerging applications, several consistent limitations are evident. First, systems that perform well on fixed installations with stable conditions may struggle in turbid waters, during storm events, or on highly mobile platforms. Second, rare or cryptic species continue to require expert attention, limiting the extent to which automation can reduce human involvement. Third, the interpretive value of AI-derived indicators depends heavily on accompanying information about detection effort, environmental conditions, and system performance.

Practitioners also report a learning curve in organizational adoption. Integrating AI outputs into established monitoring and reporting workflows requires changes in roles, expectations, and quality assurance processes. Where these changes are not explicitly managed, AI risks being treated as an experimental add-on, rather than as a meaningful component of the monitoring system.

5.5 Lessons for Offshore Wind Monitoring

Taken together, emerging offshore practice suggests that real-time AI species recognition is most effective when deployed incrementally and transparently. Successful applications share several characteristics: clear articulation of what AI outputs are – and are not – used for; explicit separation between screening and decision-grade evidence; and early engagement with regulators and stakeholders to build understanding of methods and limits.

These lessons reinforce the argument that AI-enabled monitoring should be evaluated not solely on technical performance, but on its contribution to better environmental decision-making. In offshore wind, where monitoring serves scientific, regulatory, and social functions simultaneously, credibility depends on aligning automation with governance and expertise. The following section examines how these considerations intersect with ecological study design, and how AI-enabled systems can be integrated without undermining statistical robustness or interpretability.

6. INTEGRATING AI MONITORING WITH ECOLOGICAL STUDY DESIGN

The integration of AI-enabled species recognition into offshore wind monitoring does not remove the need for robust ecological

study design. On the contrary, the increase in data volume and temporal resolution intensifies the importance of clearly articulated hypotheses, sampling logic, and analytical frameworks. Without these foundations, AI risks amplifying noise rather than improving ecological insight. For practitioners, the challenge is, therefore, not whether AI can collect more data, but how those data are structured, interpreted, and linked to meaningful ecological questions.

6.1 AI as an Extension, not a Replacement, of Study Design

Established approaches to impact assessment in marine environments – such as Before-After-Control-Impact (BACI) and related beyond-BACI frameworks – remain relevant in AI-enabled monitoring contexts. These frameworks provide the logic needed to distinguish project-related effects from natural variability, a distinction that automation alone cannot achieve. Continuous observation does not inherently resolve issues of confounding, pseudo-replication, or baseline selection; these must still be addressed through design.

AI can, however, extend the practical application of such frameworks. High-frequency data allow practitioners to characterize baseline variability more comprehensively, explore temporal patterns at finer resolution, and test assumptions that would otherwise remain implicit. For example, continuous imagery can reveal whether short survey windows are representative of broader conditions, informing decisions about survey timing and effort.

6.2 Detection Probability and Effort Standardization

A central issue in integrating AI outputs into ecological analysis is detection probability. Automated species recognition does not observe organisms directly; it detects visual signals that are themselves influenced by environmental conditions, camera performance, and model characteristics. Changes in detection rates may, therefore, reflect shifts in visibility, fouling, or system configuration rather than ecological change.

To address this, AI-enabled monitoring programs must explicitly define and document unit effort. This may include camera uptime, field of view, lighting regime, and environmental context (e.g., turbidity or current strength). Detection metrics should be normalized against these factors wherever possible, allowing practitioners to distinguish true biological patterns from artifacts of observation. The aquatic AI literature consistently emphasizes that failure to account for detection bias can lead to misleading conclusions, regardless of analytical sophistication [5].

6.3 Indicator Selection and Ecological Relevance

The availability of large volumes of automated detections can tempt analysts to focus on easily quantifiable metrics rather than ecologically meaningful ones. Counts of detections, for example, may be influenced by repeated observations of the same individuals or by behavioural responses to infrastructure. Integrating AI monitoring into study design, therefore, requires careful consideration of what indicators are intended to represent.

In offshore wind contexts, useful indicators may include presence-absence over defined temporal windows, relative activity levels of functional groups, or colonization trajectories on nature-inclusive design features. Importantly, indicators should be specified a priori, linked to management or learning objectives, and interpreted cautiously. AI-derived metrics gain value when they are clearly tied to hypotheses about habitat use, attraction, or avoidance, rather than treated as descriptive outputs.

6.4 Baselines, Controls, and Comparability

AI-enabled monitoring can strengthen baseline characterization by extending observations over longer periods and across a wider range of conditions. However, baseline data are only meaningful if they are comparable to subsequent observations. Changes in camera hardware, software updates, or model retraining can introduce discontinuities that complicate temporal comparisons.

Practitioners must, therefore, manage change carefully. Where system modifications are unavoidable, overlapping datasets or calibration exercises should be used to assess comparability. Similarly, where control sites are employed, consistency in sensor configuration and analytical workflows is essential. These considerations are familiar from traditional monitoring, but their importance is magnified when automated systems are involved.

6.5 From Data to Inference

Integrating AI monitoring into ecological study design ultimately concerns inference: what conclusions can legitimately be drawn from the data. Continuous automated observation can improve sensitivity to change, but it does not remove uncertainty. Statistical analysis must still account for variability, autocorrelation, and imperfect detection. Hybrid intelligence approaches, in which expert judgement informs interpretation, remain essential for translating patterns into understanding.

For offshore wind practitioners, the implication is clear. AI-enabled monitoring can enhance study design by expanding observational capacity, but it cannot substitute for ecological reasoning. When embedded within well-defined analytical frameworks, AI outputs can support more nuanced and responsive assessments of ecological change. When divorced from such frameworks, they risk becoming data-rich but insight-poor. The following section, therefore, turns to governance and data stewardship, examining how design, interpretation, and accountability intersect in AI-enabled monitoring systems.

7. GOVERNANCE AND DATA STEWARDSHIP

As AI-enabled monitoring becomes more common in offshore wind, governance and data stewardship move from supporting considerations to core design issues. Monitoring data inform regulatory decisions, influence stakeholder confidence, and shape how environmental performance is understood. In this context, the value of AI-derived evidence depends not only on technical performance, but on how data are managed, interpreted, and used in practice.

7.1 Governance beyond Technical Performance

AI-based monitoring systems influence what is detected, prioritized, and reviewed. Choices around training data, confidence thresholds, and validation protocols affect which signals are visible and which are missed. Research on so-called "smart ocean" governance – the growing use of digital and automated technologies in marine monitoring and management – shows that, without clear roles and accountability, such systems can shift decision-making authority away from regulators and subject-matter experts toward technology providers or data owners [9].

In offshore wind monitoring, this matters once automated outputs start to influence compliance or management decisions. Governance arrangements should clearly set out who interprets AI outputs, how uncertainty is addressed, and who is responsible if results are misunderstood.

7.2 Data Ownership, Access, and Transparency

Offshore wind monitoring typically involves multiple actors, including developers, consultants, regulators, and technology providers. AI-enabled systems generate large datasets that raise practical questions around ownership, access, and reuse. Clear data stewardship arrangements are essential to avoid disputes and maintain confidence in monitoring outcomes.

Data management principles such as accessibility, consistency, and reusability are increasingly referenced in environmental monitoring, but must be applied pragmatically in commercial and regulatory settings [16]. In practice, this often means tiered access to raw data, processed outputs, and visual summaries, depending on purpose and audience. Where AI is involved, transparency around how data are processed and reviewed is particularly important.

7.3 Communicating Uncertainty

Automated monitoring outputs can appear precise, especially when presented through annotated imagery or summary metrics. However, they inevitably reflect assumptions, detection limits, and environmental variability. If uncertainty is not communicated clearly, outputs may be over-interpreted or misused.

For practitioners, this places responsibility on how results are presented. Distinguishing screening information from evidence used to support decisions, documenting validation steps, and explaining known limitations are all essential. Visual outputs can support engagement, but only when accompanied by clear explanation of what they do – and do not – show [7], [9].

7.4 Regulatory Engagement and Learning

Early engagement with regulators is one of the most effective governance measures. When monitoring approaches are discussed during design, rather than after data have been collected, there is greater scope for shared understanding and improvement over time. Experience from marine governance shows that confidence in new monitoring methods benefits from transparent evidence and stakeholder engagement [9].

In offshore wind contexts, AI-enabled monitoring is most effective when positioned

as a complementary tool that supports existing regulatory frameworks. Clear governance arrangements, transparent data handling, and accountable interpretation allow innovation to add value without undermining confidence in the monitoring process.

8. RISKS, LIMITS, AND RESPONSIBLE USE

Real-time AI species recognition can add value to offshore wind monitoring, but only if applied with care. The main risks are not technological failure, but misinterpretation, overconfidence, and inappropriate use of automated outputs in decision-making.

AI-derived observations can appear precise, particularly when visualized, yet they remain indicators rather than conclusions. Without context, detections – or absences – may be over-interpreted. Uneven performance across species further complicates interpretation, as automated systems tend to be least reliable for rarer or visually difficult-to-detect taxa, including those of regulatory importance.

Ultimately, AI-enabled monitoring is most effective when used as a complementary tool that supports expert assessment and learning. Applied correctly, it can strengthen evidence and responsiveness in offshore wind management.

9. CONCLUSION

Offshore wind development is entering a phase where expectations around environmental evidence are rising as quickly as installed capacity. Biodiversity monitoring is no longer judged solely on scientific adequacy, but on its ability to provide timely, credible, and interpretable information that supports regulatory confidence, operational decision-making, and stakeholder trust. Within this context, real-time AI species recognition offers a meaningful opportunity – but only if its role is clearly defined and responsibly governed.

This paper has shown that AI-enabled species recognition can address long-standing weaknesses in offshore wind monitoring, particularly gaps in temporal coverage and data processing capacity. Continuous visual observation, combined with automated screening, allows practitioners to move beyond episodic snapshots toward a more dynamic understanding of how organisms interact with offshore infrastructure. Used appropriately, this capability supports earlier detection of patterns, more responsive adaptive management, and improved learning about ecological responses around offshore structures.

The paper also sets out clear limits to what AI-based monitoring can and cannot do. AI outputs are sensitive to conditions and species characteristics. They do not constitute decision-grade evidence without validation, interpretation, and governance. The distinction between screening information and verified evidence is, therefore, central to maintaining credibility. Hybrid intelligence – where automation augments rather than replaces expert judgement – emerges as a practical and defensible model for offshore wind monitoring.

Equally important are the institutional dimensions of AI deployment. Data ownership, transparency, accountability, and

communication of uncertainty shape whether AI-enabled monitoring strengthens or undermines trust. Governance frameworks that treat AI as a socio-technical system, rather than a neutral tool, are essential if automated monitoring is to contribute positively to environmental management and social licence.

In conclusion, real-time AI species recognition should not be framed as a technological solution in search of a problem. Its value lies in how it is integrated into well-designed monitoring programs, aligned with ecological objectives, and embedded within clear governance structures. When applied with realism and restraint, AI can help offshore wind monitoring evolve from retrospective compliance toward adaptive, evidence-informed practice – supporting both biodiversity outcomes and the responsible delivery of offshore renewable energy.

ACKNOWLEDGEMENT

Author Declaration

- Funding: The author did not receive financial support from any organization for the submitted work.
- Ethical approval: This paper does not contain any studies with human participants or animals.
- Competing interests: The author declares no competing interests.
- Availability of data and materials: Datasets used and/or analyzed during the current study are available from the corresponding author upon reasonable request.
- Artificial intelligence: During the preparation of this work, the author used Microsoft Copilot to support drafting and formatting. After using this tool, the author reviewed and edited the content as needed and takes full responsibility for the content of the publication.

REFERENCES

[1] E. S. Brondízio et al., Global Assessment Report on Biodiversity and Ecosystem Services, Intergovernmental SciencePolicy Platform on Biodiversity and Ecosystem Services, Bonn, Germany, 2019. doi: 10.5281/zenodo.3831673.

[2] Convention on Biological Diversity, "Kunming-Montreal Global Biodiversity Framework," CBD/COP/15/L.25, Dec. 18, 2022. [Online]. Available: https://www.cbd.int/gbf

[3] M. Elliott, Marine science and management means tackling exogenic unmanaged pressures and endogenic managed pressures – A numbered guide, *Marine Pollution Bulletin*, vol. 62, no. 4, pp. 651–655, 2010. doi: 1016/j.marpolbul.2010.11.033.

[4] A. Borja et al., "Moving Toward an Agenda on Ocean Health and Human Health in Europe," *Frontiers in Marine Science*, vol. 7, art. 37, 2020. doi: 10.3389/fmars.2020.00037.

[5] K. Malde, N. O. Handegard, L. Eikvil, and A.-B. Salberg, "Machine intelligence and the data-driven future of marine science," ICES *Journal of Marine Science*, vol. 77, no. 4, pp. 1274–1285, 2020. doi: 10.1093/icesjms/fsz057.

[6] S. Villon et al., "A deep learning method for accurate and fast identification of coral reef fishes in underwater images," *Ecological Informatics*, vol. 48, pp. 238–244, 2018. doi: 1016/j.ecoinf.2018.09.007.

[7] S. A. Reynolds et al., "The potential for AI to revolutionize conservation: a horizon scan," *Trends in Ecology & Evolution*, 2024. Advance online publication. doi: 10.1016/j.tree.2024.11.013.

[8] D. Dellermann, P. Ebel, M. Söllner, and J. M. Leimeister, "Hybrid Intelligence," *Business and Information Systems Engineering*, vol. 61, no. 5, pp. 637–643, 2019. doi: 10.1007/s12599-019-00595-2.

[9] K. Bakker and M. Ritts, "Smart oceans: artificial intelligence and marine governance," *Earth System Governance*, vol. 13, 2022, art. 100141. doi: 10.1016/j.esg.2022.100141.

[10] European Commission, Guidance Document on Wind Energy Developments and EU Nature Legislation, Brussels, Belgium, Nov. 18, 2020. [Online]. Available at: https://op.europa.eu/en/

publication-detail/-/publication/2b08de80-5ad4-11eb-b59f-01aa75ed71a1
[11] The Crown Estate, Offshore Wind Evidence and Change Programme, 2021. [Online]. Available at: https://www.thecrownestate.co.uk/our-business/marine/offshore-wind-evidence-and-change-programme
[12] S. Degraer, R. Brabant, B. Rumes, and L. Vigin, (eds.), Environmental Impacts of Offshore Wind Farms in the Belgian Part of the North Sea: Attraction, avoidance and habitat use at various spatial scales. Memoirs on the Marine Environment. Brussels: Royal Belgian Institute of Natural Sciences, OD Natural Environment, Marine Ecology and Management, 104 pp., 2021. [Online]. Available: https://tethys.pnnl.gov/sites/default/files/publications/winmon_report_2021_final.pdf
[13] R. Kelly, A. Fleming, and G. T. Pecl, "Social licence for marine conservation science," *Frontiers in Marine Science*, vol. 5, 2018. doi: 10.3389/fmars.2018.00414.
[14] The Rich North Sea Programme, "Monitoring and ecological research." Accessed: Sep. 2025. Available at: https://www.therichnorthsea.com
[15] RWE Renewables, "SeaMe – Sustainable ecological monitoring." Accessed: Sep. 2025. Available at: https://www.rwe.com/en/the-group/sustainability/biodiversity/seame
[16] M. D. Wilkinson et al., "The FAIR Guiding Principles for scientific data management and stewardship," *Scientific Data*, vol. 3, 2016. doi: 10.1038/sdata.2016.18.

Metocean and Geotechnical Design

Dr. Freeman Ralph

Paul Stuckey

Dr. Mark Fuglem

Arijit Arghya

Offshore wind development

Who should read this paper?

This paper is intended for offshore wind developers and technical teams, including metocean and ice specialists, geotechnical, structural, and naval architectural engineers, and power performance modellers. The paper is also relevant to organizations involved in the planning, design, and approval of offshore wind projects in cold and ice-affected regions, including government stakeholders, energy boards and regulators, and certification authorities.

Why is it important?

This paper presents a regional assessment of the environmental inputs and the structural response of offshore wind turbine structures for Atlantic Canada, considering both fixed (monopile) and floating (semi-submersible) support structures. To the authors' best knowledge, this is the first published study to evaluate multiple turbine operating modes (production, idling, and parked) across a range of environmental conditions, including operational winds, extreme hurricanes, winter storms, sea ice, and varying seabed properties for Atlantic Canada. The study integrates coupled aero-hydro-servo-elastic simulations to compare nacelle accelerations, blade tip deflections, structural forces and moments, seabed shear and moments, icing accumulation, and preliminary mooring and anchoring considerations.

It provides an initial design basis and benchmarking reference for offshore wind development projects in Atlantic Canada; it is applicable to both fixed and floating platforms. The paper also highlights topics such as critical data availability issues and knowledge gaps, helping guide future measurement programs, modelling efforts, and risk-informed design studies. Further, it highlights some of the implications of intermediate water depths on the selection of fixed versus floating support structures.

About the authors

Dr. Freeman Ralph joined C-CORE in 1999 and is presently vice president of oceans and energy having over 25 years of offshore oil and gas and alternative energy expertise. He holds three degrees from Memorial University including a bachelor's degree in naval architecture and ocean engineering, a master's degree in ship ice interaction modelling, and a doctorate degree focused on ice mechanics, ship structures, and probabilistic design. His experience includes offshore structure and ship design; environment characterization and design basis, risk analysis and probabilistic methods including extreme event and risk mitigation modelling, icing occurrence, mitigation, and operations interruption; and design and protection of subsea infrastructure including geotechnical foundation and mooring considerations.

Paul Stuckey joined C-CORE in 2003 and is currently deputy director of ice and ocean engineering. He is a professional engineer with over 25 years of experience in ice and ocean engineering, leading studies in environmental characterization, design load estimation, environmental and ice-related downtime modelling, structural analysis, and the dynamic response of fixed and floating offshore wind turbines under combined wind, wave, and ice conditions. He has made significant contributions to major developments offshore eastern Canada, including Hebron,

West White Rose, and Bay du Nord, providing the clients with design basis support from concept selection stage through to detailed engineering.

Dr. Mark Fuglem is a principal consultant at C-CORE, with over 40 years of experience, including application of probabilistic methods to determine design loads on structures, extreme event analysis, optimization of offshore oil transportation systems, risk and reliability assessments and input on design codes, and estimation of environmental downtime for offshore operations, considering forecast uncertainty, weather windows and downstaffing by helicopter, walk-to-work, and frog. Recent work includes characterization and evaluation of wind and ice load effects on fixed and floating offshore wind turbine structures, and development of a 12-DOF impact load model for floating offshore wind turbines.

Gerry Piercey

Arijit Biswas Arghya holds a master of engineering and specializes in numerical modelling and geohazard analysis. He has experience in slope stability and seepage analysis, debris-flow runout modelling, pipe-soil interaction, and offshore anchoring and foundation design under complex loading conditions. At C-CORE, he has supported major offshore and onshore projects through geotechnical characterization, geohazard analysis, finite element modelling of various anchors and buried pipelines, and development of GIS-based landslide risk maps for industry partners. He also contributes to C-CORE's experimental systems and data-driven modelling efforts, applying his programming skills to enhance the integration of field, laboratory, and numerical data for advanced geotechnical problem-solving. His master's research at Memorial University focused on debris-flow runout simulation using empirical and continuum approaches to improve geohazard prediction.

Dr. Ian Turnbull

Gerry Piercey's background is mechanical engineering, systems engineering, centrifuge modelling, and project management engineer with bachelor's and master's degrees in mechanical engineering. Working as the team lead, he manages the C-CORE laboratory and large-scale geotechnical centrifuge. His experience also includes the design, manufacturing, and commissioning of unique field equipment and unique project focused experimental equipment and the execution of the experiments for a variety of industries and projects. He has executed a wide range of centrifuge experimental projects including suction caisson performance, suction embedded and flexibility embedded plate anchors in different loading conditions, frost heave of buried pipelines, surface loading of buried pipelines, and ice soil pipe interaction studies.

Dr. Ahmed Derradji-Aouat

Dr. Ian Turnbull is a senior scientist at C-CORE with a PhD in geophysics. He has over 15 years of experience in ice and metocean environmental characterization analysis and model development. He has led projects on offshore ice and metocean characterization for development of risk-based decision support databases and has experience in modelling ice accretion on offshore structures including wind turbines.

Dr. Ahmed Derradji-Aouat works with the National Research Council of Canada (NRC) in St. John's, NL, Canada. He performs numerical simulations using advanced multi-physics software and conducts experimental work using the NRC ice tank and other large open water wave tanks. In recent years, he focused his technical work on offshore wind energy projects and uses his numerical models to predict the environmental loads (including ice loads for ice covered waters) on offshore wind turbines. The experimental tank testing work provides data to verify and validate the numerical models and simulations.

OFFSHORE WIND DEVELOPMENT IN ATLANTIC CANADA: REGIONAL METOCEAN AND GEOTECHNICAL DESIGN CONSIDERATION AND OPPORTUNITIES

Freeman Ralph[1*], Paul Stuckey[1], Mark Fuglem[1], Arijit Arghya[1], Gerry Piercey[1], Ian Turnbull[1], Ahmed Derradji-Aouat[2]

[1]C-CORE, St. John's, NL, Canada

[2]National Research Council of Canada, St. John's, NL, Canada

**Corresponding author: freeman.ralph@c-core.ca*

DOI: https://doi.org/10.48336/NHP0-M641

ABSTRACT

Offshore Atlantic Canada has enormous potential for developing wind farms given the strong winds in the region and experience developing offshore oil and gas facilities. Depending on the specific location, there can be hurricanes, strong winter storms, sea ice, icebergs, and icing conditions. Other considerations include the varying water depths, seabed soil conditions, distances to shore, and port and electricity infrastructure. The electricity demand also varies between the four provinces.

Wind turbine structures are designed to be relatively light. As a result, environmental loads can result in significant non-linear effects with coupling between the turbine and supporting structure responses, and susceptibility to fatigue. The choice of structure type will be critical. A significant part of the region is at water depths that are intermediary between those ideal for fixed and floating structures.

The present work provides an overview of the conditions across the region and specific challenges and information gaps. It builds on previous studies of the applicable standards, such as IEC 61400-3-1 and -2, the variation of wind conditions over the region, the relative severities of hurricanes versus winter storms, and the potential for sea ice and iceberg impact loads on floating and monopile support structures. Example OpenFAST analyses are presented for monopile and semi-submersible systems to demonstrate the potential influence of soil conditions on the structural response of the monopile and mooring and anchoring considerations for the semi-submersible. The risk of icing and potential downtime is assessed.

Keywords: Offshore wind, Atlantic Canada, metocean, hurricanes, winter storms, icing, geotechnical, moorings, downtime

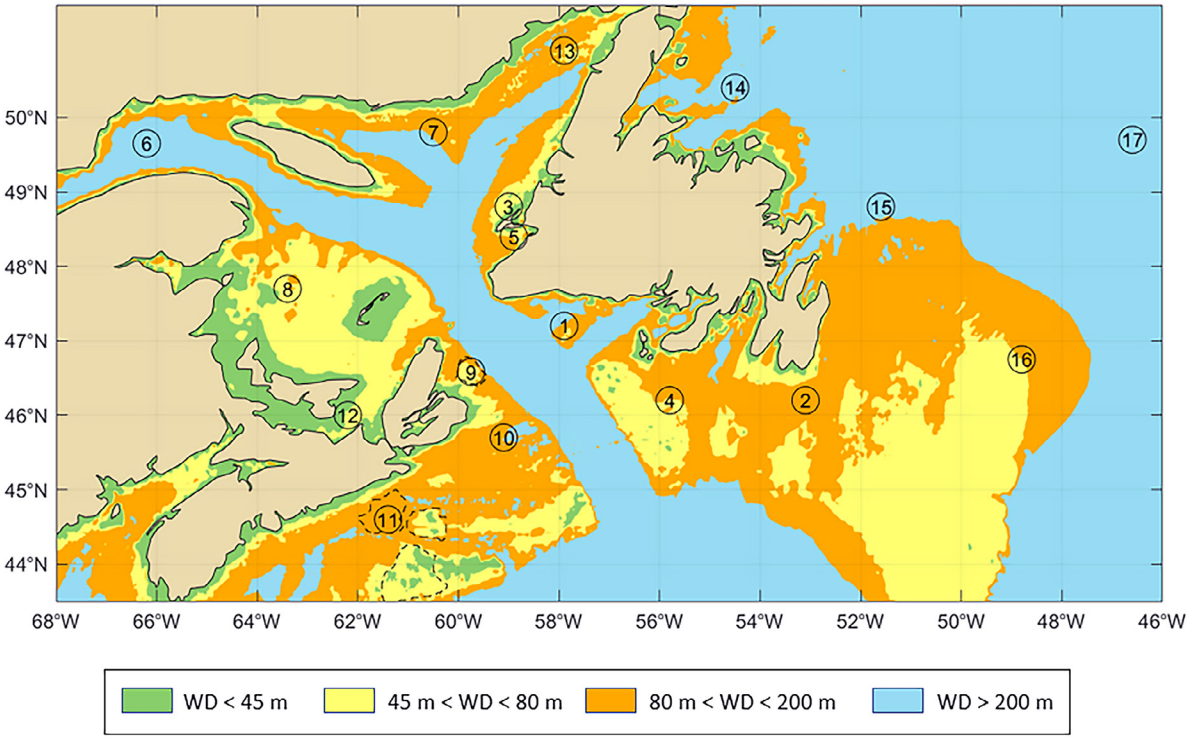

Figure 1: Region of interest showing key water depth ranges and example sites; based on [1].

1. INTRODUCTION

Atlantic Canada has substantial energy potential having strong offshore winds and large areas with suitable water depths for bottom-founded or floating wind turbines. The region of consideration is shown in Figure 1, with 17 locations identified to characterize the ice and metocean conditions [1].

Environmental parameters are provided for the sites to highlight differences in conditions that could influence the installation of wind farms. Important metocean parameters include average and extreme winds, currents, waves, sea ice, icebergs, visibility, and parameters related to potential icing. Water depth and soil conditions strongly influence the choice of viable platforms; the green, yellow and orange areas correspond to water depths less than 45 m, 80 m, and 200 m, respectively.

Designing Offshore Wind Turbines (OWTs) for Atlantic Canada requires comprehensive evaluation of extreme aerodynamic, hydrodynamic, and ice-induced loads, particularly under parked mode conditions when turbines are idling or shut down during severe weather. While wind and wave effects are well studied, the presence of sea ice introduces additional complexities due to limited environmental data and modelling challenges related to ice-structure interaction.

This paper presents numerical simulations of environmental loads on a 15 MW OWT operating in production and parked modes subjected to wind, wave, current, and ice loads. Building on a prior regional assessment of 17 potential offshore wind sites in Atlantic Canada [1], this study focuses on offshore turbines situated in two water depths: 45 m and 150 m. The 45 m water is

representative of shallow water conditions in regions such as offshore western Newfoundland (e.g., Site 3 in Figure 1). This location is within the range suitable for monopile foundations. The second location has a water depth of 150 m, representative of conditions for a floating foundation such as a semi-submersible.

The simulations utilize OpenFAST, a widely used, open-source aero-hydro-servo-elastic simulation tool, to capture coupled turbine and environmental interactions. Several IEC 61400 Design Load Cases (DLCs) specific to the production and parked design situations were selected to examine the responses of the turbine and the platform to typical production loads and extreme loads such as that from hurricanes. This approach enables a comprehensive assessment of how environmental factors differ in impact between ice and non-ice seasons and the combined loading effects on critical turbine components including the tower, substructure, and nacelle.

The results emphasize important design considerations unique to Atlantic Canada and identify significant gaps in environmental data especially related to sea ice thickness and dynamics. These findings support the development of more robust design and operational strategies to harness offshore wind energy safely and efficiently in cold-climate regions.

2. RELEVANT STANDARDS

The development and design of OWTs are governed by a combination of national regulations, international standards, certification practices, and, in some cases, classification requirements. The International Electrotechnical Commission (IEC) and DNV publish standards that define the principal technical requirements for offshore wind farms, while referencing International Organization for Standardization (ISO) standards for more general offshore design and operational considerations. In parallel, certification bodies and classification societies such as DNV, ABS, Bureau Veritas, and Lloyd's Register publish guidelines for fixed and floating offshore wind structures. These generally align with the design situations and load cases defined in the IEC standards, but may introduce additional requirements related to certification, classing, inspection, and life cycle assurance.

IEC 61400-3-1 (fixed OWTs) and IEC 61400-3-2 (floating OWTs) address design for the offshore environment, including wind, waves, and ice for structures such as monopiles, jackets, spars, semi-submersibles, and Tension-Leg Platforms (TLP). A set of defined design situations (including power production, fault conditions, start-up, shutdown, parked, and transport conditions) is combined with prescribed DLCs involving wind, wave, current, and water level conditions. These load cases are evaluated for ultimate and fatigue limit states using partial safety factors that distinguish between normal and abnormal conditions.

OWTs are highly non-linear systems due to the interaction between aerodynamic loading, turbine control systems, structural dynamics, and hydrodynamics. As a result, compliance

with DLCs requires coupled time-domain simulations using stochastic environmental inputs. Key response parameters include structural forces and moments, nacelle accelerations, blade deflections, and, for floating systems, platform motions and mooring line tensions. Fatigue damage accumulation is a critical design consideration, particularly for moorings, weld details, and dynamic electrical cables.

In Canada, the Canadian Standards Association (CSA) is accredited by the Standards Council of Canada to develop and maintain national standards. CAN/CSA C61400-3 was adopted from IEC 61400-3:2009 with Canadian deviations. Following the division of IEC 61400-3 into separate fixed and floating standards, CSA is in the process of adopting IEC 61400-3-1 with Canadian deviations, while a decision on adoption of IEC 61400-3-2 has not yet been made. As a result, floating offshore wind projects in Canada may rely directly on IEC or DNV standards, subject to regulatory acceptance.

Several proposed Canadian deviations to IEC 61400-3-1 relate to ice loading, reflecting the significant regional variability in ice conditions offshore eastern Canada. In many areas, ice advects into the region rather than forming locally, and the characteristics of ice features and interaction mechanisms can differ substantially from those assumed in generic offshore wind guidance. It has, therefore, been suggested that ice loads be determined using ISO 19906, which provides a more comprehensive framework for ice-structure interaction across a wider range of metocean and ice conditions. Direct calculation of ice loads, rather than reliance on level-ice thickness alone, may also better capture local effects, including non-horizontal loading components.

DNV offshore wind standards, including DNV-ST-0126 for fixed structures and DNV-ST-0119 for floating structures, define design situations and load cases broadly consistent with IEC, but differ in load calculation methods, safety factors, and treatment of regional conditions. DNV standards also address accidental loads such as vessel collision and dropped objects, and provide detailed guidance on ice crushing, bending, splitting, and ridge loading. Compared to IEC, the ISO 19900-series standards employ higher return periods and explicitly define abnormal limit states for manned hydrocarbon facilities; OWTs, being unmanned and without hydrocarbon storage, generally adopt less stringent criteria.

Beyond regulatory compliance, project developers may elect to pursue either certification alone or full classification. Certification demonstrates compliance with applicable standards at the design and construction stages, whereas classification typically includes ongoing inspection and verification throughout the operational life of the structure. Insurers and lenders often view classification as reducing project risk, particularly for floating wind turbines and novel structural concepts, and this can influence the choice of standards and conformity assessment route. These considerations are particularly relevant in eastern Canada, where offshore wind development must address large variations in

Table 1: Structure types and depth ranges.

Structure	Depth Range (m)	Comments
Fixed		
Gravity based	5 to 50	• Costs increase significantly with water depth and associated increased overturning moments due to waves. • Need a well-prepared and sufficiently solid base.
Steel Monopile	5 to 70	• Most common support structure for offshore wind turbines. • Higher range for extra-large monopiles, but these have increased weight and cost.
Jacket	5 to 100	• Simple, conventional gravity based offshore support structure.
Guyed Monopile/Truss	Up to 150	• Simple, single column. • Light weight, small footprint.
Articulated Wind Column	70 to 250	• Novel, no guyed wires. • Single footprint; no anchors.
Floating		
Spar	Greater than 100 m	• Spars typically have drafts in the range of 80 to 120 m and so require greater water depth.
Semi-submersible	50 to 500	• Wide range of structure types consisting of cylinders, columns, and pontoons. • Conventional spread mooring systems.
Tension-Leg Platform	Greater than 40 m	• Needs very strong vertical anchoring.

water depth, soil conditions, ice regimes, and infrastructure constraints, and where experience with offshore wind remains limited.

Offshore substations are generally treated as intermittently manned installations and are, therefore, subject to more stringent safety requirements than turbine support structures. While IEC 61400-3-1 and -3-2 provide a wind-specific framework, substations are typically designed using offshore platform standards such as ISO 19900 series, together with classification society rules. This introduces explicit consideration of accidental and abnormal limit states, higher environmental return periods, and additional load cases such as vessel impact and fire. These requirements become particularly influential for floating substations and for developments in ice-prone waters.

3. STRUCTURES

There are a number of different support structures available for OWTs, ranging from fixed-bottom concepts to different floating solutions. Table 1 provides a summary of the different types of support structures, the associated water depth range, and some general comments. Monopiles work well in water depths up to approximately 45 m, provided soil conditions are sufficiently stiff, while jacket structures extend the feasibility of bottom-founded structures up to 100 m water depth but with increased cost and installation complexity. Beyond 100 m depth, floating concepts, such as semi-submersibles, spars and TLPs, are suitable due to their broad depth. Spar platforms typically require greater water depth due to their large draft. Floating concepts typically require three or four mooring lines. Mooring system layouts can become quite complex for larger

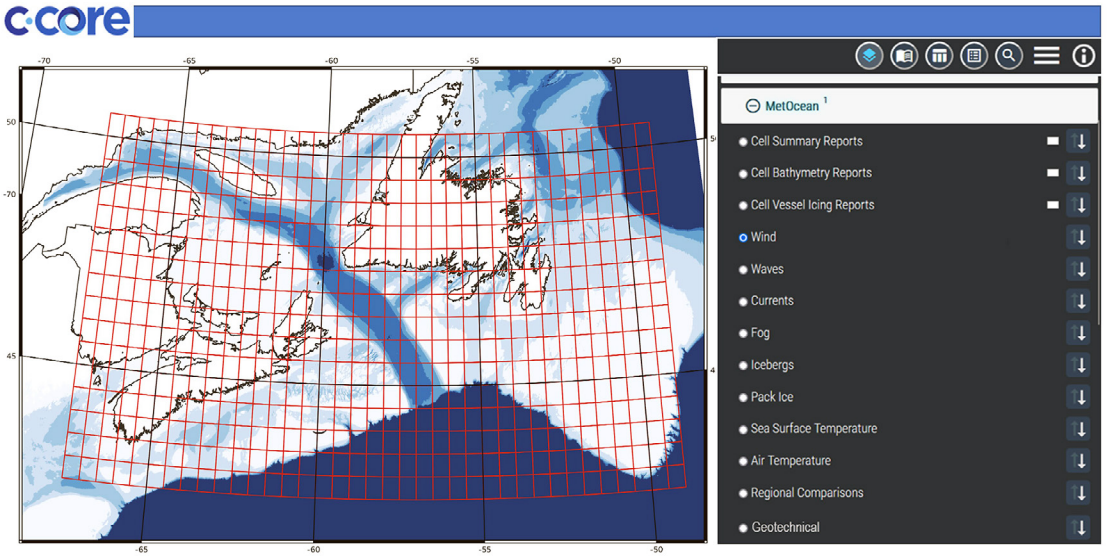

Figure 2: Atlantic Canada Wind Development Database.

wind farms and the idea of shared anchors to reduced costs and environmental footprint has been considered. TLPs require vertical anchoring that may be challenging in glacial soils. There are several new novel concepts that bridge the gap between monopiles and semi-submersibles, including the Entrion Fully Restrained Platform Monopile [2], the OSI Renewables FTLP Wind Platform [3], and the AWC Tech Articulated Wind Column [4]. The overlap in water depth ranges highlights that support structure selection in Atlantic Canada is governed not only by water depth, but also by soil stiffness, environmental loading, and installation constraints. As a result, comparing monopile and semi-submersible concepts at similar turbine ratings provides a meaningful assessment of structural response across the fixed-to-floating transition that is highly relevant for regional offshore wind development.

4. METOCEAN AND ICE CONDITIONS

4.1 Overview

Atlantic Canada offshore region is characterized by varying metocean and ice conditions. To support developments, C-CORE is building an ice, metocean, environmental, and geotechnical design focused database for Atlantic Canada to assist in enabling wind energy development. The regional coverage of the database and the included parameters are shown in Figure 2. The database will provide detailed statistics on historical metocean and ice conditions for a range of variables within defined grid cells over the region of interest. The database is modelled after Insight (https://insight.oilconl.com/ReportViz/Index), which is an ice and metocean database for offshore Newfoundland and Labrador developed for OilCo. The new database will offer onshore and offshore wind developers an initial planning tool to de-risk Atlantic Canada by providing information needed to make design and investment decisions on where to develop wind farms that optimize design and power generation and minimize downtime and maintenance costs. A listing of the datasets and corresponding qualifiers is given in Table 2.

Table 2: Data sources in wind development database for Atlantic Canada.

Data Source	Qualifier
Wind: ERA5	Re-analysis dataset from the European Centre for Medium-Range Weather Forecasts providing hourly, gridded hindcast wind data on land and ocean from 1940s to present.
Waves: MSC50 dataset	Hindcast wind and wave dataset for offshore Canadian waters developed by Oceanweather Inc. for Meteorological Services of Canada, Environment and Climate Change Canada. Contains either hourly or three-hour recordings of wind and wave values for 68 years from 1954 to 2021, measured in m/s at a height of 10 metres above mean sea level.
Current: Hybrid Coordinate Ocean Model (HYCOM)	The HYCOM database covers a temporal range of 22 years from January 1994 to December 2015 and provides ocean current velocity components, u and v, in eastward and northward directions, respectively with a spatial resolution of 1/12° × 1/12° and temporal resolution of three hours.
Fog: North American Regional Reanalysis (NARR) hindcast model	Fog occurrence estimated using the horizontal visibility data. The visibility data in NARR are available at a 0.3° (approximately 32 km) spatial resolution and at a three-hourly temporal frequency. Available data covers the period from January 1979 to August 2021.
Sea Surface Temperature: ERA5 Reanalysis data	Data available from 1979 to present having a 0.25° (approximately 28 km) spatial resolution, and a one-hourly temporal resolution.
Air Temperature: ERA5 Reanalysis data	Data available from 1979 to present at 2 m height and having a 0.25° (approximately 28 km) spatial resolution, and a one-hourly temporal resolution.
Sea Ice: Canadian Ice Service (CIS)	Data within the CIS archives are available in two formats: weekly regional charts and daily charts, depending on location and year.
Icing: physics-based model	Calculated using the following inputs from given sources: sea surface temperature (ERA5 dataset), 10 m height wind speed (ERA5 dataset), 2 m height air temperature (ERA5 dataset), sea ice concentration (ERA5 dataset), precipitation type (ERA5 dataset), and sea surface salinity (Copernicus Marine Environment Monitoring Service dataset).
Bathymetry: General Bathymetric Chart of the Oceans	A global 30 arc-second grid largely generated by combining quality-controlled ship depth soundings with interpolation between sounding points guided by satellite-derived gravity data.

Fuglem et al. [1] describe the characterization of wind, waves, currents, and sea ice conditions for the 17 locations shown in Figure 1. In that study, wind speed and significant wave height date were taken from the MSC50 [5]. Ocean current data were extracted from the Global Ocean Physics Analysis and the Hybrid Coordinate Ocean Model (HYCOM). Sea ice data were extracted from the Canadian Ice Service daily and weekly sea ice charts.

4.2 Estimating Icing Accretion and Corresponding Downtime

Wind turbine icing can impede power

generation efficiency by altering the aerodynamic profile of the blades, damage turbine blades in extreme ice build-up scenarios, and can present hazards to personnel in their vicinity due to ice falling off the turbine blades. For floating OWTs, ice build-up can additionally create balance issues. The rate of ice build-up due to super-cooled sea spray freezing on contact with the turbines is a function of the air and sea surface temperatures, the wind speed, and the saltwater freezing point (e.g., see [6]). When precipitation icing occurs, the rate of ice accretion on turbine blades is a function of the wind speed, the liquid water content of the precipitation, the mean droplet size, the fraction of the precipitation that freezes, and the efficiency with which the turbine blades collect the freezing precipitation. In the present work, the rate of precipitation icing on wind turbines is not modelled as an explicit function of air temperature, as it occurs only due to freezing rain or wet snow when air temperatures are typically 0-3°C (e.g., see [7]).

Icing was modelled on a wind turbine at Site 10. Hourly data were acquired from the ERA5 global reanalysis (see [8]) for wind velocity, 2 m air and sea surface temperature, sea ice concentration, and precipitation type for 2003-2024 (22 years). An icing event was defined by a minimum threshold of 0.7 cm per hour of ice accretion on a turbine blade, which is the minimum icing rate for "moderate" icing according to [6], [9], [10]. Figure 3 shows the distribution, cumulative probability, and exceedance probabilities for icing event total accretions modelled for a wind turbine blade in the 6 o'clock position at 50 m above the sea surface. At this height, the blade tip reaches within the sea spray icing zone, which is assumed to extend to 60 m height [11], with sea spray icing rate decreasing exponentially with height. Ice accretion due to precipitation can occur anywhere on the turbine structure. Figure 4 shows the distribution of icing event durations in hours (with a Weibull curve fit), which is assumed to correspond with operational downtime. Over 2003-2024, an average of around 10 icing events per year were modelled (Figure 3 and Figure 4).

The extreme values of the total icing event accretion thicknesses for each section of the turbine structure were determined for the 1, 5, 10, 50, and 100-year return periods (see Table 3). First, the annual maximum icing event accretion was determined for each year. The probabilities (P_R) for each return period, R, were calculated according to:

$$P_R = 1 - \frac{1}{R} \quad (1)$$

where extreme values for each return period were then determined from an inverse Weibull cumulative distribution function.

The results in Figure 3, Figure 4, and Table 3 show that icing is not severe at Site 10, with 50% of events lasting less than two days with ice accretion less than 2 cm on the blade tip in the sea spray zone. In this region, icing prevention and mitigation methods such as using hydrophobic paint on the blades may reduce icing downtime further.

5. GEOTECHNICAL CONSIDERATIONS

As noted earlier, the Atlantic Canada Region has considerable geotechnical variability

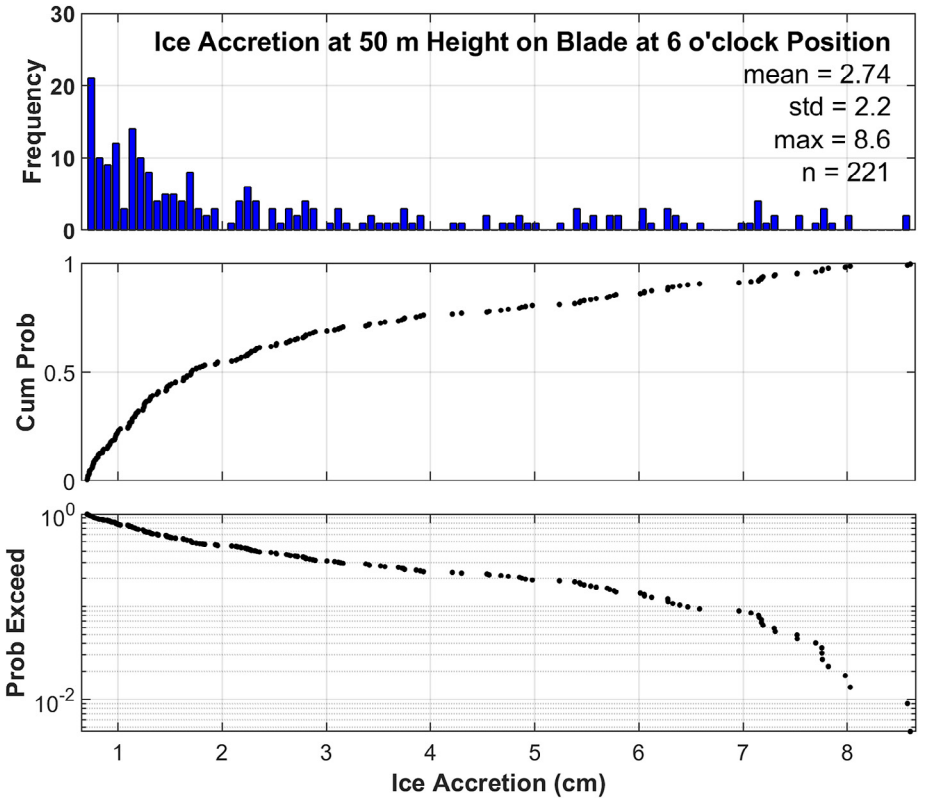

Figure 3: Modelled icing event total accretion.

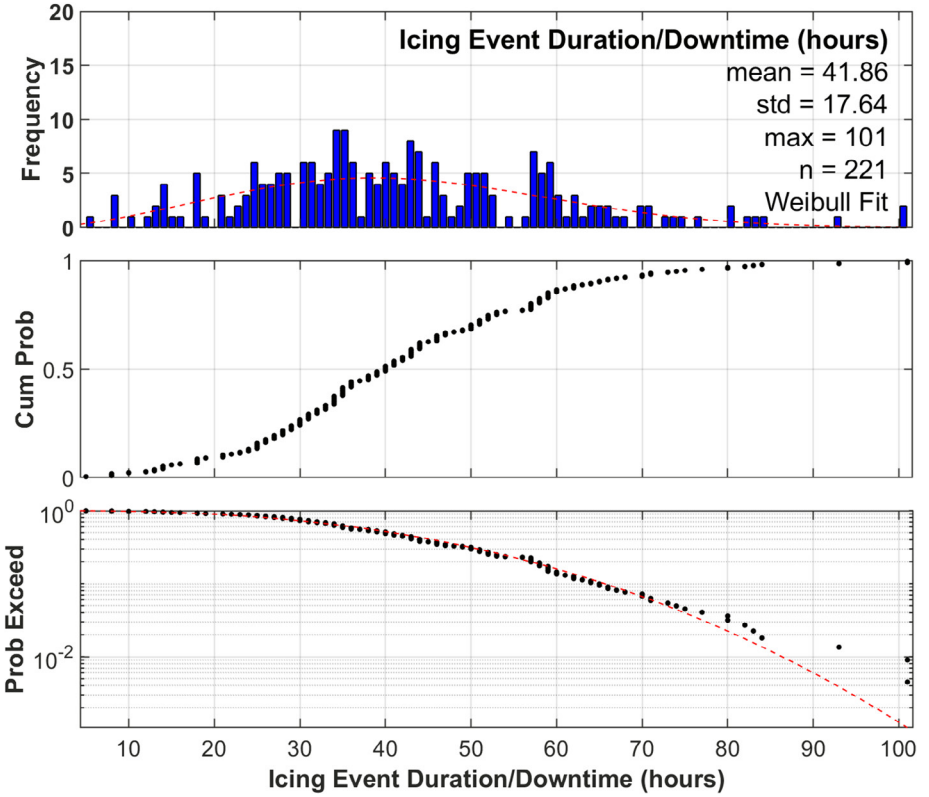

Figure 4: Modelled icing event operational downtime.

Table 3: Estimated icing event downtime (hours) by return period.

	Extreme Value Return Period (Years)				
	1	**5**	**10**	**50**	**100**
Downtime Hours	0	86	91	100	103

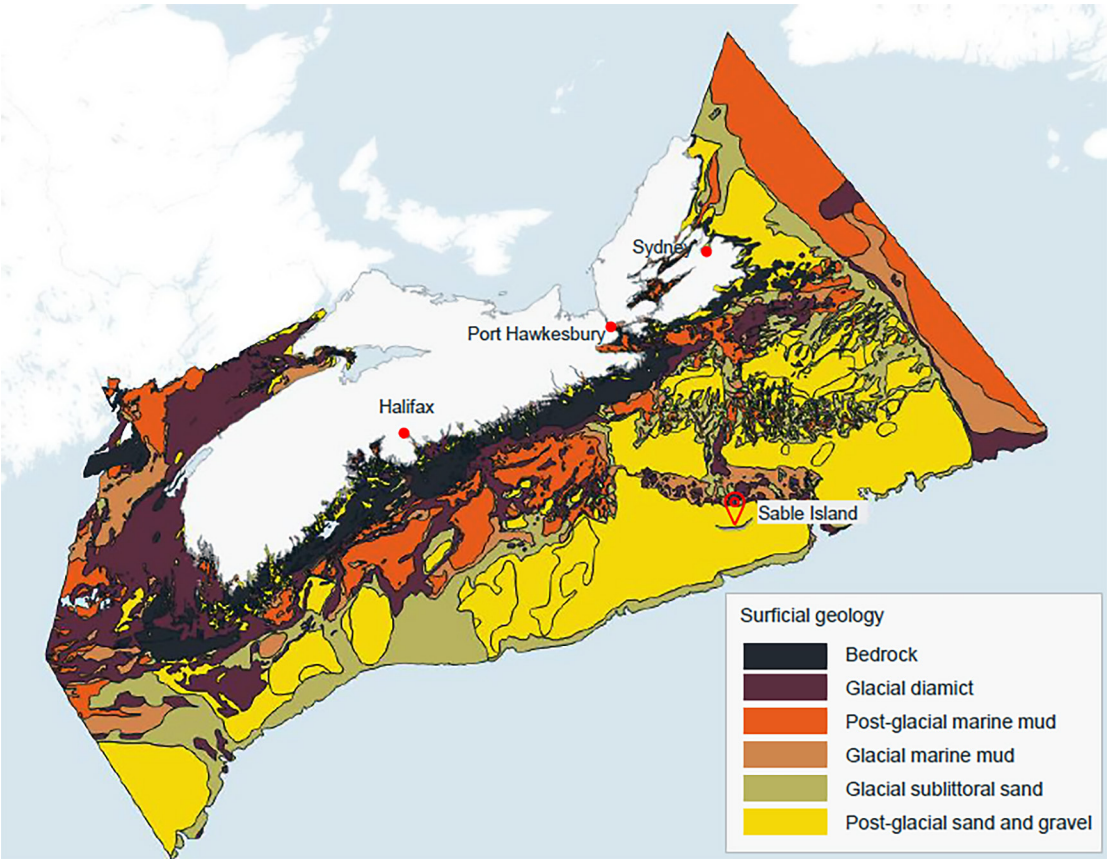

Figure 5: Surficial geology of the Scotian Shelf Bioregion; offshore Nova Scotia and New Brunswick, Canada; [13] after [14].

including post-glacial sand and gravel, glaciomarine mud, post-glacial marine mud, glacial till, and bedrock as illustrated in Figure 5. Offshore wind development areas lie within a region mapped as post-glacial sand or gravel, which is the same surficial geological unit that characterizes Sable Island. Borehole logs from the Sable Island area [12] illustrate this geological unit as being dominated by granular material, fine to medium sand, and sand-gravel mixtures with limited fines. This geological unit occurs across the region, and its thickness depends on location. On the outer banks, post glacial sand and gravel forms thick deposits (>20 m), whereas on the inner shelf, it appears as thin surface layers (<1 m) or patchy deeper accumulation (>10 m). The surficial geological maps provide confidence in the material type, a granular cohesionless sand-gravel mixture, but do not indicate how thick this unit is. Therefore, site-specific Cone Penetration Test (CPT) or borehole data are required for development.

The typical characteristics of post-glacial sand or gravel are consistent with the behaviour of dense sand. Post glacial sand and gravel are generally described as well drained, non-cohesive, and frictional, with unit weights on the order of 15.7 to 19.6 kN/m³ and friction angles ranging from 36° to 45°. Material of this kind allows for efficient pile installation, as they provide predictable drivability and reduced risk of premature refusal compared with cohesive or variable seabeds. Once installed, monopiles embedded in such soils exhibit high lateral stiffness and reliable resistance to cyclic loading, owing to the frictional nature of the sand-gravel matrix and its tendency to mobilize strong passive resistance under lateral displacement. Taken together, these geological characteristics suggest that the selected region offers favourable geotechnical conditions for monopile foundations.

In contrast, post-glacial marine muds typically exhibit very low undrained shear strength (approximately 1-6 kPa), resulting in low lateral resistance and excessive lateral displacements for large diameter monopiles [12]. These deposits are, therefore, generally unsuitable for monopile foundations. Consequently, monopile feasibility on the Atlantic shelf is governed primarily by local soil conditions, with post-glacial sand and gravel representing the preferred founding material.

5.1 Soil-Pile Modelling

Given the dominance of post-glacial sand and gravel within the selected offshore wind energy area, lateral soil-pile interaction for the monopile foundation was characterized using the sand p-y method described in API RP 2GEO. This methodology is widely adopted for representing the non-linear lateral resistance of cohesionless soils and provides a consistent basis for feasibility-level analyses using representative soil parameters. In this formulation, the soil reaction at any depth is governed by an ultimate lateral resistance dependent on depth, effective unit weight, and friction angle. The resulting non-linear cyclic p-y curves for dense sand are shown in Figure 6.

5.2 Linearization of p-y Curves for Dynamic Soil-Structure Interaction Analysis

The cyclic p-y curves were converted into an equivalent linear soil-structure interaction representation for use in OpenFAST. As OpenFAST requires the foundation to be defined through a linear stiffness matrix at the mudline, the cyclic p-y relationships were linearized using a secant stiffness evaluated at a small reference displacement equal to 1% of the pile diameter. The resulting depth-dependent stiffness profile was applied to a beam-on-elastic-foundation model of the embedded monopile and subsequently condensed to obtain an equivalent 6×6 foundation stiffness matrix. This approach is widely used to represent monopile foundations in dynamic OWT analyses [15], [16].

5.3 Mooring Considerations for Varying Soil Types

For floating structures, mooring system performance in different soil types need consideration and verification. Table 4 highlights mooring types, soil preference, load resistance orientation, and qualifying comments. As highlighted above, soil conditions and depth vary considerably across

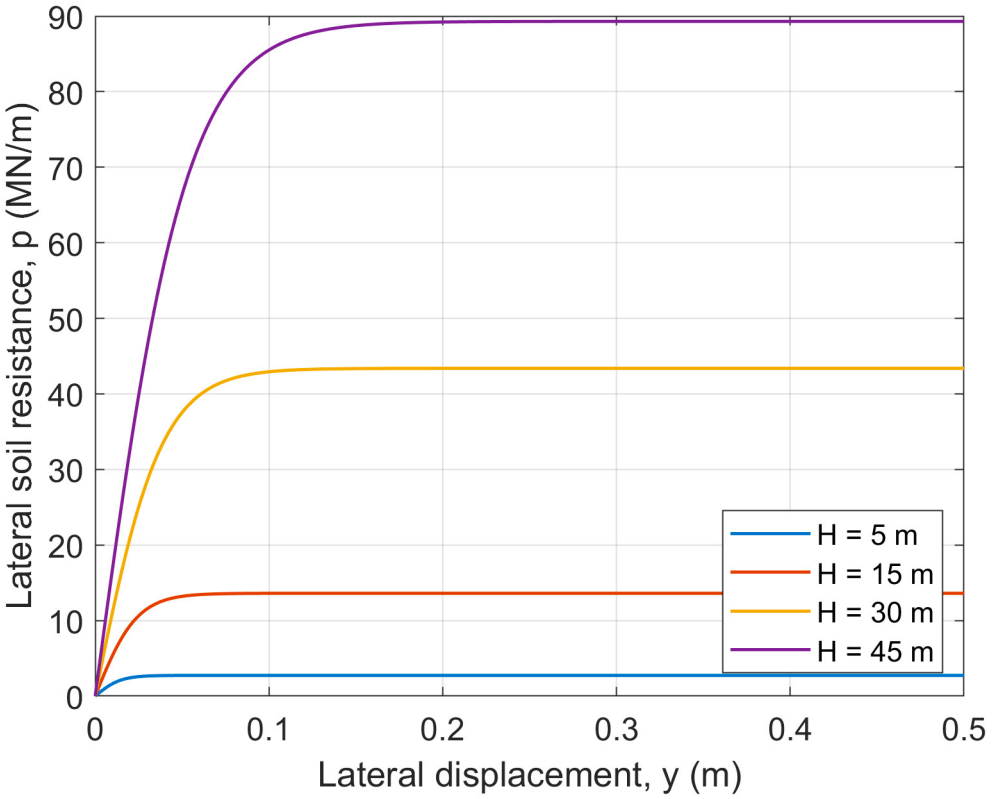

Figure 6: Cyclic p-y curves for monopile in dense sand.

Table 4: List of anchor types and applicability.

Anchor type	Soil preference	Typical load orientation	Comments
Drag embedment anchor	Soft to medium sand, silt	Primarily horizontal	Simple, inexpensive; high horizontal capacity; vertical capacity low.
Vertically loaded anchor	Soft clay, silt, some sand	Vertical (and horizontal)	Can be installed with suction caisson; good vertical capacity; resists horizontal loads.
Suction caisson	Soft clay, silty clay	Both vertical and horizontal	Excellent vertical capacity; height greater than width; installation requires specialized vessel.
Suction bucket	Soft clay or mud	Horizontal	Excellent horizontal capacity; width greater than height; simpler installation than suction caisson.
Driven pile anchor	Soft to medium clay, sand, silt	Both horizontal and vertical	Fast installation in suitable soils; well-understood capacity; limited in hard soils or rock; moderate cost.
Drilled and grouted pile anchor	Stiff clay, sand, gravel, rock	Both horizontal and vertical	Applicable in hard soils; high capacity; slow and expensive installation; specialized rig required.
Gravity base anchor	Any	Horizontal and vertical	Relies on weight of structure; requires flat seabed; heavy in deep water; installation cost high.

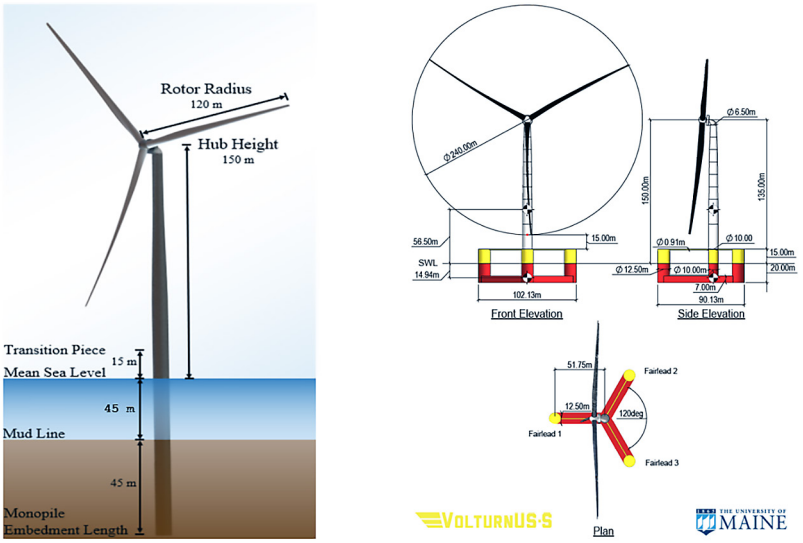

(a) IEA Wind 15-Megawatt Offshore Reference Wind Turbine (b) UMaine VolturnUS-S Reference Platform

Figure 7: Monopile and semi-submersible platforms analyzed in this study.

the region. Depending on the spatial arrangement and size of a farm, different mooring systems may be required, or systems that can perform in different conditions may be more desirable. This highlights the importance of good geotechnical data across a development region.

6. EXAMPLE APPLICATION

6.1 Approach

OpenFAST is used to evaluate multiple DLCs defining production and parked design situations for two 15 MW OWTs (one with a monopile foundation and the other supported by a semi-submersible platform). The simulations are conducted using OpenFAST v3.5.3, an open-source, coupled aero-hydro-servo-elastic analysis tool developed and maintained by the US National Renewable Energy Laboratory (NREL) [17]. Atmospheric turbulence is represented using wind fields generated with TurbSim, NREL's stochastic wind field simulator [18]. Together, these tools provide a comprehensive framework for assessing the dynamic response of OWTs subjected to combined environmental loading, including wind, wave, and ice effects.

The wind turbine model is based on the IEA Wind TCP 15 MW reference turbine, classified as IEC 61400-3-1 Class IB (Figure 7, left). The turbine has a rotor diameter of 240 m and a hub height of 150 m. Two distinct support structures are considered. The first is a 10 m-diameter monopile installed in 45 m water depth; additional details of the monopile model are provided in [19]. The monopile is assumed to be rigid at the mudline.

The second is the UMaine VolturnUS-S semi-submersible platform, a concrete-based floating foundation developed by the University of Maine's Advanced Structures and Composites Center [20] (Figure 7, right). Both support structures are coupled to the same IEA Wind TCP 15 MW reference turbine.

Table 5: Summary of OpenFAST cases.

Case No.	Description	Design Situation	DLC	Ws (m/s)	Hs (m)	Tp (s)	Current Speed (m/s)	Ice Thick (m)	Ref Ice Str. (MPa)	Monopile base at mudline
1	Monopile; production	Production	1.1	15	2.22	7.05	0.37	N/A	N/A	Rigid
2		Production	1.1	10	1.25	5.54	0.37	N/A	N/A	Rigid
3		Production	1.1	20	3.34	8.30	0.37	N/A	N/A	Rigid
4	Monopile; production, with level ice	Production	1.1	15	N/A	N/A	0.37	1	1	Rigid
5		Production	1.1	15	N/A	N/A	0.37	0.5	1	Rigid
6		Production	1.1	15	N/A	N/A	0.37	1.5	1	Rigid
7	Monopile; production, accounting for soil stiffness	Production	1.1	15	2.22	7.05	0.37	N/A	N/A	Flexible
8		Production	1.1	15	1.25	5.54	0.37	N/A	N/A	Flexible
9		Production	1.1	15	1.25	5.54	0.37	N/A	N/A	Flexible
9.1		Production	1.1	15	1.25	5.54	0.37	N/A	N/A	Flexible
10	Monopile; parked mode* and hurricane check	Parked/stand.	6.1	43	9.1	12.3	0.67	N/A	N/A	Rigid
11		Parked/Idling	6.1	43	6.7	10.3	0.67	N/A	N/A	Rigid
12		Parked/stand.	I1	55	10.3	12	0.67	N/A	N/A	Rigid
13		Parked/Idling	I1	55	10.3	12	0.67	N/A	N/A	Rigid
101	Semi; production	Production	1.1	15	2.22	7.05	0.37	N/A	N/A	N/A
102		Production	1.1	10	1.25	5.54	0.37	N/A	N/A	N/A
103		Production	1.1	20	3.34	8.30	0.37	N/A	N/A	N/A

*Two parked modes are considered in accordance with IEC 61400 series: (1) idling (parked with blades free to rotate, typically not producing power), and (2) standstill (parked with the rotor locked or secured in position).

In total, 17 simulation cases are defined for analysis in OpenFAST: 14 cases for the monopile and three cases for the semi-submersible platform. Cases 1 to 3 represent production mode at wind speeds of 10, 15, and 20 m/s. Cases 4 to 6 introduce ice loads from level ice using the IceFloe module (see [21] for details). Cases 7 to 9.1 consider varying soil strength and account for a flexible monopile. In Cases 10 and 11, the monopile is in a parked condition under a 50-year wind speed, while Cases 12 and 13 represent hurricane conditions with 500-year wind speeds. Cases 1 to 3 and 10 to 13 are also repeated for a semi-submersible platform. A complete summary of all cases is provided in Table 5.

6.2 Monopile Results

Fourteen OpenFAST simulations were performed for the wind turbine supported by the monopile foundation situated in 45 m water depth. As recommended in the IEC 61400 series, multiple simulations with unique random seeds are run for 600 seconds to capture the relevant stochastic variability of wind and wave loading. Here, only one simulation has been done for each case for expediency. Table 6 provides 90th percentile values for a selection of OpenFAST output parameters. Note these results do not include the normal/abnormal partial safety factors described in the IEC 64100 series.

For the monopile production (Cases 1-3), increasing wind speed from 10 to 20 m/s increases aerodynamic and structural loading, with both fore-aft and lateral nacelle accelerations increasing slightly, and tower top

Table 6: Summary of 90th percentile output parameters from OpenFAST simulations.

No.	Ice, Fx	Nac. Accel.		Rot. Thrust	TwTip Disp.	Tower Base				Mudline			
		X	Y			Fx	Fy	Mx	My	Fx	Fy	Mx	My
	MN	m/s^2	m/s^2	MN	(m)	MN	MN	MN·m	MN·m	MN	MN	MN·m	MN·m
1	N/A	0.15	0.25	2.69	1.49	2.54	0.13	32.4	275	3.15	0.60	46.3	424
2	N/A	0.21	0.31	1.77	0.81	1.69	0.18	48.9	156	3.04	0.63	65.9	276
3	N/A	0.25	0.37	1.42	0.57	1.41	0.17	54.0	114	3.40	0.77	77.6	228
5	2.86	0.18	0.30	1.77	0.88	1.69	0.15	41.7	154	4.64	0.74	61.8	356
4	4.84	0.21	0.30	1.78	0.97	1.77	0.19	41.2	158	6.69	0.95	68.0	441
6	6.86	0.26	0.31	1.78	1.06	1.87	0.23	41.1	162	8.81	1.19	76.5	531
7	N/A	0.20	0.30	1.78	0.81	1.70	0.16	45.2	157	3.03	0.62	62.1	274
8	N/A	0.20	0.30	1.78	0.81	1.70	0.16	45.2	157	3.03	0.62	62.1	274
9	N/A	0.20	0.30	1.78	0.81	1.70	0.16	45.2	157	3.03	0.62	62.1	274
9.1	N/A	0.46	0.37	1.82	1.71	1.98	0.27	67.6	196	3.56	1.30	84.2	283
10	N/A	0.81	0.35	0.56	0.57	1.63	0.39	61.4	113	6.45	0.83	87.0	294
11	N/A	0.88	0.28	0.57	0.64	1.72	0.32	38.5	125	6.47	0.54	60.7	310
12	N/A	1.02	0.23	0.62	0.78	1.90	0.26	48.5	146	7.26	0.59	66.4	355
13	N/A	1.03	0.19	0.62	0.78	1.91	0.22	25.0	147	7.26	0.38	38.4	353

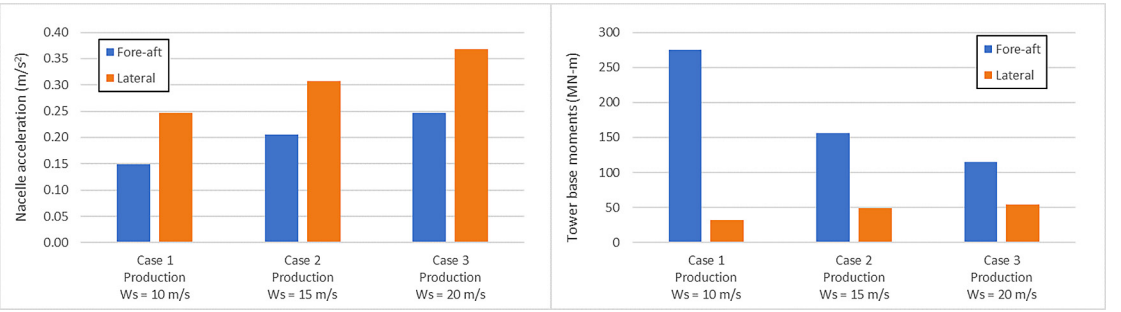

Figure 8: Nacelle acceleration and tower base moments for production cases.

fore-aft displacements decreasing (see Figure 8 and Table 6). Fore-aft tower-top motion and fore-aft loads decrease with wind speed due to blade pitch regulation by the controller.

When operating in production mode, the structure benefits from strong aerodynamic damping, which results in relatively low nacelle accelerations and tower motions. When the turbine transitions to parked conditions at higher wind speeds (Cases 10-13), the structural response changes, as the aero-dynamic damping is reduced or eliminated (Figure 9). Fore-aft nacelle accelerations increase significantly relative to production, reaching about 0.8-1.0 m/s², though these accelerations are less than the 0.3 G upper limit that is sometimes referenced. Lateral accelerations remain lower and comparable. Even under extreme winds and hurricanes, idling operation provides a small amount of aerodynamic damping to noticeably reduce lateral tower base and mudline loads compared with full standstill; fore-aft moments remain similar.

Introducing stochastic ice loads (Cases 4, 5, and 6) increases the fore-aft structural loading of the structure (see Figure 10). Fore-aft nacelle accelerations, tower top displacement, and tower base shear forces increase slightly compared to the equivalent production case (Case 1). Loads at the mudline show a more

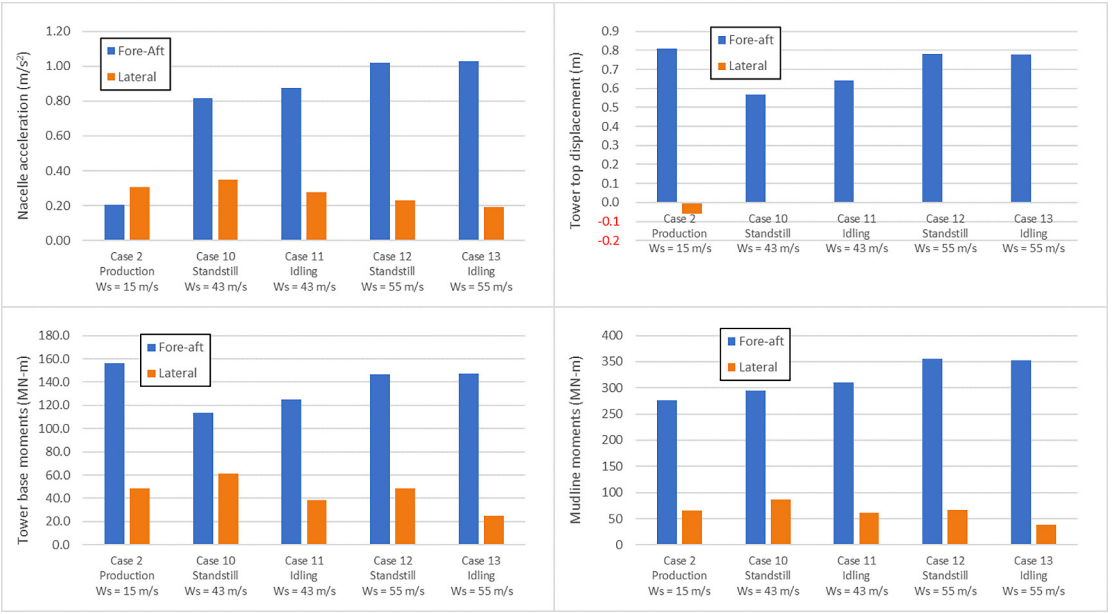

Figure 9: Comparison of production, idling, and standstill cases.

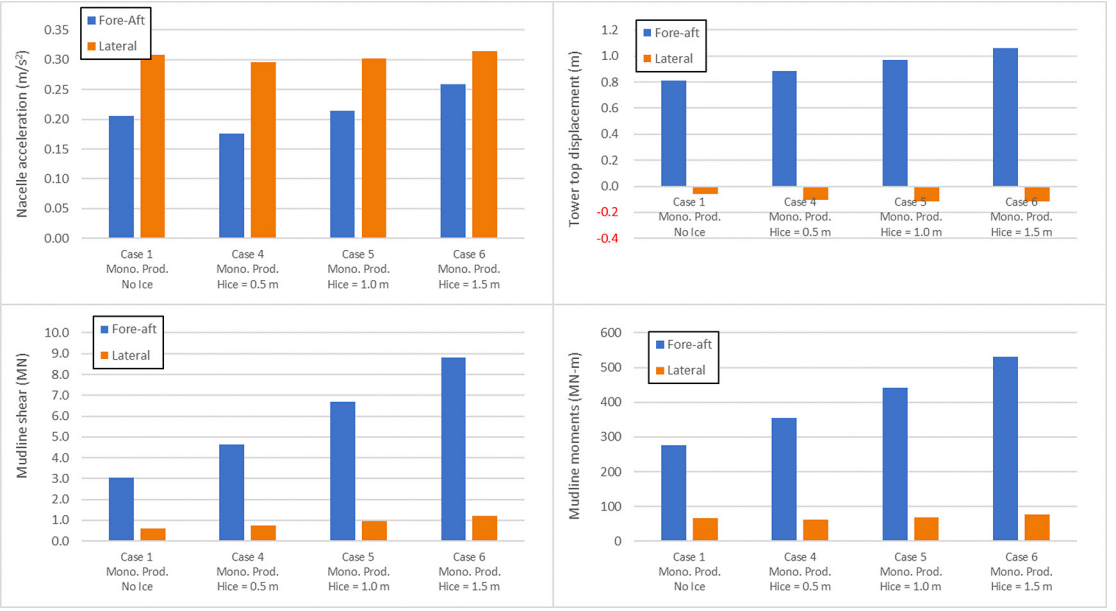

Figure 10: Comparison of different ice loads (thicknesses) for the monopile.

significant increase, especially in the fore-aft direction where loads for the case with the thickest (but less frequently observed) ice are nearly doubled those of the non-ice case. Overall, ice loading increases both tower-top motions and mudline loads, highlighting its effect on monopile structural response. In design, a probabilistic assessment of ice loads is needed to accurately capture the effects of the thickest, though least likely, ice interactions, and the effects of misaligned wind and ice directions.

In a previous study assessing a wind turbine supported by a monopile foundation [21], it

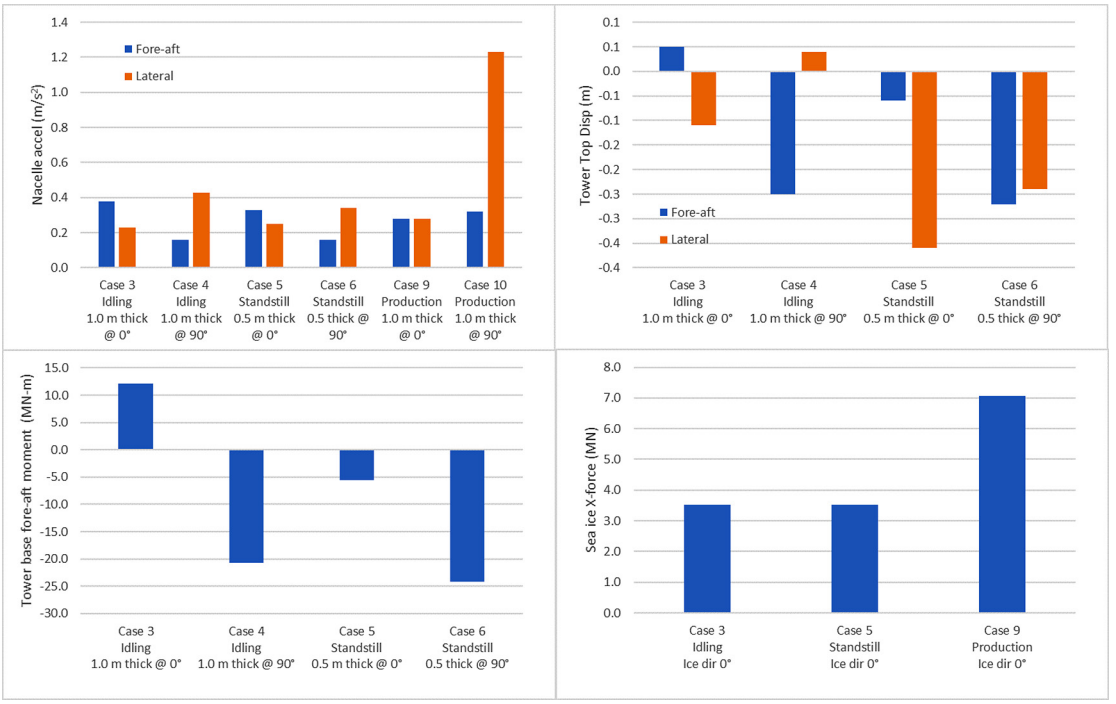

Figure 11: Comparison of sea ice results from [21]. Note the definition and numbering of cases in this table are based on Table 5 in [21] and are provided here to illustrate how ice drift direction impacts turbine response.

was shown that, for the parked cases, lateral ice loading, compared to inline ice loading, produced significant damping effects on fore-aft mudline moments and nacelle accelerations (see Figure 11). Tower base moments are considerably higher when ice moves at 90° relative to wind, as there is no aerodynamic damping. Further, nacelle accelerations are largest for production case when ice moves at 90° relative to the wind and damping on vibrations associated with random ice crushing is the smallest. Coupling these with a softer (vs. rigid) seabed will introduce different damping effects that will further influence forces, moments, and nacelle accelerations, which should be studied further. Different ice load models may need to be considered for the cases of ice-induced vibration and sloped structures.

For the monopile, soil stiffness will influence the structural response as illustrated in Figure 12. The equivalent 6×6 foundation stiffness matrix developed in Section 5.2 was based on post-glacial sand and gravel and, when introduced to the OpenFAST simulation, resulted in no changes to output parameters. Sensitivity cases, where the stiffness values were scaled by factors of 2 and 0.5, also showed no difference when compared to the base case stiffness results. One thought is that the base case stiffness matrix was very high (approaching "rigid" responses) and that factoring by 0.5 still resulted in a very high stiffness. Further, reducing the stiffness by a factor of 100 (Case 9.1) resulted in noticeable increases in tower motions and mudline shear forces. Nacelle accelerations increased significantly, with smaller increases in the tower top motions and mudline shear. This sensitivity analysis underscores the importance of collecting in-situ soil data and developing accurate modelling inputs.

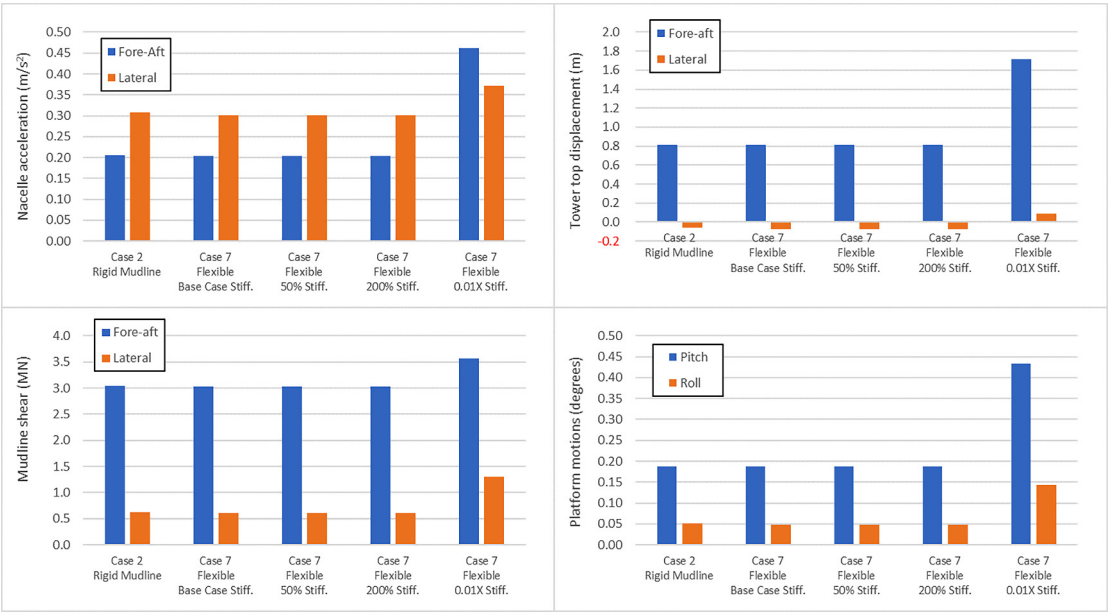

Figure 12: Comparison of various soil stiffness models for the monopile.

Table 7: Summary of 90th percentile output parameters from OpenFAST simulations.

No.	Nac. Accel		Rot Thr.	TwTip Disp.	Tower Base				Mooring Line 1		Platform	
	X	Y			Fx	Fy	Mx	My	Fair. Ten.	Anch. Ten.	Pitch	Roll
	m/s²	m/s²	MN	(m)	MN	MN	MN·m	MN·m	MN	MN	Deg.	Deg.
101	0.25	0.07	2.55	13.6	4.01	75.9	51.2	370	8.8	8.0	4.41	0.66
102	0.23	0.08	1.95	10.0	2.96	2.83	62.4	260	8.4	7.6	3.19	0.79
103	0.29	0.15	1.51	7.30	2.30	31.4	81.8	193	8.2	7.4	2.32	1.03

6.3 Semi-submersible Results

6.3.1 OpenFAST Results

Three production cases are analysed for the semi-submersible platform and 90th percentile values for a selection of parameters are presented in Table 7.

Structural loads and platform responses are notably different for the semi-submersible compared to the monopile; refer to Figure 13. The semi-submersible reduces lateral nacelle accelerations but has larger global motions, including a tower top displacement of about 7 to 14 m; fore-aft accelerations remain comparable. For the monopile, lateral nacelle accelerations are higher, while tower-top displacements remain relatively small, indicating high stiffness for the fixed monopile. With the much higher tower motions, the fore-aft tower base shear and moments for the semi-submersible are much higher compared to the monopile.

6.3.2 Sea Ice Loads

For this study, an analysis of sea ice loads on the semi-submersible was not carried out but should be in subsequent studies as the additional dynamics and damping effects from sea ice will influence structural forces and moments, mooring tensions, platform motions, blade deflections, and nacelle accelerations.

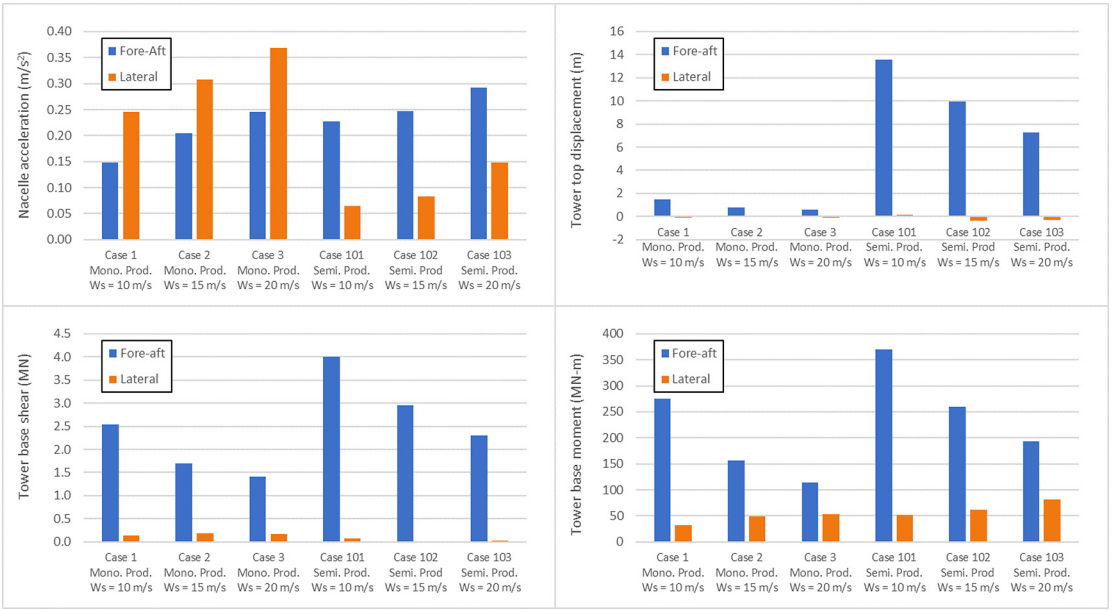

Figure 13: Comparison of tower motions and loading for the monopile and the semi-submersible.

The interaction of floes with a flexible moored structure introduces added complexity where pack ice floe diameter, ice driving forces, ice failure forces and dynamics, as well as mooring stiffness (and flexibility) all need to be considered. As wind, waves, and currents push an ice floe, tension increases in the mooring until the force at which ice failure can occur on the structure is reached. Then the floater will crush forward into the floe. This distance is limited and continues until tension drops, the force to fail the ice drops, and only driving forces remain. This cyclic process continues until the floe has moved past the platform. Two important items are noted. The IEC standard requires 600 seconds of simulation to verify whether lock-in frequencies occur, which will be limited by cyclic process noted above. Also, the diameter of floes further to the south will continually reduce as higher average water temperatures weaken the ice and wave action breaks them up, limiting the amount of distance available for floe crushing (and dynamics) to occur. Coupled with low annual occurrence in most areas, exposure will be reduced, further mitigating sea ice effects.

6.3.3 FEPLA Anchoring System

In this study, a Flexible Embedded Plate Anchor (FEPLA) was considered as a mooring option in dense sand. This included physical verification testing of the capacity of a 7.6 × 3 m FEPLA (see Figure 14) at different depths. This was part of a centrifuge-based demonstration test studying the performance of a FEPLA under different embedment depths.

Suction Embedded Plate Anchors (SEPLA) have been proven for application in soft clays with the advantages being relatively low cost and having a high installation positioning accuracy. As the offshore wind industry continues to expand, there is a growing need for the evolution of mooring designs to

Figure 14: Illustration of plate anchor and the Acteon Flexible Embedded Plate Anchor (FEPLA) system.

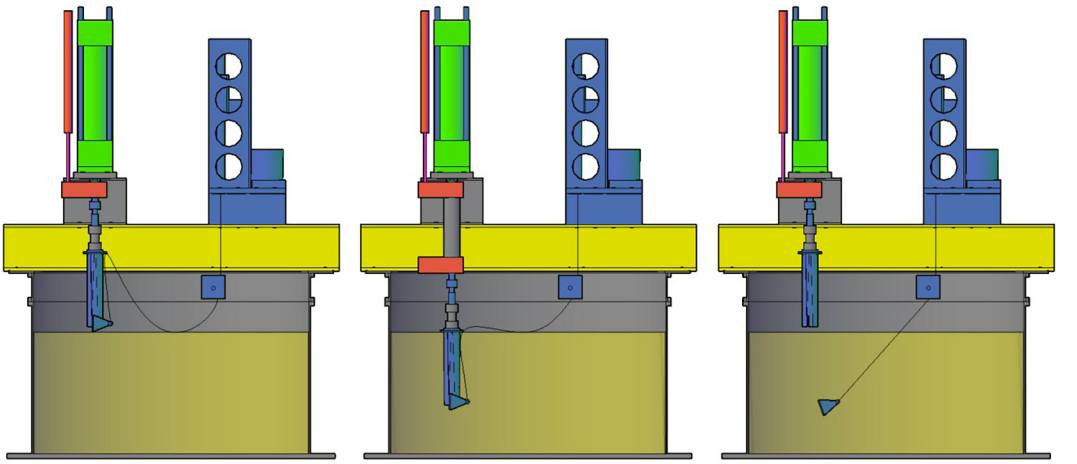

Figure 15: Illustration of centrifuge testing of the Acteon Flexible Embedded Plate Anchor (FEPLA) including installation and pulling.

provide even more effective, accurate, and cost-efficient alternatives. The FEPLA offers several advantages over traditional anchors, including deployment in shallow waters, stronger seabeds, and close proximity to other anchors. It has a hybrid embedment method that combines vibro hammering and impact hammering.

A geotechnical centrifuge test was carried out on a scaled FEPLA in saturated dense silica sand. A 1/60th scale centrifuge model of the FEPLA was manufactured (see Figure 15). The soil sample was prepared using air pluviated silica sand simulating a common shallow shelf soil. The model testbed was vacuum water saturated. A cone test was completed demonstrating a repeatable and consistent relative density (Dr = 85%).

The anchor was installed at a low G level at installation depths of 2 and 3 times the fluke height (H = 3 m). When at the target G level, the anchor was pulled to soil failure. Measuring that capacity at varied installation depths was the goal of this demonstration test. Full scale ultimate holding capacity of 12.5 MN at 3H depth and 6.3 MN at 2H depth was measured. An Abaqus finite element model of the centrifuge test was carried out modelling both the installation and pullout. Loads in the Abaqus model compared well, within 6%, of the centrifuge model results.

Based on these results, the expected FEPLA installation depth for the example floating turbine assessed in the previous section with peak tension of 8 MN would be just over 2H or 6-8 m depth.

Future testing could be completed to study additional prototype geometries, push or hammer installation, pull velocities, and pull angles. Additional studies could be completed considering cyclic loading, displacement under sustained tension and anchor tilt. Building on SEPLA technology, these new anchors can be precisely positioned without the use of suction, making them suitable for the dense clustering needed in offshore wind installations in sand and shallow waters.

7. CONCLUSION AND RECOMMENDATIONS

The findings of this study highlight some of the unique aspects of offshore wind development in Atlantic Canada. Conditions vary significantly across the region including water depths, soil types, exposure to extratropical storms, weakened hurricanes, icing, and, in more northerly regions, seasonal sea ice. Structures selected will be optimized based on the local conditions, and, in some cases, different structure types and different mooring systems may be required within the same development.

The analyses in this paper emphasize the critical role of turbine operational mode and the effect on structural loading, especially under extreme wind conditions. Idling provides aerodynamic damping, which reduces extreme motions but introduces higher thrust and nacelle accelerations. Production based forces and moments are larger than parked or idle modes.

As discussed in [1], hurricanes can reach Atlantic Canada but are often diminished in strength by the time they arrive. IEC 61400-1 recommends performing a robustness check for hurricanes using the 500-year wind speed combined with a partial safety factor of 1.0, compared to a partial safety factor of 1.25 applied for production DLCs. For example, from Table 6, the production loads (e.g., Cases 1, 2, and 3) factored by 1.25 are similar to the hurricane generated loads factored by 1.0 (Cases 12 and 13). This confirms the use of idling (free rotor) control as an effective load mitigation strategy during high wind events such as hurricanes.

Canada is presently adopting the IEC 61400-3-1 standard for fixed wind turbine structures with deviations, including reference to methods for determining ice loads referenced in ISO 19906. The IEC 61400-3-2 standard for floating wind turbine structures has not yet been adopted in Canada; it is of note that this standard defers to ISO 19906 for ice loads. While ISO 19906 generally has methods for determining design ice loads, the methods were developed for oil and gas drilling and production platforms and typically define fixed design loads. Further guidance may be needed on developing load time series and modelling coupled wind and ice load effects, with added emphasis on intermittent crushing and ice-induced vibrations.

It is important to initiate enhanced measurements of wind, wave, current, and ice occurrence and mobility at locations where wind power production may be considered to accurately characterize conditions and avoid overly conservative assumptions. In many regions in Atlantic Canada, ice floes are typically small, and floes with sufficient diameter to achieve lock-in failure frequency vibrations are unlikely – unlike Baltic conditions where fixed installations are being designed for ice loading. Developing improved modelling techniques to assess the potential influence of wind turbine arrays on sea ice conditions and movements is equally important, particularly for production mode.

Site-specific detailed geotechnical investigations will be essential to quantify stratigraphy, density variability, friction angle, stiffness profiles, and the presence of gravel or shell layers that may influence drivability or

lateral capacity. CPTs, boreholes, and laboratory characterization will allow site-specific soil models to be developed and will refine estimates of drained strength and deformation behaviour in accordance with offshore design standards. Such data will also enable more accurate soil-structure interaction modelling, which is required for final monopile sizing and verification of lateral performance under operational and extreme load conditions. While not specifically addressed in this paper, certifying mooring systems for certain applications requires an in-situ pull test to verify capacity. In the case of a large offshore wind energy development with hundreds of moored turbines, this approach of verification is not practical, and alternative approaches will be required. These may include more accurate seabed/soil profiling coupled with physical testing (e.g., centrifuge) and calibrated numerical finite element modelling.

Finally, in accordance with the IEC 61400 series, the design of a single turbine is typically based on extreme metocean conditions with a 50-year return period. However, as the size of farms increase, the design philosophy may need to move from a "per turbine" design to an overall wind farm design where the consequence of the failure of one or more turbines is considered. This may result in the need to design to a higher reliability target.

ACKNOWLEDGMENT

The authors gratefully acknowledge funding from the Department of Industry, Environment and Technology, Government of Newfoundland and Labrador, for supporting the development of the drive actuator used to install the FEPLAs in the centrifuge. The authors also acknowledge the collaborative support of Acteon in providing dimensions of a FEPLA as well as technical support for performance modelling.

Authors' Declaration

- Ethical approval: This paper does not contain any studies with human participants or animals.
- Competing interests: The authors declare that they have no competing interests.
- Availability of data and materials: Datasets used and/or analyzed during the current study are available from the corresponding author upon reasonable request.
- Artificial intelligence was not used in this work.

REFERENCES

[1] M. Fuglem, P. Stuckey, A. Derradji-Aouat, R. McKenna, and F. Ralph, "Development of Offshore Wind in Atlantic Canada: Regulations, Standards and Technical Challenges," in *OCEANS 2024 – Halifax*, Halifax, NS, Canada, Sept. 2024, pp. 1–10. doi: 10.1109/OCEANS55160.2024.10753762.

[2] Entrion Wind. "Fully-restrained Platform Monopile Foundation." entrionwind.com. Accessed Dec. 2025. [Online]. Available: https://www.entrionwind.com/technology

[3] OSI Renewables, "FTLP Floating Wind Platform." 2025. [Online]. Available: https://www.osirenewables.com/wp-content/uploads/2023/04/23-03-FTLP-Flysheet-Protected.pdf

[4] AWC Tech. "Articulated Wind Column (AWC)." AWCtech.co.uk. Accessed: Dec. 2025. [Online]. Available: https://awctech.co.uk/

[5] V. Swail et al., "The MSC50 wind and wave reanalysis," in *Proceedings of the 9th International Workshop on Wave Hindcasting and Forecasting*, Victoria, BC, Canada, 2006, p. 29. https://www.oceanweather.com/about/papers/The%20MSC50%20Wind%20and%20Wave%20Reanalysis.pdf

[6] J. E. Overland, "Prediction of Vessel Icing for Near-Freezing Sea Temperatures," *Weather*

Forecasting., vol. 5, no. 1, pp. 62–77, Mar. 1990, doi: 175/1520-0434(1990)005<0062:POVIFN>2.0.CO;2.

[7] J. Laforte and M. Allaire, "Évaluation du Givromètre d'Hydro-Québec à Différentes Intensités de Givrage Sec et Humide," Montreal, Canada, Hydro-Québec, Études et Normalisation Équipement de Transport Rapport HQ-92-02, 1992.

[8] H. Hersbach et al., "The ERA5 global reanalysis," *Quarterly Journal of the Royal Meteorological Society*, vol. 146, no. 730, pp. 1999–2049, July 2020, doi: 10.1002/qj.3803.

[9] P. Guest, "Vessel Icing," in NOAA's Marine Weather Log, vol. 49, no. 3, 2005. [Online]. Available at: https://www.vos.noaa.gov/MWL/dec_05/ves.shtml

[10] S. Mintu and D. Molyneux, "Experimental Study of Combined Wave and Ice Loads on a Fixed Offshore Structure," in *Volume 7: Polar and Arctic Sciences and Technology*, Virtual, Online: American Society of Mechanical Engineers, Jun. 2021, p. V007T07A010. doi: 10.1115/OMAE2021-66442.

[11] AEGIR Insights, "Value Mapping Nova Scotia's Offshore Wind resources," 2023. [Online]. Available at: https://netzeroatlantic.ca/sites/default/files/2023-04/Value%20Mapping%20Nova%20Scotia%20Offshore%20Wind%20Resources.pdf

[12] G. Philibert et al., "Updated surficial geology compilation of the Scotian Shelf bioregion, offshore Nova Scotia and New Brunswick, Canada," Natural Resources Canada, Open File 8911, 2022.

[13] J. Eamer, J. Shaw, E. King, and K. MacKillop, "Seabed conditions on the inner shelves of Atlantic Canada," Geological Survey of Canada, Open File 8731, 2020.

[14] P. Passon, "Derivation and description of the soil-pile-interaction models," University of Stuttgart, Stuttgart, Germany, Memo. pp. 1–9, 2006.

[15] S. Aasen, A. M. Page, K. Skjolden Skau, and T. A. Nygaard, "Effect of foundation modelling on the fatigue lifetime of a monopile-based offshore wind turbine," *Wind Energy Science*, vol. 2, no. 2, pp. 361–376, July 2017, doi: 10.5194/wes-2-361-2017.

[16] National Renewable Energy Laboratory, *OpenFAST 3.5.1*. [Online]. Available: https://github.com/OpenFAST

[17] B. J. Jonkman, "TurbSim User's Guide: Version 1.50," National Renewable Energy Laboratory, Golden, CO, USA, NREL/TP-500-46198, Sep. 2009. [Online]. Available: https://www.nrel.gov/docs/fy09osti/46198.pdf

[18] E. Gaertner et al., "Definition of the IEA 15-Megawatt Offshore Reference Wind Turbine," National Renewable Energy Laboratory, Golden, CO, USA, NREL/TP-5000-75698, Mar. 2020. [Online]. Available: https://www.nrel.gov/docs/fy20osti/75698.pdf

[19] C. Allen et al., "Definition of the UMaine VolturnUS-S Reference Platform Developed for the IEA Wind 15-Megawatt Offshore Reference Wind Turbine," National Renewable Energy Laboratory, Golden, CO, USA, NREL/TP-5000-76773, Jul. 2020. [Online]. Available: https://docs.nrel.gov/docs/fy20osti/76773.pdf

[20] C. Allen et al., "Definition of the UMaine VolturnUS-S Reference Platform Developed for the IEA Wind 15-Megawatt Offshore Reference Wind Turbine," International Energy Agency. [Online]. Available: https://docs.nrel.gov/docs/fy20osti/76773.pdf

[21] P. Stuckey, A. Derradji-Aouat, M. Fuglem, and I. Turnbull, "Evaluation of Monopile Wind Turbine Platforms for Extreme Design Conditions," in *Proceedings of 28th International Conference on Port and Ocean Engineering under Arctic Conditions*, St. John's Canada, 2025.

Seabed Characterization

George Marling

A desktop assessment

Who should read this paper?

Parties and people interested in offshore wind development of the Canadian East Coast and those who wish to gain a high-level understanding of the geological conditions and development constraints of the Nova Scotia designated Wind Energy Areas (WEAs) will be interested in this paper.

Why is it important?

This work compiles existing data, often consisting of recent geophysical and geotechnical survey works, to develop a high-level understanding of the seabed and sub-seabed conditions of each of the Nova Scotia WEAs. It offers an understanding of the development and geological constraints of the WEAs and of the amount of data that is (and will be) publicly available. Finally, it enables early planning to address the most significant construction/development constraints and highlights the potential development works, key considerations, and site characterization data.

About the author

George Marling is a chartered senior geotechnical engineer at OWC, a specialist renewables engineering consultancy, where he takes a leading role supporting offshore windfarm developers in the Americas. He brings a wealth of experience as geoscience lead, having fulfilled various geoscience package management and cables owners engineer roles in Taiwan, South Korea, and the US. Based in New York, he acts as OWC's regional coordinator for geo projects in the Americas region, which includes Canada, the US, Brazil, and Colombia, working closely with offshore wind developers to de-risk their projects through site investigations, site characterization, ground modelling, geo-hazard identification, and front-end engineering design.

GEOLOGICAL CHARACTERIZATION OF OFFSHORE WIND ENERGY AREAS ON THE SCOTIAN SHELF

George Marling
OWC, An ABL Group Company, New York, NY, USA
Corresponding author: george.marling@owcltd.com
DOI: https://doi.org/10.48336/Y49H-FN24

ABSTRACT

The Scotian Shelf offshore Nova Scotia has emerged as a region of significant interest for large-scale offshore wind development, with four designated Wind Energy Areas (WEAs): French Bank, Middle Bank, Sable Island Bank, and Sydney Bight. These WEAs are notable for their exceptional spatial extent, variable water depths, and complex geological history shaped through glacial processes, sea level fluctuations, and post-glacial marine reworking. This paper synthesizes publicly available geological data to provide an integrated desktop assessment of seabed and sub-seabed conditions across the Nova Scotia WEAs. Particular attention is given to surficial sediment distribution, shallow stratigraphy, bedrock exposure, glacial landforms, and geological hazards such as shallow gas and challenging minerology. The implications of these conditions for offshore wind foundation concepts, cable installation, and development strategy are discussed. The analysis highlights that while large portions of the WEAs are broadly suitable for offshore wind development, spatial heterogeneity in seabed conditions will strongly influence site selection, turbine layout optimization, and engineering design. Early-stage geological understanding is, therefore, critical to de-risk development and to identify viable sub-areas within these exceptionally large lease zones.

1. INTRODUCTION

Global offshore wind is gaining momentum as nations seek to decarbonize electricity systems while maintaining energy security. Canada, particularly Atlantic Canada, has recently emerged as a frontier region for offshore wind development. Nova Scotia's offshore environment is characterized by high wind resource potential, proximity to North American markets, and an established offshore energy and marine engineering legacy. In recognition of this potential, several sizeable Wind Energy Areas (WEAs) have been identified on the Scotian Shelf, offshore Nova Scotia.

While the wind resource and electrical export potential of these areas are increasingly well recognized, the geological and geotechnical conditions of the Scotian Shelf introduce both opportunities and challenges for offshore wind development. Unlike many established offshore wind regions, such as the southern North Sea, the Scotian Shelf retains a strong imprint of glaciation, limited fluvial sediment input, and locally extensive shallow bedrock. These characteristics can significantly affect foundation feasibility, installation methodology, and project cost.

This paper presents a geological desktop study of the Nova Scotia WEAs, synthesizing existing datasets from federal and provincial sources, academic literature, and offshore surveys. The objective is to characterize seabed and shallow subsurface conditions at a scale relevant to early-stage offshore wind development and to assess the implications for engineering design and development strategy.

2. STUDY AREA AND WIND ENERGY AREAS

2.1 Regional Setting

The Scotian Shelf is a broad continental shelf extending from the coastline of Nova Scotia into the northwest Atlantic Ocean. It is bounded to the south by the continental slope and to the northeast by the Laurentian Channel. The shelf has been shaped by repeated Pleistocene glaciations, with ice sheets advancing across the shelf and retreating during interglacial periods. These processes have produced a complex seabed morphology consisting of banks, basins, ridges, and palaeochannels.

Unlike many sediment-rich continental shelves, the Scotian Shelf has experienced relatively limited riverine sediment input. As a result, glacial and post-glacial sediments are often thin, and bedrock is locally exposed or shallowly buried, particularly in nearshore and mid-shelf settings.

2.2 Wind Energy Areas

Four WEAs have been identified offshore Nova Scotia for further development (Figure 1):

- French Bank (approximately 20 km offshore)
- Sydney Bight (approximately 25 km offshore)
- Middle Bank (approximately 60 km offshore)
- Sable Island Bank (up to approximately 110 km offshore) [1]

These WEAs are exceptionally large, ranging from approximately 1,285 km² (Sydney Bight)

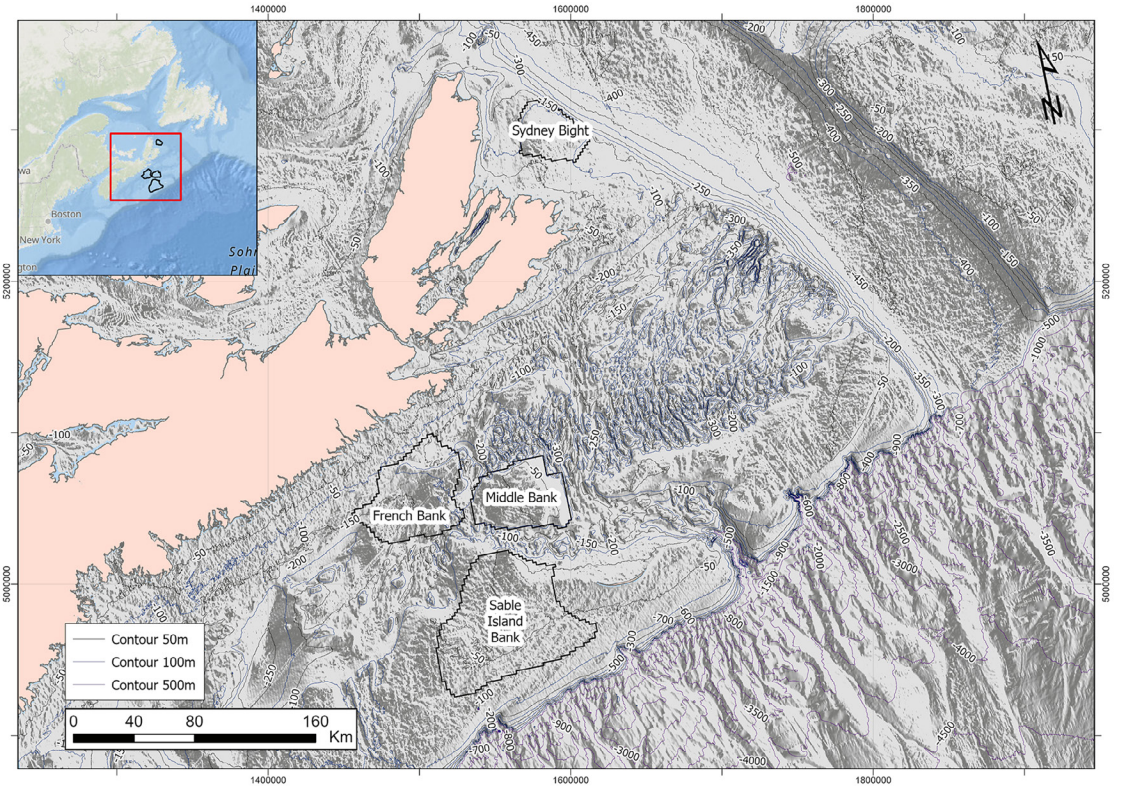

Figure 1: Location of Nova Scotia Wind Energy Areas (WEAs). Map developed by OWC.

to approximately 5,850 km² (Sable Island Bank) [2]. For context, Hornsea 2, currently the world's largest operational offshore wind farm, occupies approximately 460 km² [3]. The scale of the Nova Scotia WEAs implies that only a subset of each area is likely to be developed, with geological and bathymetric constraints playing a key role in determining viable development zones.

2.3 Water Depths and Bathymetry

Water depths across the WEAs vary substantially (Figure 2):

- French Bank: ~70-210 m (deepest of the four)
- Middle Bank: ~40-160 m
- Sydney Bight: ~50-150 m
- Sable Island Bank: ~20-80 m (shallowest)

Publicly available bathymetric data indicate that large areas of the WEAs are relatively flat, which is favourable for offshore wind development. However, localized ridges, scarps, and depressions are present, reflecting underlying geological structures and glacial landforms (Figure 3).

3. DATA SOURCES AND METHODOLOGY

This study is based on a desktop review of publicly available geological and geophysical datasets, including:

- Surficial geology compilations of the Scotian Shelf from Natural Resources Canada
- Bathymetric datasets and seabed morphology interpretations from

General Bathymetric Chart of the Oceans
- Geological Survey of Canada seismic stratigraphy studies
- Grab sample and seabed imagery from recent survey expeditions
- Peer-reviewed academic literature on Scotian Shelf geology

The analysis focuses on seabed and shallow subsurface conditions (upper tens to one hundred metres), which are most relevant to offshore wind foundations and cable installation. No new field data were collected as part of this study; rather, existing data were synthesized to provide a development oriented geological interpretation.

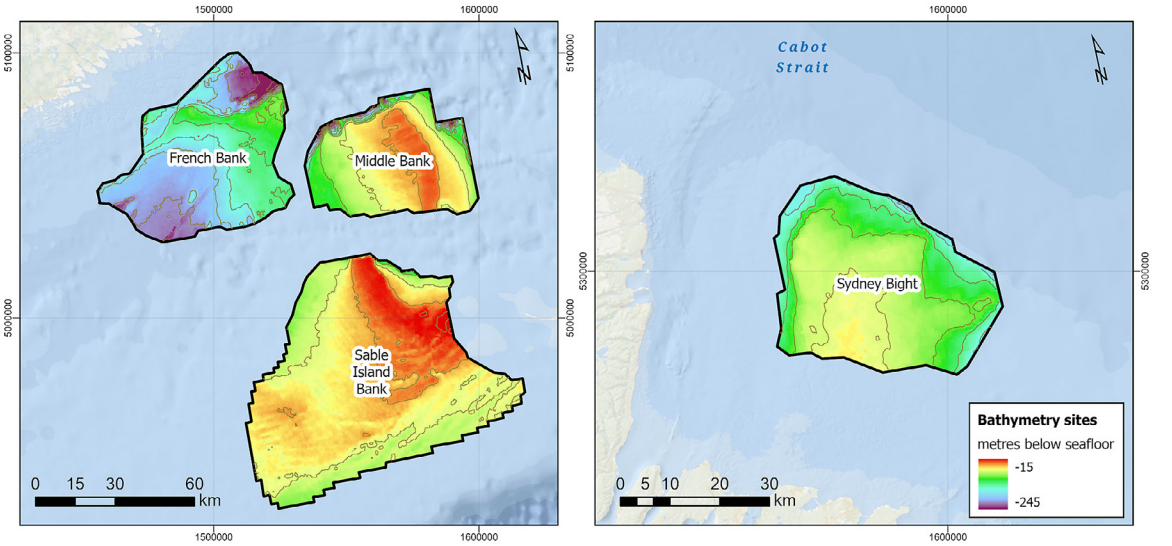

Figure 2: Bathymetry of the Wind Energy Areas (WEAs). Map developed by OWC with data sourced from [4].

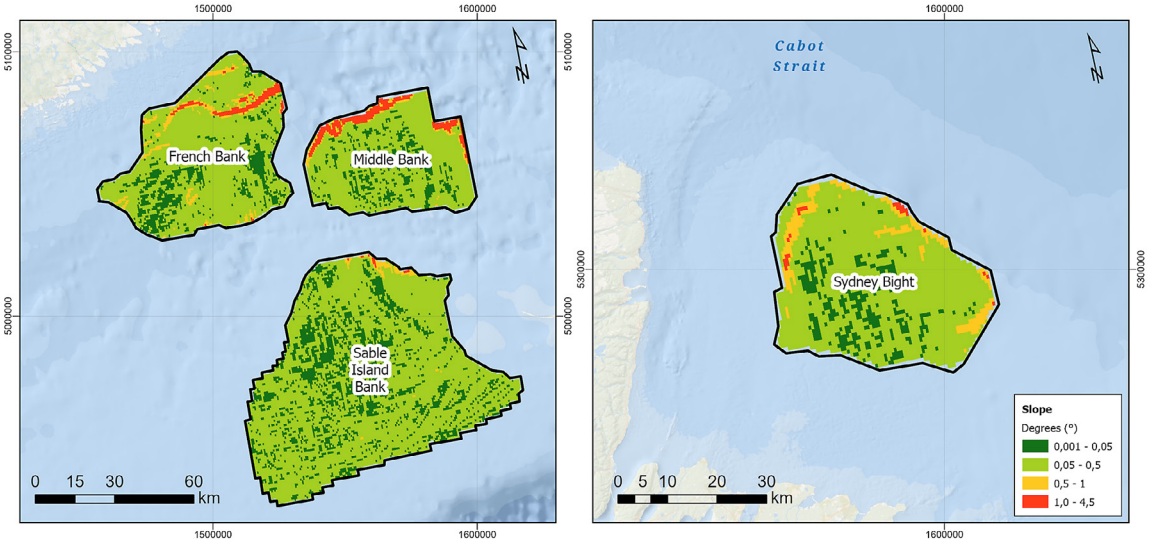

Figure 3: Seabed slopes of the Wind Energy Areas (WEAs). Map developed by OWC with data sourced from [4].

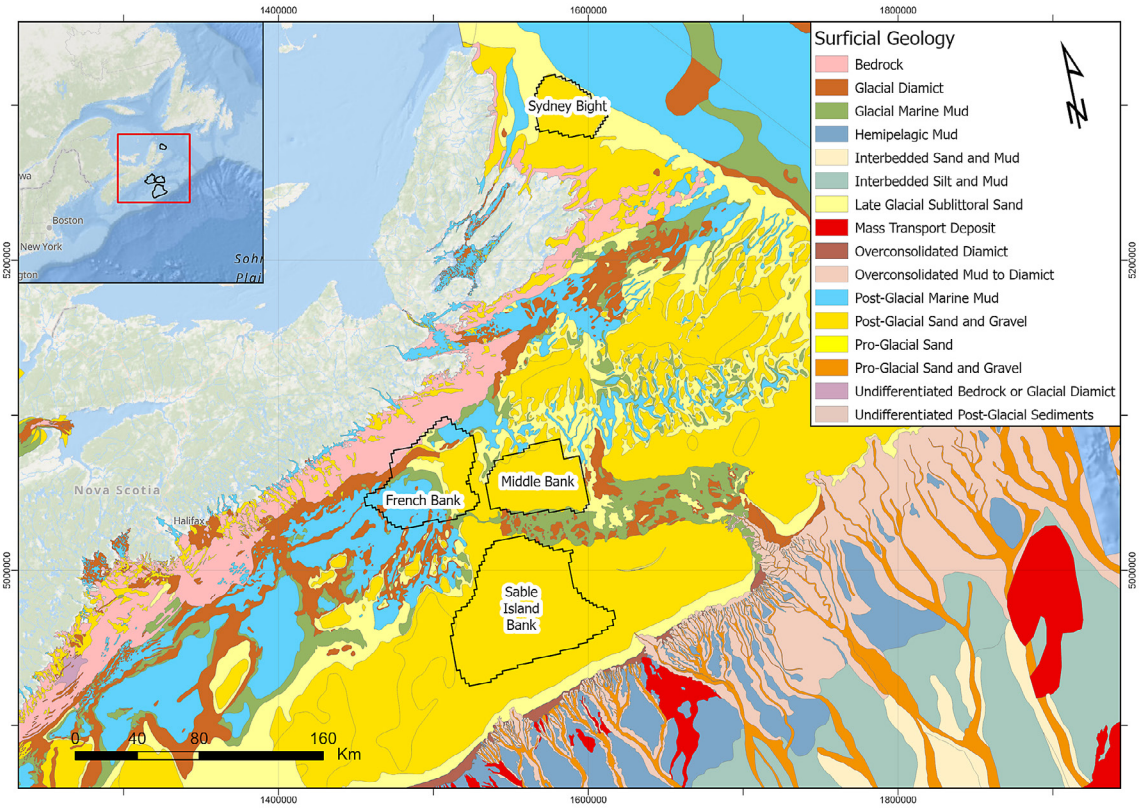

Figure 4: Seabed sediments across the Scotian Shelf. Map developed by OWC with data sourced from [5].

4. SURFICIAL SEABED SEDIMENTS

4.1 Overview of Sediment Types

The surficial geology of the Nova Scotia WEAs is dominated by post-glacial sands and gravels, with local occurrences of glacial diamict, marine muds, and exposed bedrock (Figure 4). Sediment distribution varies between WEAs, reflecting differences in glacial history, water depth, and post-glacial marine processes (sea level transgression).

4.2 Sydney Bight

Sydney Bight is characterized predominantly by post-glacial sand and gravel deposits. At water depths less than approximately 100 m, sediments are often thin, with bedrock locally exposed through a veneer of sand and gravel. The seabed is generally flat, but minor roughness occurs, where bedrock ridges may be present. Coal-bearing formations extend offshore in this region, reflecting the geological continuity between Cape Breton and Newfoundland.

4.3 French Bank

French Bank exhibits a more diverse assemblage of surficial sediments, including:

- Post-glacial sand and gravel
- Late glacial sublittoral sands
- Glacial and post-glacial marine muds
- Glacial diamict
- Local bedrock exposure

This diversity reflects the strong influence of glacial deposition and ice-marginal processes in the near- to mid-shelf environment.

4.4 Middle Bank

Middle Bank is dominated by post-glacial sand and gravel deposits. Recent surveys indicate generally flat seabed conditions with local scour depressions. In some locations, geophysical data suggest the presence of a "competent" layer sitting 10-20 m beneath the seabed, interpreted as either dense glacial material or shallow bedrock [6].

4.5 Sable Island Bank

Sable Island Bank is characterized by thick, sand-dominated deposits formed through repeated cycles of deposition and erosion associated with sea level transgression and storm-dominated marine processes. While clay-rich tills are not expected to be widespread, local interbedded clays and scattered cobbles and boulders are likely to be present beneath the thick sand sequences, particularly in palaeochannel fills [7]. Surficial cobbles and boulders are also likely to be present in the north-northwest areas of Sable Island Bank.

5. SUBSURFACE GEOLOGICAL FRAMEWORK

5.1 Glacial Landforms and Deposits

The inner shelf regions, particularly around French Bank, display classic glacial landforms such as moraines and drumlins. These features reflect ice movement and glacial deposition across the shelf and are associated with glacial till deposits. Such deposits can vary significantly in grain size, density, and strength over short distances, posing challenges for foundation design.

5.2 Bedrock Characteristics

Bedrock lithologies identified in the region include slate, greywacke, and quartzite, all of which are known to be hard, competent materials (Figure 5). Shallow bedrock such as this presents challenges for driven foundations and cable burial. In areas where bedrock is exposed or covered by only a thin sediment layer, alternative installation techniques may be required.

5.3 Palaeochannels and Stratigraphic Complexity

Across the Scotian Shelf, numerous palaeochannels have been identified. These channels are incised into bedrock or competent sediments, and partially infilled with sand, gravel, and locally clay-rich sediments. The infill materials are often highly variable in composition and compaction, introducing uncertainty in geotechnical behaviour.

5.4 Sable Island Bank Stratigraphy

Seismic stratigraphy studies of Sable Island Bank reveal a classic sequence stratigraphic framework, with cyclic transgressions and regressions of sea level producing layered sedimentary sequences (Figure 6). Sediments generally thicken as we look further offshore, with older and potentially more indurated units present at depth.

6. GEOLOGICAL HAZARDS AND ENGINEERING CONSIDERATIONS

6.1 Shallow Bedrock

Shallow bedrock (i.e., bedrock located at the seabed surface to approximately 30-40 m below seabed) has been identified across the Scotian Shelf and is likely present at French Bank and Sydney Bight WEAs. It has not been

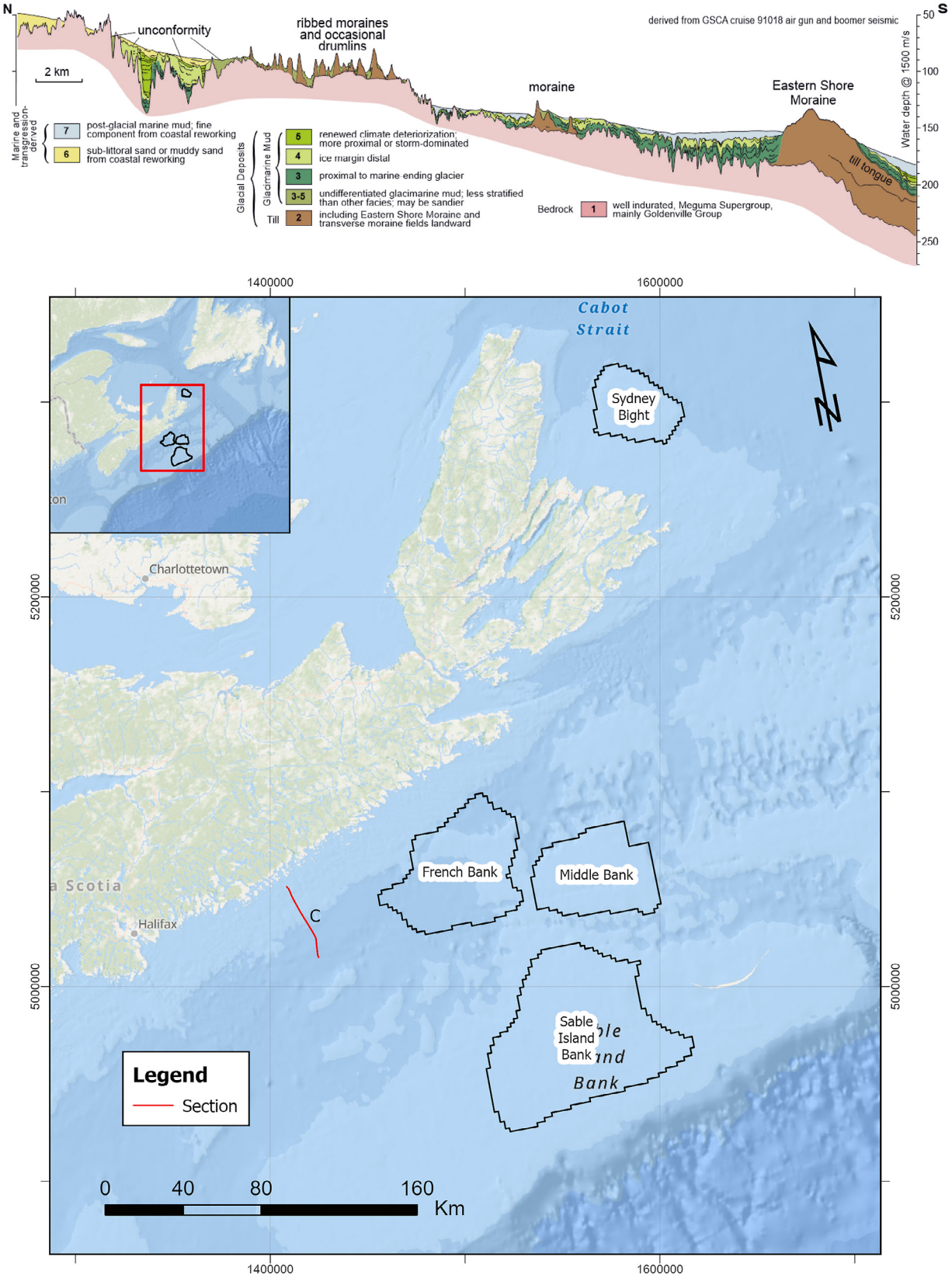

Figure 5: Subsurface profile (top) [8]. Map (bottom) developed by OWC providing approximate location of the profile in relation to the Wind Energy Areas (WEAs).

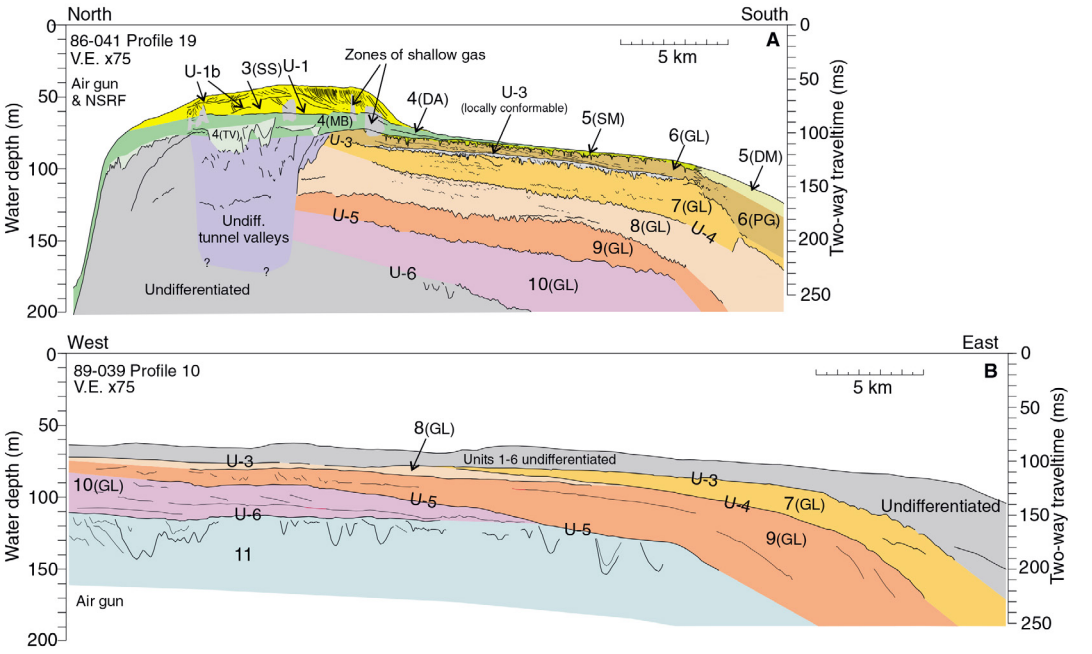

Figure 6: Soil profiles extracted from [7]. Both profiles are in close proximity to Sable Island Bank Wind Energy Area (WEA) site. Top image shows profile from nearshore to offshore (left-right), displaying clear layering of sediments, getting thicker as the profile progresses toward the Outer Continental Shelf. Bottom image shows profile running parallel to shore, where palaeochannels can be identified as anomalies within the normal layering of sediments.

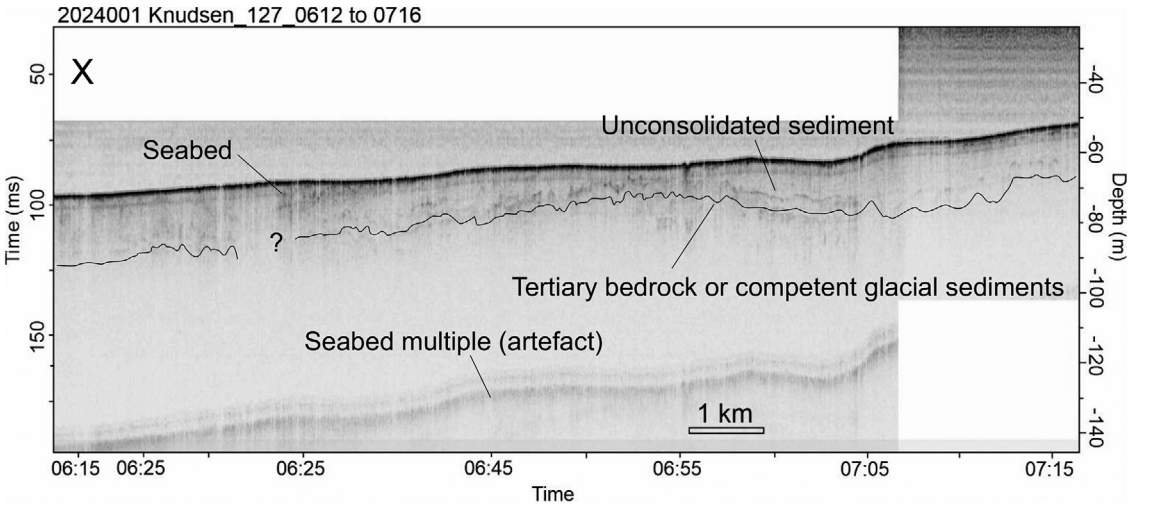

Figure 7: Subsurface soil profile acquired at a central location within Middle Bank Wind Energy Area (WEA). Profile extracted from [6].

verified whether Middle Bank also has areas of shallow bedrock; however, a sub-surface seismic profile acquired in 2023 indicates the presence of a competent soil layer within the first 10-20 m below seabed (Figure 7).

6.2 Shallow Gas

Shallow gas has been identified in parts of Sable Island Bank, generally at a local scale. While not necessarily widespread, the presence of shallow gas requires careful consideration during site investigation and foundation design. This is due to potential health risks to crew during drilling operations and stability of soils during asset installation/operation [7].

6.3 Glauconite or "Green Sand"

Recent research has identified glauconite content in parts of the Scotian Shelf, most notably at Sable Island Bank WEA [6]. Glauconite, that appears as a green sand, has gained infamous recognition in the US, where it has caused pile installation challenges for offshore wind projects offshore Massachusetts and Rhode Island. Although glauconite has so far been identified primarily in grab samples of seabed sediments, its potential presence warrants further investigation.

6.4 Seabed Mobility

Sand-dominated environments, particularly on Sable Island Bank, are subject to seabed mobility under storm-dominated wave and current regimes. Sandwaves and megaripples, bedforms that indicate the risk of seabed mobility, are likely to be present at Sable Island Bank WEA, and recent bathymetric survey data at Middle Bank show signs of scour depressions [9]. Bedform migration and scour around foundations may be significant and must be accounted for in foundation design and cable protection measures for offshore wind projects.

7. IMPLICATIONS FOR OFFSHORE WIND DEVELOPMENT

7.1 Foundation Concepts

The geological diversity of the Nova Scotia WEAs suggests that no single foundation concept will be universally applicable. Potential foundation solutions include:

- Large-diameter monopiles (with or without pre-drilling)
- Drilled monopiles or socketed foundations in hard ground
- Suction caissons in suitable sedimentary conditions
- Floating foundations in deeper water areas (French Bank)

Experience from projects such as the Saint-Nazaire offshore wind farm demonstrates that drilled extra-large monopiles can be successfully deployed in rocky seabed conditions – although significant installation times, equipment damage, and expensive drilling apparatus will likely increase costs significantly.

7.2 Cable Installation

Cable routing may be challenging in areas with shallow bedrock, ridges, and variable sediment cover. However, in deeper water areas, cable burial may not be required, potentially simplifying installation. As many of the WEA names suggest, each of the sites sit on a bank, an area of relatively flat, elevated seabed. Between each of the banks is a basin or rougher terrain, which will need to be

navigated to successfully route export cables back to shore. It is, therefore, not sufficient to simply investigate the WEAs themselves but also potential cable routes back to Nova Scotia or further afield.

7.3 Development Strategy

Given the immense size of the WEAs, early-stage geological screening is essential to identify favourable sub-areas for development. Targeting zones with relatively uniform sediments, moderate water depths, and limited geological hazards can significantly reduce development risk and cost.

8. DISCUSSION

The Nova Scotia WEAs represent a geologically complex but highly promising offshore wind region. Compared to more established offshore wind provinces, the Scotian Shelf presents greater geological variability and uncertainty, particularly related to glacial landforms, shallow bedrock, and sediment heterogeneity. However, these challenges are not insurmountable and can be addressed through appropriate site investigation, engineering innovation, and adaptive development strategies.

9. CONCLUSION

1. The Scotian Shelf offshore Nova Scotia exhibits complex seabed and sub-seabed geology shaped by glaciation and post-glacial marine processes.
2. Surficial sediments are dominated by post-glacial sands and gravels, with localized glacial diamict, marine muds, and bedrock exposure (most notably at French Bank).
3. Geological hazards such as shallow gas and glauconite require further investigation but are manageable with appropriate design approaches.
4. The exceptional size of the WEAs necessitates selective development, guided by early-stage geological understanding.
5. With informed planning and engineering, the Nova Scotia WEAs offer strong potential for large-scale offshore wind development.

ACKNOWLEDGMENT

The author acknowledges Natural Resources Canada and the Geological Survey of Canada for the availability of geological datasets, and OWC for support in compiling and interpreting the available data.

Author Declaration

- Funding: The author did not receive financial support from any organization for the submitted work.
- Ethical approval: This paper does not contain any studies with human participants or animals.
- Competing interests: The author declares that he has no competing interests.
- Availability of data and materials: Datasets used and/or analyzed during the current study are available from the corresponding author upon reasonable request.
- Artificial intelligence was not used in this work.

REFERENCES

[1] Natural Resources Canada-Nova Scotia Department of Energy, “Proposed Wind Energy Areas for

the Canada-Nova Scotia Offshore," Discussion Paper, Mar. 2025. [Online]. Available at: https://novascotia.ca/offshore-wind/docs/offshore-wind-energy-areas-discussion-paper.pdf

[2] Natural Resources Canada, "Designated Offshore Wind Energy Areas," [Online]. Available at: https://novascotia.ca/offshore-wind/docs/designated-offshore-wind-energy-areas.pdf

[3] Orsted, "Hornsea 2 Offshore Windfarm." Accessed Jan. 2026. [Online]. Available at: https://orsted.co.uk/energy-solutions/offshore-wind/our-wind-farms/hornsea2

[4] General Bathymetric Chart of the Oceans (GEBCO), "Gridded bathymetry data." Accessed Jan. 2026. [Online]. Available at: https://www.gebco.net/data-products/gridded-bathymetry-data

[5] Nova Scotia Department of Natural Resources and Renewables, "Downloadable GIS data." Accessed Jan. 2026. [Online]. Available at: https://novascotia.ca/natr/meb/download/gis-data-maps.asp

[6] J.B.R. Eamer et al., "Recent research in support of a low-carbon economy at the Geological Survey of Canada – Atlantic," Geological Survey of Canada¸ Open File 9204, 1 poster, 2024. doi: 10.4095/p4vptgc1s2.

[7] E.K. King, "A glacial origin for Sable Island: ice and sea-level fluctuations from seismic stratigraphy on Sable Island Bank, Scotian Shelf, Offshore Nova Scotia," Geological Survey of Canada, 2001. doi: 10.4095/212173.

[8] E.L. King, "Surficial geology and features of the inner shelf of Eastern shore, offshore Nova Scotia," Natural Resources Canada, 2018. [Online]. Available at: https://publications.gc.ca/collections/collection_2019/rncan-nrcan/m183-2/M183-2-8375-eng.pdf

[9] D.C. Campbell, "RRS Discovery Expedition 2023-003 (DY169 Leg 01): seabed investigations of the eastern Scotian Shelf and canyons, offshore Nova Scotia," Geological Survey of Canada, 2024. [Online]. Available at: https://publications.gc.ca/collections/collection_2025/rncan-nrcan/m183-2/M183-2-9179-eng.pdf

Informative

Cutting Edge

Provocative

Challenging

Thought Provoking

International

thejot.net

marine renewables canada

2026 CONFERENCE & EXHIBITION

THE ONLY NATIONAL CONFERENCE DEDICATED TO OFFSHORE WIND, TIDAL, WAVE, AND RIVER CURRENT ENERGY

2025 CONFERENCE HIGHLIGHTS

700+ ATTENDEES! THAT'S 100% GROWTH YEAR-OVER-YEAR!

135 SPEAKERS, 46 OF THEM INTERNATIONAL

40 EXHIBITORS, INCLUDING INDIGENOUS BUSINESSES

33 SESSIONS: WORKSHOPS, INDUSTRY PANELS, & TECHNICAL PRESENTATIONS

November 17-19, 2026
The Westin Ottawa
Ottawa, Canada

marinerenewablesconference.ca

REGISTER TODAY FOR EARLY BIRD PRICING!